

**Reaction Pathways of Binuclear Aromatics Containing 5-membered Rings**

by

Riya

A thesis submitted in partial fulfillment of the requirements for the degree of

Master of Science

in

Chemical Engineering

Department of Chemical and Materials Engineering

University of Alberta

© Riya, 2018

## ABSTRACT

There is a growing need to decrease the viscosity of bitumen using minimal diluent addition to reduce the cost of transportation. However, due to the inherently free radical rich nature of bitumen, even on exposure to low autoxidative conditions adverse effects on the viscosity and hardening of bitumen were observed. These effects were postulated to be caused by a compound class containing 5-membered rings attached to an aromatic ring since they have a high propensity to undergo free radical addition reactions.

The objective of the work was to develop a better fundamental understanding of addition reactions in binuclear aromatic compounds with one 5-membered ring when exposed to different reaction environments. The compounds selected for this study were: indene, indane, indole, benzofuran and thianaphthene. The reaction environments focused on initiation of addition reactions caused by the addition and removal of hydrogen from the compounds. This was achieved by performing reactions in the presence of acids, bases, thermal conversion conditions and supported metal hydrogenation conditions.

The reactions with acids and bases were performed at very low temperatures of 70 and 120 ° C in the presence of nitrogen at atmospheric pressure with a dilution in toluene of 2 wt% acid/base with 10 wt% model compounds. On reactions with acids, the aromatics containing a 5-membered ring polymerized to form much denser and heavier compound chains. The polymers in the cases of indole and benzofuran formed solid particles upon reactions with acids. Bases, however, did not react with indene, indole and benzofuran. Thianaphthene reacted only in the presence of NaH.

Thermal cracking conditions of 400 °C and 2 MPa promoted free radical reactions in indene, indole and benzofuran. While indane and thianaphthene did not react, indene, indole and benzofuran underwent addition reactions. The addition reactions led to formation of heavier compounds. Indene also produced asphaltenes in the product. The increase in asphaltene formation was linked to an increase in temperature.

Hydrogenation in the presence of a metal supported catalyst was performed in a flow reactor in the presence of H<sub>2</sub> gas. The reactions were performed between a temperature range of 150-180 °C at a gauge pressure of 1 MPa, for indene, indole and benzofuran. The compounds hydrogenated in the descending order: indene >> benzofuran ~ indole. Thianaphthene, however, did not undergo hydrogenation at 180 °C, it required a higher temperature of 220 °C.

## ACKNOWLEDGEMENTS

I would, first and foremost, like to thank Professor Arno de Klerk for taking me in as a master's student in your group and giving me this opportunity and for all the guidance that you have given throughout my thesis. Thank you for all the support and interest you showed during our discussions about my future goals and ambitions. Most importantly thank you for being so patient and calm whenever I would start panicking. I have learned a lot as an engineer and a person under your supervision.

I would like to thank everyone in the group for being so helpful and supportive throughout these two years. I would especially like to thank Cloribel, Isabel, Joy and Giselle for all your help in the lab and during the thinking/writing process.

This chapter of my life has not only helped me grow professionally but emotionally as well. I'm grateful for meeting a lot of wonderful people through this journey, who I have grown very close to. In addition to the people mentioned above, I would also like to thank Shirley, Natalia and Adriana. Thank you for your friendship, and for all the emotional support and the encouragement. I could not have asked to be surrounded by a better group of people who showered me with love when I needed it the most.

I would not have achieved anything in life and be where I'm now without the help of my mom and dad. You have always been so supportive of all my choices and given me complete freedom in directing my life as I wanted. Despite the time difference and the distance, you always kept checking up on me and encouraging me to do the best I can.

Lastly, I would like to thank Nexen for supporting and sponsoring this project.

## TABLE OF CONTENTS

<b>CHAPTER 1: INTRODUCTION.....</b>	<b>1</b>
1.1 Background .....	1
1.2 Objective .....	3
1.3 Scope of work.....	3
1.4 References .....	3
<b>CHAPTER 2 : LITERATURE REVIEW .....</b>	<b>5</b>
2.1 Introduction .....	5
2.2 Acid catalysis .....	5
2.3 Base catalysis .....	8
2.4 Free radical chemistry .....	9
2.5 Metal catalysis.....	13
2.6 References .....	15
<b>CHAPTER 3 : REACTIONS OF AROMATIC COMPOUNDS CONTAINING 5- MEMBERED RINGS WITHS ACIDS.....</b>	<b>18</b>
3.1 Introduction .....	19
3.2 Experimental .....	19
3.2.1 Materials .....	20
3.2.2 Equipment and procedure .....	21
3.2.3 Analyses.....	22
3.3 Results .....	23
3.3.1 Quantifying water content in Amberlyst® 15.....	23

3.3.2 Results for indene .....	25
3.3.3 Results for indole .....	33
3.4 Results for benzofuran .....	37
3.3.5 Results for thianaphthene.....	45
3.3.6 Results for tetrahydrothiophene.....	47
3.4 Discussion .....	47
3.4.1 Addition reactions in the presence of acids .....	47
3.4.2 Solid formation in indole on reaction with acids .....	49
3.4.3 Impact of results on upgrading in oilsands .....	50
3.5 Conclusion.....	50
3.6 References .....	51
<b>CHAPTER 4 : REACTIONS OF AROMATIC COMPOUNDS 5-MEMBERED RINGS WITH BASES.....</b>	<b>53</b>
4.1 Introduction .....	54
4.2 Experimental .....	54
4.2.1 Materials .....	54
4.2.2 Equipment and procedure .....	55
4.2.3 Analyses.....	56
4.3 Results.....	58
4.3.1 Reactions with Ambersep® 900 .....	58
4.3.2 Reaction with sodium hydroxide and ammonium hydroxide.....	60
4.3.3 Reactions with sodium hydride.....	60
4.4 Discussion .....	63
4.4.1 Unreactive behavior of alkalis with naphtheno-aromatic compounds.....	63
4.4.2 Reduction in the presence of sodium hydride.....	63
4.5 Conclusion.....	65
4.6 References .....	65

**CHAPTER 5 : FREE RADICAL ADDITION REACTIONS OF AROMATIC COMPOUNDS CONTAINING FIVE MEMBERED RINGS UNDER THERMAL CONVERSION CONDITIONS..... 67**

5.1 Introduction .....	68
5.2 Experimental .....	68
5.2.1 Material .....	68
5.2.2 Equipment and Procedure .....	69
5.2.3 Analysis.....	70
5.3 Results .....	72
5.3.1 Physical changes .....	72
5.3.2 Asphaltene content.....	73
5.3.3 Gas Chromatograms.....	74
5.3.4 Presence of heavier boiling fractions.....	85
5.3.5 Free radicals in products .....	88
5.3.6 Investigating the presence of phenols .....	90
5.3.7 Reaction of indane and indene together.....	91
5.4 Discussion .....	96
5.4.1 Heavier product formation and ring-opening reactions.....	96
5.4.2 Reaction chemistry of indene and indane .....	99
5.4.3 No reaction in thianaphthene despite pyrolysis of benzofuran .....	100
5.5 Conclusion.....	100
5.6 References .....	101

**CHAPTER 6 : HYDROGENATION OF AROMATIC COMPOUNDS CONTAINING 5-MEMBERED RINGS OVER A SUPPORTED METAL HYDROGENATION CATALYST IN A FLOW REACTOR IN THE PRESENCE OF H<sub>2</sub> GAS ..... 103**

6.1 Introduction .....	104
6.2 Experimental .....	105
6.2.1 Material .....	105
6.2.3 Preparation of catalyst.....	105

6.2.4 Catalyst activation.....	106
6.2.5 Catalyst characterization.....	106
6.2.6 Reactor design.....	109
6.2.7 Reactor operation.....	110
6.2.8 Analysis.....	111
6.2.9 Calculations.....	113
6.3 Results.....	113
6.3.1 Identification of the peaks for hydrogenated products.....	113
6.3.2 Effect of temperature and space velocity on conversion of indene.....	125
6.3.3 Low conversion rates after hydrogenation of indole, benzofuran and thianaphthene.....	127
6.3.4 Elemental analysis of spent catalyst vs. fresh catalyst.....	130
6.4 Discussion.....	131
6.4.1 Hydrogenation of aromatic compounds containing 5-membered rings.....	131
6.4.2 Ring-opening reactions followed by hydrogenation.....	132
6.5 Conclusion.....	133
6.6 References.....	134
<b>CHAPTER 7: CONCLUSIONS AND FUTURE WORK.....</b>	<b>135</b>
7.1 Conclusions.....	135
7.2 Other deliverables.....	137
7.3 Future work.....	137
<b>BIBLIOGRAPHY.....</b>	<b>137</b>
<b>APPENDIX A.....</b>	<b>A1</b>

## LIST OF FIGURES

<b>Figure 1.1</b> Flow Diagram for the partial upgrading process, highlighting the presence of naphtheno-aromatic compounds.....	2
<b>Figure 2.1</b> Indene (left) and the expected protonation product of indene (right).....	6
<b>Figure 2.2</b> Reaction mechanism for formation of major products on reaction of thianaphthene with aqueous metal sulfates.....	7
<b>Figure 2.3</b> Reaction pathways during conversion of dibenzothiophene in decalin with sodium...	8
<b>Figure 2.4</b> Possible initiation steps in the thermal decomposition of indene.....	10
<b>Figure 2.5</b> Ring fission of indene at 700 °C giving three possible primary radicals.....	10
<b>Figure 2.6</b> Primary reaction in furan pyrolysis at >827 °C.....	11
<b>Figure 2.7</b> Reaction mechanism for thianaphthene in continuous flow pyrolysis at temperatures between 750-850 °C.....	12
<b>Figure 3.1</b> Experimental setup.....	21
<b>Figure 3.2</b> Heat curve obtained using the TGA (red) overlapped with the mass loss (black) of Amberlyst® 15 with respect to temperature under nitrogen.....	23
<b>Figure 3.3</b> Absorbance of sulfur dioxide and water at 1360 and 1650 cm <sup>-1</sup> respectively, during the degradation of Amberlyst® 15 as a function of temperature under nitrogen.....	24
<b>Figure 3.4</b> Chromatograms obtained from the reactions of indene with acids where a) shows the retention time from 2.5- 15 minutes while b) goes from 9.5 to 28 minutes.....	26

<b>Figure 3.5</b> GC-MS results for the a) indene control sample and reaction of indene with b) H <sub>3</sub> PO <sub>4</sub> and c) Amberlyst® 15.....	<b>28</b>
<b>Figure 3.6</b> Chemical structure for 1-methyl-2-[(E)-2-(2-methylphenyl)ethenyl]benzene and 1-(1-indanylidene)indan.....	<b>30</b>
<b>Figure 3.7</b> Mass spectrum for peak 11 and 14 at a retention time of 13.312 min for reactions of indene with Amberlyst® 15 and H <sub>3</sub> PO <sub>4</sub> .....	<b>31</b>
<b>Figure 3.8</b> Crystallization following on reaction from a saturated solution of indole seen from Zeiss StereoMicroscope over a period of time.....	<b>33</b>
<b>Figure 3.9</b> Chromatographs obtained from the reactions of indole with acids using the GC-MS..	<b>34</b>
<b>Figure 3.10</b> Solid formed during the reaction of indole with sulfuric acid at a temperature of 120 °C (left) and 70 °C (right).....	<b>35</b>
<b>Figure 3.11</b> Solid formed during the reaction of indole with phosphoric acid.....	<b>36</b>
<b>Figure 3.12</b> Chromatographs obtained from the reactions of benzofuran with acids where a) reaction with selected acids and control b) peaks present in benzofuran provided by supplier c) reaction of benzofuran with Amberlyst® 15 d) reaction with H <sub>3</sub> PO <sub>4</sub> e) reaction with H <sub>2</sub> SO <sub>4</sub> f) and reaction with HCl.....	<b>39</b>
<b>Figure 3.13</b> Mass spectrum for peak 9 for reactions of benzofuran with Amberlyst®15.....	<b>41</b>
<b>Figure 3.14</b> Mass spectrum for a) peak 13, b) peak 14 and 15 for reactions of benzofuran with HCl.....	<b>43</b>
<b>Figure 3.15</b> GC-MS results for the reaction of thianaphthene with a) selected acids and b)Amberlyst®.....	<b>44</b>
<b>Figure 3.16</b> Structure for 2,5-diphenyl-1,4-dithiine.....	<b>45</b>
<b>Figure 3.17</b> Reaction chemistry for formation of isomers of 1-(1-indanylidene)indan.....	<b>46</b>

<b>Figure 3.18</b>	Structure of 3-(2,3-dihydro-1-benzothiophen-3-yl)-1-benzothiophene.....	<b>47</b>
<b>Figure 3.19</b>	Reaction of indole in the presence of sulfuric acid.....	<b>48</b>
<b>Figure 4.1</b>	GC-MS result for the reaction of indene with Ambersep® 900 at 55 °C.....	<b>56</b>
<b>Figure 4.2</b>	Heat flow obtained from DSC for pure indene versus reaction of indene with Ambersep® 900.....	<b>57</b>
<b>Figure 4.3</b>	GC-MS result for the reaction of thianaphthene with NaH at 120 °C.....	<b>58</b>
<b>Figure 4.4</b>	Mass spectrums obtained for reaction of thianaphthene with NaH for peaks a)3 and c) 4.....	<b>60</b>
<b>Figure 5.1</b>	Images of products obtained after the reaction of a) indene b) indole and c) benzofuran captured using the Zeiss microscope.....	<b>71</b>
<b>Figure 5.2</b>	Asphaltene content for indene at reaction times of 30 and 60 min.....	<b>72</b>
<b>Figure 5.3</b>	Results from gas chromatography obtained for the <i>n</i> -pentane soluble fractions of indene between the retention times of 1.5 to 20 minutes for a 60 min reaction of indene at 2 MPa and 400 °C. Numbered peaks are identified in Table 5.2.....	<b>73</b>
<b>Figure 5.4</b>	Mass spectrum for peak 14 at retention times of a)12.52 min, 12.84 min and, peak 16 at a retention time of b) 13.59 min, for reaction of indene for 60 min.....	<b>76</b>
<b>Figure 5.5</b>	Results from gas chromatography obtained for benzofuran between the retention times of 1.5 to 20 minutes for a 60 min reaction at 2 MPa and 400 °C. Numbered peaks are identified in Table 5.3.....	<b>77</b>
<b>Figure 5.6</b>	Mass spectrum for peaks a) 9, b) 11 and c) 12, from reaction of benzofuran for 60 min.....	<b>81</b>

<b>Figure 5.7</b> Boiling curve acquired using SIMDIS for the product of indene obtained after reacting for 60 min in a batch reactor.....	<b>83</b>
<b>Figure 5.8</b> Boiling curve acquired using SIMDIS for the product of indole obtained after reacting for 60 min in a batch reactor.....	<b>84</b>
<b>Figure 5.9</b> Boiling curve acquired using SIMDIS for the product of benzofuran obtained after reacting for 60 min in a batch reactor.....	<b>85</b>
<b>Figure 5.10</b> First derivative electron spin resonance curve obtained using ESR for indene for reactions at 30 and 60 min.....	<b>86</b>
<b>Figure 5.11</b> First derivative electron spin resonance curve obtained using ESR for benzofuran for reactions at 30 and 60 min.....	<b>87</b>
<b>Figure 5.12</b> FTIR results for samples obtained from benzofuran under thermal cracking conditions with different reaction times of 60 and 30 min.....	<b>88</b>
<b>Figure 5.13</b> Results from gas chromatography obtained for the <i>n</i> -pentane soluble fractions of indane and indene between the retention times of 1.5 to 20 minutes for a 60 min reaction at 2MPa and 400 °C.....	<b>89</b>
<b>Figure 5.14</b> Mass spectrum for peaks 17-19 from reaction of indene and indane for 60 min.....	<b>90</b>
<b>Figure 5.15</b> Asphaltene content for a reaction with indane and indene in equal ratios performed at thermal cracking conditions for a reaction time of 60 min.....	<b>91</b>
<b>Figure 5.16</b> Boiling curve acquired using SIMDIS for the product of indene and indane reacted together for 60 min in a batch reactor.....	<b>92</b>
<b>Figure 5.17</b> First derivative electron spin resonance curve obtained using ESR for reaction between indene and indane for reactions at 60 min.....	<b>93</b>

<b>Figure 5.18</b> Reaction mechanism of free radical addition reaction of indene under thermal cracking conditions.....	<b>94</b>
<b>Figure 5.19</b> Reaction mechanism for the ring opening of benzofuran under thermal cracking conditions.....	<b>95</b>
<b>Figure 5.20</b> Reaction mechanism for indanyl formation from indene under thermal cracking Conditions.....	<b>96</b>
<b>Figure 6.1</b> SEM results for nickel catalyst impregnated on a $\gamma$ -Al <sub>2</sub> O <sub>3</sub> support at magnifications of 20 K and 50 K.....	<b>105</b>
<b>Figure 6.2</b> Process flow diagram of plug flow reactor used for hydrogenation.....	<b>109</b>
<b>Figure 6.3</b> Images of lab scale reactor which was designed, constructed and commissioned as part of this project.....	<b>110</b>
<b>Figure 6.4</b> GC-MS result for the reaction of indene in the flow reactor.....	<b>115</b>
<b>Figure 6.5</b> GC-MS result for the reaction of indole in the flow reactor.....	<b>117</b>
<b>Figure 6.6</b> GC-MS result for the reaction of benzofuran in the flow reactor.....	<b>120</b>
<b>Figure 6.7</b> Mass spectrums obtained for retention times of a) 2.75 min and b) 4.89 min, respectively, during the hydrogenation reaction of benzofuran in a plug flow reactor.....	<b>122</b>
<b>Figure 6.8</b> GC-MS result for the reaction of thianaphthene in the flow reactor.....	<b>123</b>
<b>Figure 6.9</b> Mass spectrums obtained for retention times of a) 2.47 min and b) 2.76 min, respectively, during the hydrogenation reaction of thianaphthene in a plug flow reactor.....	<b>126</b>
<b>Figure 6.10</b> Hydrogenation reactions for binuclear aromatic compounds with one 5-membered ring.....	<b>132</b>

**Figure 6.11** Possible reaction sequence for the ring opening reaction of benzofuran and thianaphthene.....133

### LIST OF TABLES

<b>Table 3.1</b>	Materials employed in this study.....		<b>18</b>
<b>Table 3.2</b>	Products from reactions of indene with acids.....		<b>28</b>
<b>Table 3.3</b>	Products from reactions of benzofuran with acids.....		<b>40</b>
<b>Table 4.1</b>	Materials employed in this.....		<b>51</b>
<b>Table 4.2</b>	Methods built in the DSC corresponding to each of the model compounds selected for the study.....		<b>55</b>
<b>Table 4.3</b>	Products of reactions of thianaphthene with NaH.....		<b>59</b>
<b>Table 5.1</b>	Materials employed in this study.....		<b>67</b>
<b>Table 5.2</b>	Compound list from the GC-MS results for a 60 min reaction of indene at 2 MPa and 400 °C.....		<b>74</b>
<b>Table 5.3</b>	Compound list from the GC-MS results for a 60 min reaction of benzofuran at 2 MPa and 400 °C.....		<b>78</b>

<b>Table 5.4</b> Temperatures for heaviest boiling fractions for the model compounds obtained using the SIMDIS at reaction times of 30 and 60 min.....	<b>82</b>
<b>Table 5.5</b> Compound list from the GC-MS results for a 60 min reaction between indene and indane at 2 MPa and 400 °C.....	<b>89</b>
<b>Table 6.1</b> Materials employed in this study.....	<b>102</b>
<b>Table 6.2</b> Operating conditions for the flow reactor for each of the model compounds.....	<b>112</b>
<b>Table 6.3</b> Response factors for the selected model compounds acquired from the GC-FID.....	<b>113</b>
<b>Table 6.4</b> Products from hydrogenation reaction of indene in the presence of nickel catalyst...	<b>116</b>
<b>Table 6.5</b> Products from hydrogenation reaction of indole in the presence of nickel catalyst....	<b>118</b>
<b>Table 6.6</b> Products from hydrogenation reaction of benzofuran in the presence of nickel catalyst.....	<b>120</b>
<b>Table 6.7</b> Products from hydrogenation reaction of thianaphthene in the presence of nickel catalyst.....	<b>124</b>
<b>Table 6.8</b> GC-FID results obtained from product samples of experimental runs with indene compared to theoretical feed concentration.....	<b>127</b>
<b>Table 6.9</b> GC-FID results obtained from product samples of experimental runs with indole compared to theoretical feed concentration.....	<b>129</b>
<b>Table 6.10</b> GC-FID results obtained from product samples of experimental runs with benzofuran compared to theoretical feed concentration.....	<b>129</b>

**Table 6.11** GC-FID results obtained from product samples of experimental runs with thianaphthene compared to theoretical feed concentration.....**130**

**Table 6.12** CHNS elemental analysis of the fresh catalyst and the spent catalyst.....**131**

## CHAPTER 1: INTRODUCTION

### 1.1 Background

The main objective of partial upgrading in oilsands is to produce an oil with a lower viscosity by using minimal amount of diluent, thereby increasing the capacity of the pipelines.<sup>1</sup> Any upgrading technology involves complex feed and product mixtures, and multiple reactions that include cracking, hydrogenation, dehydrogenation, asphaltene formation, and removal of sulphur and nitrogen. They are conversion based processes and are focused on improving density and elemental composition of the products.<sup>2</sup> Partial upgrading uses a subset of these technologies.

Cracking is an important partial upgrading process and it is the primary conversion unit of the Nexen BituMax™ field upgrading technology (Figure 1.1). Thermal cracking takes place by a free radical process.

Free radical addition reactions in combination with hydrogen disproportionation can occur at temperatures lower than 350 °C. Since bitumen is inherently rich in free radicals,<sup>3</sup> it was realized that these reactions were taking place during in situ recovery, process heating and distillation operations. Free radical addition reactions are undesirable, because they potentially reduce conversion. It was of interest to investigate the possible compound classes that are to blame for addition reactions undermining thermal conversion.

A research lead on possible compound classes that could result in addition reactions under free radical reaction conditions was found in a different type of study. On exposure of bitumen to air under autoxidative conditions, which also proceeds by free radical reaction, it was found that low temperature oxidation had adverse effects on the viscosity and hardening of bitumen. An increase in density meant that heavier compounds were formed due to addition reactions. Addition reactions are an important class of side-reactions that can be initiated by oxidation contributing to bitumen hardening.<sup>4</sup> Although these reactions were caused by oxidation, free radical addition does not require oxygen to proceed. The compound classes that were mainly responsible for the hardening in bitumen, were compounds with a 5-membered ring attached to an aromatic ring.<sup>4</sup>

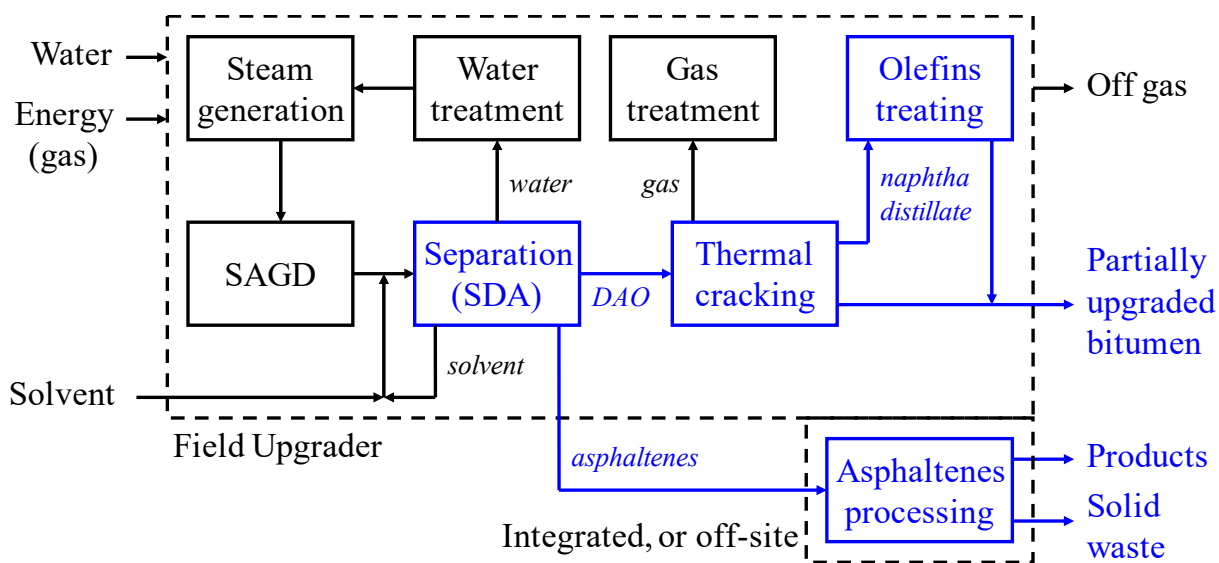


**Figure 1.1** Flow Diagram for the partial upgrading process, highlighting the presence of naphtheno-aromatic compounds

Bitumen is a complex feed. Aromatics such as alkylaromatics, naphtheno-aromatics and alkyl naphthenes are present in large quantities in bitumen. Bitumen constitutes of higher degree of heteroatoms which are rich in nitrogen, oxygen and sulfur containing compounds. Heavy oils are known to contain a H/C ratio between 1.4-1.6. A H/C ratio of 1.5 is indicative of presence of a higher concentration of naphtheno-aromatic compounds.<sup>5</sup> From the study performed by Siddiquee<sup>6</sup>, certain compounds were found to be highly inclined to forming free radicals. The order of propensity of these compounds to undergo free radical addition reactions, listed in the decreasing order, was: indene > indole > benzofuran >> thianaphthene.<sup>6</sup>

From figure 1.1, the compounds of interest were not only present in thermal cracking unit of a partial upgrader, but they are formed during the solvent deasphalting of bitumen, in both layers i.e. asphaltenes and the DAO. The compounds present in the form of substrates of a bigger molecule, move up in the chain to the olefin treating segment of the process.

The compounds in this list can all be classified as bicyclic, aromatic, and containing one 5-membered ring. Although these specific compounds would not be found in bitumen, larger molecules that contain such substructures could be present in bitumen. For ease of study binuclear aromatic compounds with one 5-membered ring were selected for study, exploring the main reaction environments that could be considered for bitumen processing: thermal conversion, acid conversion, base conversion and hydroprocessing conversion.

## 1.2 Objective

The objective of the work was to develop a better fundamental understanding of addition reactions in binuclear aromatic compounds with one 5-membered ring when exposed to different reaction environments.

## 1.3 Scope of work

The key focus of reaction environments studied, revolved around the removal and addition of hydrogen in different ways to the 5-membered ring, since this was postulated to be responsible for initiation of addition reactions. The compounds selected for this study were indane, indene, indole, thianaphthene, and benzofuran. The chapter layout is described below:

Chapter 2: Literature Review

Chapter 3: Reactions of aromatic compounds containing 5-membered rings with Acids

Chapter 4: Reactions of aromatic compounds containing 5-membered rings with Bases

Chapter 5: Free radical addition reactions of aromatic compounds containing 5-membered rings under Thermal conversion conditions

Chapter 6: Hydrogenation of aromatic compounds containing 5-membered rings over a supported metal hydrogenation catalyst in a flow reactor in the presence of H<sub>2</sub> gas

Chapter 7: Conclusions

## 1.4 References

- (1) Zou, C. Heavy Oil and Bitumen. *Unconv. Pet. Geol.* **2013**, 307–335
- (2) Gray, M. R. *Upgrading Oilsands Bitumen and Heavy Oil*, 1st ed.; The University of Alberta Press: Edmonton, 2015.
- (3) Niizuma, S.; Steele, C. T.; Gunning, H. E.; Strausz, O. P. Electron spin resonance study of free radicals in Athabasca asphaltene. **1977**, *56*, 249–256.
- (4) Siddiquee, M. N.; De Klerk, A. Hydrocarbon addition reactions during low-temperature

- autoxidation of oilsands bitumen. *Energy and Fuels* **2014**, 28 (11), 6848–6859.
- (5) Strausz, O. P.; Lown, E. M. *The chemistry of Alberta oil sands, bitumens and heavy oils*; Alberta Energy Research Institute: Calgary, AB, 2003.
- (6) Siddiquee, M. N.; De Klerk, A. Heterocyclic addition reactions during low temperature autoxidation. *Energy and Fuels* **2015**, 29 (7), 4236–4244.

## CHAPTER 2 : LITERATURE REVIEW

### 2.1 Introduction

This literature review is focused on understanding how the selected binuclear aromatic with 5-membered rings react under different processing conditions. The conditions revolve around the four different transformations relevant to industry:

- a) Acid catalysis
- b) Basic catalysis
- c) Free radical chemistry (thermal conversion)
- d) Metal catalysis

The review will investigate into how indane, indene, indole, benzofuran and thianaphthene, have been known to react in the presence of the above reaction environments and what could potentially occur.

### 2.2 Acid catalysis

Heterocyclic 5-membered rings present in the bicyclic aromatic compounds are susceptible to protonation. They polymerize when treated with strong acids, leading to chain growth catalyzed by acids. The degree of polymerization, i.e. multiple addition reactions, is dependent on the strength of the acid and the structure of the compounds.<sup>1</sup> Since polymerization was an expected outcome of the reactions of the model compounds with acids, the focus of the literature review was on possible polymerizations of the compounds in the presence of a proton.

In one study<sup>2</sup>, the reaction of indene with  $\text{H}_3\text{PO}_4$  and  $\text{H}_2\text{SO}_4$  was investigated. The study was focused on understanding the monomer and in turn isomerized dimer formation of indene. The yield and distribution of dimers in the product, on reactions with acids, was higher in comparison to boron trifluoride, a strong Lewis acid. Sulfuric acid produced lower quantities of oligomer and higher quantities (10 times more) of dimers. Phosphoric acid led to similar results but required a longer reaction time of 24 h compared to 8 h in the case of sulfuric acid.



**Figure 2.1** Indene (left) and the expected protonation product of indene (right)

In the presence of an acid, indene forms an indan-1-ylum ion (figure 2.1) which in the presence of another indene molecule reacts to form a dimer of 2-(2',3'-dihydro-1'H-inden-1'-yl)-1H-indene. Different isomers of the same compound can form based on the delocalization of the positive charge in the dimer.<sup>2,3</sup>

Ability of benzofuran, indene and 1,2-dihydronaphthalene to polymerize were compared in a study performed by Mizote and Tanaka.<sup>4</sup> The study involved comparison of parameters like ring strain, ring stabilization and steric hindrance in the transition state during the polymerization of the three compounds. These parameters were also compared with those of styrene. It is known that benzofuran, similar to indene, can be easily polymerized by cationic catalysts.<sup>4</sup> Unlike aliphatic cyclic olefins, benzofuran and indene do not produce crystalline polymers. The compounds were heated at 30 °C, in the presence of IBr solution in glacial acetic acid as a catalyst. The degree of polymerization is in the decreasing order: indene > benzofuran > styrene >> 1,2- dihydronaphthalene.<sup>4</sup>

Indole is an aromatic compound with a high activity towards even weak electrophiles. Although indole is classified as a neutral nitrogen-containing compound, indole is reactive to electrophilic reagents, like acids, and undergoes protonation in the presence of strong acids. These electrophiles can initiate polymerization or dimerization, resulting in large amounts of byproducts.<sup>5,6</sup> Indoles are rendered susceptible to attack by electrophiles due to high electron density and low localization energy for substitution of electrophiles. Indole and its substituents are known to polymerize on reaction even with moderately strong acids, for example nitrous and phosphoric acids. In the presence of a strong acid, however, it completely protonates, largely in the C<sub>3</sub> position to form an iminium ion. On addition of high concentrations of sulfuric and perchloric acids, instantaneous precipitation of the acid salts of indole are formed.<sup>5</sup>

Not much literature was available on the reactions of acids with thianaphthene. Literature was found on reactions of thianaphthene with sulfates of metallic ions. The reactions with the aqueous metals species were performed at 240 °C, to create steam stimulation conditions in heavy-oil reservoir for a period of 28 days. The proton donation was due to the dissociation of the water molecule from the aqueous metal ions. The aqueous metal species produced an acidic solution by solvolysis mechanism. Products 6-8 in figure 2.2 were the major compounds produced from the reaction. However, metal ions appeared to have more drastic product formation as compared to HCl and H<sub>2</sub>SO<sub>4</sub>, which resulted in little reaction.<sup>7</sup>

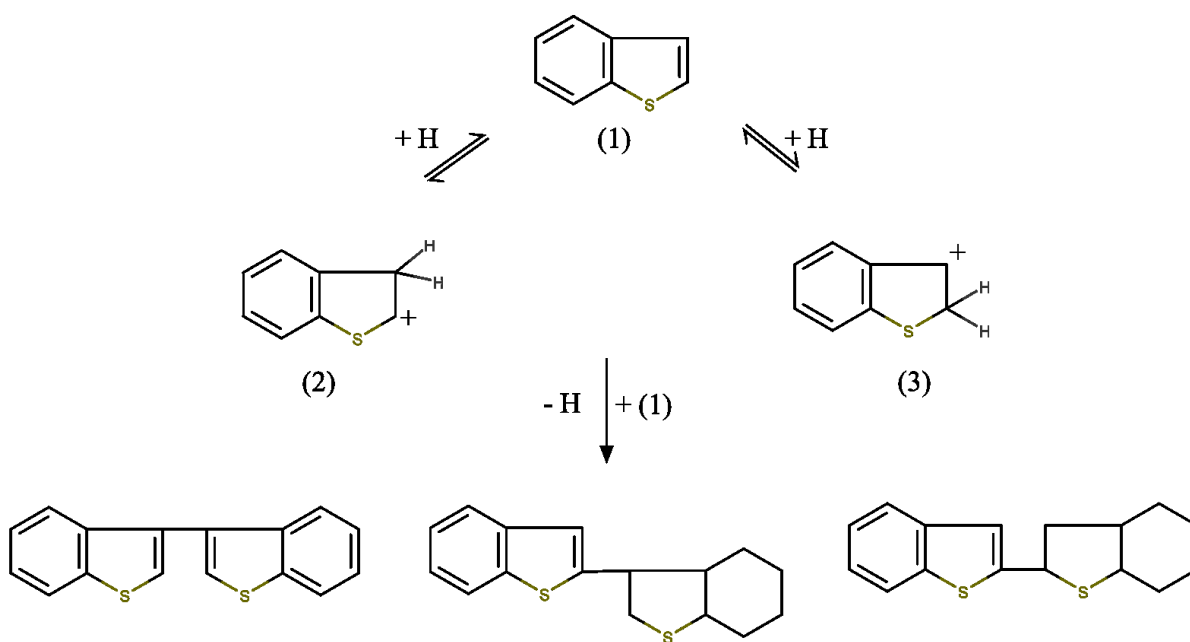


**Figure 2.2** Reaction mechanism for formation of major products on reaction of thianaphthene with aqueous metal sulfates<sup>7</sup>

Indane, is not susceptible to acid catalyzed conversion, expect under very forcing conditions, where the Haag-Dessau mechanism of protolysis is active.<sup>8</sup>

## 2.3 Base catalysis

Base-catalyzed reactions for hydrocarbons are dependent on the ease of removal of a proton or the acidity of the hydrocarbons. Since hydrocarbons are naturally less acidic in nature, a strong base as catalyst is needed for a reaction. An effective example of a strong alkali metal used as a base would be sodium, potassium, and cesium.<sup>9</sup>

Alkali metals could be used for desulfurization of multinuclear aromatics. Base catalyst like sodium hydride is used as a strong reducing agent. It facilitates conversion by having sodium as a strong electron donor, or in the case of sodium hydride, the hydride ion as a strong electron donor. The aromatic acts as the ion acceptor during the reaction. During the hydrogen exchange reactions, the aromatic is susceptible to partial hydrogenation.

Sodium can be used to desulfurize thiophenes. In one study, the conversion was studied under nitrogen atmosphere using different solvents to compare conversion based on hydrogen availability in the matrix. The solvents selected for the study were decalin (hydrogen rich) and 1-methylnaphthalene (hydrogen poor). The hydrogen donor capacity did favor desulfurization by hydrogenolysis (figure 2.3). However, desulfurization through hydrogenolysis is a reversible reaction. The desulfurization in the presence of hydrogen was favored in the presence of sodium hydride, but it led to precipitation without removal of sulfur from the product.<sup>10</sup>

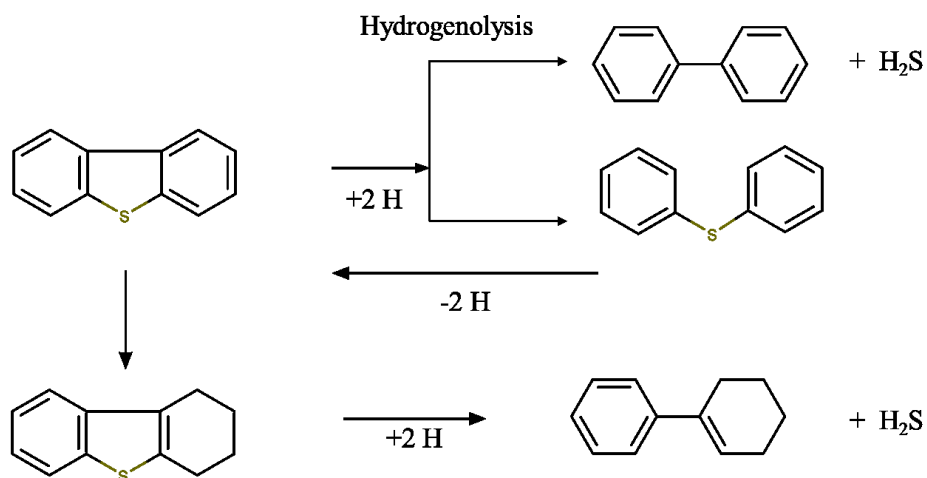


**Figure 2.3** Reaction pathways during conversion of dibenzothiophene in decalin with sodium<sup>10</sup>

Looking further into the possible hydrogenation of unsaturated compounds in the presence of base-catalyzed reactions, the hydrogenation is known to take place for alkenes between temperatures of 170-250 °C. Hydrogenation at low temperatures takes place from alkadienes and cycloalkadienes. However, polynuclear aromatic hydrocarbons undergo hydrogenation at 250 °C. The hydrogenation reactions take place through addition of alkali metals from the hydrides to the C-C bonds. This is followed by hydrogenolysis with molecular hydrogen.<sup>9</sup>

## 2.4 Free radical chemistry

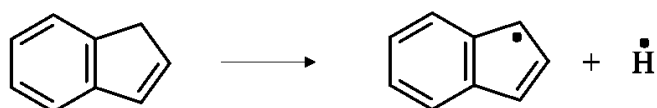
Free radicals can be formed by three different processes: irradiation, thermal homolysis and oxidation-reduction reactions. The focus of this literature review will be thermal homolysis. It is defined as a bond dissociation of a molecule creating two radicals, because of heat addition. The propagation reaction, that is of interest in this literature review, is by hydrogen abstraction. This occurs as a principle or a side reaction during almost all radical reactions.<sup>11</sup>

A study was performed by Laskin and Lifshitz, aimed at better understanding of the combustion process of polyaromatic hydrocarbons, in specific, indene.<sup>12</sup> The work investigated on the product distribution, pyrolysis mechanism and kinetic modelling. The pyrolysis was studied behind reflected shock waves in a single-pulse shock tube. The temperatures attained for the study were in the range of 877-1627 °C. The products formed at 1147 °C were lighter compounds starting from the very base of methane, ethane, prop-1,2-diene, etc., onto heavier molecules like isomers of naphthalene. The thermal decomposition of the indene is initiated by the formation of a hydrogen radical following the reaction shown in figure 2.4a. The indenyl ion is formed by breaking of the  $sp^3$  C-H bond in the heterocycle. Depending on the location of breakage and hydrogen migration *ortho*-ethynyl benzyl and  $\alpha$ -ethynyl benzyl radicals can be formed.

Another radical formation could be that of indanyl radical, by addition of a free radical to the indene structure at the  $\pi$  bond of the 5 membered ring (figure 2.4b). The two radicals, indenyl and indanyl, are the competing fragments as the source of product formation. The fragments undergo recombination and hydrogen disproportionation to produce much heavier compounds.<sup>12</sup>

There is also the possibility of molecule-induced hydrogen transfer leading to free radical formation.<sup>13</sup> In this type of reaction two neutral molecules (indene) would participate in a bimolecular interaction leading to hydrogen disproportionation to produce two free radicals as products.

a)



b)

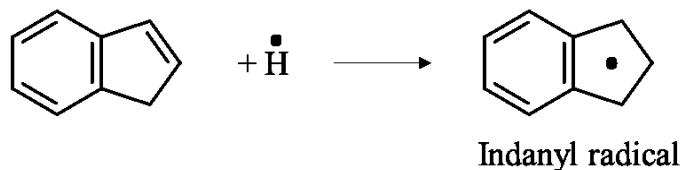


**Figure 2.4** Possible initiation steps in the thermal decomposition of indene<sup>12</sup>

Pyrolysis of indene was performed at 700 °C, by Badger and Kimber<sup>14</sup>, by passing indene vapour through a silica tube filled with porcelain chips, using nitrogen gas. Similar to the study above, gases containing methane and ethane were detected. Several heavier compounds were identified in the study, but chrysene was the major product with a 31.7 wt% composition in the product. Based on bond dissociation, figure 2.5 shows the three possible primary radicals which help in explaining all the suitable reactions.

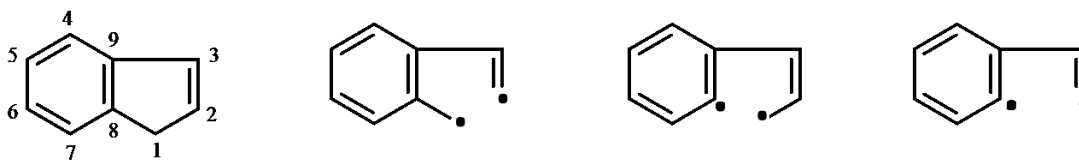


**Figure 2.5** Ring fission of indene at 700 °C giving three possible primary radicals<sup>14</sup>

Based on the bond dissociation energies, it is harder to break the bond at positions 2,3 and 3,9 in comparison to bonds at positions of 1,2 and 1,8. Therefore, dimerization of the first suggested primary radical is expected to bind with in duplicates and give chrysene or 1,2-benzanthracene.<sup>14</sup>

Laskin and Lifshitz<sup>15</sup> also studied the pyrolysis of pyrrolic compounds resulting from reflected shocks in a pressurized single-pulse shock tube over the temperature range of 777-1377 °C. The most reactive site on the indole ring is at the C(3) position. In a pyrrole ring, the C(2) and C(5) positions were seen as the most reactive sites. The presence of a benzene ring impacted the location of the  $sp^3$  C-H bond location. Isomerization reactions were identified as the main reactions as a result of the shock heating. The three primary products leading to isomerization products were benzyl cyanide, *o*- and *m*-tolunitriles. At a lower temperature of 1127 °C, the decomposition products outweighed the isomerization products. Ring opening products like C<sub>2</sub>H<sub>2</sub>, HCN, HC≡C-CN, C<sub>4</sub>H<sub>2</sub>, C<sub>6</sub>H<sub>5</sub>-CN, CH<sub>3</sub>-CN, C<sub>6</sub>H<sub>6</sub> were majority of the products formed. At higher temperatures, the three primary products form fragments to produce heavier compounds.<sup>15</sup>

Literature was scarce on the pyrolysis of benzofuran and thianaphthene but pyrolysis of furan and thiophene was a topic of abundant available research. It is important to note, however, the aromatic ring influences the reactivity of the compounds. The reactive positions in heterocyclic rings attached to a benzene ring are different from that of the 5-membered ring on its own.

Pyrolysis on furan behind reflected shocks in a pressurized single-pulse shock tubes over the temperature range of 827-1427 °C was performed by Organ and Mackle.<sup>16</sup> Carbon monoxide was the major product formed during the pyrolysis at all temperatures. The primary reactions that acted as the initiation steps are shown in figure 2.6. The initiation was postulated to occur by the unimolecular C-O ring scission to form a biradical, which further decomposed.

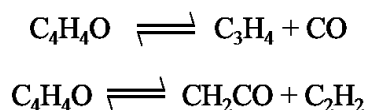


**Figure 2.6** Primary reaction in furan pyrolysis at >827 °C<sup>16,17</sup>

The problems realized in the second reaction suggested, was that through experimental work, acetylene and ketene were not found in equal concentrations. There was an excess production of acetylene suggesting that there was secondary reaction which produced acetylene or a secondary reaction that caused decomposition of ketene.<sup>16</sup>

In a continuous flow pyrolysis of thianaphthene at a temperature range of 500-1100 °C under atmospheric pressure, polycyclic aromatic hydrocarbons and sulfur-containing polycyclic hetarenes were observed. The reactions were temperature dependent. At temperatures lower than 800 °C, oligomers were main products due to radical recombination reactions. Above 800 °C, benzo[b]naphtho[2,1-d]thiophene and [1]benzothieno[2,3-b][1]benzothiophene were obtained as products. From figure 2.7, the first step is initiated at a temperature of 600 °C and increases above 700 °C.<sup>18</sup>

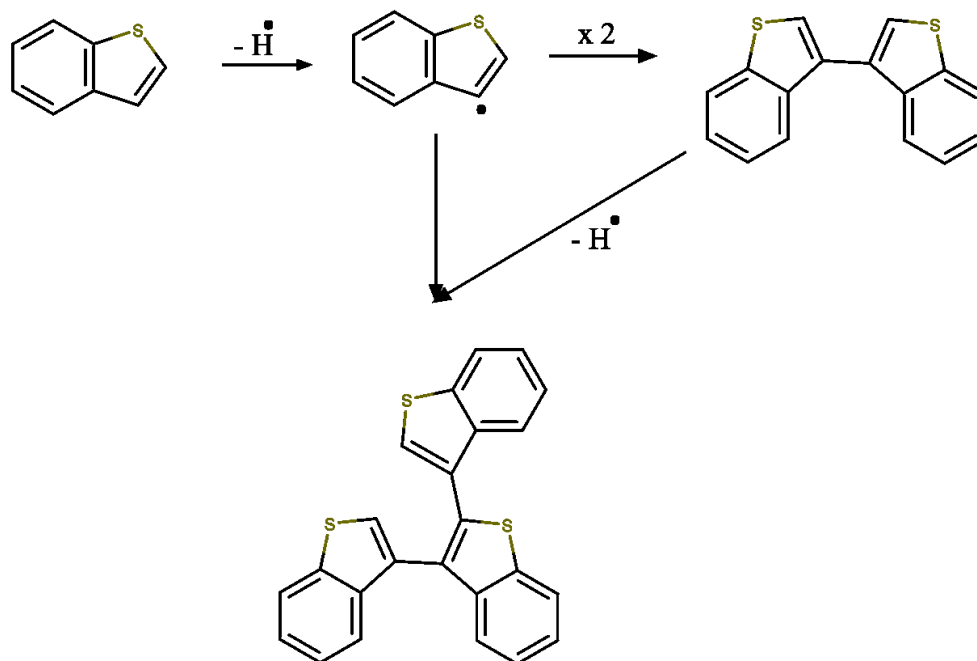


**Figure 2.7** Reaction mechanism for thianaphthene in continuous flow pyrolysis at temperatures between 750-850 °C<sup>18</sup>

Indane contains a saturated 5-membered ring, with two benzylic  $CH_2$  groups. It is likely that thermal cracking would proceed by thermal homolysis to producing a ring-opened product with a  $C_1$  and  $C_2$  alkyl group attached to the benzene ring. Depending on conditions, it is also possible

to facilitate cleavage at different positions. For example, in the presence of H<sub>2</sub>, it was found that some cleavage between the benzene and the benzylic carbon was possible to produce a C<sub>3</sub> alkyl group attached to the benzene ring.<sup>19</sup>

## 2.5 Metal catalysis

Catalysts used for hydrotreating are required to be highly active, have good selectivity to targeted hydrogenated products and should be suitable for use in large-scale reactors. Nickel is known to be used as a metal in hydrogenation catalysts in a wide variety of industries, because it is one of the least expensive of the transition metals and has high hydrogenation activity.<sup>20</sup> Since Ni was employed in the present investigation, a brief overview of Ni catalyzed hydrogenation of the target compounds is provided.

Indene can be hydrogenated to form indane and hexahydroindane. For example, hydrogenation was performed in a rotating autoclave in the presence of a nickel-kieselguhr catalyst. At an initial hydrogen pressure of 10 MPa and a temperature of 30 °C indene is hydrogenated to form indane. Using the same apparatus at a higher temperature of 160 °C, and pressure of 10 MPa, indene could be hydrogenated to hexahydroindane.<sup>21</sup>

Another study hydrogenated indene in the presence of 10 % nickel catalyst, pressurized at 7 MPa at a temperature of 100 °C in a batch reactor. Indene was hydrogenated to indane and the major side-product in this reaction was of hexahydroindane.<sup>22</sup>

Indole reduces to indoline on catalytic hydrogenation. While hydrogenating indole to indoline is the most straightforward method of forming indoline, it comes with additional challenges:<sup>23</sup>

- a) Indole has a high resonance stability and thus requires higher temperature and pressure conditions to react;
- b) Difficulty in achieving high selectivity leading to by-product formation because of over hydrogenation and possible polymerization reactions.
- c) Catalyst deactivation from indoline.

Initial reports stated that hydrogenation on unprotected indole requires severe conditions, i.e. a temperature of 227 °C and pressure of 15 MPa, under the influence of hydrogen gas. The reaction achieve a conversion of 82 % using nickel on silica-alumina catalyst.<sup>24</sup>

To perform the same reaction at relatively less severe conditions, a more expensive catalyst, Pt/C, was employed. The reaction was performed in acidic solution. The selectivity of this reactions was 100 % on performing the reaction at ambient temperature with H<sub>2</sub> pressure of 3 MPa.<sup>6</sup>

In a study performed by Entel and Ruof,<sup>25</sup> benzofuran was selected as an oxygen containing compound to investigate the hydrogen absorption in bituminous coals. Compared to indene and furan, benzofuran was found to have a slower hydrogen absorption rate. In the presence of Raney nickel, benzofuran reduces to 2,3-dihydrobenzofuran at a temperature of 120 °C and a pressure of 13.8 MPa. The reaction was conducted over a time of 18 h and with a ratio of 1.88 moles of H<sub>2</sub> per mole of benzofuran. Under over hydrogenation conditions, after the breaking of the double bond in the furan ring, the benzene ring saturates and the furan ring ruptures hydrogenolytically to produce phenols and alcohols.<sup>25-27</sup>

Direct conversion to 2,3-dihydrobenzothiophene by reduction of thianaphthene was found in the presence of a sulfided catalyst of palladium on  $\gamma$ -alumina. A conversion of 50 % with a high selectivity of 91 % is achievable under certain reaction conditions. A study was based on understanding the reaction conditions on achieving that conversion rate. To do so, the experiment was carried out in a stainless-steel shaken reactor, pressurized with hydrogen. Pressure of hydrogen was kept constant at 5 MPa while changing temperature, contact time and the concentration of thianaphthene during the reaction. The reaction product constituted of 2,3-dihydrobenzothiophene and ethylbenzene. Change in concentration had no effect on the conversion. On increasing the contact time from 0.25-3.0 h, there was an increase in the yield of 2,3-dihydrobenzothiophene while keeping temperature, thianaphthene conversion and ethylbenzene yield constant. This was found to be a linear relationship. The same trend was also observed on increasing temperature. Increase in temperature from 160-200 °C led to an increase in desirable product yield. However, the selectivity of 2,3-dihydrobenzothiophene is dependent on the degree of conversion of thianaphthene which in any case should be below 60 %.<sup>28</sup>

An important difference between the use of Ni as hydrogenation catalyst for all of the compounds except thianaphthene, is that the Ni can be employed as reduced metal. When hydrogenating thianaphthene, release of H<sub>2</sub>S would lead to sulfidation of the Ni and the Ni is then employed as a sulfided hydrogenation catalyst. A detailed discussion of the differences between reduced and sulfided Ni catalysts can be found in the work by Pines.<sup>29</sup>

## 2.6 References

- (1) Solomons, T. W. G.; Fryhle, C. *Organic Chemistry*, 10th ed.; John Wiley & Sons, Inc.: Hoboken, N.J, 2011.
- (2) Jovanović, J.; Spitteller, M.; Elling, W. Indene Dimerization Products. *J. Serbian Chem. Soc.* **2002**, *67* (6), 393–406.
- (3) Jovanović, J.; Spitteller, M.; Spitteller, P. NMR Analysis of 2-(2', 3'-Dihydro-1'H-Inden-1'-Yl)-1H-Indene. *J. Serbian Chem. Soc.* **2001**, *66* (11–12), 753–763.
- (4) Mizote, A.; Tanaka, T.; Higashimura, T.; Okamura, S. Cationic Polymerization of Cyclic Olefins. *J. Polym. Sci. Part A-1 Polym. Chem.* **1966**, *4* (4), 869–879.
- (5) J. Houlihan, W. *Indoles*; Wiley-Interscience: New York, 1972.
- (6) Kulkarni, A.; Zhou, W.; Török, B. Heterogeneous Catalytic Hydrogenation of Unprotected Indoles in Water: A Green Solution to a Long-Standing Challenge. *Org. Lett.* **2011**, *13* (19), 5124–5127.
- (7) Clark, P. D.; Lesage, K. L.; Tsang, G. T.; Hyne, J. B.; Tn, C. Reactions of Benzo [B] Thiophene with Aqueous Metal Species: Their Influence on the Production and Processing of Heavy Oils. *Energy Fuels* **1988**, *2* (4), 578–581.
- (8) Kotrel, S.; Knözinger, H.; Gates, B. C. The Haag-Dessau Mechanism of Protolytic Cracking of Alkanes. *Microporous Mesoporous Mater.* **2000**, *35–36*, 11–20.
- (9) Pines, H.; Stalick, W. M. *Base-Catalyzed Reactions of Hydrocarbons and Related Compounds*; Academic Press: New York, 1977.
- (10) Styles, Y.; De Klerk, A. Sodium Conversion of Oilsands Bitumen-Derived Asphaltenes. *Energy Fuels* **2016**, *30* (7), 5214–5222.
- (11) A. Pryor, W. *Free Radicals*; McGraw-Hill: New York, 1966.
- (12) Lifshitz, A.; Suslensky, A.; Tamburu, C. Thermal Decomposition of 4-Methylpyrimidine. Experimental Results and Kinetic Modeling. *J. Phys. Chem. A* **2001**, *105* (14), 3542–

- 3554.
- (13) Rüchardt, C.; Gerst, M.; Ebenhoch, J. Uncatalyzed Transfer Hydrogenation and Transfer Hydrogenolysis: Two Novel Types of Hydrogen-Transfer Reactions. *Angew. Chemie Int. Ed. English* **1997**, *36* (1314), 1406–1430.
  - (14) Badger, B. G. M.; Kimber, R. W. L. The Formation of Aromatic Hydrocarbons at High Temperatures. Part V1. The Pyrolysis of Tetralin. *J. Chem. Soc.* **1960**, 266–270.
  - (15) Laskin, A.; Lifshitz, A. Isomerization and Decomposition of Indole. Experimental Results and Kinetic Modeling. *J. Phys. Chem. A* **1997**, *101* (42), 7787–7801.
  - (16) Organ, P. P.; Mackie, J. C. Kinetics of Pyrolysis of Furan. *J. Chem. Soc. Faraday Trans.* **1991**, *87* (6), 815–823.
  - (17) Urness, K. N.; Guan, Q.; Golan, A.; Daily, J. W.; Nimlos, M. R.; Stanton, J. F.; Ahmed, M.; Ellison, G. B. Pyrolysis of Furan in a Microreactor. *J. Chem. Phys.* **2013**, *139* (12), 124305(1-10).
  - (18) Winkler, J. K.; Karow, W.; Rademacher, P. Gas-Phase Pyrolysis of Heterocyclic Compounds, Part 1 and 2: Flow Pyrolysis and Annulation Reactions of Some Sulfur Heterocycles: Thiophene, Benzo[b]thiophene, and Dibenzothiophene. A Product-Oriented Study. *J. Anal. Appl. Pyrolysis* **2002**, *62* (1), 123–141.
  - (19) Slotboom, H. W.; Penninger, J. Mechanism and Kinetics of the Thermal Hydrocracking of Single Polyaromatic Compounds. *ACS Symp. Ser.* **1975**, *32*, 444–456.
  - (20) Chianelli, R. R. Fundamental Studies of Transition Metal Sulfide Hydrodesulfurization Catalysts. *Catal. Rev.* **1984**, *26* (3–4), 361–393.
  - (21) Ipatieff, B. Y. V. N.; Meisinger, E. E.; Pines, H. Destructive Hydrogenation of Indan and Hexahydroindan. *J. Am. Chem. Soc.* **1949**, *71* (8), 2685–2687.
  - (22) Kutz, W. M.; Nickels, J. E.; McGovern, J. J.; Corson, B. B. Catalytic Alkylation of Indan and Tetralin by Olefins, Alcohols and Diethyl Ether. *J. Am. Chem. Soc.* **1948**, *70* (12), 4026–4031.
  - (23) Deng, D. S.; Han, G. Q.; Zhu, X.; Xu, X.; Gong, Y. T.; Wang, Y. Selective Hydrogenation of Unprotected Indole to Indoline over N-Doped Carbon Supported Palladium Catalyst. *Chinese Chem. Lett.* **2015**, *26* (3), 277–281.
  - (24) Shaw, J. E.; Stapp, P. R. Regiospecific Hydrogenation of Quinolines and Indoles in the Heterocyclic Ring. *J. Heterocycl. Chem.* **1987**, *24* (5), 1477–1483.

- (25) Entel, J.; Ruof, C. H.; Howard, H. C. Reactions of Benzofurans with Hydrogen. *J. Am. Chem. Soc.* **1951**, *73* (9), 4152–4158.
- (26) Karakhanov, É. A.; Drovyannikova, G. V.; Viktorova, E. A. Catalytic Alkylation of Benzofurans. *Chem. Heterocycl. Compd.* **1971**, *7* (8), 953–955.
- (27) Lee, C. L.; Ollis, D. F. Catalytic Hydrodeoxygenation of Benzofuran and O-Ethylphenol. *J. Catal.* **1984**, *87* (2), 325–331.
- (28) Zirka, A. A.; Ryzhova, G. L.; Slizhov, Y. G.; Mashkina, A. V. Catalytic Hydrogenation of Benzothiophene to 2,3-Dihydrobenzothiophene. *React. Kinet. Catal. Lett.* **1983**, *23* (1–2), 7–12.
- (29) Pines, H. Catalytic Versatility of Nickel as a Function of Its Preparation and Modification. *Adv. Catal.* **1987**, *35*, 323–373.

## **CHAPTER 3 : REACTIONS OF AROMATIC COMPOUNDS CONTAINING 5-MEMBERED RINGS WITHS ACIDS**

### **Abstract**

Acids are present in the oilsands upgrading processes, starting from the presence of naphthenic acid in composition of bitumen to use of solid acid catalysts in refining processes. The objective of this chapter was to study the impact of some of the common acids on selected binuclear aromatic compounds with 5-membered rings under mild conditions. Reactions were performed by heating a dilution 2 wt% acid and 10 wt% model compounds in toluene, to 70 and 120 °C. The organic layer of the solution was then analyzed further. On studying the results, it was found that all compounds oligomerized depending on the selection of acids. Compounds like indene, indole and benzofuran further went through physiochemical changes. Indene not only polymerized to form heavier compounds but also showed formation of ring opening structures. Indole and benzofuran produced solids, as byproducts of the reactions.

**Keywords:** Acids, oligomerization.

### 3.1 Introduction

Acids are present in various steps during upgrading and refining of oilsands. To start off, bitumen contains 1-2 % of naphthenic acids which could undergo hydrolysis in the presence of calcium salts to form hydrochloric acid.<sup>1</sup> Like hydrochloric acid, some acids appear as a result of reactions while some other acids are used as catalysts. For example, sulfuric acid is used as a catalyst in alkylation units where excess isobutane is reacted with alkenes to produce alkanes.<sup>1</sup> Similarly, solid catalysts impregnated with phosphoric acid are used in alkylation desulfurization of fluid catalytic cracking of gasoline.<sup>2</sup>

Hydrogen disproportion reactions are considered key intermediate steps in free radical addition reactions; however, hydrogen can also be transferred by Bronsted acids as  $H^+$ . Given the deleterious behavior of binuclear aromatics attached to 5-membered compounds, the aim was to understand the fundamental chemistry during the presence of protons ( $H^+$ ) from the acids. The acids selected for this study were HCl,  $H_2SO_4$ ,  $H_3PO_4$  and Amberlyst® 15.

The objective of this chapter is focused on studying the possible implications that different acids could have on reacting with the alicyclic and heterocyclic compounds attached to aromatic rings at lower temperatures.

### 3.2 Experimental

### 3.2.1 Materials

All the chemicals used in the reactions are listed in table 3.1. The aromatic compounds with a five membered ring were reacted in the presence of acids. The use of a variation of acids was based on different acidic strengths, phases and availability of hydrogen atoms.

Amberlyst® 15 was used as an acid resin. It is strongly acidic macroporous chain of styrene-divinylbenzene, with a sulfonic acid functional group.

Deionized water was used for the water washes during the experimental runs. The deionized water was obtained from a Millipore water purification system with a conductivity of less than 3  $\mu\text{S}/\text{cm}$  at 25 °C.

**Table 3.1** Materials employed in this study

Compound	Formula	CASRN <sup>a</sup>	Mass fraction purity <sup>b</sup>	Supplier
<i>Chemicals</i>				
Indene	C <sub>9</sub> H <sub>8</sub>	95-13-6	0.90	Sigma-Aldrich
Indole	C <sub>8</sub> H <sub>7</sub> N	120-72-9	0.99	Sigma-Aldrich
Benzofuran	C <sub>8</sub> H <sub>6</sub> O	271-89-6	0.99	Sigma-Aldrich
Thianaphthene	C <sub>8</sub> H <sub>6</sub> S	95-15-8	0.95	Sigma-Aldrich
Tetrahydrothiophene	C <sub>4</sub> H <sub>8</sub> S	110-01-0	0.99	Sigma-Aldrich
Hydrochloric acid 1N solution	HCl	7647-01-0	- <sup>c</sup>	Fisher Scientific
Sulfuric acid solution 1M	H <sub>2</sub> SO <sub>4</sub>	7664-93-9	- <sup>c</sup>	Fluka
Phosphoric acid	H <sub>3</sub> PO <sub>4</sub>	7664-38-2	0.98	Sigma-Aldrich
Amberlyst® 15 hydrogen form	-	39389-20-3	- <sup>c</sup>	Sigma-Aldrich
Methanol	CH <sub>3</sub> OH	67-56-1	0.995	Fisher Scientific
Sodium carbonate anhydrous	Na <sub>2</sub> CO <sub>3</sub>	497-19-8	0.995	Fisher Scientific
Sodium hydroxide solution 1M	NaOH	1310-73-2	- <sup>c</sup>	Fisher Scientific
Toluene	C <sub>7</sub> H <sub>8</sub>	108-88-3	0.995	Fisher Scientific
<i>Cylinder gases</i>				
Nitrogen	N <sub>2</sub>	7727-37-9	0.99999 <sup>d</sup>	Praxair

<sup>a</sup> CASRN = Chemical Abstracts Services Registry Number

<sup>b</sup> This is the purity of the material guaranteed by the supplier; material was not further purified

<sup>c</sup> Mass fraction purity not specified

<sup>d</sup> Mole fraction purity

### 3.2.2 Equipment and procedure

Reactions in the presence of acids were performed in 250 mL three-neck round bottom flasks. The solution was prepared using toluene as the solvent with 10 % model compound and 2 % acid. Since the acid was insoluble in the organic layer, the mixture comprised of two liquid phases. The round bottom flask was placed in metal blocks, to ensure uniform distribution of heat over the entire solution. A magnetic stir bar was added to the flask for constant mixing of the solution while heating. The metal block was left on the heating plate connected to the condenser, which was circulating water at a temperature of 3 °C, for 1 h. The reactant was heated at two temperature ranges of 70 °C and 120 °C with magnetic stirrer rotating at 200 rpm, after purging the system with nitrogen gas for 5 min at a flow rate of 200 mL/min. After leaving the reaction on for 1 h, the flask was left to cool for 30 min.

If the acids are considered catalysts, both, homogenous and heterogeneous catalysts were used. Homogenous reactions involved reactions with hydrochloric acid, sulfuric acid and phosphoric acid while the heterogeneous reactions were performed with Amberlyst® 15.

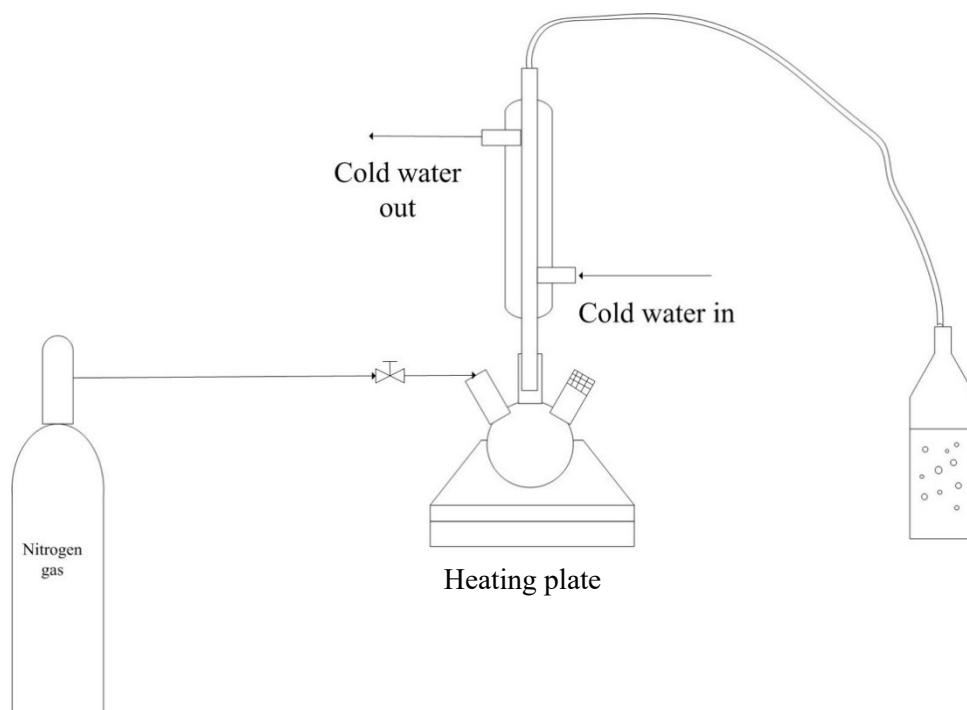


**Figure 3.1** Experimental setup

In the case of homogenous catalysis, after the reaction, the solution was further transferred to a 500 mL separation funnel for liquid-liquid extraction. 10 mL of sodium hydroxide solution was added to neutralize the acid. The product was washed three times using 100 mL of water. Since water is a polar solvent in comparison with the non-polar nature of toluene, water was used to dissolve all the acid from the product, thereby separating it from the organic layer. Sodium carbonate was added after the last wash with water to remove any water molecules present in the organic layer. The product was collected in a vial and weighed on a Mettler Toledo balance XP1203S, to ensure there was not a significant loss of product. The scale had a readability limit of 1 mg with a maximum capacity of 1210 g. It was observed that some products had an accumulation of solids at the bottom of the flask that were insoluble in toluene and water. The solids were dissolved in methanol and collected in a vial to be analyzed. Using the rotovap (Heizbad Hei-VAP from Heidolph), toluene was separated from the product under 7.7 kPa of pressure at 44 °C.

On the other hand, heterogeneous catalysis did not require water washing. The liquid product was transferred to a vial using 0.2 µm membrane filter attached to a syringe to separate the solid catalyst from the organic liquid.

Control experiments were run for each of the model compounds. This was done to have a reference point for comparison with any changes that might arise because of the reactions with acids. For control runs, the reactions were run with a solution of 10 % model compound with toluene, without the presence of any acid. The same set up was used as above and the solution was heated to 120 °C. After the reaction had cooled down, toluene was separated from the mixture using the rotovap and the samples were further analyzed. All experiments were performed once.

### *3.2.3 Analyses*

The gas chromatograph with mass spectrometer (GC-MS) and Zeiss StereoMicroscope were used for analyzing samples in this chapter. The working principle behind these analyses can be found in Section 5.2.3 of Chapter 5.

Thermogravimetric Analysis (TGA) connected to ABB MB 3000 FTIR (TGA-FTIR) was used. Any gases released from the sample in the TGA during the pyrolysis process were carried over to the FTIR through a PIKE heated gas flow cell via a line that was heated and kept at a constant temperature of 200 °C. Amberlyst® 15 was placed in a 70 L alumina crucible and weighed using a Mettler–Toledo dual range analytical balance (Model XS105) with a readability of 10 µg, in the range of 0–41 g and a readability of 100 µg for the remaining range, until 120 g. It was heated, starting at 40 °C to 600 °C in the presence of a constant flow of 100 mL/min of nitrogen gas at increments of 10 °C/min. A spectrum was captured using the FTIR at intervals of 10 °C at a resolution of 8 cm<sup>-1</sup> and an average of 20 scans.

### 3.3 Results

The results are arranged based on the effects of the acids on each model compound. Model compounds reacted differently in the presence of different acids. However, the results from the GC coupled with mass spectroscopy were identical for the two temperature selections of 70 °C and 120 °C for each set of reactions. The nature of the products formed at 70 and 120 °C was similar, but the reaction rate at higher temperature was higher. All reactions were compared with the control samples for the respective model compound. On analyzing the pure compounds with the help of the GC-MS and comparing with the control samples, the results obtained were the same.

#### 3.3.1 *Quantifying water content in Amberlyst® 15*

In some of the results obtained from the GC-MS, there were compounds containing oxygen. However, the reactions were performed under inert atmosphere. There were no other sources of

oxygen present during the reaction. Therefore, to understand whether Amberlyst® 15 could have been a potential source of oxygen present during the reactions, the TGA was used. The TGA-FTIR was able to provide more accurate figures on the amount of water present in the solid resins.

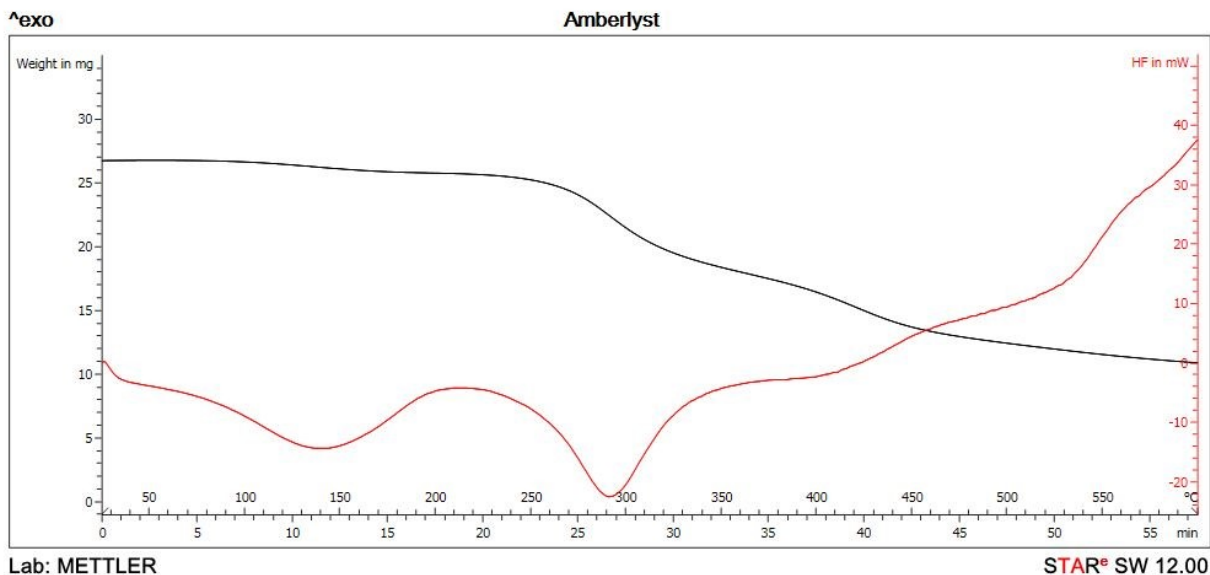


**Figure 3.2** Heat curve obtained using the TGA (red) overlapped with the mass loss (black) of Amberlyst® 15 with respect to temperature under nitrogen. Figure 3.2 shows the TGA curve obtained. There is a considerable mass loss starting around 275 °C, declining at 450 °C. The drop in mass during the degradation of the solid resins has one major stage of mass loss, which can be directly correlated to the decomposition of sulfonic acid groups to release sulfur dioxide (SO<sub>2</sub>) since no other significant changes in peaks were observed at any other wavenumber.

Figure 3.3 shows the highest release of SO<sub>2</sub> and water at a temperature of 300 °C. The expected sulfur dioxide peak at 1360 cm<sup>-1</sup> was distinctly visible amongst all others. The water peak was expected to be observed close to the wavenumber of 1650 cm<sup>-1</sup>.

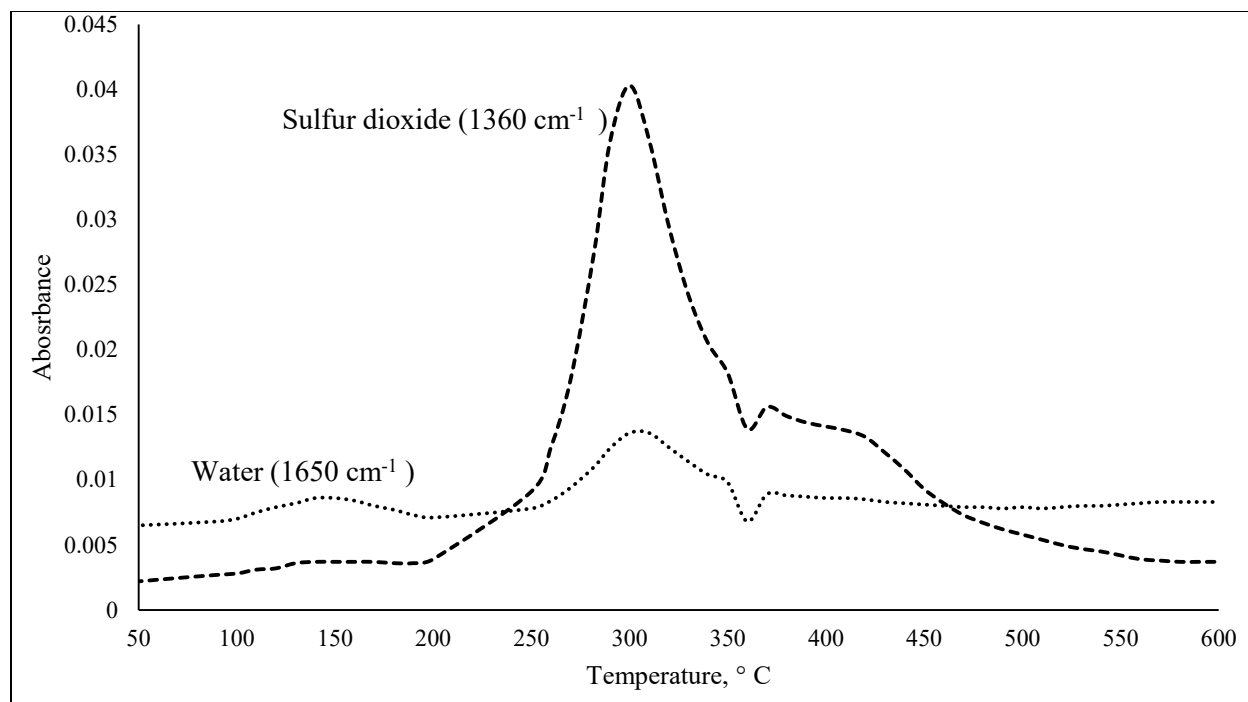


**Figure 3.3** Absorbance of sulfur dioxide and water at 1360 and 1650  $\text{cm}^{-1}$  respectively, during the degradation of Amberlyst® 15 as a function of temperature under nitrogen

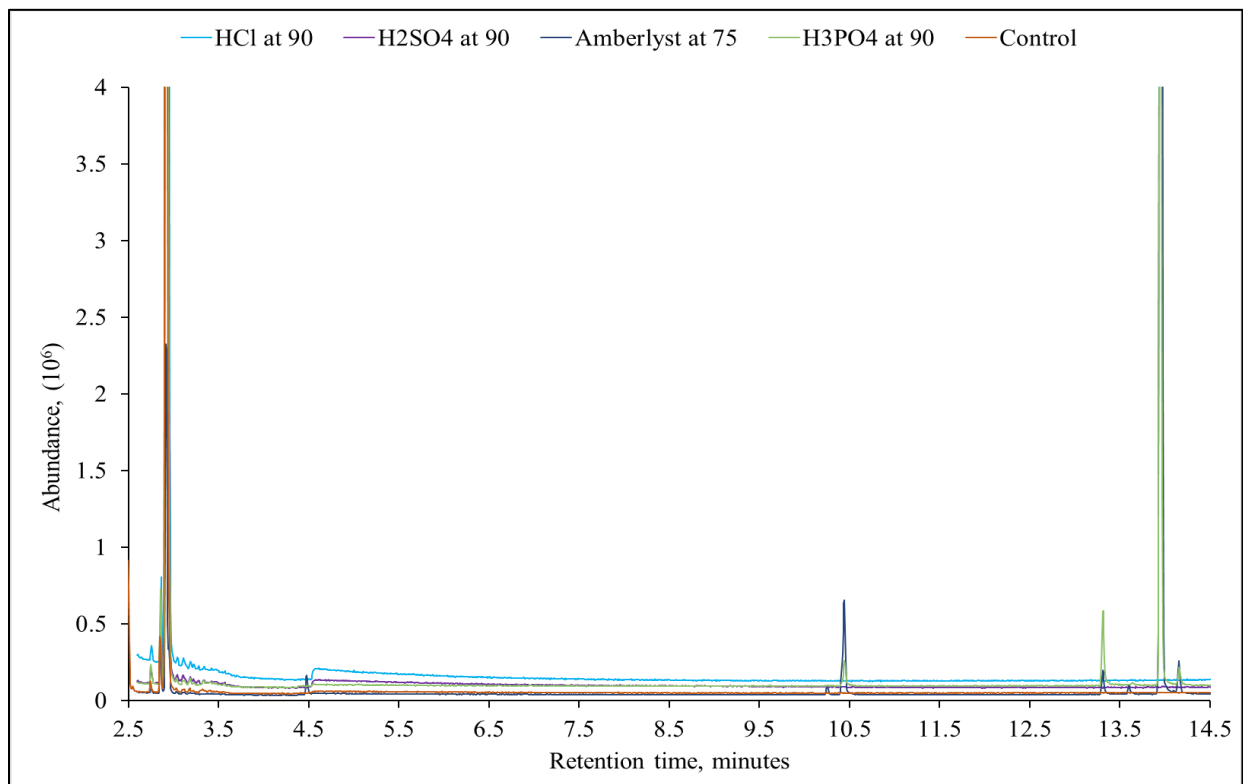
From figure 3.2 and 3.3, it can be observed that there are three different events taking place. The first event, between the temperature range of 100-200 °C, is the region of adsorbance of water on the acid resin. Very small amount of water is seen to decompose within that range. The second peak (between 200-350 °C) takes place at a higher temperature due to release of water during the decomposition of the sulfonic group, as a byproduct. Therefore, only the first event was taken into consideration for the possible presence of water initially in Amberlyst® 15. From figure 3.2, the mass loss in the temperature range of 100-200 °C was calculated to be 0.6 mg (2.2 wt%) which is in close approximation with the specifications provided by the manufacturer i.e.  $\leq 1.60$  % water content.

### 3.3.2 Results for indene

#### 3.3.2.1 Gas chromatography for reactions with indene

A comparison of the chromatograms obtained of the reagents and the products after reaction with HCl and H<sub>2</sub>SO<sub>4</sub> indicated that no reactions took place. However, in the reaction of indene with Amberlyst® 15 and H<sub>3</sub>PO<sub>4</sub>, sharp peaks were observed around the retention time region of 14 and 21 min, and several other smaller peaks were found after the 9 min mark. Figure 3.4 shows the peaks for reaction with all acids.

a)



b)

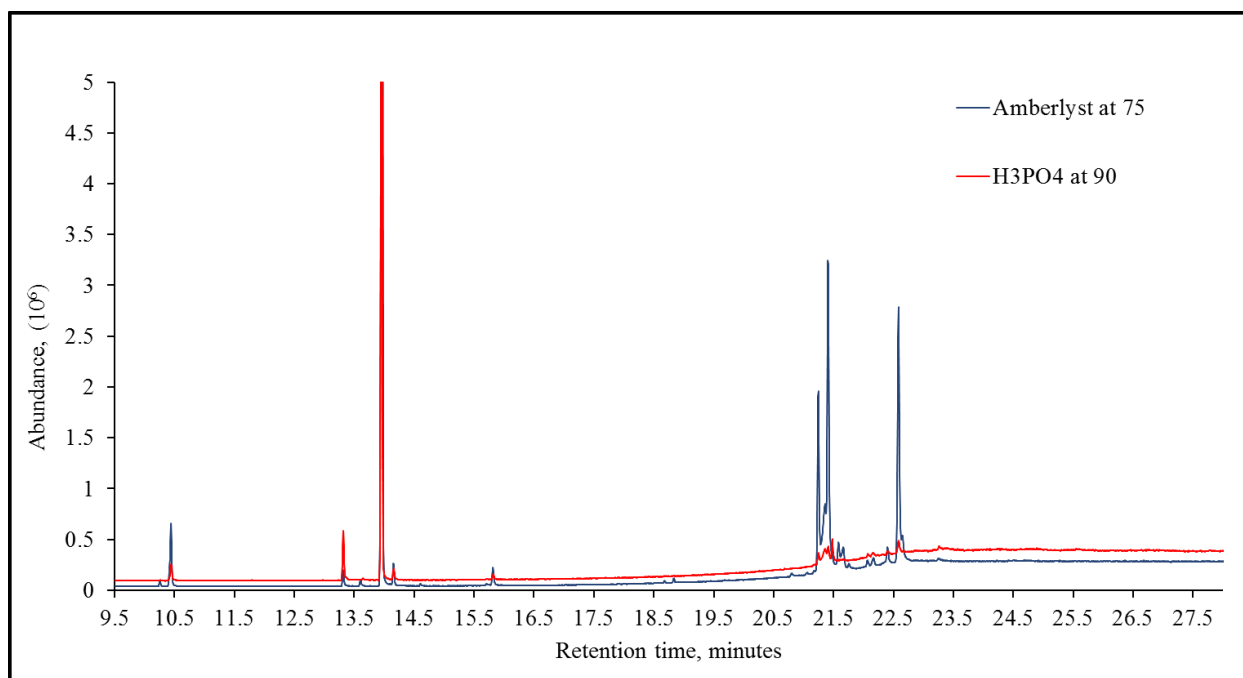
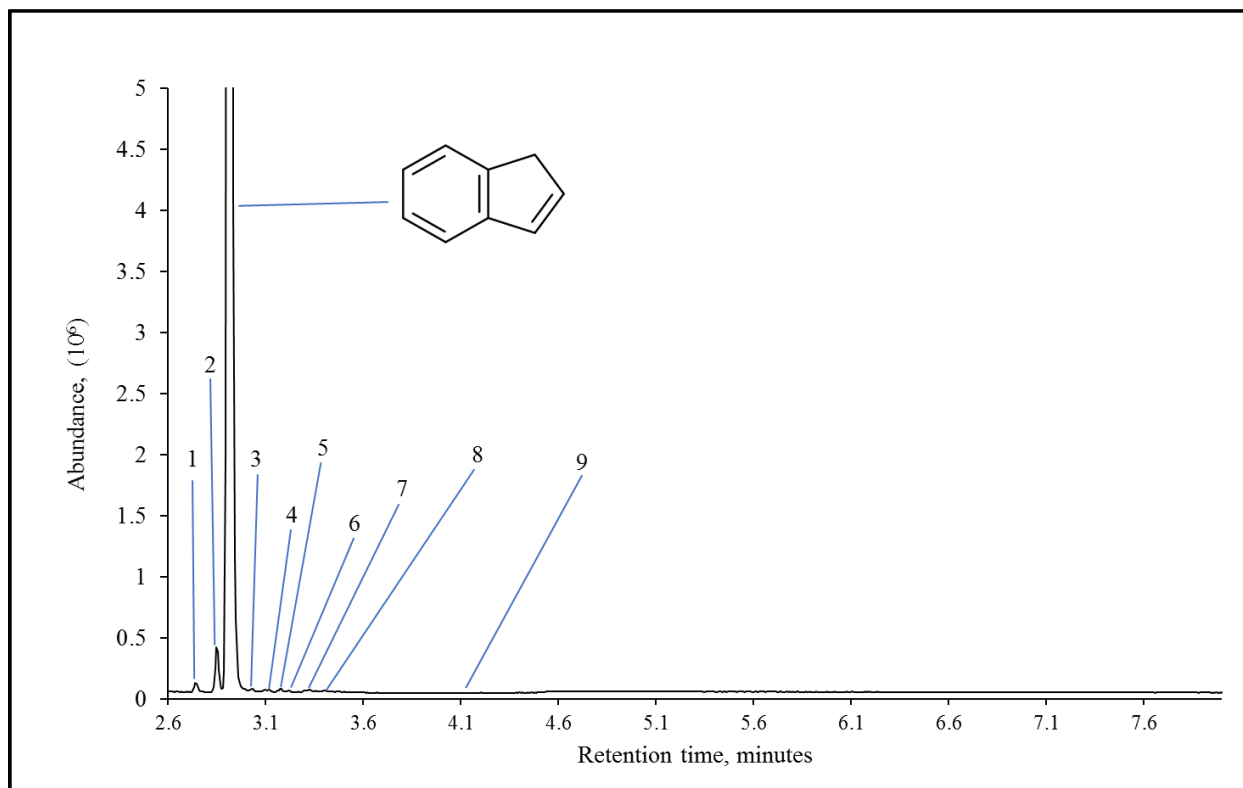


**Figure 3.4** Chromatograms obtained from the reactions of indene with acids where a) shows the retention time from 2.5- 15 minutes while b) goes from 9.5 to 28 minutes

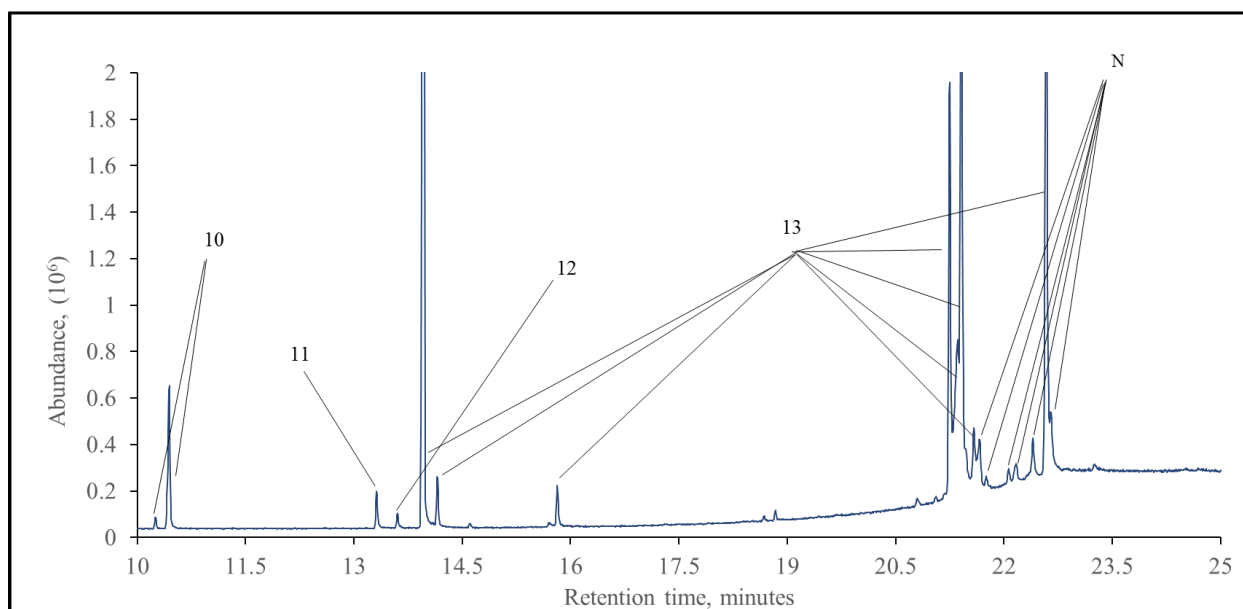
Bumps in figure 3.4 a) at a retention time of 4.5 min which are significantly bigger in the cases of HCl and H<sub>2</sub>SO<sub>4</sub> were due to acid decomposition. It is possible that the product samples were contaminated with acids even after the water washes.

The peaks between the retention time of 2.5 and 4 min overlap with the control experiment. These peaks were found to be present in the indene provided by the supplier when the compound was analyzed using the GC-MS. The peaks were further labelled and identified for the control sample for better understanding (figure 3.5 and table 3.2). Majority of the peaks were present in very low concentrations and their mass spectrums were added in Appendix A. Peaks obtained from the reaction of indene with Amberlyst® 15 and H<sub>3</sub>PO<sub>4</sub> at longer retention times are also further labelled and identified in figure 3.5 and table 3.2.

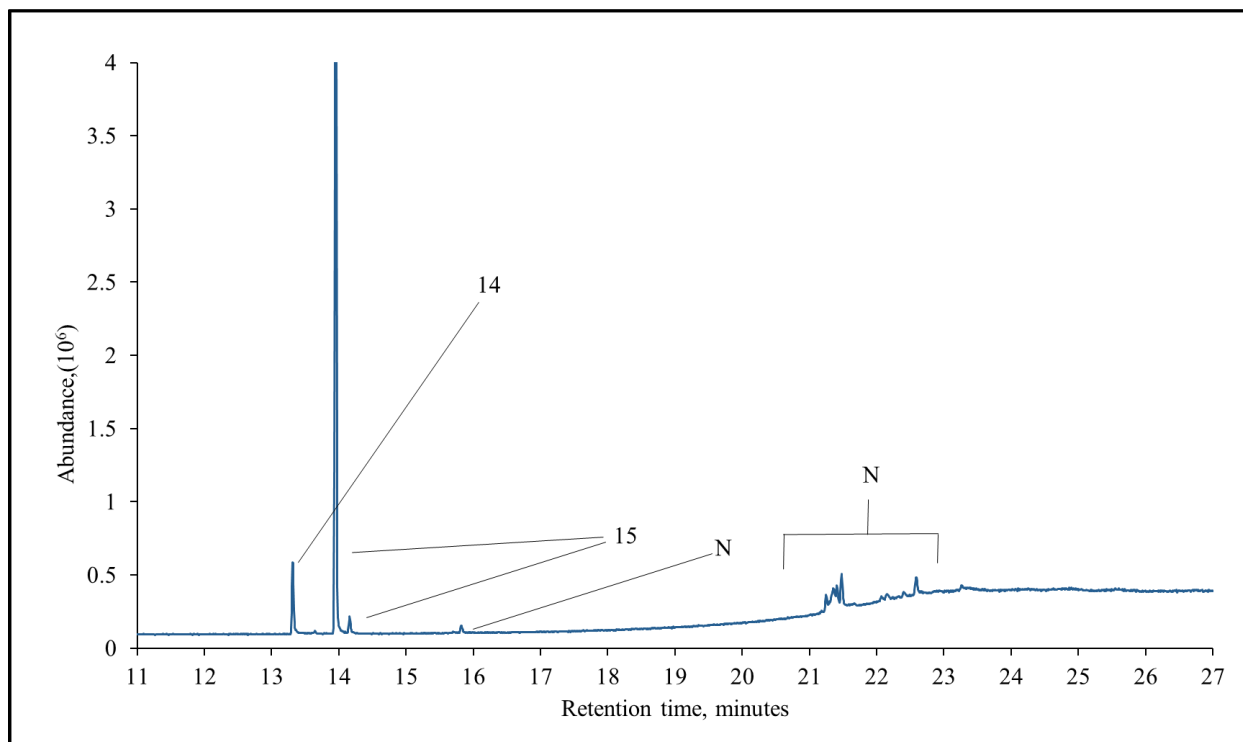
a)



b)



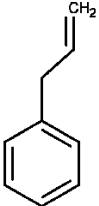
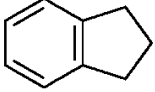
c)

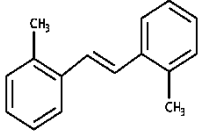
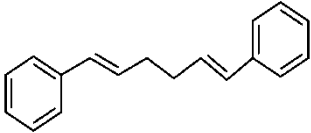
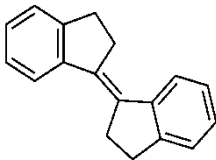
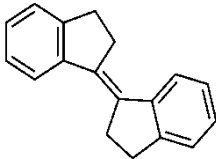


\*N- Bleeding in the column.

**Figure 3.5** GC-MS results for the a) indene control sample and reaction of indene with b)  $H_3PO_4$  and c) Amberlyst® 15

**Table 3.2** Products from reactions of indene with acids

Peak	Retention time (min)	Compound name	Structure
1 <sup>a</sup>	2.75	2-Propenyl benzene	
2 <sup>a</sup>	2.85	Indane	
3 <sup>a</sup> - 9 <sup>a</sup>	3.03 - 4.10	- <sup>b</sup>	-

10 <sup>c</sup>	10.26, 10.45	Isomers of 1-methyl-2-[(E)-2-(2-methylphenyl)ethenyl]benzene	
11 <sup>c</sup>	13.31	Mass spectrum shown below (figure 3.7)	Unidentified
12 <sup>c</sup>	13.60	1,1'-(1,5-hexadiene-1,6-diyl)bisbenzene	
13 <sup>c</sup>	13.96, 14.15, 15.82, 21.25, 21.36, 21.41, 21.59, 22.59	Isomers of 1-(1-indanylidene)indan	
14 <sup>c</sup>	13.31	Mass spectrum shown below (figure 3.7)	Unidentified
15 <sup>c</sup>	13.95, 14.20	Isomers of 1-(1-indanylidene)indan	

a Peak present in the pure compound acquired from the supplier as an existing impurity or unidentified compound.

b Mass spectrum for the respective retention time is shown in Appendix A.

c These compounds should be seen only as being indicative of the nature of the products. The true

identities of these compounds have not been confirmed.

Several peaks were observed after the retention time of 9 min. On further speculation the majority of the peaks, in case of reactions with Amberlyst® 15, pointed to the formation of 1-(1-Indanylidene)indan. Meanwhile, the majority of the peaks for reactions with H<sub>3</sub>PO<sub>4</sub> were due to the formation of 1-methyl-2-[(E)-2-(2-methylphenyl)ethenyl]benzene. A plausible hypothesis was that peaks at different retention times imply that various isomers of the two compounds were formed for the products of each of the acids in the injected samples.

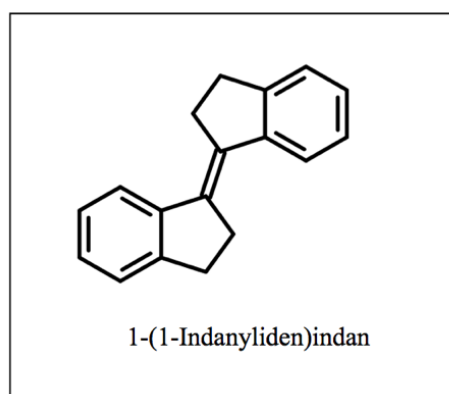
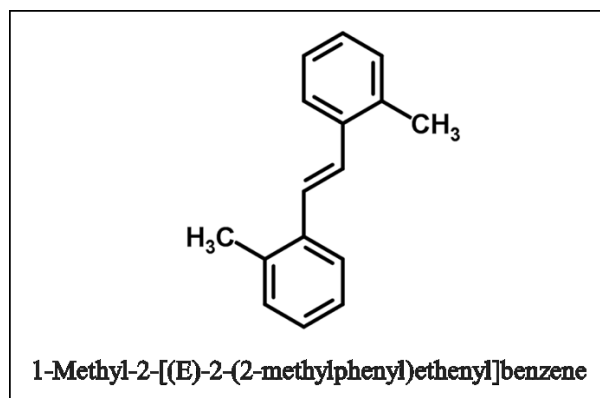


**Figure 3.6** Chemical structure for 1-methyl-2-[(E)-2-(2-methylphenyl)ethenyl]benzene and 1-(1-indanylidene)indan

Quantitative comparison is not a viable option using the GC-MS, however, on comparing the intensities of the peaks for the product of the reaction between indene and Amberlyst® 15, the peak for the polymer of 1-(1-indanylidene)indan was comparably larger than the indene peak. 1-(1-indanylidene)indan produced the largest peak at a retention time of 13.9 min which was 6.8 times higher than the indene peak. Therefore, a significant amount of indene had taken part in the reaction over Amberlyst® 15.

The fragment ion at 18 m/z is present in all compounds because of the presence of 0.03 % in toluene provided by the supplier, that was used as a solvent and for sample preparation in the GC-MS.

The unidentified peaks 11 and 14 had the same mass spectrum, as shown in figure 3.7. From the mass spectrum, the base molecular ion in the spectrum is at 116 m/z. Molecular ion of 91 m/z is

a fragment related to toluene and might also suggest that the presence of an alkyl benzene group. Therefore, the compound does contain benzene rings. The molecular weight of the compound is expected to be approximately 232 g/mol from the spectrum. Given the neighborhood that the peak lies in, the compound is expected to contain 17 carbons. The formula that can be predicted by reading the spectrum is  $C_{17}H_{28}$ .

Unknown; InLib=-1032

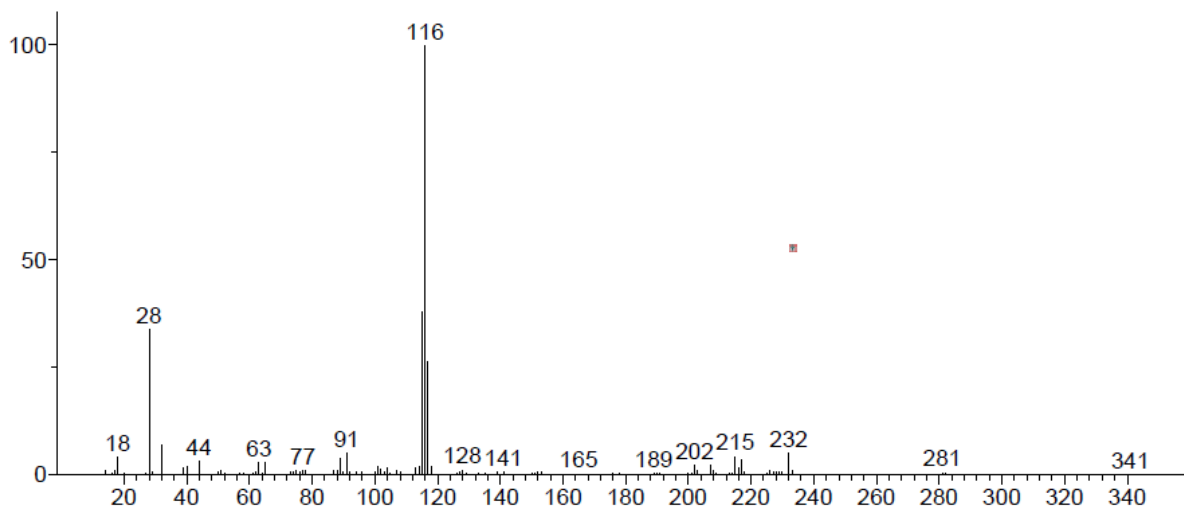


**Figure 3.7** Mass spectrum for peak 11 and 14 at a retention time of 13.31 min for reactions of indene with Amberlyst® 15 and  $H_3PO_4$

The unlabeled compounds between retention times of 14-21 minutes are peaks representative of bleeding in the column.

### 3.3.2.2 Physical changes observable in reaction of indene with acids

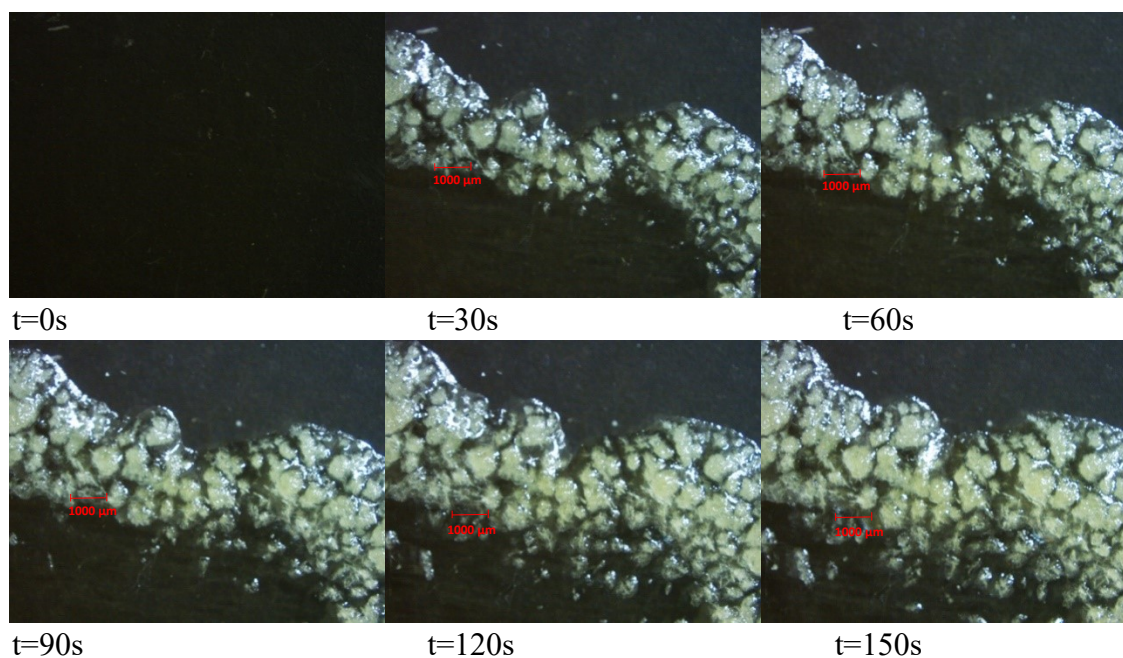
Physical changes in the products obtained after the reaction of indene with Amberlyst® 15 were distinct. The liquid was more viscous in comparison and sticky in nature. The sticky liquid formed was observed to be no longer soluble in toluene. The change in liquid properties is directly related to the formation of the dimer, 1-(1-indanylidene)indan and potentially heavier oligomers.

These changes were not as striking in the products from the phosphoric acid due to relatively low amount of dimer formation with different chemical structure and properties.

### 3.3.3 Results for indole

#### 3.3.3.1 Photoreactions in indole on exposure to light and atmospheric conditions

While performing the analysis for the products from reaction of indole with acids, it was observed that on exposure to atmospheric conditions the liquid would quickly start solidifying. To further understand this phenomenon, a saturated solution of indole dissolved in toluene was prepared. The solution was then observed under the Zeiss StereoMicroscope with respect to time. Figure 3.8 shows the changes that the solution underwent; each frame was taken after an interval of 30 seconds. Indole is light sensitive; it is susceptible to photoreactions in the presence of a solvent which can be seen from figure 3.8. On exposure to light and atmospheric conditions, physical changes are evident which advocate further investigation towards the chemical changes.



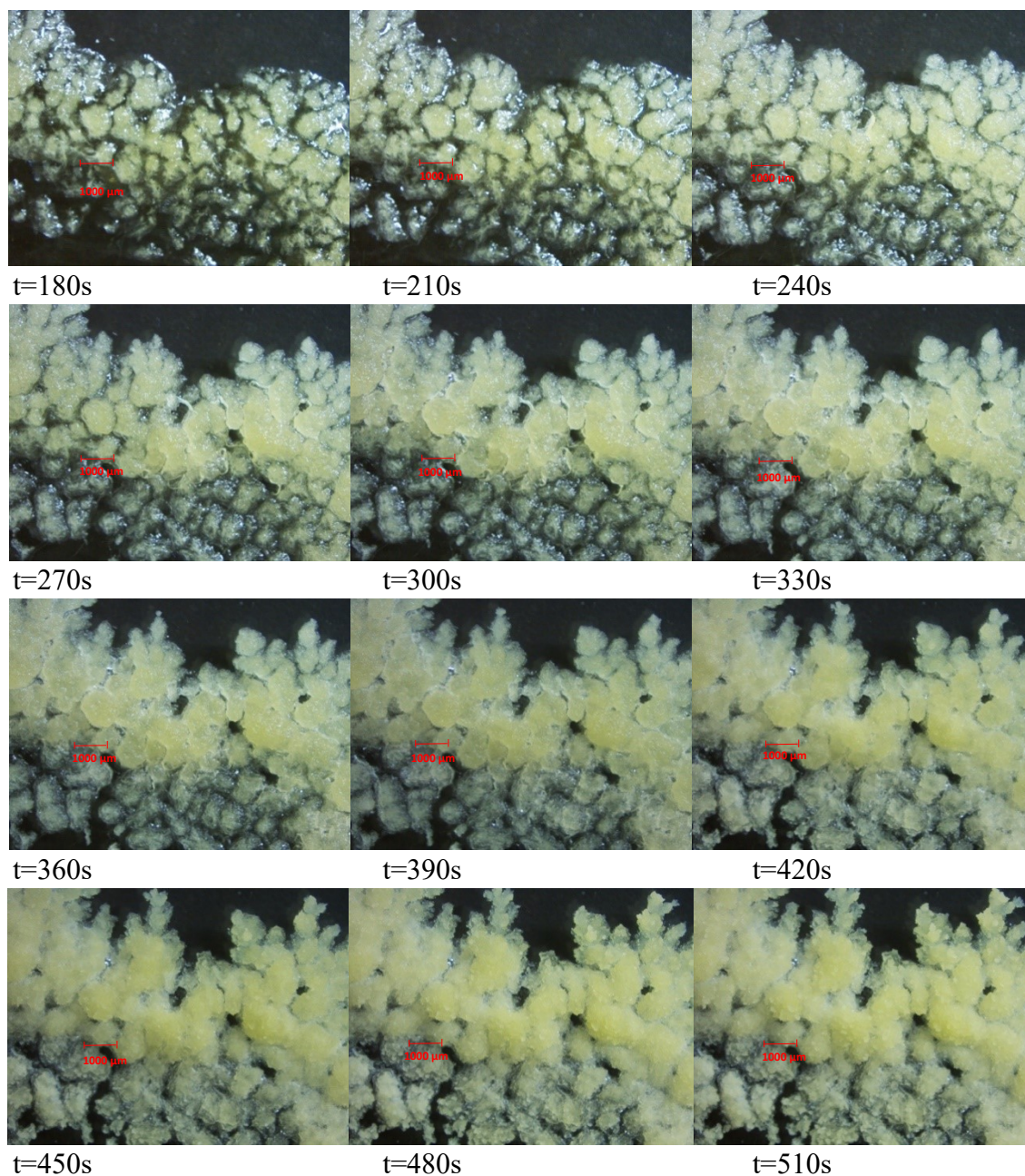


**Figure 3.8** Crystallization following on reaction from a saturated solution of indole seen from Zeiss StereoMicroscope over a period of time

### 3.3.3.2 Gas chromatography for reactions with indole

The chromatogram of the reactions of indole with respect to change in temperature while keeping the catalyst constant overlapped with no deviations. However, there were physical changes visible in the products after the reaction. Much heavier compounds were present in the product with a boiling point much higher than 325 °C, which is the highest temperature the GC-MS can reach. From the GC-MS results, even though the dominant fragments in terms of molecular weight were lighter components 28, 14, 32 and 69 but there were heavier peaks with the  $m/z$  value of up to 327, 355 and as high as 446 captured by the detector. These heavier compounds point towards the formation of gum through addition reactions. These reactions are enhanced over time with the exposure of the products to atmosphere. The peaks after the 17 min mark arise due to the bleeding of the column.

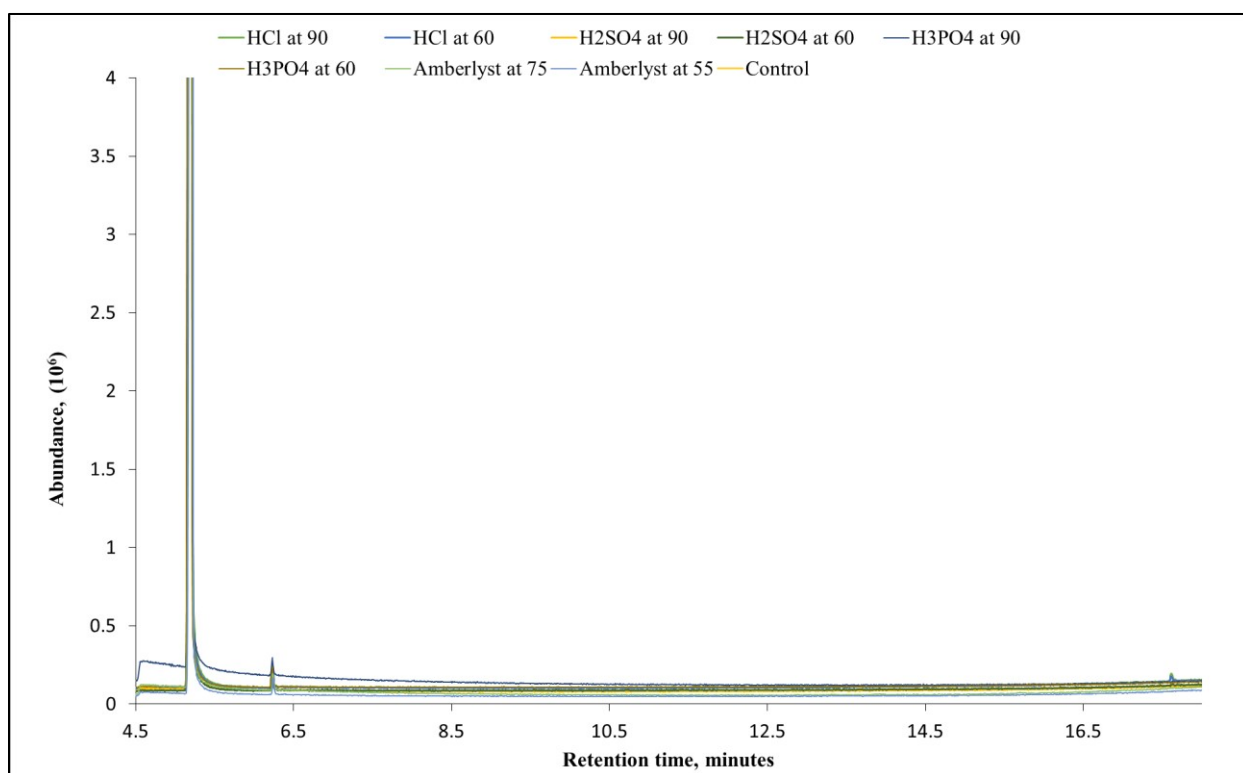


**Figure 3.9** Chromatographs obtained from the reactions of indole with acids using the GC-MS

The peak at a retention time of 6.269 min was an impurity in indole provided by the supplier. The mass spectrum for the peak can be found in Appendix A.

### 3.3.3.3 Solid products under the microscope

All catalyst, in the case of indole, lead to the precipitation of solids at the bottom of the flask after the reaction, except for Amberlyst® 15. The accumulated solids were insoluble in toluene and had to be extracted with the help of methanol, a more polar solvent. In case of the reaction of indole with HCl, the solids completely dissolved in the methanol. The solids precipitated in methanol in the case of sulfuric and phosphoric acids. On testing the methanol samples containing the solids, there was no difference in the chromatogram using the GC-MS, it was similar to that of indole.

Solids obtained from reactions of indole with sulfuric acid produced two different colors of solids at different temperatures, as is shown in figure 3.10. All of these results indicated that the products formed were of higher boiling point than could be eluted during GC-MS analysis.

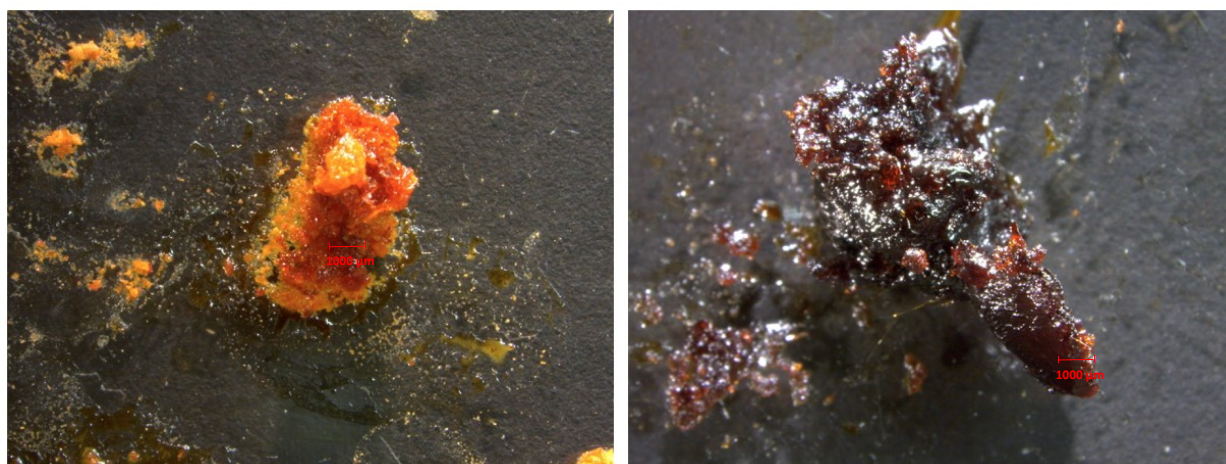


**Figure 3.10** Solid formed during the reaction of indole with sulfuric acid at a temperature of 120 °C (left) and 70 °C (right)

The products that reacted in the presence of phosphoric acid had solids collect at the bottom of the vial. On vigorous shaking, the solid particles would stay suspended in the liquid. When viewed under the microscope, the tiny solid particles were found to be rapidly moving in the

liquid and then slowly started to agglomerate, with time. After a considerable amount of time the solids settled at the bottom of the vial.

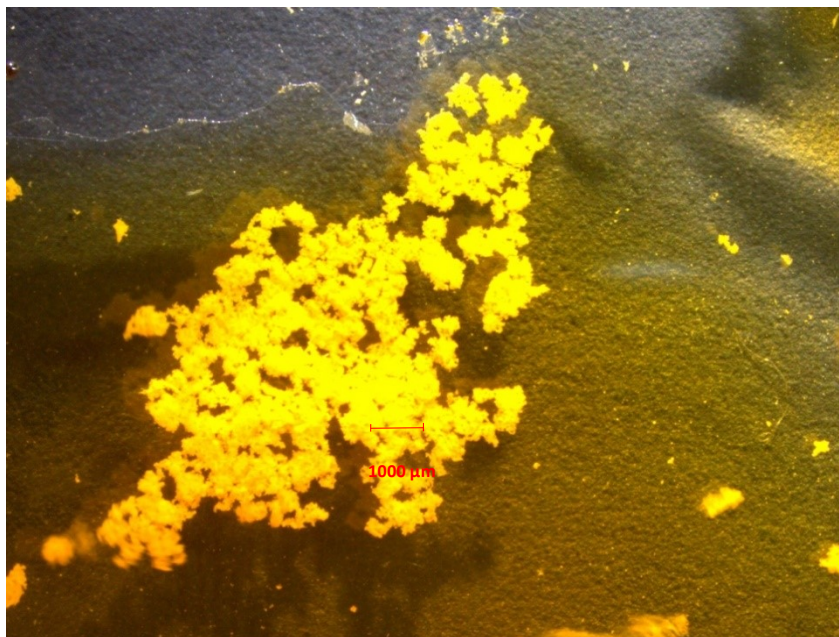


**Figure 3.11** Solid formed during the reaction of indole with phosphoric acid

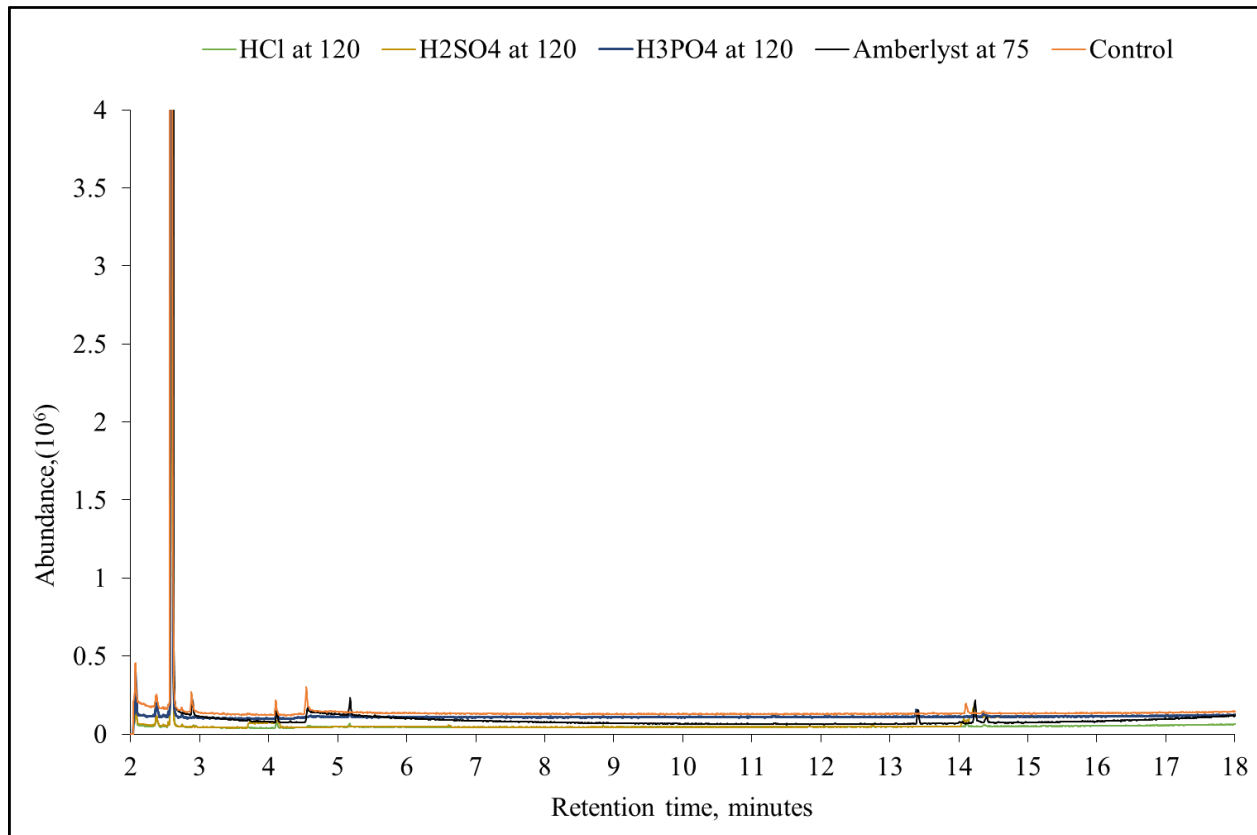
### *3.4 Results for benzofuran*

The reaction with  $\text{H}_2\text{SO}_4$  and  $\text{H}_3\text{PO}_4$  also accumulated a black liquid at the bottom of the flask which dissolved in methanol. The GC-MS further was only able to confirm the presence of benzofuran in the solids, but no other peak provided substantial information on the composition of the liquid.

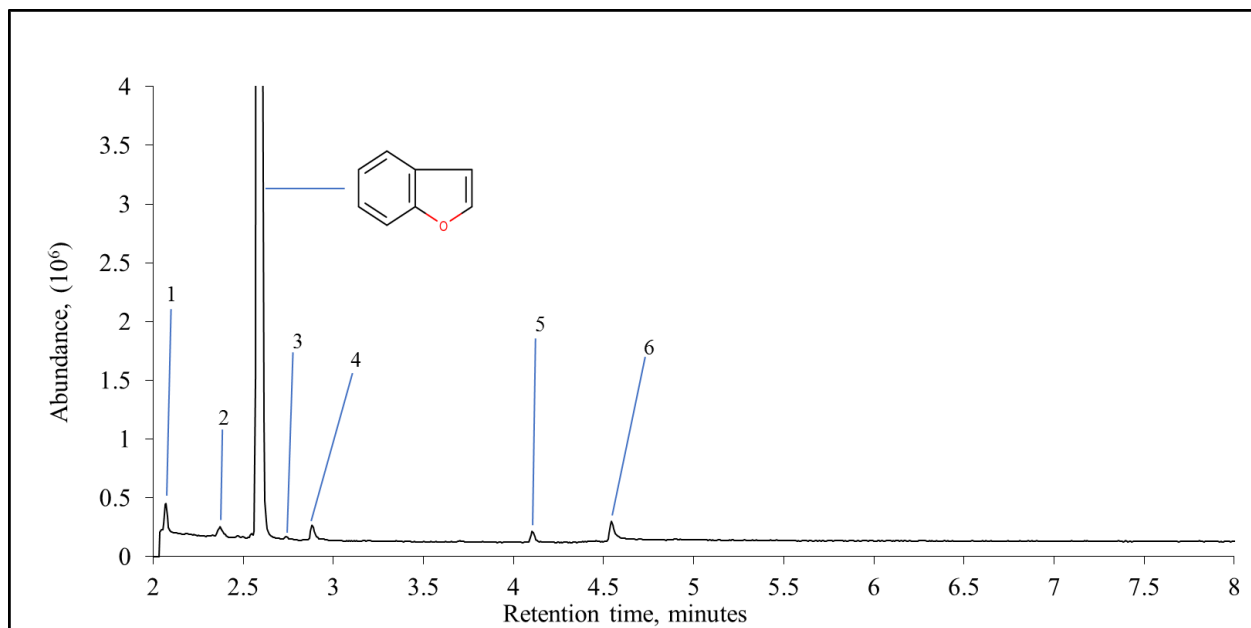
#### *3.4.1 Gas chromatography for reactions with benzofuran*

Similar to the other model compounds, temperature did not play a role in differentiating the products formed after the reaction. The presence of all acid catalysts resulted in addition reactions. The reactions led to an overall generation of a compound much heavier than benzofuran. After a retention time of 13 min, much heavier compounds with a molecular weight higher than 234 were detected by the GC-MS for Amberlyst® 15, HCl,  $\text{H}_2\text{SO}_4$  and  $\text{H}_3\text{PO}_4$ .

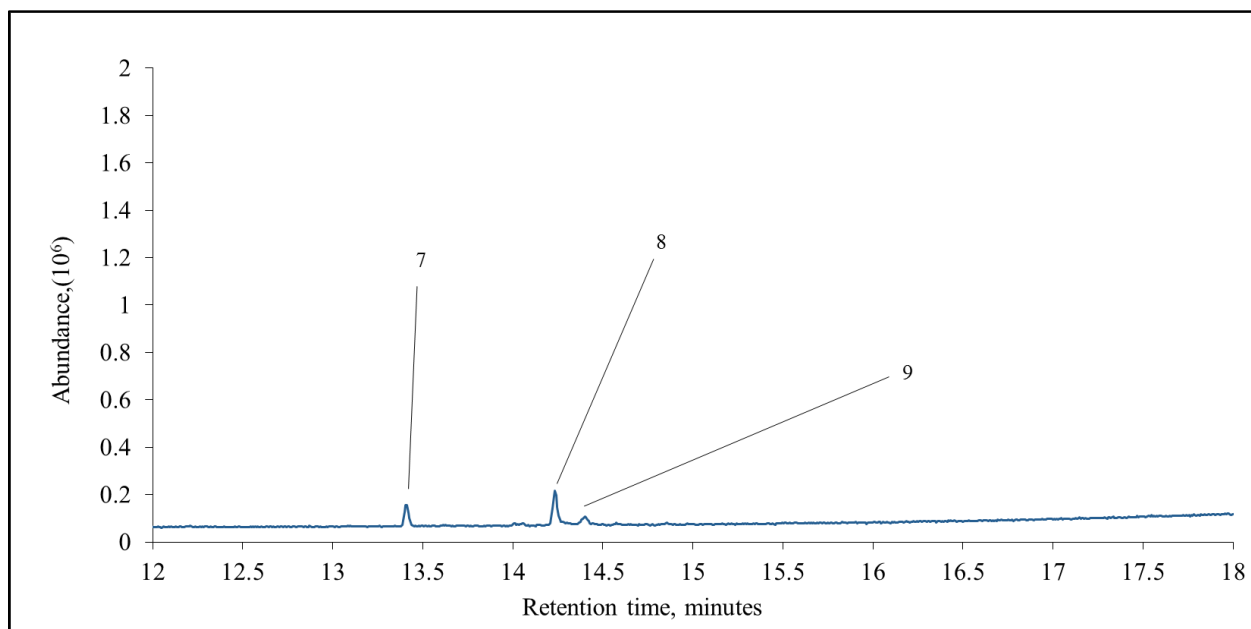
a)



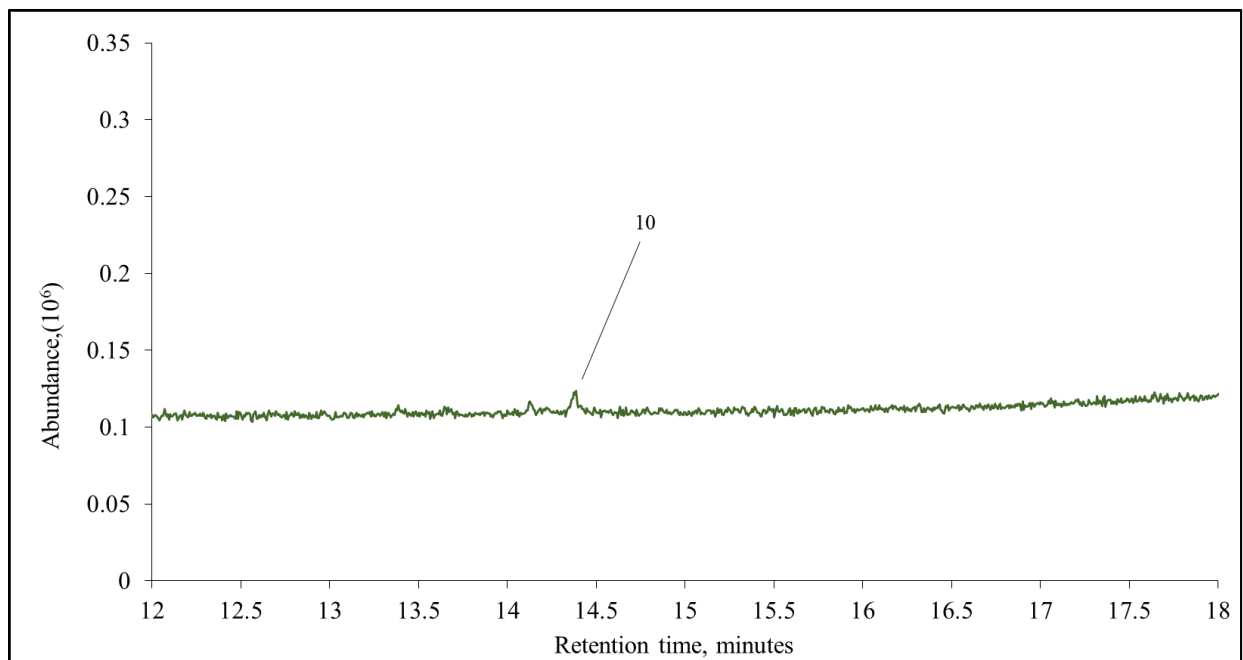
b)



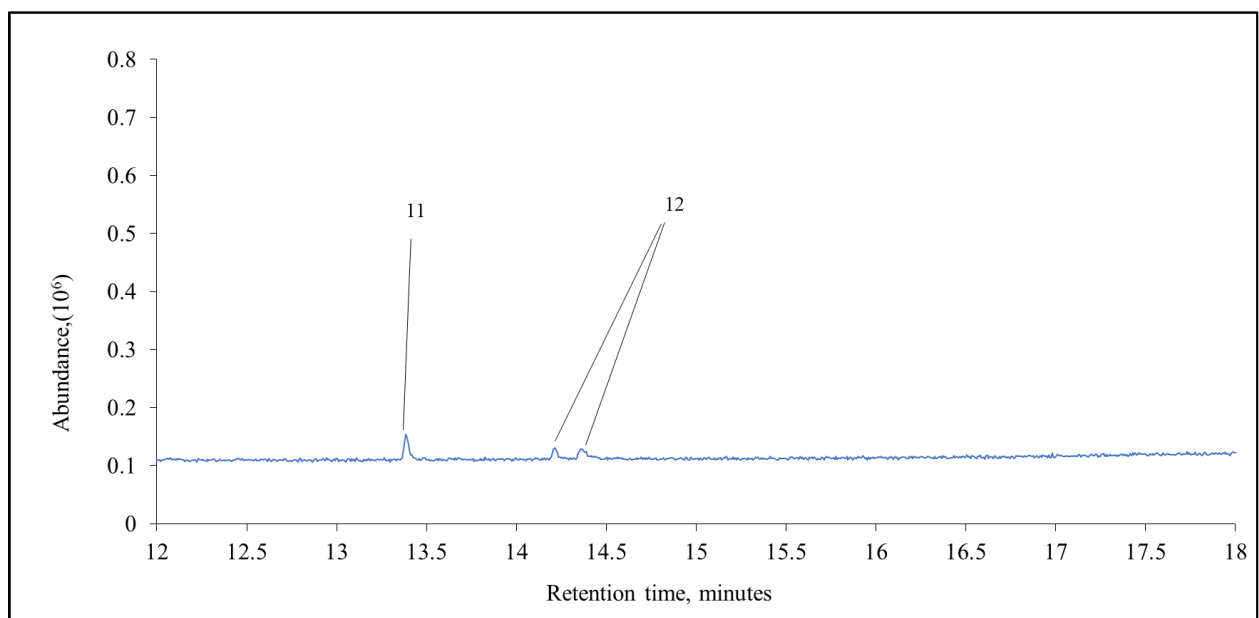
c)



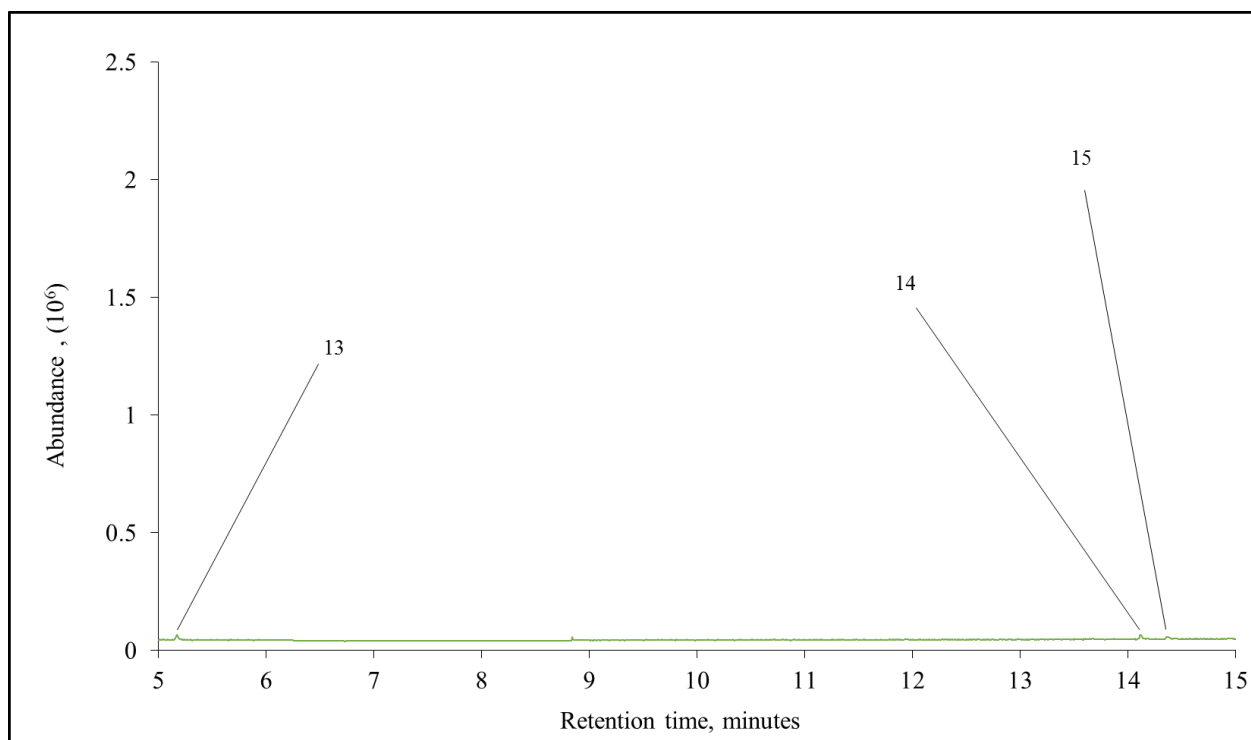
d)



e)

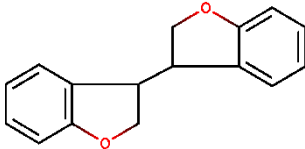
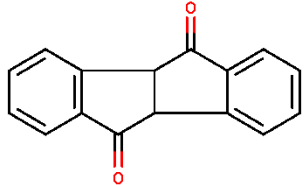


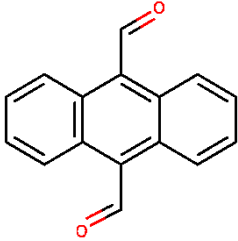
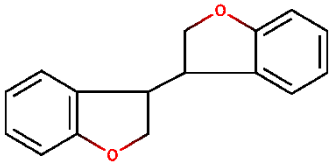
f)



**Figure 3.12** Chromatographs obtained from the reactions of benzofuran with acids where a) reaction with selected acids and control b) peaks present in benzofuran provided by supplier c) reaction of benzofuran with Amberlyst® 15 d) reaction with H<sub>3</sub>PO<sub>4</sub> e) reaction with H<sub>2</sub>SO<sub>4</sub> f) reaction with HCl

**Table 3.3** Products from reactions of benzofuran with acids

Peak	Retention time (min)	Compound name	Structure
1 <sup>a</sup> – 6 <sup>a</sup>	2.07 – 4.11	- <sup>b</sup>	-
7 <sup>c</sup>	13.41	3-(2,3-Dihydro-1-benzofuran-3-yl)-2,3-dihydro-1-benzofuran	
8 <sup>c</sup>	14.23	Tetracyclo[7.7.0.0 <sup>2</sup> , 7.0 <sup>10,15</sup> ]hexadeca-2(7),3,5-triene-8,16-dione	

9 <sup>c</sup>	14.40	Mass spectrum shown below (figure 3.13)	Unidentified
10 <sup>c</sup> , 12 <sup>c</sup>	14.38, 14.23, 14.38	Isomers of Anthracene-9,10- dicarbaldehyde	
11 <sup>c</sup>	13.41	3-(2,3-Dihydro-1-benzofuran-3- yl)-2,3-dihydro-1-benzofuran	
13 <sup>c</sup>	5.17	Mass spectrum shown below (figure 3.14a)	Unidentified
14 <sup>c</sup>	14.13	Mass spectrum shown below (figure 3.14b)	Unidentified
15 <sup>c</sup>	14.37	Mass spectrum shown below (figure 3.14b)	Unidentified

a Peak present in the pure compound acquired from the supplier as an existing impurity or unidentified compound.

b Mass spectrum for the respective retention time is shown in Appendix A.

c These compounds should be seen only as being indicative of the nature of the products. The true

identities of these compounds have not been confirmed.

All other peaks which have not been labelled in the above chromatogram are peaks for bleeding in the column.

The mass spectrum for peak 9 was obtained after the reaction of benzofuran with Amberlyst®15 at a retention time of 14.41 min (figure 3.13). The compound is formed as an addition product and is expected to lie on the heavier end. On studying the compounds prior to the peak, the compound is expected to have at least 16 carbons or more, with a molecular weight of

approximately 252 g/mol. A peak at 91 m/z is present for toluene fragment, possibly also suggesting an alkyl benzene group. Studying the difference between the fragments of 118 m/z and 207m/z, there is a possible molecular ion of  $C_3H_7OC=O$  present in the compound. Not much else can be said about the structure of the final compound.

Unknown; InLib=-1562

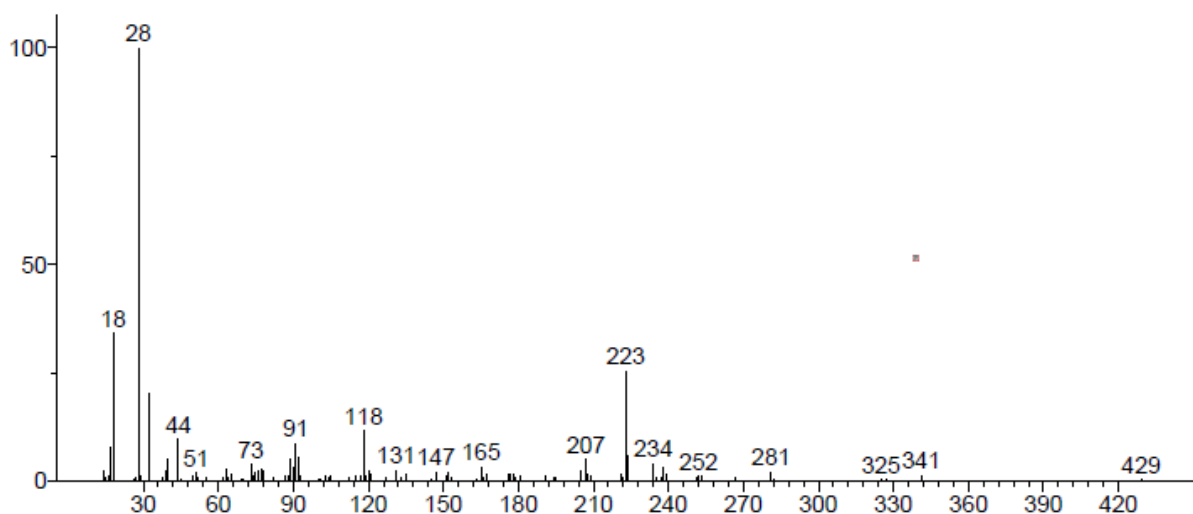


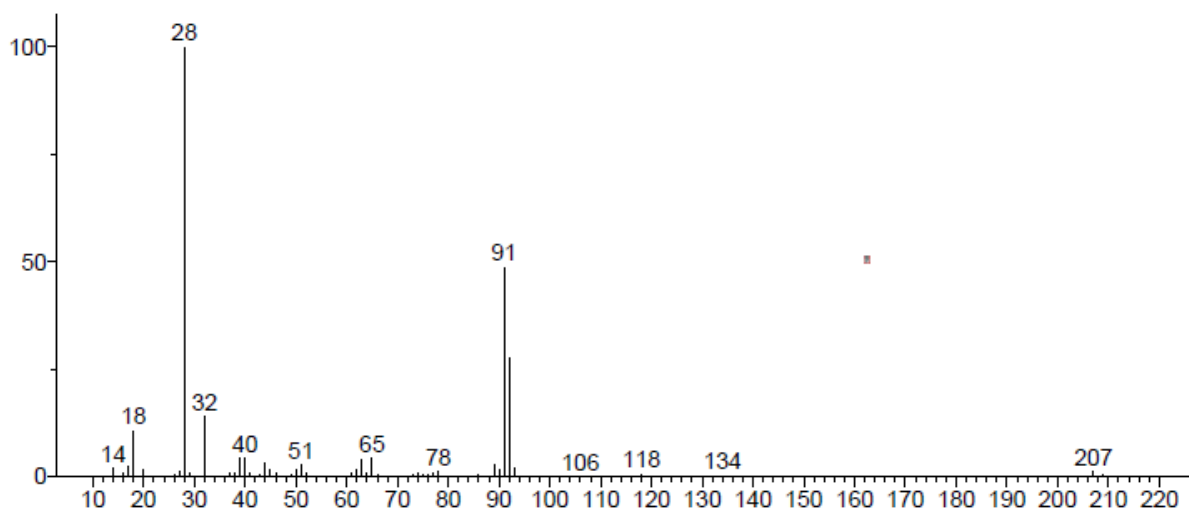
**Figure 3.13** Mass spectrum for peak 9 for reactions of benzofuran with Amberlyst®15

Peak 13 was found at a retention time of 5.17 min for a reaction between benzofuran and HCl (figure 3.14a). The compound is likely to constitute of 9-10 carbons including the presence of a benzene ring (molecular fragment of 78 m/z). The expected molecular weight is expected to be 134 g/mol. The molecular fragment of 91 m/z is representative of toluene, also likely a methyl benzene group. The 118 m/z peak is the same as the one present for benzofuran. The difference between the 134 and 118 m/z fragments gives a propyl group.

The mass spectrums for peaks 14 and 15 were the same, indicating that the two peaks are possibly isomers of the same compound. The spectrum is shown in figure 3.14b. The molecular weight of the compound is expected to be 238 g/mol. On studying the chromatograms for the reaction of benzofuran with other acids, the expected compound should constitute of 16 carbons. The rest of the composition of the compound is not known.

a)

Unknown; InLib=-591



b)

Unknown; InLib=-550

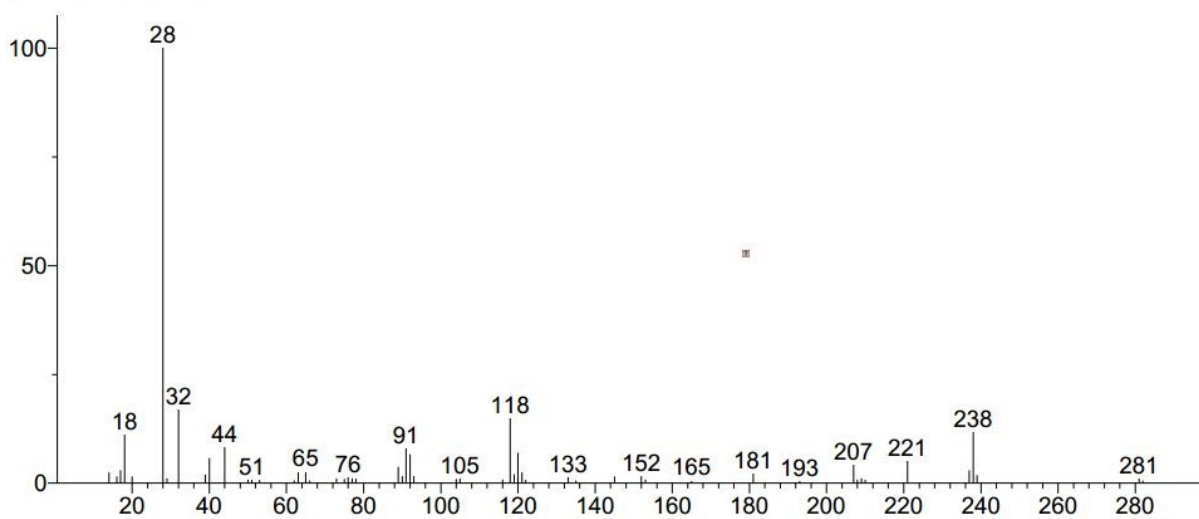


**Figure 3.14** Mass spectrum for a) peak 13, b) peak 14 and 15 for reactions of benzofuran with HCl

Chemical compounds associated with peaks 7,8,10,11 and 12, are tentatively assigned based on the mass spectra. The mass spectrums for the compounds are shown in appendix A.

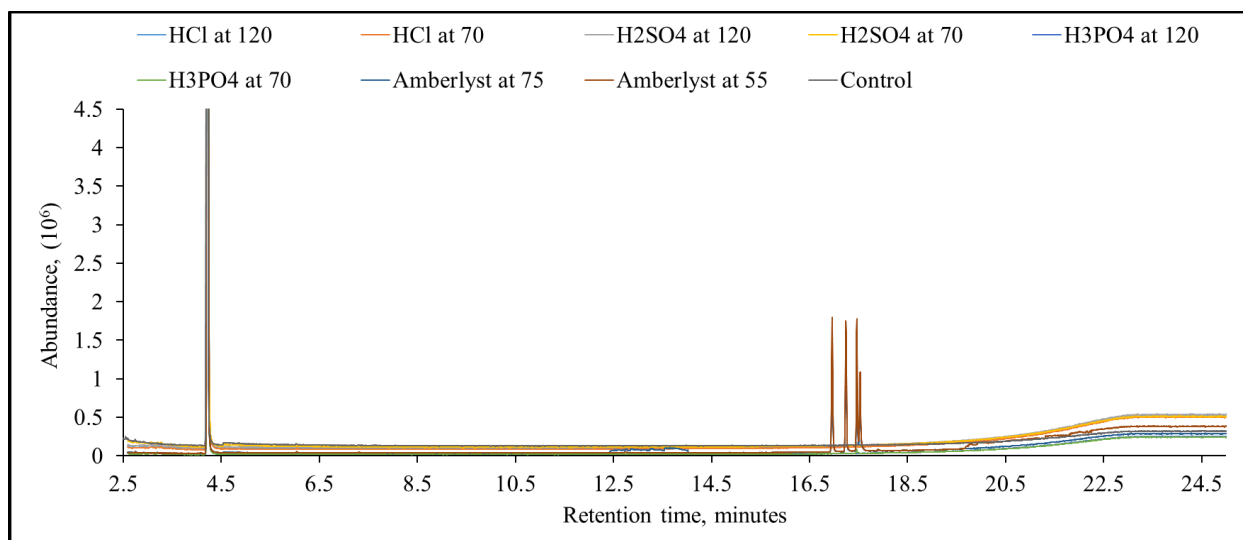
### *3.3.5 Results for thianaphthene*

There were no physical changes observed in the products obtained during the reaction of thianaphthene with acids.

#### *3.3.5.1 Gas chromatography for reactions with thianaphthene*

Amberlyst®15 was the only acid that reacted with thianaphthene. No other acids showed any difference in the GC-MS results. Figure 3.15 shows a comparison between the chromatograms obtained for thianaphthene. After a retention time of 16.5 min, similar to results in case of other model compounds, several peaks were grouped and labelled as 1 (figure 3.16). These peaks indicated the formation of isomers of 3-(2,3-dihydro-1-benzothiophen-3-yl)-1-benzothiophene (figure 3.16). The smaller peaks between 12.5-14.5 min indicate bleeding in the column and can be discarded.

a)



b)

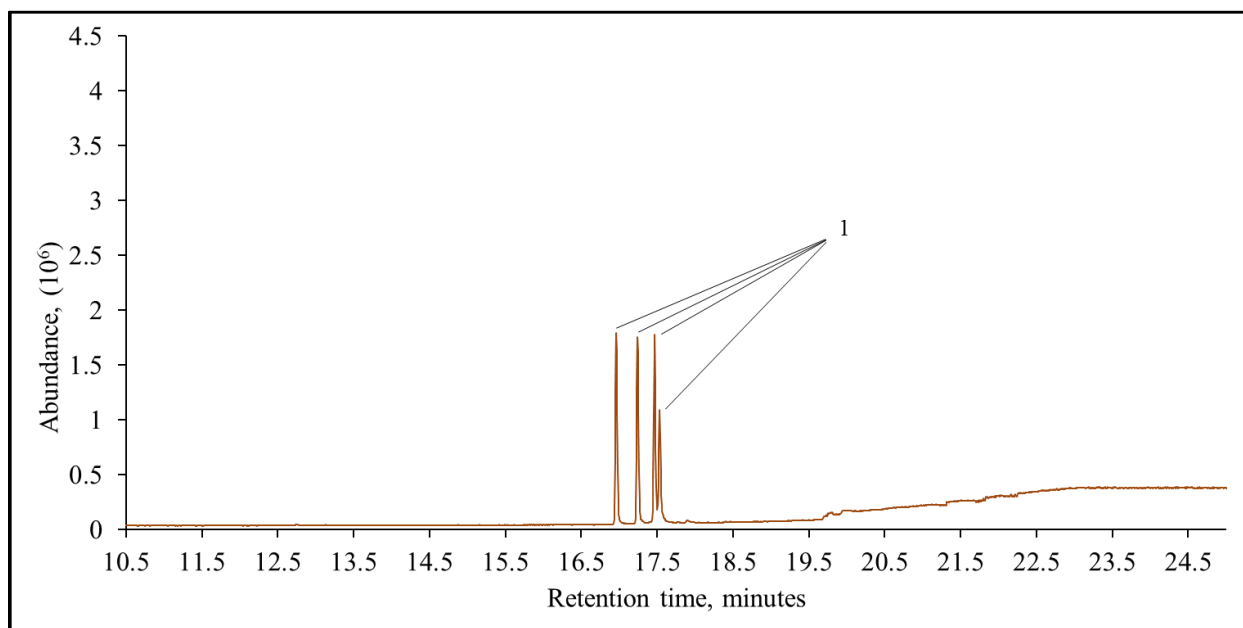


**Figure 3.15** GC-MS results for the reaction of thianaphthene with a) selected acids and b) Amberlyst® 15

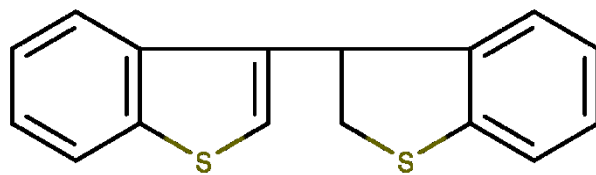


**Figure 3.16** Structure for 3-(2,3-dihydro-1-benzothiophen-3-yl)-1-benzothiophene

### 3.3.6 Results for tetrahydrothiophene

The reactions of tetrahydrothiophene with acids were performed to get a better understanding for the heterocyclic ring present in thianaphthene. On analyzing the products in the GC-MS from the reactions of thianaphthene in the presence of the selected group of acids, no reaction took place. All chromatograms aligned with the control run for all acids for temperatures of 70 °C and 120 °C.

## 3.4 Discussion

### 3.4.1 Addition reactions in the presence of acids

Oligomerization reactions were achieved in reactions of acids in indene, indole, benzofuran and thianaphthene. Moderately strong acids create pathways for dimerization and trimerization of heterocyclic compounds.<sup>3</sup>

Indene is known to easily undergo polymerization reactions. A visible spectrum change from yellow to red and further to dark red, occurs in the presence of acids.<sup>4</sup> From the results, indene was exposed to very mild reaction conditions. There was not a visible change in color, however, it is recognized from the results obtained in the GC-MS that the product dimerized (figure 3.5).

Indene is known to not polymerize in the presence of only hydrochloric acid, although it does have a susceptibility to undergo attack by cationic reagents. During reaction of indene with Lewis acids such as boron trifluoride and titanium tetrachloride, in the presence of hydrochloric acid used as a co-catalyst alongside water, heavier polymers were formed.<sup>5</sup>

In the presence of  $\text{H}_3\text{PO}_4$  and Amberlyst® 15, indene formed the indan-1-ylum ion which in addition to another indene molecule formed several isomers of 1-(1-indanylidene)indan (figure 3.17).<sup>6</sup> From the results of just the GC-MS it is difficult to relate each isomer to the respective peak.

From literature, indene oligomerizes on reaction with concentrated  $\text{H}_2\text{SO}_4$ .<sup>6</sup> However, it was not applicable in the reaction conditions used in accordance with results from this chapter due to lower concentration of sulfuric acid. However, when a stronger sulfonic group (Amberlyst® 15) was available during reaction, large amounts of dimerization was observed.

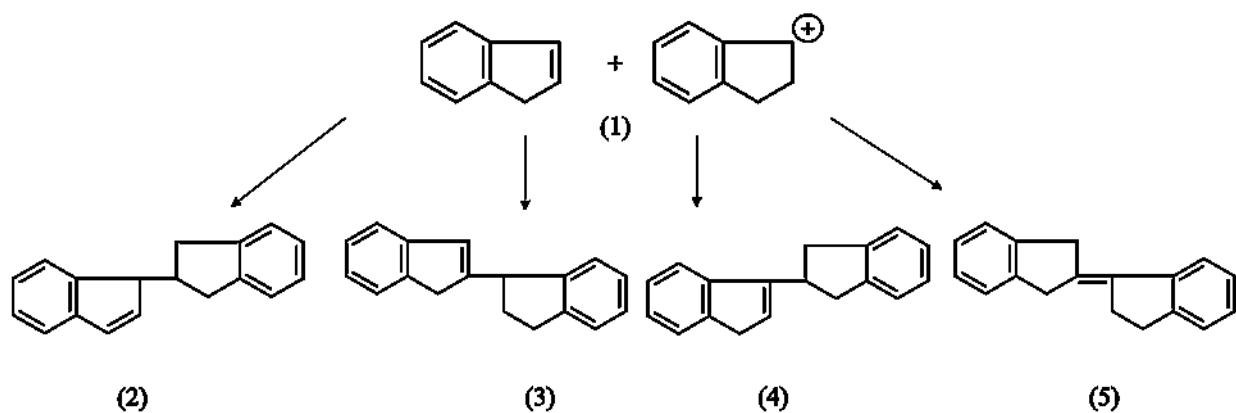


**Figure 3.17** Reaction chemistry for formation of isomers of 1-(1-indanylidene)indan<sup>6</sup>

Indene and benzofuran are known to easily polymerize in the presence of cationic catalysts at low temperatures, which in this case are  $\text{HCl}$ ,  $\text{H}_2\text{SO}_4$ ,  $\text{H}_3\text{PO}_4$  and Amberlyst® 15.<sup>7</sup> From peaks 7 and 11 in table 3.3, benzofuran polymerizes through the  $\text{C}_3$  position of the cyclic olefin. The reaction is initiated by the proton added from the acids. It propagates through the olefinic bond opening in the furan ring.<sup>7,8</sup> And terminates with a release of proton from one of the benzofuran molecules in the dimer.

Thianaphthene is the least reactive compound in comparison to the selected model compounds, however, it reacted with Amberlyst® 15. Upon reviewing literature, it was found that with

addition of a proton in the presence of an aqueous metal species, thianaphthene polymerizes to form isomers of 3-(2,3-dihydro-1-benzothiophen-3-yl)-1-benzothiophene (figure 3.18). The possible mechanism is shown in chapter 2 (figure 3.2).<sup>9</sup>

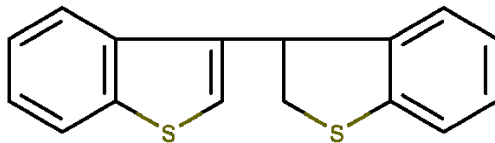


**Figure 3.18** Structure of 3-(2,3-dihydro-1-benzothiophen-3-yl)-1-benzothiophene

### 3.4.2 Solid formation in indole on reaction with acids

Without increase in temperature, indole on exposure to air and in the presence of toluene goes through physiochemical changes and forms a crystal-like structure following on reaction from a saturated solution. This was seen through figure 3.8 and can be correlated to gum formation.

Hydrocarbons present in gasoline have been known to form gum on reaction with absorbed atmospheric oxygen at ambient temperature. One of the reasons for the gum formation is due to the presence of reactive nitrogen containing compounds present in gasoline.<sup>10</sup> This plays a crucial role in the instability of gasoline over extended periods, also creating non-optimal conditions not only during transportation but combustion of fuel and engine efficiency.<sup>10</sup>

Acid catalyzed reactions promote electrophilic substitution reactions which can lead to polymerization. Indole is a highly activated aromatic compound. On forming weak electrophiles, polymerization can be initiated with ease.<sup>11,12</sup> Indole undergoes dimerization and trimerization in the presence of acids, the rate of oligomerization is dependent on the acid strength. When treated with acids, indole also forms acidic salts of dimers. In the reactions of indole with HCl, H<sub>2</sub>SO<sub>4</sub> and H<sub>3</sub>PO<sub>4</sub>, solid precipitates were formed. In the case of sulfuric acid, the acid salts precipitated as red and black solids (figure 3.10). From studies, sulfuric acid completely protonates indoles, the protonation in indole takes place at the C<sub>3</sub> position as shown below (figure 3.19).<sup>13</sup> The GC-MS was not able to detect the presence of any compounds because of limitation of working temperature.<sup>3</sup>



**Figure 3.19** Reaction of indole in the presence of sulfuric acid.<sup>13</sup>

### 3.4.3 Impact of results on upgrading in oilsands

The presence of acids occurs in various stages of the upgrading process. Polymerization with selected binuclear naphtheno-aromatics compounds, i.e. indene, indole, benzofuran and thianaphthene in the presence of acids, occurs at lower temperatures. This gives rise to the formation of much heavier compounds and, in some cases, solids. Presence of such compounds in different fractions of the process can impact the viscosity of bitumen, fouling of equipment, bitumen recovery and storage stability.<sup>14</sup>

Polymerization in fuels can lead to increased fuel density, heavier boiling distillates and increased concentration of olefins. All these factors create economic problems due to increase in expenses during processing and reduced fuel quality.<sup>10</sup>

## 3.5 Conclusion

Binuclear aromatic compounds with 5-membered ring were reacted in the presence of acids at temperatures of 70 and 120 °C. The reactions were performed to understand the impact that the presence of the selected compounds could potentially have on alicyclic and heterocyclic compounds attached to aromatic rings at different stages of the upgrading process under mild conditions. The main conclusions and observations were as follows:

- a) Oligomerization of the model compounds lead to much heavier product formation. Indene polymerized in the presence of H<sub>3</sub>PO<sub>4</sub> and Amberlyst® 15. Indole reacted with

HCl, H<sub>3</sub>PO<sub>4</sub> and H<sub>2</sub>SO<sub>4</sub>. Benzofuran reacted with HCl, H<sub>3</sub>PO<sub>4</sub>, Amberlyst® 15 and H<sub>2</sub>SO<sub>4</sub>. Lastly, thianaphthene polymerized in the presence of Amberlyst® 15.

- b) Indene, indole and benzofuran underwent physiochemical changes. Indene formed a product that was sticky in nature on reactions with both H<sub>3</sub>PO<sub>4</sub> and Amberlyst® 15. Indole and benzofuran formed acid salts on reactions with HCl, H<sub>3</sub>PO<sub>4</sub> and H<sub>2</sub>SO<sub>4</sub>. These physical changes could possibly have bigger repercussions during transportations due to fouling in the pipelines.
- c) Indole forms gum at ambient temperature in the presence of light and absorbed oxygen.

### 3.6 References

- (1) Gray, M. R. *Upgrading Oilsands Bitumen and Heavy Oil*, 1st ed.; The University of Alberta Press: Edmonton, 2015.
- (2) Wang, R.; Li, Y.; Guo, B.; Sun, H. Catalytic Mechanism of MCM-41 Supported Phosphoric Acid Catalyst for FCC Gasoline Desulfurization by Alkylation: Experimental and Theoretical Investigation. *Energy Fuels* **2011**, *25* (9), 3940–3949.
- (3) J. Houlihan, W. *Indoles*; Wiley-Interscience: New York, 1972.
- (4) Bhadani, S. N.; Baranwal, P. P. The Electro-Initiated Cationic Polymerization of Indene , 1. *Macromol. Chem. Phys.* **1977**, *178*, 1049–1060.
- (5) Eckard, A. D.; Ledwith, A.; Sherrington, D. C. Cationic Polymerization of Indene. *Polymer (Guildf)*. **1971**, *12* (7), 444–451.
- (6) Jovanović, J.; Spitteller, M.; Elling, W. Indene Dimerization Products. *J. Serbian Chem. Soc.* **2002**, *67* (6), 393–406.
- (7) Mizote, A.; Tanaka, T.; Higashimura, T.; Okamura, S. Cationic Polymerization of Cyclic Olefins. *J. Polym. Sci. Part A-1 Polym. Chem.* **1966**, *4* (4), 869–879.

- (8) Redingungen, D. Optically Active Polymers : Some New Results and Remarks on the Asymmetric Polymerization of Benzofuran. *Macromol. Chem. Phys.* **1963**, *61* (1), 79–89.
- (9) Clark, P. D.; Lesage, K. L.; Tsang, G. T.; Hyne, J. B.; Tn, C. Reactions of Benzo [ B ] Thiophene with Aqueous Metal Species: Their Influence on the Production and Processing of Heavy Oils. *Energy Fuels* **1988**, *2* (4), 578–581.
- (10) Pradelle, F.; Braga, S. L.; Martins, A. R. F. A.; Turkovics, F.; Pradelle, R. N. C. Gum Formation in Gasoline and Its Blends: A Review. *Energy Fuels* **2015**, *29* (12), 7753–7770.
- (11) Laskin, A.; Lifshitz, A. Isomerization and Decomposition of Indole. Experimental Results and Kinetic Modeling †. *J. Phys. Chem. A* **1997**, *101* (42), 7787–7801.
- (12) Kulkarni, A.; Zhou, W.; Török, B. Heterogeneous Catalytic Hydrogenation of Unprotected Indoles in Water: A Green Solution to a Long-Standing Challenge. *Org. Lett.* **2011**, *13* (19), 5124–5127.
- (13) Eicher, T.; Hauptmann, S.; Speicher, A. *The Chemistry of Heterocycles*, 2nd ed.; Weinheim: Wiley-VCH: Federal Republic of Germany, 2004.
- (14) Siddiquee, M. N.; de Klerk, A. Heterocyclic Addition Reactions during Low Temperature Autoxidation. *Energy Fuels* **2015**, *29* (7), 4236–4244.

## CHAPTER 4 : REACTIONS OF AROMATIC COMPOUNDS 5-MEMBERED RINGS WITH BASES

### Abstract

Bases are added during the extraction process to enhance liberation of bitumen. Caustics are added in upgrading to minimize slime coating and improve the recovery of bitumen by increasing the pH levels. The objective of this chapter was to study the impact of different bases on 5-membered aromatic compounds under mild conditions. The bases selected for this study were NaOH, NH<sub>4</sub>OH, Ambersep® 900 and NaH. Reactions were performed by heating a dilution of 2 wt% base and 10 wt% model compounds in toluene, to 70 and 120 °C. The organic layer of the solution was then analyzed further. Based on the analyses, it was concluded that the model compounds did not react in the presence of NaOH, NH<sub>4</sub>OH and Ambersep® 900. However, thianaphthene reacted with NaH.

**Keywords:** Bases, sodium reduction

## 4.1 Introduction

For the recovery of bitumen from oilsands, the bitumen extraction process is aimed at separating unwanted solids and water from bitumen. However, after the froth treatment of mined bitumen there are still remains of contaminants (solids) on the surface of the aerated bitumen droplets, which is called a slime coating. The slime is responsible for poor recovery of bitumen.<sup>1,2</sup> To minimize slime coating and to achieve improved bitumen recovery, the pH of the oilsands needs to be raised. Caustics are added to the process to minimize slime coating and improve bitumen recovery by increasing the pH levels.<sup>3</sup> Both ammonium hydroxide and sodium hydroxide are used in the upgrading industry to enhance liberation of bitumen.<sup>3,4</sup>

Strong bases namely alkali metal such as sodium are also utilized in processes like desulfurization. Sodium is known to ease the removal of sulfur and produce low-sulfur content petroleum oil.<sup>5</sup> This was thought of as an alternative to higher hydrogen consumption during hydrodesulfurization.<sup>6</sup>

Bases are used in upstream processes prior to upgrading of bitumen, as well as, downstream processes. The reactions of 5-membered naphtheno-aromatic compounds with bases were studied to better understand how compounds like indene, indole, benzofuran and thianaphthene would behave in the presence of a proton accepting or hydride ( $H^-$ ) donating groups. In this chapter, selected bases namely NaOH,  $NH_4OH$ , Ambersep® 900 and NaH were reacted with the model compounds.

The objective of this chapter is focused on studying the possible implications that different bases could have on reacting with the heterocyclic compounds attached to aromatic rings at lower temperatures.

## 4.2 Experimental

### 4.2.1 Materials

The list of chemicals used can be found in Section 3.2.1 of Chapter 3 (acids). Additional chemicals that were used are listed below (table 4.1).

Ambersep® 900 was used as a base resin. It is strongly basic, macroreticular polymer of styrene-divinylbenzene, with quaternary ammonium anion.

**Table 4.1** Materials employed in this study

Compound	Formula	CASRN <sup>a</sup>	Mass fraction purity <sup>b</sup>	Supplier
Sodium hydride	NaH	7646-69-7	0.95	Sigma-Aldrich
Ammonium hydroxide 1N solution	NH <sub>4</sub> OH	1336-21-6	- <sup>c</sup>	LabChem
Ambersep® 900 hydroxide form	-	9017-79-2	- <sup>c</sup>	Sigma-Aldrich
Ethanol (anhydrous)	C <sub>2</sub> H <sub>5</sub> OH	64-17-5	0.999	Sigma-Aldrich

<sup>a</sup> CASRN = Chemical Abstracts Services Registry Number

<sup>b</sup> This is the purity of the material guaranteed by the supplier; material was not further purified

<sup>c</sup> Mass fraction purity not specified

#### 4.2.2 Equipment and procedure

The same experimental procedure and setup was mentioned in section 3.2.2 of Chapter 3. Instead of acids, bases were used in this chapter.

Homogenous reactions involved reactions with ammonium hydroxide, sodium hydroxide and sodium hydride. While the heterogeneous reactions were performed with Ambersep® 900.

In the case of homogenous catalysis (except the reaction with sodium hydride), after the reaction, the solution was further transferred to a 500 mL separation funnel for liquid-liquid extraction. 10 mL of hydrochloric acid was added to neutralize the base. The product was washed three times using 100 mL of water. Since water is a polar solvent in comparison with the non-polar nature of toluene, water was used to dissolve all the base from the product, thereby separating it from the organic layer. Anhydrous sodium carbonate was added after the last wash with water to remove any water molecules present in the organic layer. The product was collected in a vial and weighed to ensure there was not a significant loss of product.

For the reaction with sodium hydride, the model compound and the base were added in equal mass of 0.5 g because of the extremely reactive nature of sodium hydride. The reactions were performed only at one temperature of 120 °C. A deactivation procedure had to be followed after the reaction. Excess amount of ethanol was added to the solution in small amounts till the

solution stopped fuming completely. 200 mL water was added to the solution which created a visible phase separation with the organic layer. The solution was transferred to a 500 mL separation funnel and the water layer was flushed out. The organic layer was collected in a vial and analyzed further.

Heterogeneous catalysis did not require water washing. The liquid product was transferred to a vial using 0.2  $\mu\text{m}$  membrane filter attached to a syringe.

All experiments were only performed once.

Control experiments performed in Chapter 3 were used as references for analyses in this chapter. The control runs were not repeated.

#### *4.2.3 Analyses*

Gas chromatograph coupled with mass spectrometer (GC-MS) was used for analyzing samples in this chapter. The working principle behind these analyses can be found in Section 5.2.3 of Chapter 5.

Differential Scanning Calorimetry (DSC) analysis was performed using Mettler Toledo DSC1 Star<sup>e</sup> System. The DSC was used to investigate the presence of heavier boiling compounds present in the products obtained after the reactions based on the thermal behavior of the samples. The instrument was calibrated for temperature and heat flow using an indium standard. Samples were weighed in 40  $\mu\text{L}$  aluminum crucibles using a Mettler Toledo Model XS105 Dual Range Analytical Balance with a readability of 10  $\mu\text{g}$ , in the range of 0–41 g and a readability of 100  $\mu\text{g}$  for the remaining range, until 120 g. A hole was pierced into the lids using a needle with a diameter of 1mm. The crucibles were then sealed shut with the help of a sealing press. All runs were performed under a nitrogen flow of 100 mL/min. The method (table 4.2) for each model compound was designed with an isotherm segment around their boiling points.

**Table 4.2** Methods built in the DSC corresponding to each of the model compounds selected for the study.

<b>Compound</b>	<b>Method</b>
Indene	80 to 140 °C with increments of 20 K/min 140 to 180 °C with increments of 5 K/min Isotherm segment : 180 °C for 3 min 180 to 500 °C with increments of 15 K/min
Indole	80 to 140 °C with increments of 20 K/min 140 to 255 °C with increments of 5 K/min Isotherm segment : 255 °C for 3 min 255 to 500 °C with increments of 15 K/min
Benzofuran	80 to 140 °C with increments of 20 K/min 140 to 174 °C with increments of 5 K/min Isotherm segment : 174 °C for 3 min 174 to 500 °C with increments of 15 K/min
Thianaphthene	80 to 170 °C with increments of 20 K/min 170 to 220 °C with increments of 5 K/min Isotherm segment : 220 °C for 3 min 220 to 500 °C with increments of 15 K/min

## 4.3 Results

### 4.3.1 Reactions with Ambersep® 900

Reactions of the model compounds with Ambersep® 900 did not produce any results based on the information obtained from the GC-MS. Figure 1 shows the chromatogram obtained for indene on reaction with the base resin. All the peaks on the chromatogram were present in the compound and solvent as impurities, labelled in chapter 3. No peaks were observed between the retention time of 12-35 min. The bump in the chromatogram at a retention time of 4.5 min is the decomposition of an inorganic compound, or salt formed during the water wash.

On analyzing the GC-MS results obtained from reactions of Ambersep® 900 with the other model compounds, the chromatograms for each of the model compounds overlapped with the control samples. Therefore, from the results, no reaction took place to elute products in the temperature range covered by GC-MS analysis. There were no visible changes in the compounds either, unlike for the products obtained after reactions with acids.

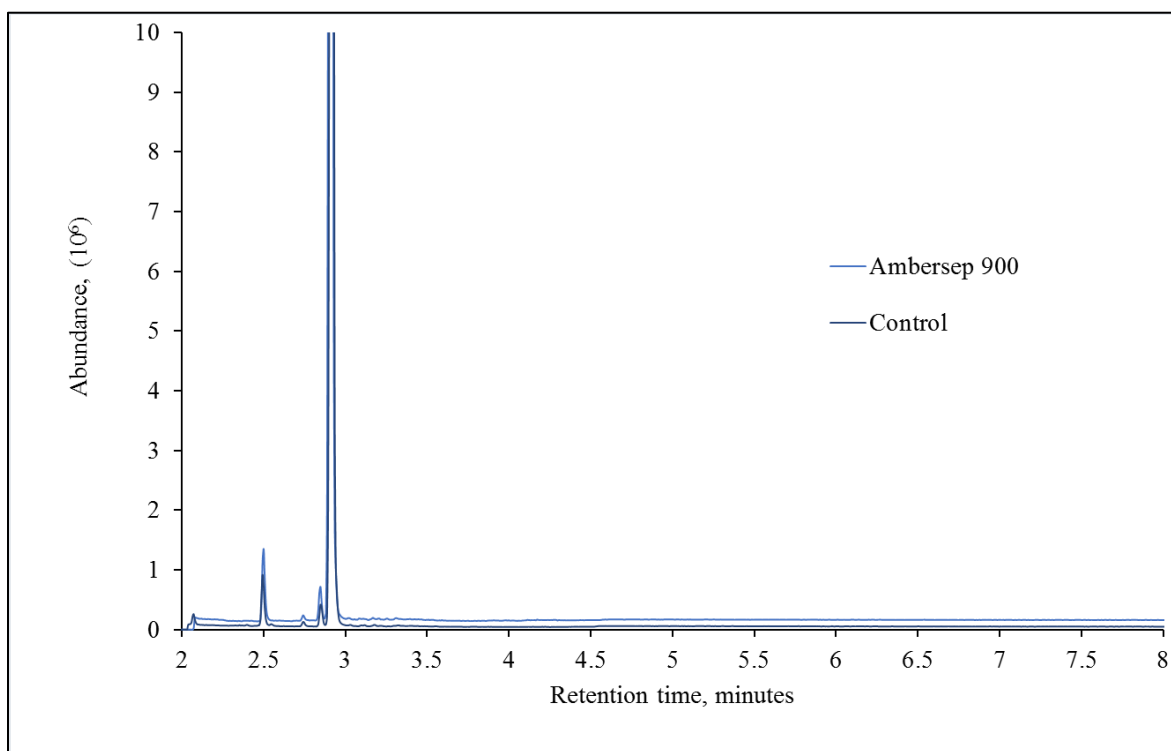


**Figure 4.1** GC-MS result for the reaction of indene with Ambersep® 900 at 55 °C

DSC analysis was carried out to reaffirm that there was no presence of heavier fractions in the products. All products were run under methods that had a temperature range of 80 to 500 °C. According to the results obtained from the DSC, on comparing the curve for the pure compound versus the product obtained after the reaction of indene with Ambersep® 900 can be seen in figure 4.2. The product from the reaction had traces of toluene present. Therefore, all the dips in the heat flow curve are associated with evaporation of a combination of toluene and indene. However, no peaks are observed after a temperature of 180 °C on the heat flow curve. There were no indications of any reactions taking place from the heat flow curve including and beyond the temperature at which products could be eluted by the GC-MS.

From the rest of the reactions with the model compounds, the biggest dip in the heat flow was in the corresponding range of the boiling points of indene and toluene. Figure 4.2 shows results obtained for reaction of Ambersep® 900 with indene from the DSC, respectively.

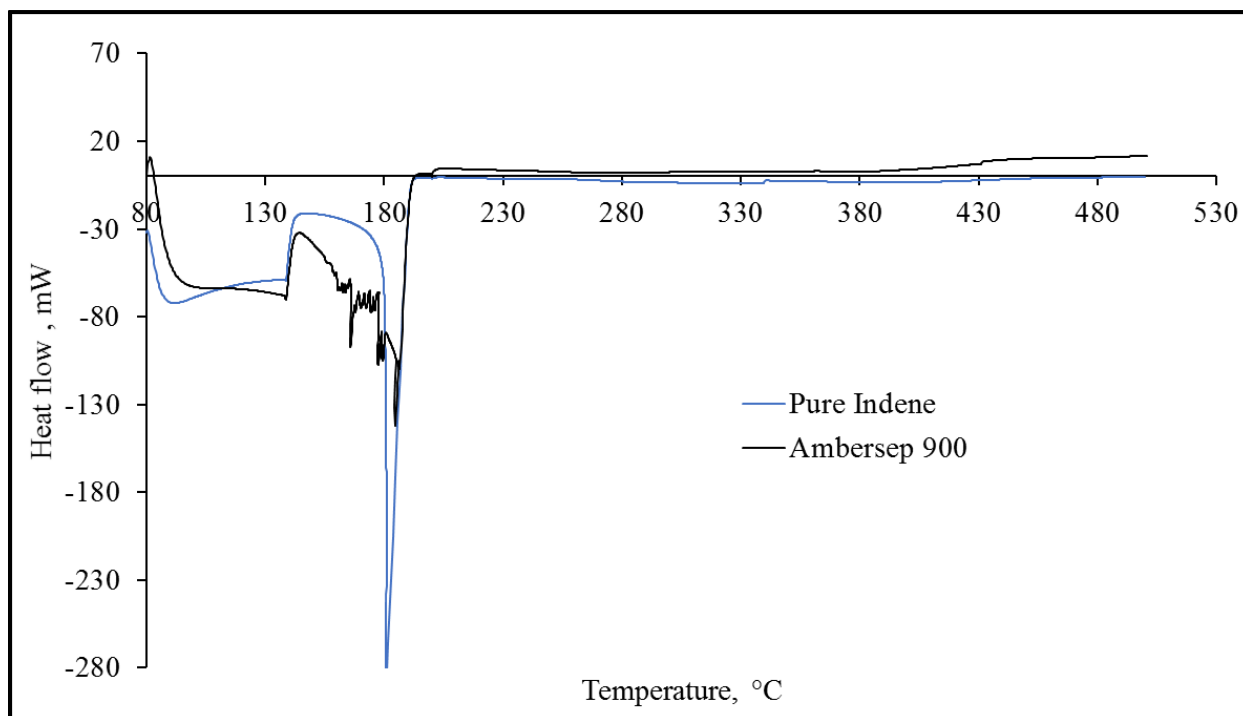


**Figure 4.2** Heat flow obtained from DSC for pure indene versus reaction of indene with Ambersep® 900

#### 4.3.2 Reaction with sodium hydroxide and ammonium hydroxide

On studying the results obtained from the GC-MS and DSC for reactions of 5-membered naphtheno-aromatic compounds with NaOH and NH<sub>4</sub>OH, there were no reactions. The GC-MS results for each model compound overlapped with the chromatograms of the control samples. In DSC heat flow curves, the product curves did not go beyond the corresponding boiling point of the corresponding model compound.

#### 4.3.3 Reactions with sodium hydride

It is known that alkali metals and their hydrides have been used for base-catalyzed hydrogenation of unsaturated hydrocarbons.<sup>7</sup> On conducting experiments in the presence of a strong base like sodium hydride, thianaphthene experienced hydrogenation reaction. The remaining model compounds i.e. indene, indole and benzofuran, did not react. As can be seen from the GC-MS result shown in figure 4.3, there is a defined peak at a retention time of 4.59 min. The remaining peaks were present in the control sample and therefore have not been labelled.

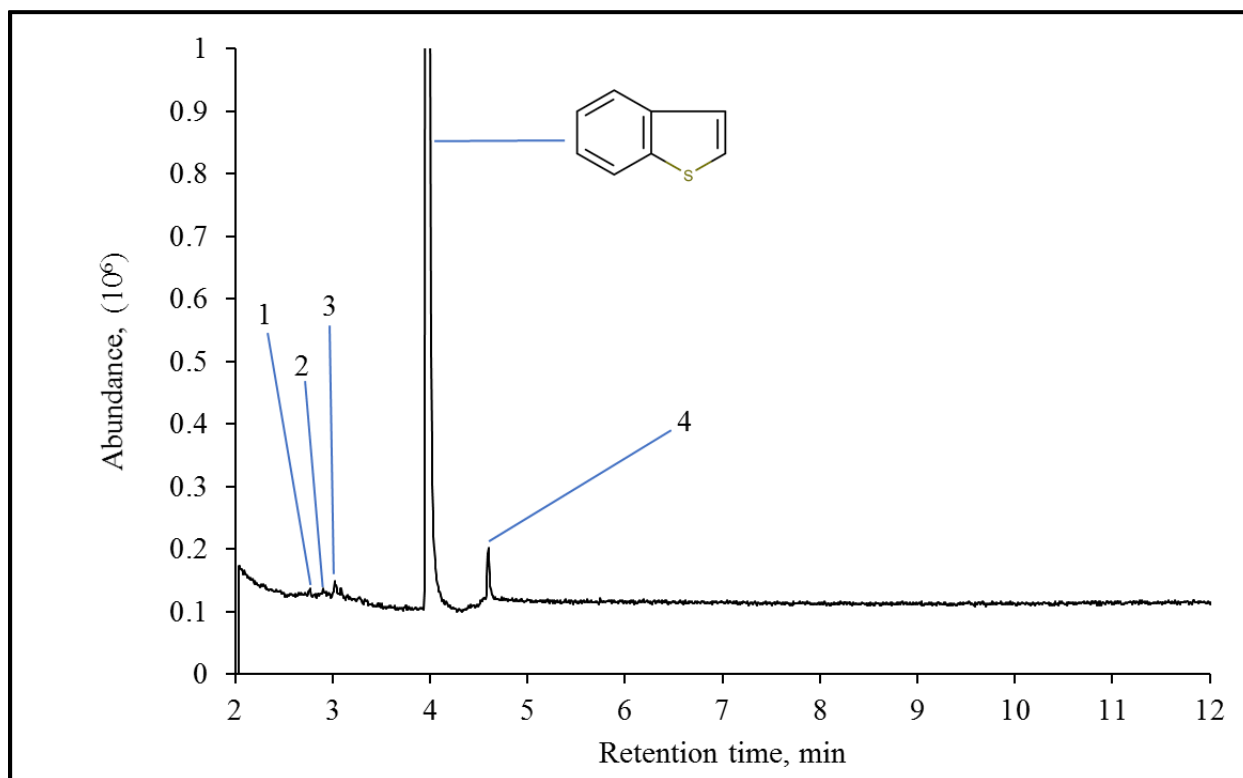


**Figure 4.3** GC-MS result for the reaction of thianaphthene with NaH at 120 °C

**Table 4.3** Products of reactions of thianaphthene with NaH

Peak	Retention time (min)	Compound name	Structure
1 <sup>a</sup>	2.77	- <sup>b</sup>	-
2 <sup>a</sup>	2.91	- <sup>b</sup>	-
3 <sup>c</sup>	3.03	Mass spectrum shown below (figure 4.4a)	Unidentified
4 <sup>c</sup>	4.60	Mass spectrum shown below (figure 4.4b)	Unidentified

a Peak present in the pure compound acquired from the supplier as an existing impurity or unidentified compound.

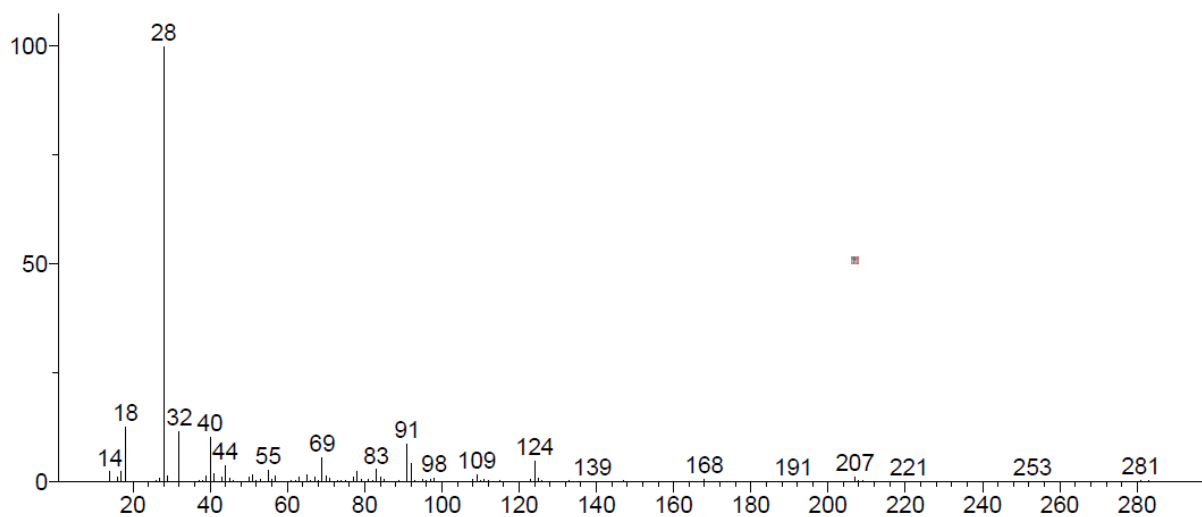
b Mass spectrum for the respective retention time is shown in Appendix A.

c These compounds should be seen only as being indicative of the nature of the products. The true identities of these compounds have not been confirmed.

From figure 4.4 a), at a retention time of 3.03 min, the molecular weight from the mass spectrum is expected to be 124 g/mol. The molecular ion of 91 m/z is related to toluene and might suggest the presence of alkyl benzene group. The difference between the last two fragment ions is 33 m/z. Given the molecular weight of 32 g/mol, it is expected to have a -SH functional group. Therefore, a possible formula of compound could be C<sub>7</sub>H<sub>8</sub>S.

a)

Unknown; InLib=-1589



b)

Unknown; InLib=-441

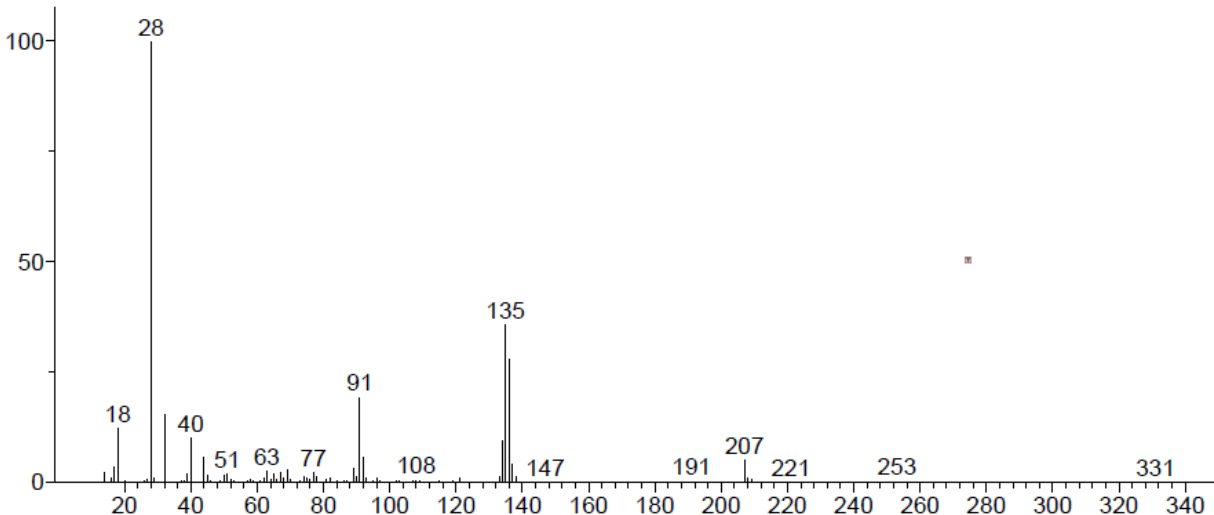


**Figure 4.4** Mass spectrums obtained for reaction of thianaphthene with NaH for peaks a)3 and b) 4

The mass spectrum at a retention time of 4.60 min (peak 4), is shown in figure 4.4 b). The molecular weight from the spectrum is expected to be 136 g/mol. Similar to part a), the molecular ion of 91 m/z is representative of toluene or a possible alkyl benzene fragment. From

the chromatogram, since the peak lies close to the peak for thianaphthene, it can be assumed that the compound constitutes of 8 carbons. Given the difference of 44 m/z, in the last two fragments and the possible composition of the compound containing sulfur, the remaining 12 m/z can account for an extra carbon atom. Therefore, the possible structure of the compound is expected to be C<sub>8</sub>H<sub>8</sub>S. A possible suggestion from the NIST library based on the mass spectrum was 2,3-dihydro-1-benzothiophene.

## 4.4 Discussion

### 4.4.1 Unreactive behavior of alkalis with naphtheno-aromatic compounds

Based on the results from section 4.3.1 and 4.3.2, no reactions took place in the presence of NaOH, NH<sub>4</sub>OH and Ambersep® 900. The bases dissociate into a cation and a hydroxide (OH<sup>-</sup>) ion. Aromatic compounds are weakly acidic in nature. Aromatic compounds commonly take on the role of nucleophiles (electron-rich).<sup>8</sup> In the presence of a hydroxide group (OH<sup>-</sup>), under the reaction conditions in this study there was not sufficient activation energy for the compounds to react with the OH<sup>-</sup> group. Therefore, no reaction was observed with alkalis.

### 4.4.2 Reduction in the presence of sodium hydride

Several studies have been previously shown to have used sodium as an alternative pathway for the removal of sulfur from oil distillates.<sup>5,6,9</sup> Alkali metals are used as strong reducing agents. In the process of desulfurization, the thiophene ring attached to an aromatic is susceptible to undergo hydrogenation in the presence of sodium.<sup>6,10</sup> Sodium was observed to reduce the thiophenic ring and led to the formation of 2,3-dihydro-1-benzothiophene.

To understand the acidity of the model compounds, factors like electronegativity, inductive effect and stability of the conjugate base, need to be compared. Looking at the individual electronegativities of the molecules involved, oxygen is the most electronegative followed by

$N \gg S > C > H$ . Compared to oxygen and nitrogen, sulfur is the least electronegative molecule. The acid dissociation constant ( $pK_a$ ) for deprotonation of C-H bond at the C<sub>3</sub> position, was in the order of indole ( $pK_a = 38.1$ ) > benzofuran ( $pK_a = 33.2$ ) > thianaphthene ( $pK_a = 32.4$ ). Since  $pK_a$  is a negative log value, the lower the  $pK_a$ , stronger the acid is. Therefore, thianaphthene is a relatively stronger acid in comparison to benzofuran and indole.

For reactions with strong bases, the aromatic compounds form conjugate bases. The aromatic compound with the most stable conjugate base, acts as the strongest acid.

In the reaction of hydrogenation of thianaphthene to form 2,3-dihydro-1-benzothiophene in the presence of sodium hydride, the sodium is most likely to partake in the reaction pathway. One proposed mechanism of the thianaphthene reacting with NaH, is the addition of a positively charged sodium ion. From literature it is known that, when a sulfur is present next to an alkene, the  $\pi$ -bond in C=C is disrupted. The reaction shown below takes place.<sup>11</sup>



If the heterocycle follows the mechanism mentioned above, and delocalization of charges takes place, the negative charge is transferred to the benzene ring, giving the structure a negative charge.

Sodium reacts with a binuclear aromatic. It attacks the sulfur in the compound, forming an intermediate for the reaction. To completely understand the chemistry, however, the aqueous layer separated during the deactivation must be analyzed further. Since the aqueous phase was not analyzed, the reaction chemistry can not be described with accuracy.

## 4.5 Conclusion

Binuclear aromatic compounds with 5-membered rings were reacted in the presence of bases at temperatures of 70 and 120 °C. The reactions were performed to understand the impact that the presence of the selected compounds could potentially have on alicyclic and heterocyclic compounds attached to aromatic rings at different stages of the upgrading process under mild conditions. The main conclusions and observations were as follows:

- a) Caustics used for washing of oilsands, like NaOH and NH<sub>4</sub>OH, on reaction with 5 membered rings attached to aromatics did not form any products. Therefore, there is no reason for concern of these compounds creating byproducts or undergoing deleterious reactions based on the current extraction process.
- b) To investigate the behavior of the model compounds with a stronger base resin with a hydroxide group, reactions were performed. No reaction was observed.
- c) On exposing thianaphthene to a strong reducing agent, namely NaH, it reduced to 2,3-dihydro-1-benzothiophene.

## 4.6 References

- (1) Masliyah, J.; Zhou, Z. J.; Xu, Z.; Czarnecki, J.; Hamza, H. Understanding Water-Based Bitumen Extraction from Athabasca Oil Sands. *Can. J. Chem. Eng.* **2008**, 82 (4), 628–654.
- (2) Liu, J.; Xu, Z.; Masliyah, J. Interaction Forces in Bitumen Extraction from Oil Sands. *J. Colloid Interface Sci.* **2005**, 287 (2), 507–520.

- (3) Tamiz Bakhtiari, M.; Harbottle, D.; Curran, M.; Ng, S.; Spence, J.; Siy, R.; Liu, Q.; Masliyah, J.; Xu, Z. Role of Caustic Addition in Bitumen-Clay Interactions. *Energy Fuels* **2015**, *29* (1), 58–69.
- (4) Flury, C.; Afacan, A.; Tamiz Bakhtiari, M.; Sjoblom, J.; Xu, Z. Effect of Caustic Type on Bitumen Extraction from Canadian Oil Sands. *Energy Fuels* **2014**, *28* (1), 431–438.
- (5) Fink, T. E.; Bearden, R. Alkali Metal Desulfurization Process for Petroleum Oil Stocks Using Low Pressure Hydrogen. 3,787,315, 1974.
- (6) Styles, Y.; De Klerk, A. Sodium Conversion of Oilsands Bitumen-Derived Asphaltenes. *Energy Fuels* **2016**, *30* (7), 5214–5222.
- (7) Pines, H.; Stalick, W. M. *Base-Catalyzed Reactions of Hydrocarbons and Related Compounds*; Academic Press: New York, **1977**.
- (8) Solomons, T. W. G.; Fryhle, C. *Organic Chemistry*, 10th ed.; John Wiley & Sons, Inc.: Hoboken, N.J, **2011**.
- (9) Sternberg, H. W.; Donne, C. L. D.; Markby, R. E.; Friedman, S. Reaction of Sodium with Dibenzothiophene. A Method for Desulfurization of Residua. *Ind. Eng. Chem. Process Des. Dev.* **1974**, *13* (4), 433–436.
- (10) Friedman, S.; Kaufman, M. L.; Wender, I. Alkali Metals As Hydrogenation Catalysts for Aromatic Materials. *J. Org. Chem.* **1971**, *36* (5), 694–697.
- (11) Price; Caole, C.; Oae, S. *Sulfur Bonding*; Ronald Press Co: New York, **1962**.

## CHAPTER 5 : FREE RADICAL ADDITION REACTIONS OF AROMATIC COMPOUNDS CONTAINING FIVE MEMBERED RINGS UNDER THERMAL CONVERSION CONDITIONS

### Abstract

Thermal cracking reaction pathway is applied in upgrading of bitumen to break larger molecules. The objective of this chapter was to study the effect of thermal cracking conditions on five membered rings attached to aromatic compounds. To study this, selected model compounds were pressurized in a batch reactor under nitrogen and heated to a temperature of 400 °C, for reaction times of 30 and 60 min. It was found that under these conditions, indene, benzofuran and indole went through free radical addition reactions. This led to the formation of much heavier compounds and ring-opening polymerization in some cases. Indene being highly susceptible to free radical reactions, formed *n*-pentane soluble fractions. With increase in reaction time there was an increase in the *n*-pentane soluble fractions. On the other hand, indane and thianaphthene did not react and they did not show any presence of free radicals in their products.

**Keywords :** Thermal cracking, free radical addition reaction, asphaltene formation

## **5.1 Introduction**

Fouling, catalyst deactivation, weathering, higher viscosity and storage instability, are major concerns in the upgrading and refining processes. It was suspected that fouling, higher viscosity and premature onset of coking can be blamed on free radical addition reaction chemistry.<sup>1</sup> Five membered rings attached to aromatic compounds have shown to form addition products. From previous studies performed on heterocyclic compounds attached to aromatics, under autoxidative conditions, it was found that these compounds had high propensity to undergo free radical addition reactions. They have tendencies to form stable free radical intermediates in the order of indene, followed by derivatives containing N>O>>S. These reactions were held responsible for increased viscosity of bitumen and weathering of oilsands.<sup>2</sup>

Based on the evidence, in the presence of these compounds and their derivatives in bitumen, it is important to study their impact on the upgrading process.

A study was done to better understand the tendency of all the selected compounds to undergo free radical reactions. This chapter investigates the impact of thermal cracking conditions, i.e. 2 MPa and 400 °C, on model compounds in a micro-batch reactor without the presence of any other compound affecting the reaction. Thermal cracking conditions were selected for this chapter to study effects of indene, indane, indole, benzofuran and thianaphthene on the upgrading processes, olefin treatment, as well as asphaltene processing where the exposed conditions are much more intensified.

## **5.2 Experimental**

### *5.2.1 Material*

All chemicals used are listed in table 5.1. Only model compounds were used for experimentation purposes in batch reactors without the presence of any solvent. Pentane was used to determine asphaltene content after obtaining the products from the batch reactors.

**Table 5.1** Materials employed in this study

Compound	Formula	CASRN <sup>a</sup>	Mass fraction purity <sup>b</sup>	Supplier
<i>Chemicals</i>				
Indene	C <sub>9</sub> H <sub>8</sub>	95-13-6	0.90	Sigma-Aldrich
Indane	C <sub>9</sub> H <sub>10</sub>	496-11-7	0.95	Sigma-Aldrich
Indole	C <sub>8</sub> H <sub>7</sub> N	120-72-9	0.99	Sigma-Aldrich
Benzofuran	C <sub>8</sub> H <sub>6</sub> O	271-89-6	0.99	Sigma-Aldrich
Thianaphthene	C <sub>8</sub> H <sub>6</sub> S	95-15-8	0.95	Sigma-Aldrich
Carbon Sulfide	CS <sub>2</sub>	75-15-0	0.999	Fisher
<i>n</i> -pentane	C <sub>5</sub> H <sub>12</sub>	109-66-0	0.994	Fisher
<i>Cylinder gases</i>				
Nitrogen	N <sub>2</sub>	7727-37-9	0.99999 <sup>c</sup>	Praxair

<sup>a</sup> CASRN = Chemical Abstracts Services Registry Number

<sup>b</sup> This is the purity of the material guaranteed by the supplier; material was not further purified

<sup>c</sup> Mole fraction purity

### 5.2.2 Equipment and Procedure

Thermal cracking is expected to occur at a temperature of 400 °C and pressure of 2 MPa. Conversion for the selected model compounds were performed under those conditions in Swagelok 316 stainless steel micro batch reactors (1 inch in diameter and 3.4 inch in length). In a typical experiment the selected model compound was transferred to a glass vial and weighed on a Mettler Toledo balance XP1203S. The scale had a readability limit of 1 mg with a maximum capacity of 1210 g. The glass vial was placed in a micro batch reactor. The batch reactor was closed, and a leak test was performed with the help of nitrogen. On purging the reactor of any air, nitrogen gas was used to pressurize the reactor to 2 MPa. A fluidized sand bath (SBS-4 from Techne) with a set point temperature of 400 °C was used to heat the batch reactor with a low-pressure air flow for fluidizing the sand and ensuring good heat transfer. The reactors were left in the bath for two different intervals of 30 and 60 min.

After removing the reactor from the sand bath, the reactor was left to cool down and reach room temperature. The gas present in the reactor was released into the fumehood. The reactor was then

opened and the glass vial with the product was retrieved. The products were stored under nitrogen atmosphere to prevent any further reactions. All runs were performed only once.

### 5.2.3 Analysis

To study the asphaltene content, 2 g of the product was transferred into an amber vial. 80 mL of *n*-pentane was added to the vial and was left to stir at room temperature for 1 h. After 24 h, vacuum filtration technique was used to separate any solids present from the liquid solution using a filter paper. The solids collected on the 0.22  $\mu\text{m}$  filter papers were left to dry in the fumehood for 24 h before weighing them. The pentane was evaporated from the liquid sample using the rotovap (Heizbad Hei-VAP from Heidolph) at 40  $^{\circ}\text{C}$  at atmospheric pressure. The liquid obtained was further analyzed.

The gas chromatograph coupled with mass spectrometer (GC-MS) was used to analyze the composition of the liquid products. The instrument used was an Agilent 7820A gas chromatograph with a 5977E mass selective detector. The instrument employed a HP-5 capillary column with dimensions of 30 m x 0.25 mm x 0.25 $\mu\text{m}$ . Helium gas was the mobile phase flowing in at a rate of 1 mL/min. Samples for the GC analysis were prepared by diluting 1 vol% of the product sample in toluene or *n*-pentane. *n*-Pentane was used for dilution for liquid products obtained from the asphaltene content analysis, the rest of the samples were diluted in toluene. For all samples, the method was set to have the oven temperature at 100  $^{\circ}\text{C}$  before sample injection. After injection, there was an increase of 10  $^{\circ}\text{C}/\text{min}$  to 320  $^{\circ}\text{C}$  and the temperature stayed at 320  $^{\circ}\text{C}$  for 13 min. The solvent delay was different based on the solvent selection for dilution. In case of toluene, the detector was turned off between the retention time of 1.5-2 min while for *n*-pentane the detector was off from 1.3-1.5 min.

Electron Spin Resonance analysis was run on the liquid products using Active Spectrum Micro-ESR. Studying the electron spin of the electrons helped understand the presence of free radicals in the system. Spin calibration was done using 2,2-diphenyl-1-picrylhydrazyl (DPPH). 20 mg of the sample was diluted in 600  $\mu\text{L}$  of toluene in Norell<sup>®</sup> Standard Series <sup>™</sup> 5mm NMR tubes. 7

sweeps were performed in the sweep field of 3400-3500 G. The microwave power was set to 15 mW.

Simulated Distillation by gas chromatography (SIMDIS Agilent Technologies Model 7890B) helped provide a boiling point curve for products. The column installed in the instrument was DB-HT-SIMDIS 5 m x 0.53 mm x 0.15  $\mu\text{m}$ . Detailed working principle of the SIMDIS can be found in ASTM D7169-11. The curve was able to provide information on the heavier fractions present in the samples with normal boiling point temperatures as high as 750  $^{\circ}\text{C}$ . Two standards were run in the SIMDIS- Polywax 655 and reference material 5010. Polywax 655 was run for the calibration of retention time to build a boiling point curve. Reference material 5010 was used for calibrating response factor of the detector to calculate quantitative recovery of sample. The two references were selected in accordance with the method. The selected method was aimed at obtaining boiling point distribution for incompletely eluting samples.<sup>3</sup> Sample preparation was carried out by preparing a dilution of 1 wt% product in  $\text{CS}_2$ .

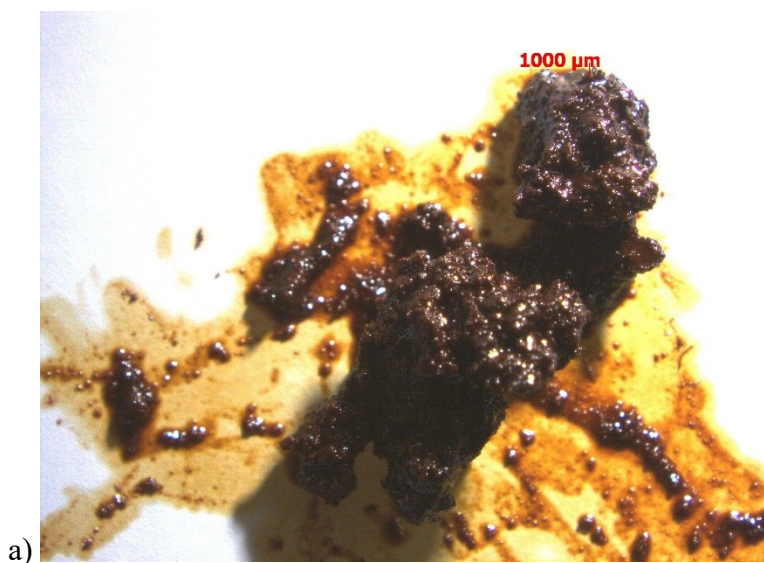
Fourier Transform infra-red (FTIR) spectroscopy was performed using an ABB MB 3000. The FTIR spectra were used to confirm the presence of specific functional groups in the products. 120 scans were performed at a resolution of 4  $\text{cm}^{-1}$  and detector gain of 243. The spectrum data was collected within a wavenumber range of 400-4000  $\text{cm}^{-1}$  under a transmittance acquisition mode.

Carl Zeiss StereoMicroscope Discovery V2.0 helped magnify images of products that underwent visible changes in their appearance and structures. Photos of the images were taken and added in the chapter. The microscope had a zoom range of 20:1. The images were able to be magnified up to 345x using a 10x eyepieces.

## 5.3 Results

### 5.3.1 Physical changes

The first indication that a chemical reaction had taken place inside the batch reactor under thermal cracking conditions was evident from the color of the product obtained for most of the model compounds. Model compounds, namely indene, indole and benzofuran formed products which were black in color. Figure 1 shows the images captured of the products obtained under the Ziess microscope.





c)

**Figure 5.1** Images of products obtained after the reaction of a) indene b) indole and c) benzofuran captured using the Zeiss microscope

No changes were visibly observed in the reaction products from the thermal conversion of indane and thianaphthene. The products looked similar to the pure compounds prior to reactions.

### 5.3.2 Asphaltene content

Based on physical changes, it was hypothesized that there were heavier products formed during the reaction. Indene, indole and benzofuran were in turn good candidates to perform the asphaltene content, to study the possible amount of solid formation, if any. In order to do so, the pure model compounds of the three, were tested for their solubility in *n*-pentane. In case of benzofuran and indole, even though the final products were black in color, the asphaltene content was a meaningless measure, because the pure form and the final product obtained were both insoluble in *n*-pentane.

However, indene was found to contain *n*-pentane insoluble solids (asphaltenes) which were separated using vacuum filtration. The solid formation was observed to increase with increase in reaction times from 30 to 60 min. 35.1% solids were formed for a reaction time of 30 min and the amount approximately doubled to 71.9% when the reaction ran for a period of 60 min.

Figure 5.2 provides a comparison for the ratios of solid and liquid formed by conversion of indene at reaction time of 30 and 60 min.

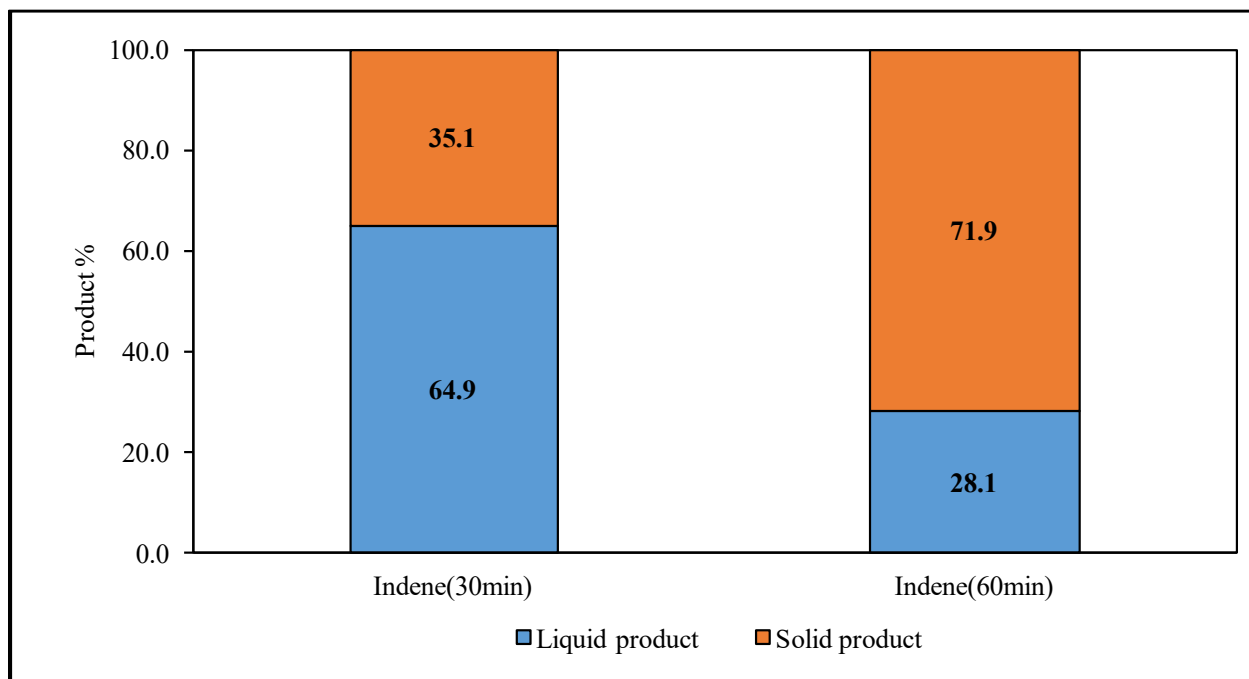


**Figure 5.2** Asphaltene content for indene at reaction times of 30 and 60 min

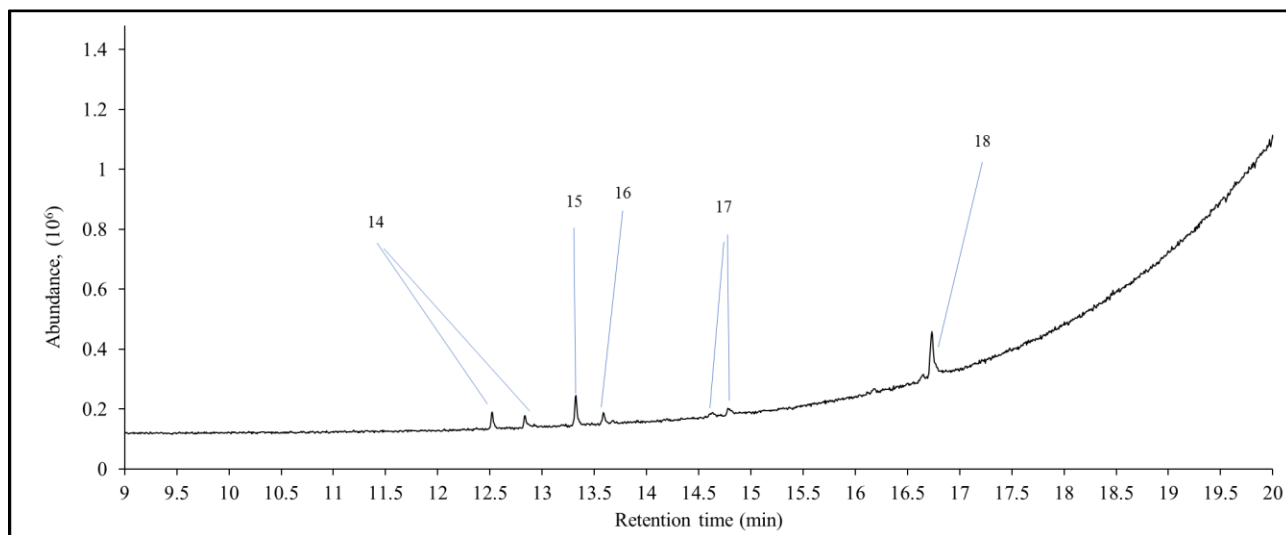
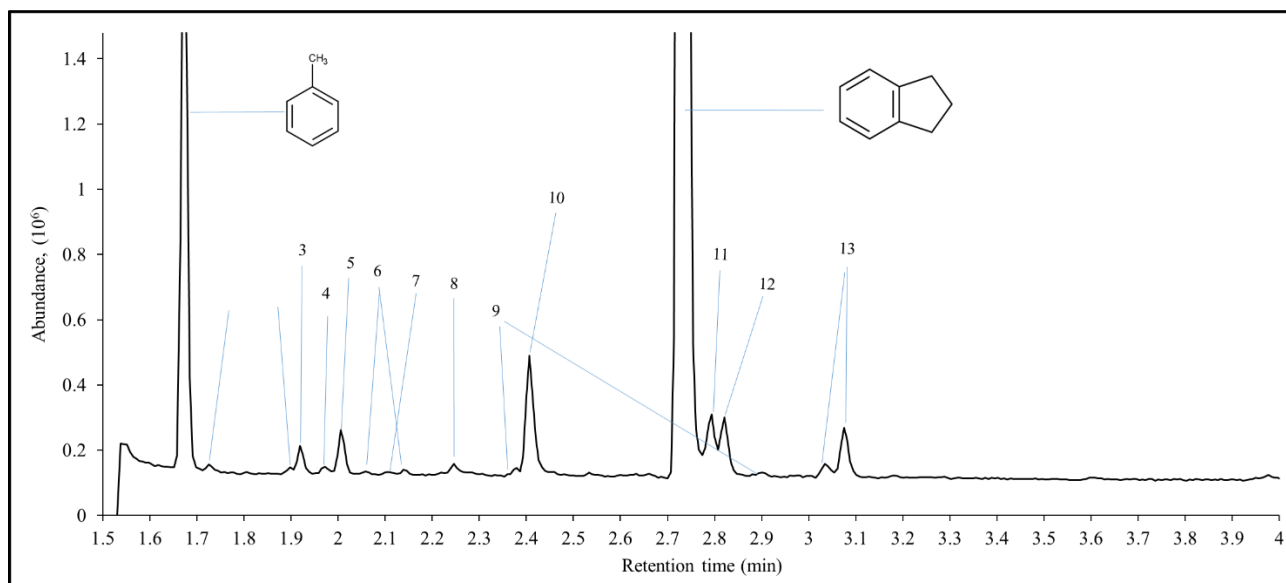
### 5.3.3 Gas Chromatograms

On analyzing all the samples using gas chromatography mass spectroscopy, the only model compounds that had detectable peaks, other than the initial reactant, were benzofuran and the *n*-pentane soluble fractions of indene.

No new peaks were displayed for the product obtained for indane. It was speculated that indane was unreactive at the test conditions because there were no hydrogen acceptors, only indane. Further reactions were performed in a batch reaction with equal proportions of indene and indane which will be discussed later in section 5.3.7 of this chapter.

The final indene product had solid fractions present which were insoluble in the pentane. From the gas chromatogram obtained for the soluble fraction (figure 5.3), minute amount of indene at a

retention time of 2.8 min was present. The largest peak was at a retention time of 2.7 min for indane. Hence, indane was formed in abundance. The peak for toluene was present at a retention time of 1.7 min because it was used as a cleaning solvent and had not completely evaporated from the walls of the reactor. Some compounds point towards two or more different peaks and displayed the same major fragment ion peaks in their mass spectrum reports. Those peaks are representative of presence of isomers for the respective compounds.



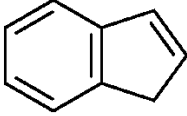
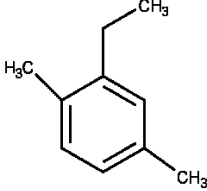
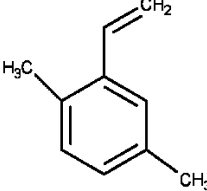
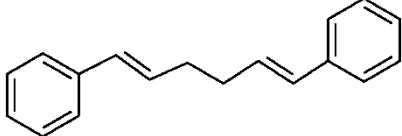
*\*Unlabeled peaks from retention time 9-20 min are indicative of column bleeding*

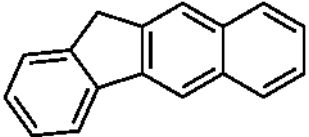
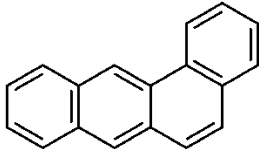
**Figure 5.3** Results from gas chromatography obtained for the *n*-pentane soluble fractions of indene

between the retention times of 1.5 to 20 minutes for a 60 min reaction of indene at 2 MPa and 400 °C. Numbered peaks are identified in Table 5.2

Peaks 1-9 are impurities present in either in the solvent (*n*-pentane) or indene, provided by the supplier. The compounds eluting at those retention times were already present before the reaction.

**Table 5.2** Compound list from the GC-MS results for a 60 min reaction of indene at 2 MPa and 400 °C

	Retention time (min)	Compound name	Chemical structure
1 <sup>a</sup> -10 <sup>a</sup>	1.73 - 2.41	- <sup>b</sup>	-
11 <sup>c</sup>	2.79	Indene	
12 <sup>c</sup>	2.81	2-Ethyl-1,4-dimethylbenzene	
13 <sup>c</sup>	3.05, 3.08	Isomers of 2-Ethenyl-1,4-dimethylbenzene	
14 <sup>c</sup>	12.52, 12.84	Mass spectrum shown below (figure 4a)	Unidentified
15 <sup>c</sup>	13.33	[(1E,5E)-6-Phenylhexa-1,5-dien-1-yl]benzene	
16 <sup>c</sup>	13.59	Mass spectrum shown below (figure 4b)	Unidentified

17 <sup>c</sup>	14.53, 14.69	Isomers of 11H-Benzo[b]fluorene	
18 <sup>c</sup>	16.74	Benz[a]anthracene	

a Peak present in the pure compound acquired from the supplier as an existing impurity or unidentified compound.

b Mass spectrum for the respective retention time is shown in Appendix A.

c These compounds should be seen only as being indicative of the nature of the products. The true

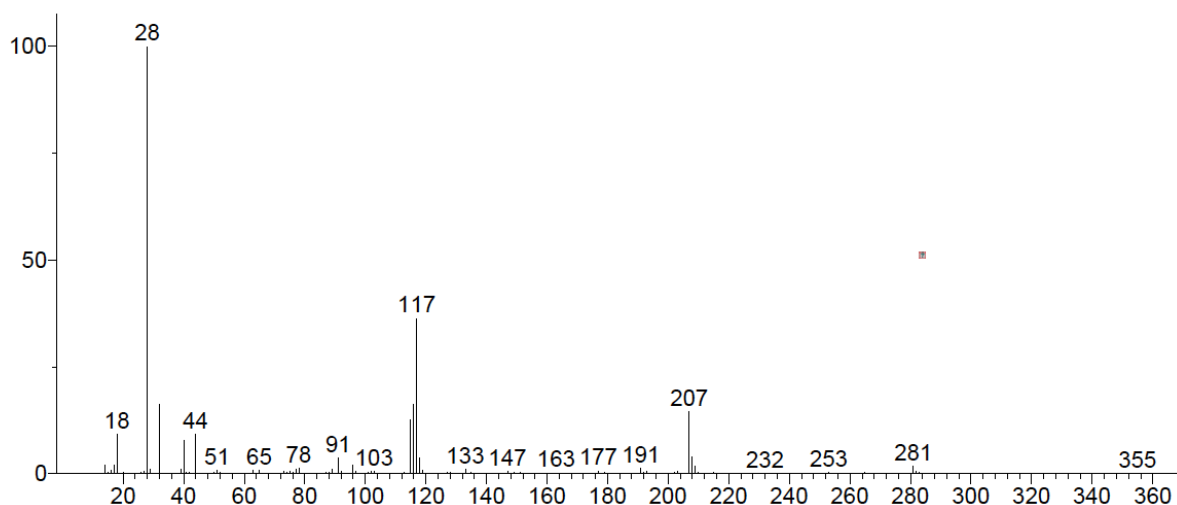
identities of these compounds have not been confirmed.

From figures 5.3, it is evident that there are reactions involving both ring opening and polymerization when subjected to thermal cracking conditions. They constitute both addition reactions and bond breakage.

For a retention time of 12.52 min and 12.84 min, the mass spectrum obtained were identical. The mass spectrum for peak 14 is shown in figure 5.4 for a retention time of 12.52 min. Since a heavier molecule does not elute before the retention time of 12.52 min, it can only be assumed based on the peak 15, that the compound might constitute of 16 carbon atoms. The expected molecular weight from the spectrum is expected to be 207 g/mol. Therefore, the compound is likely to have the molecular formula of C<sub>16</sub>H<sub>15</sub>.

a)

Unknown; InLib=-2179



b)

Unknown; InLib=-1589

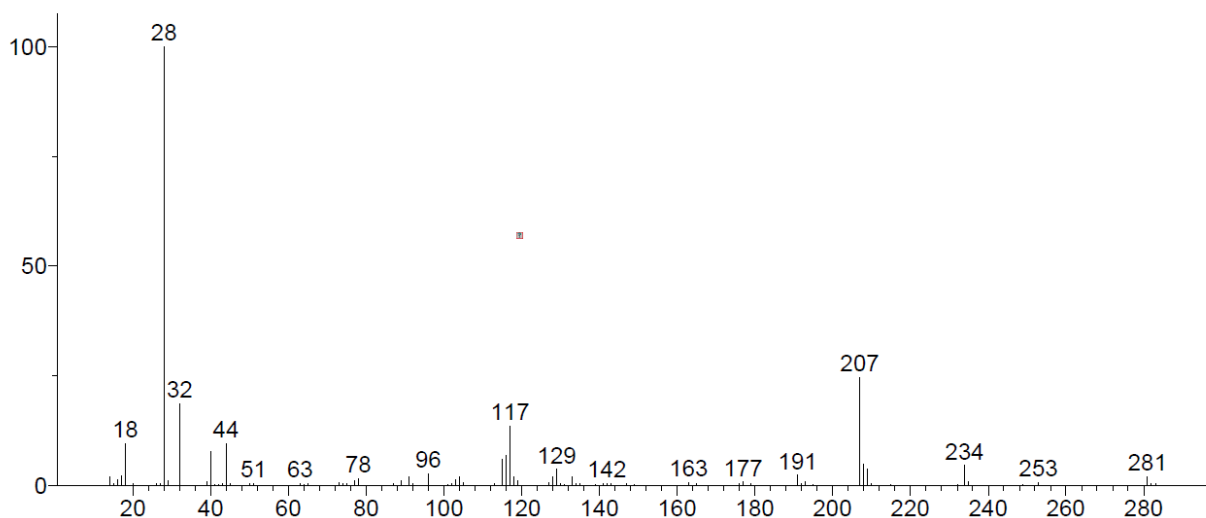


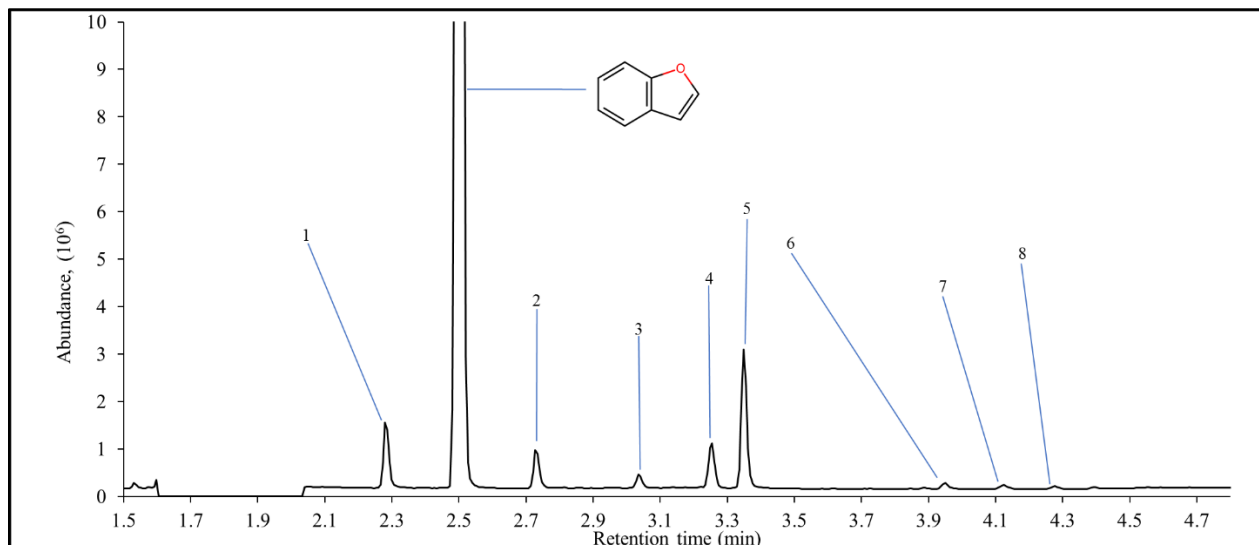
**Figure 5.4** Mass spectrum for peak 14 at retention times of a) 12.52 min, 12.84 min and, peak 16 at a retention time of b) 13.59 min, for reaction of indene for 60 min

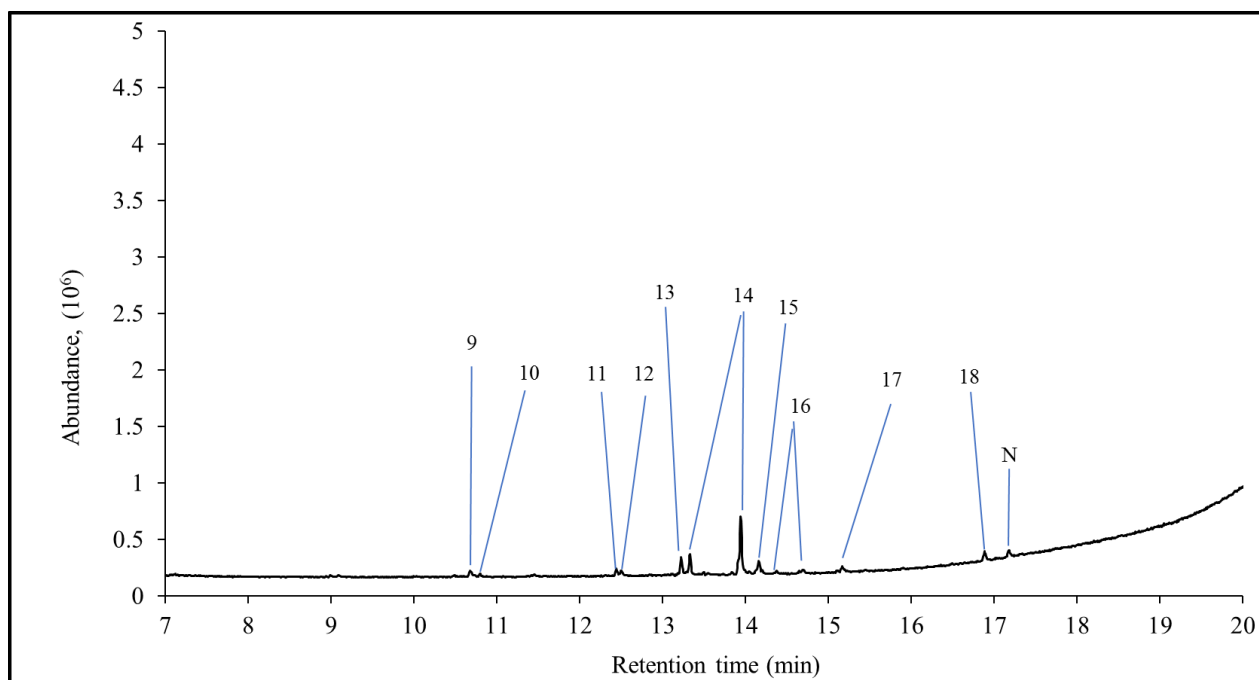
At a retention time of 13.59 min, for peak 16, the expected molecular weight is approximately 281 g/mol. On studying the major molecular ions, there is a peak at 78 m/z, demonstrating presence of a benzene ring. The difference between 207 m/z and 129 m/z also indicates elution of another benzene ring. Therefore, the compound constitutes of 2 benzyl rings in the structure. Calculating the differences in the remaining fragments, there is a presence of a 39 m/z, 12 m/z

and 27 m/z. Together, that indicates presence of 6 carbon atoms, in addition to 12 carbons for the two benzene rings. The molecular formula of the compound, therefore, is C<sub>18</sub>H<sub>18</sub>.

Benzofuran still had remains of the model compound as the most abundant peak according to the gas chromatography (figure 5.5). There was a weak presence of 1,3-dihydro-2-benzofuran at a retention time of 3.0 minutes, indicating a loss of the double bond. The presence of the –OH functional group is strongly visible in a few of the compounds formed. This was analyzed using the FTIR and will be further discussed in section 5.3.6 of this chapter.

Similar to indene, benzofuran also underwent both ring opening, and polymerization reactions as can be seen from figure 5.4.

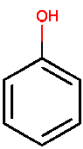
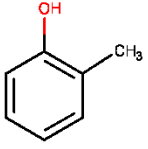
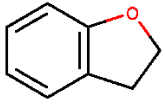


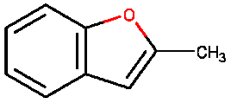
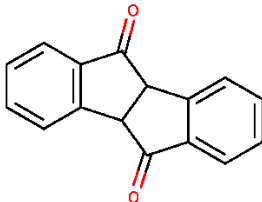
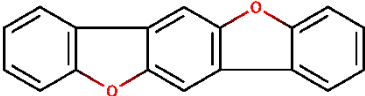


*\*N- Bleeding of the column*

**Figure 5.5** Results from gas chromatography obtained for benzofuran between the retention times of 1.5 to 20 minutes for a 60 min reaction at 2 MPa and 400 °C. Numbered peaks are identified in Table 5.3

**Table 5.3** Compound list from the GC-MS results for a 60 min reaction of benzofuran at 2 MPa and 400 °C

	Retention time (min)	Compound name	Chemical structure
1	2.29	Phenol	
2 <sup>a</sup>	2.73	2-Methylphenol <sup>b</sup>	
3	3.05	2,3-Dihydro-1-benzofuran	

4 <sup>c</sup>	3.26	2-Methyl-1-benzofuran	
5	3.35	2-Ethylphenol	
6 <sup>a</sup> , 7 <sup>a</sup> , 8 <sup>a</sup>	3.94, 4.11, 4.26	- <sup>b</sup>	-
9 <sup>c</sup> - 12 <sup>c</sup>	10.67- 12.48	Mass spectrum shown below (figure 6)	Unidentified
13 <sup>c</sup>	13.23	- <sup>b</sup>	Unidentified
14 <sup>c</sup>	13.33, 13.95	Isomers of 4b,9b-dihydroindeno[2,1-a]indene-5,10-dione	
15 <sup>c</sup> , 18 <sup>c</sup>	14.13, 16.86	Isomers of benzo[1,2-b:4,5-b']bisbenzofuran	
16 <sup>c</sup>	14.35, 14.67	- <sup>b</sup>	Unidentified
17 <sup>c</sup>	15.16	- <sup>b</sup>	Unidentified

a Peak present in the pure compound acquired from the supplier as an existing impurity or unidentified compound.

b Mass spectrum for the respective retention time is shown in Appendix A.

c These compounds should be seen only as being indicative of the nature of the products. The true

identities of these compounds have not been confirmed.

From the mass spectrum of peak 9, the molecular weight is expected to be close to 207 g/mol. There is a presence of a benzyl group, since there is a molecular ion peak at 77 m/z. An oxygen atom is also expected to be present in the molecular composition given the difference of 16 between the molecular ions of 131 m/z and 115 m/z. Looking at the major molecular peaks after 131 m/z, there is a possibility of presence of another benzyl ring (difference between 207 m/z

and 131 m/z). Therefore, the molecule is expected to constitute of 2 benzyl rings and an oxygen atom, connected by an alkyl chain.

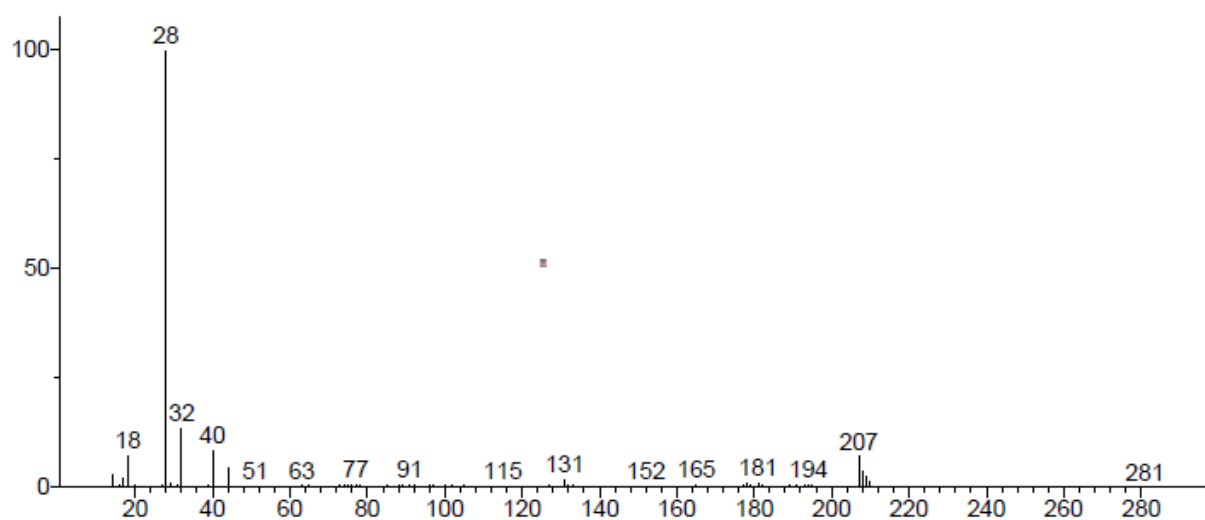
The compound corresponding to the mass spectrum for peak 10 was not able to be identified. The mass spectrum is shown in appendix A.

Focusing on the last three molecular ions present in the mass spectrum of peak 11 (figure 5.6) i.e. 210, 181 and 152 m/z, the difference between the consecutive peaks is equivalent to 29 m/z, which are representative of an ethyl group. The expected molecular mass of the compound is 210 g/mol. The peak of 152 m/z indicates the presence of 2 benzyl groups (76 m/z x 2). From the vicinity of the peak, it is predicted to have 14 carbon atoms.

Peak 12 for reaction of benzofuran, is expected to have a molecular mass of 224 g/mol. On studying the last 2 major molecular ions for peak 12 i.e. 224 and 207 m/z, it was derived that since the difference was of 17 m/z, an alcohol group (-OH) is present in the compound. The difference in the next peaks, is that of 55 m/z, indicating the presence of four carbon atoms. Similar to above, the peak of 152 m/z is representative of 2 benzyl groups. Therefore, accounting for all the carbons, the expected formula for the compound could possibly be C<sub>16</sub>H<sub>15</sub>OH.

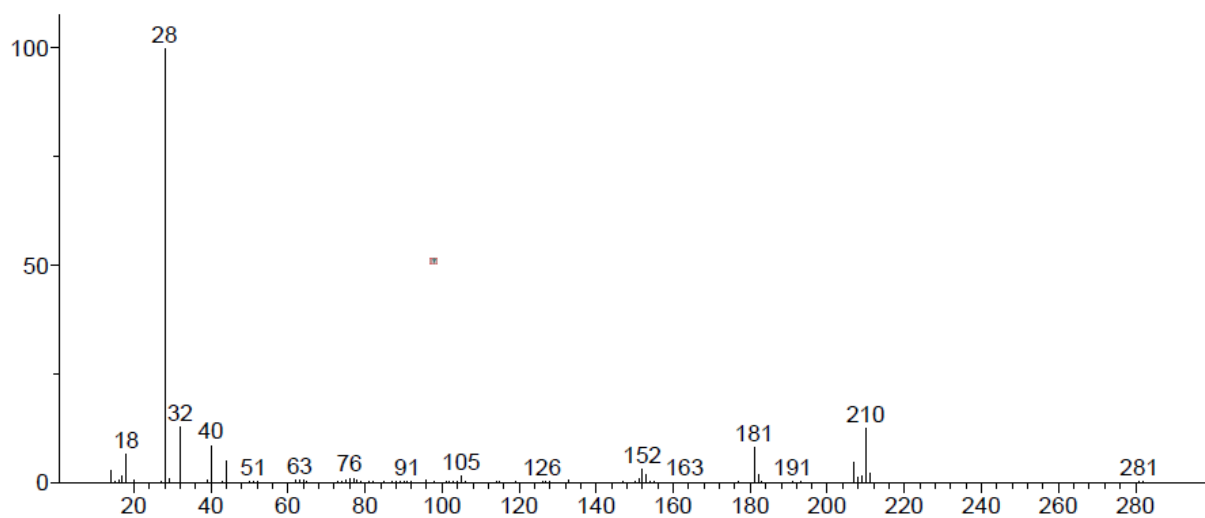
a)

Unknown; InLib=-779



b)

Unknown; InLib=-394



c)

Unknown; InLib=-1187

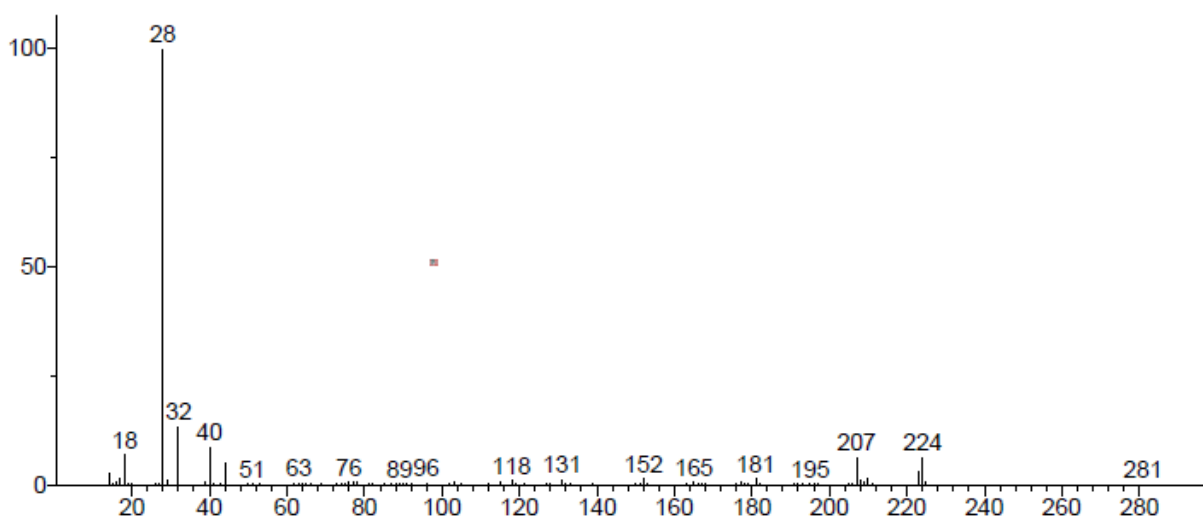


**Figure 5.6** Mass spectrum for peaks a) 9, b) 11 and c) 12, from reaction of benzofuran for 60 min

Peak 13,16 and 17 were not able to be identified and have been included in Appendix A.

Heavier compounds are visible above a retention time of 12 minutes. Isomers of 4b,9b-dihydroindeno[2,1-a]indene-5,10-dione is represented by two peaks at an interval time of 13.4 and 14 minutes, indicating isomers of *cis* and *trans* for the dimer of benzofuran.

Even though there were color changes in indole, the gas chromatogram was unable to capture any peaks apart from that of indole itself. Since the GC-MS had a maximum oven temperature constraint of 325 °C, the SIMDIS was used to investigate the presence of any heavier compounds. Meanwhile, thianaphthene did not have any visible color changes nor any revelation of peaks on the GC apart from the starting material. SIMDIS analysis was performed to confirm whether there were any heavier compounds that went by undetected by the GC-MS.

### 5.3.4 Presence of heavier boiling fractions

On analyzing the product samples using the SIMDIS, it was found that all fractions of indane and thianaphthene boiled at 176.5 °C and 221 °C, respectively. Both temperatures are significantly close to the boiling points of the pure compounds (as given in the NIST library), implying the absence of heavier boiling compounds.

**Table 5.4** Temperatures for heaviest boiling fractions for the model compounds obtained using the SIMDIS at reaction times of 30 and 60 min

Compound	Highest Boiling temperature (°C)	
	30min	60min
Indane	192.0	192.5
Indene	587.0	588.1
Indole	422.6	428.2
Benzofuran	646.9	556.9
Thianaphthene	222.9	222.8

*n*-Pentane soluble fraction of the indene product was analyzed in the SIMDIS. From figure 5.7, indene curves for both reaction times overlapped with only a minor difference. Indene has a boiling point of 182.4 °C (NIST library). Approximately 60 % of the product boils off before the boiling point of indene is reached due to the conversion of indene to indane, leaving 40 % of the mixture to boil off at higher temperatures until 588 °C. The data from the SIMDIS indicated that the highest boiling fractions present in indole consisted of polymers all the way to C<sub>52</sub>. Between the two reaction times, it was observed that for a reaction time of 60 min, the last boil off under a constant temperature of 588 °C is 10%. While for the reaction time of 30 min, at the highest temperature, the wt % distilled for the constant temperature is only 4 %.

Initially, in the plot (figure 5.7), there is a ~10 % distillation of the solvent (*n*-pentane). The bumps in the graph have been split by the degree of polymerization. There are four groups of separation- dimers, trimers, tetramers and pentamers.

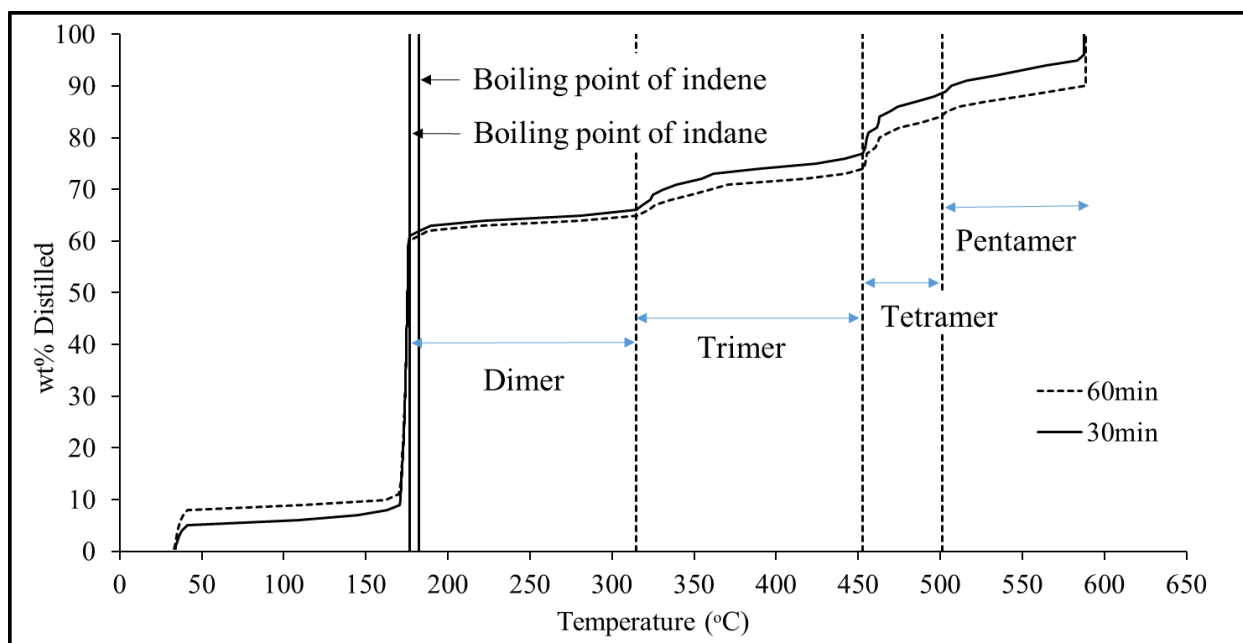


**Figure 5.7** Boiling curve acquired using SIMDIS for the product of indene obtained after reacting for 60 min in a batch reactor

Indole had heavier fractions present on reaction in a batch reactor. As can be seen from table 5.4, there was not a significant difference in the boiling points at the two different reaction times. Similar boiling curves were obtained using the SIMDIS. Indole is known to boil at a temperature of 254 °C (NIST library) which can be correlated to the majority of product boiling off close to that range. Majority of the indole product boils off between temperatures of 224-237 °C. However, approximately 7 % of the product boils at a temperature higher than the boiling point of indole. The data from the SIMDIS indicated that the highest boiling fractions present in indole consisted of polymers all the way to C<sub>26</sub>. Therefore, there is definitive proof that there are, indeed, heavier compounds present in the product which possibly were not eluted during regular temperature gas chromatography.

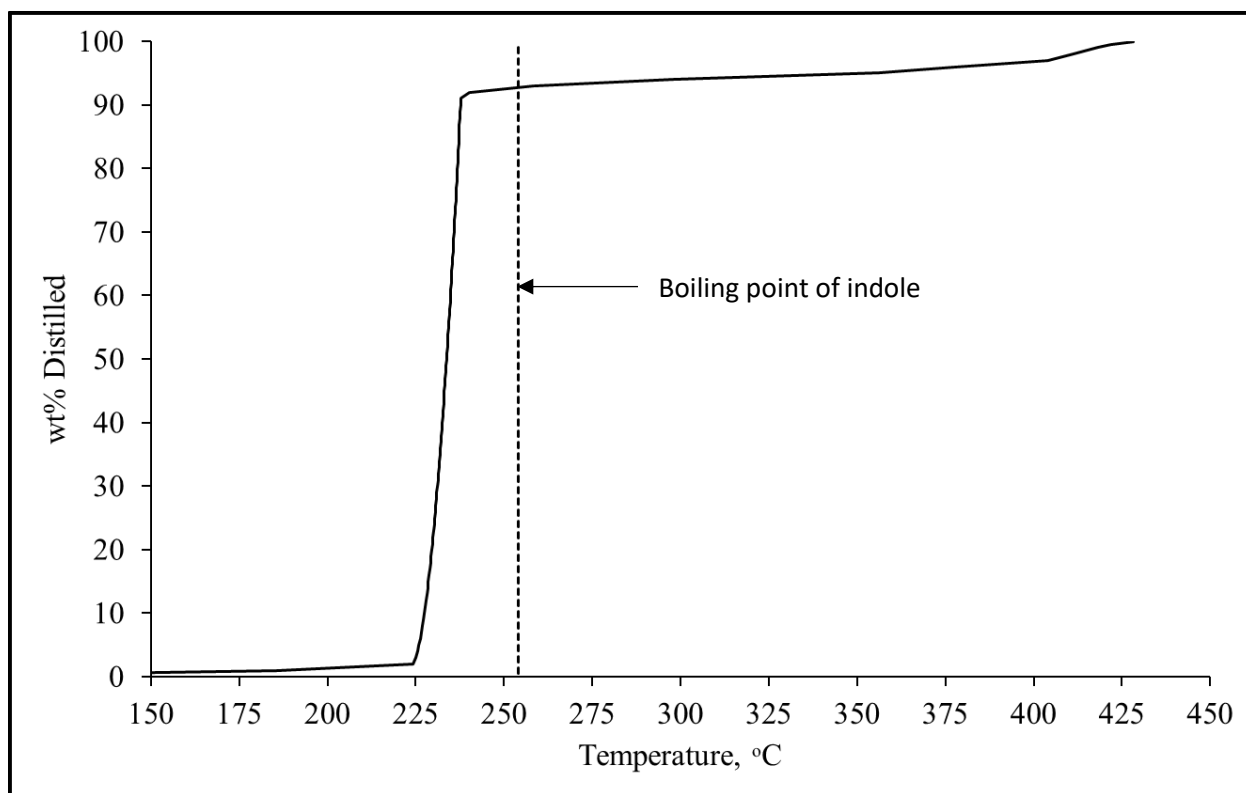


**Figure 5.8** Boiling curve acquired using SIMDIS for the product of indole obtained after reacting for 60 min in a batch reactor

Benzofuran was predicted to have heavier boiling compounds present in the free radical product for reactions at 30 and 60 min. With a boiling point of 174 °C, approximately 62% and 68 % for 60 min and 30 min, respectively were monomeric products. Much higher boiling temperatures were observed. From figure 5.9, it is evident that there are significant fractions present in the products that have higher boiling points all the way to 646.6 °C. Reaction at 30 min revealed higher boiling fractions of C<sub>70</sub> carbon chains while at 60 min, it was only as high as C<sub>46</sub> carbon chains. This demonstrated that product obtained from a lower reaction time contained heavier polymers compared to longer reaction time.

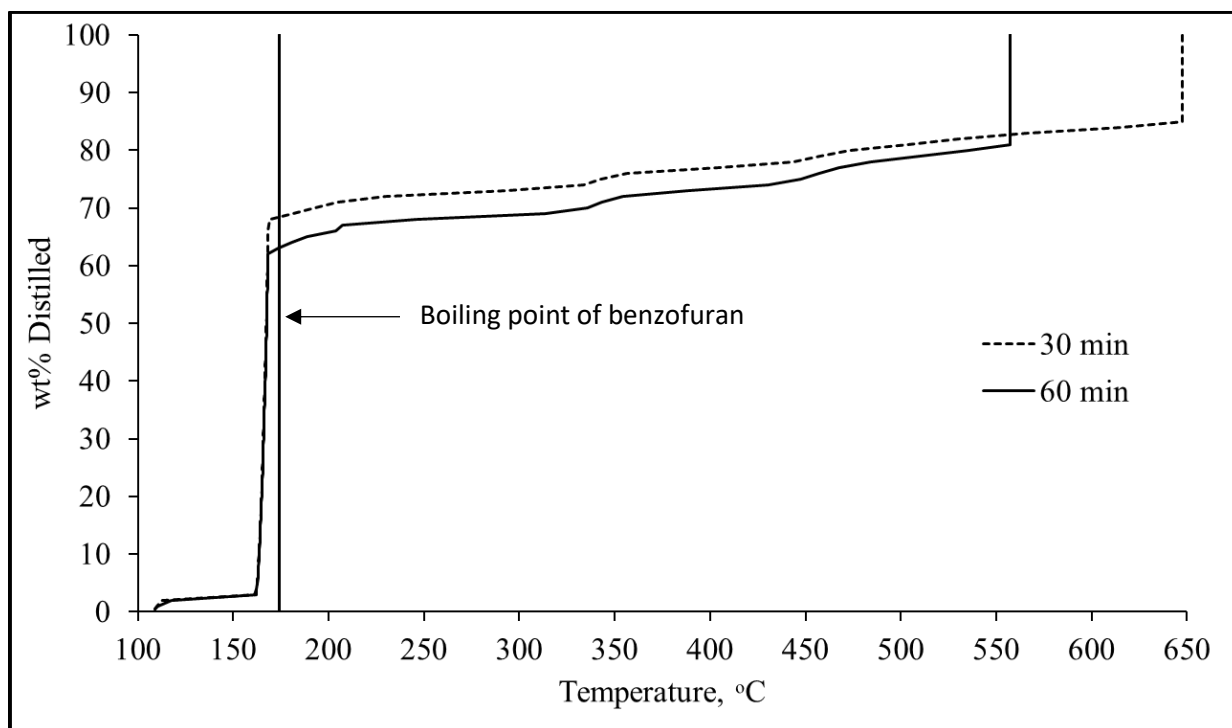


**Figure 5.9** Boiling curve acquired using SIMDIS for the product of benzofuran obtained after reacting for 60 min in a batch reactor

### 5.3.5 Free radicals in products

As hypothesized, indene may have free radicals in the products. Figure 5.10 shows ESR results obtained for both reaction times. On quantifying the results by calculating the double integrals of the curve, from the results there were  $1.4 \times 10^{18}$  spins/g of sample for the product at 60 min compared to a lower value of  $1.3 \times 10^{18}$  spins/g at 30 min. There was a general trend detected for the indene samples, namely, asphaltene content and free radicals increased with respect to reaction time.

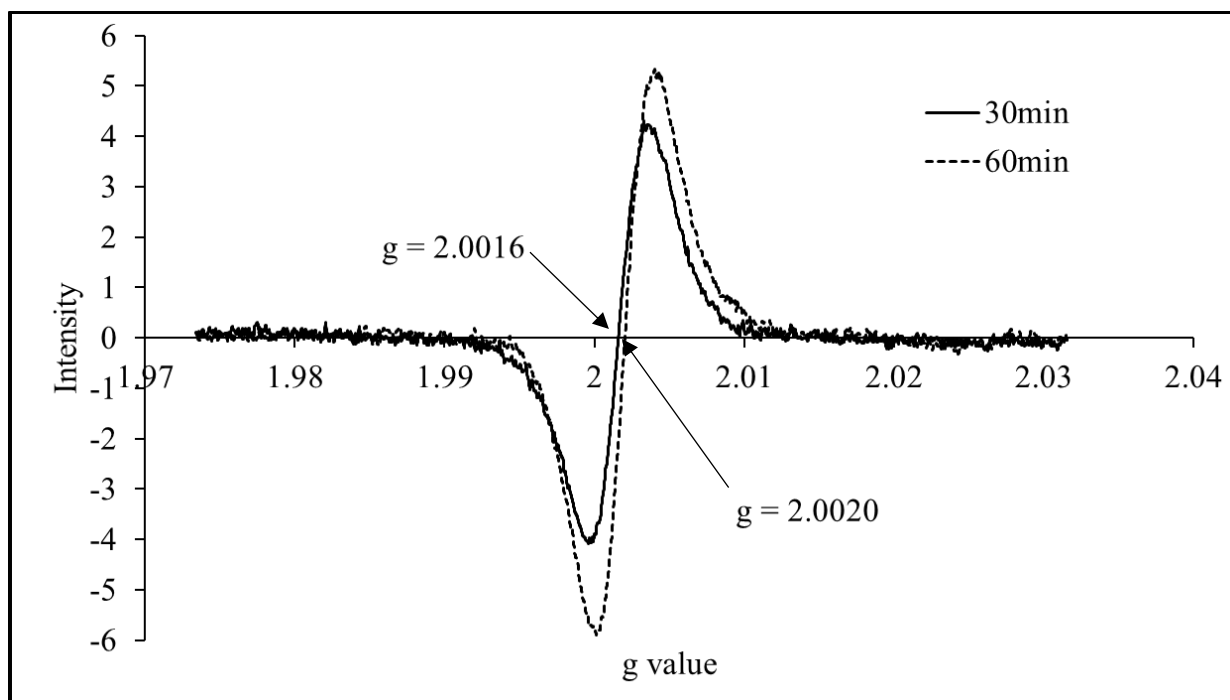


**Figure 5.10** First derivative electron spin resonance curve obtained using ESR for indene for reactions at 30 and 60 min

When tested using the ESR, the reaction products obtained from indane did not demonstrate any presence of free radicals in both reactions. Indane is known to have a propensity to form free radicals<sup>4</sup> but without the presence of any external hydrogen acceptors, there was no reaction.

Indole had an ESR signal for product obtained for the reaction performed at 30 min. However, the peak was extremely weak and barely above the baseline (i.e. order of magnitude  $10^{16}$  spins/g).

Benzofuran, on the contrary, had very distinct peaks which were similar to indene, showing  $1.3 \times 10^{18}$  spins/g and  $1.2 \times 10^{18}$  spins/g of sample for 60 and 30 min, respectively. The curves for both reaction times are shown in figure 5.11.

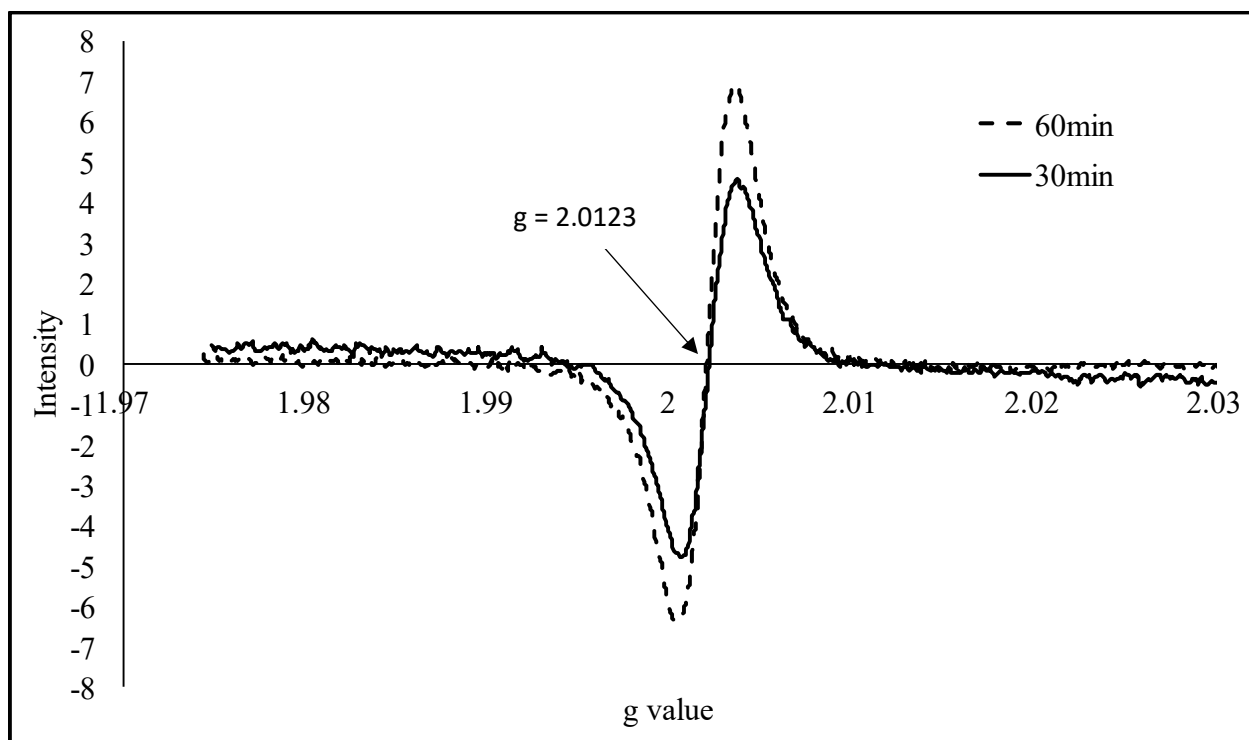


**Figure 5.11** First derivative electron spin resonance curve obtained using ESR for benzofuran for reactions at 30 and 60 min

### 5.3.6 Investigating the presence of phenols

For benzofuran, based on the results from the GC-MS, the presence of the hydroxyl (-OH) function group in various compounds needed to be confirmed. In order to do so, the products obtained for benzofuran were further analyzed using the FTIR and  $^1\text{H-NMR}$ .

In the presence of a hydroxyl group, there should be a clear peak visible in the wavenumber range of  $3500\text{-}3200\text{ cm}^{-1}$ .<sup>5</sup> In figure 5.12, in the bordered area there is no clear indication of presence of any peak in the region. Since there was still a possibility that the FTIR was not able to capture the OH group because of its presence in a very minute quantity.

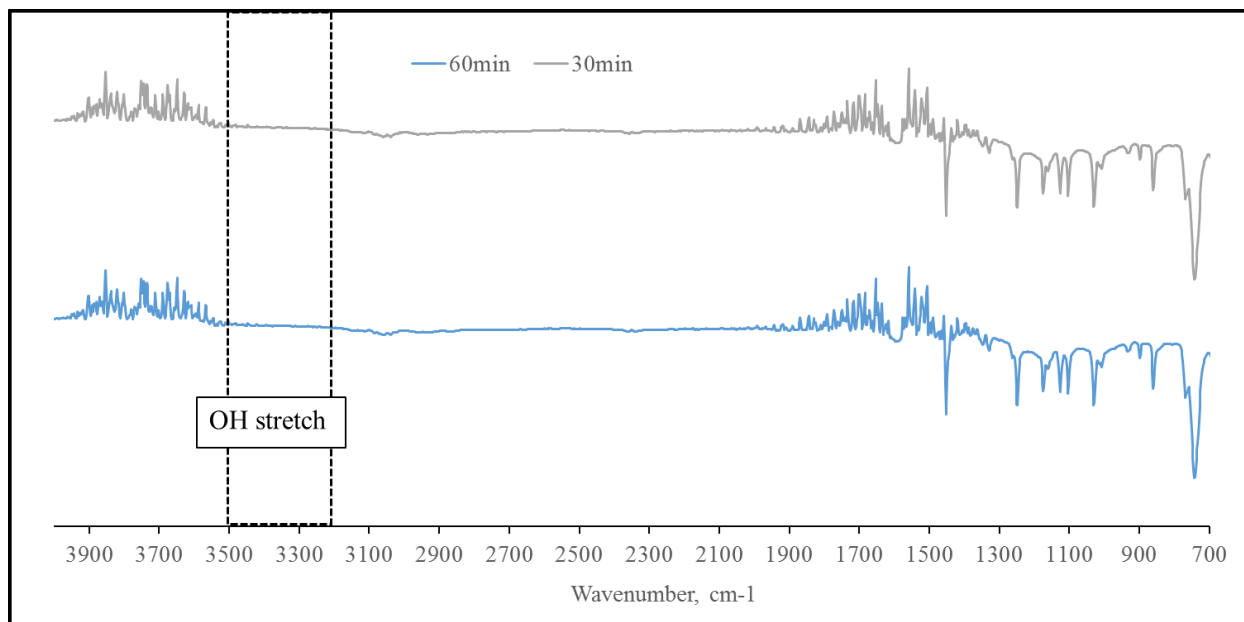


**Figure 5.12** FTIR results for samples obtained from benzofuran under thermal cracking conditions with different reaction times of 60 and 30 min

### 5.3.7 Reaction of indane and indene together

Based on the reaction from indane and indene separately, a combined reaction of both in equal proportions inside a batch reactor was performed to observe how the final product would be affected at thermal cracking conditions.

Figure 5.13 shows the spectra obtained using the GC-MS for the product at a 60 min period. The peaks are similar to those obtained for the indene products. All of indene was observed to have reacted completely to form the solid and liquid products.

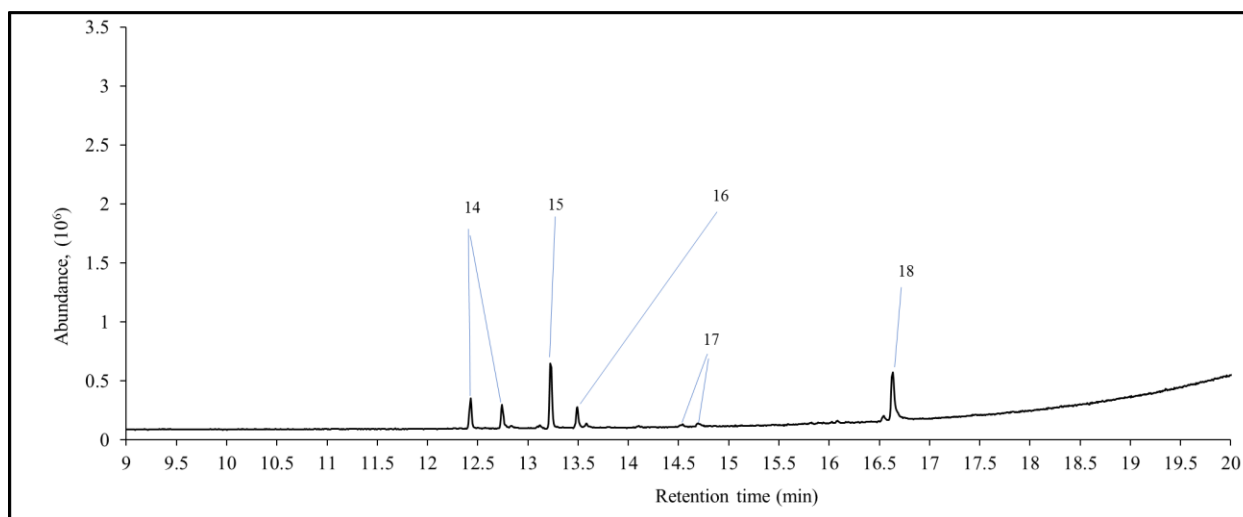
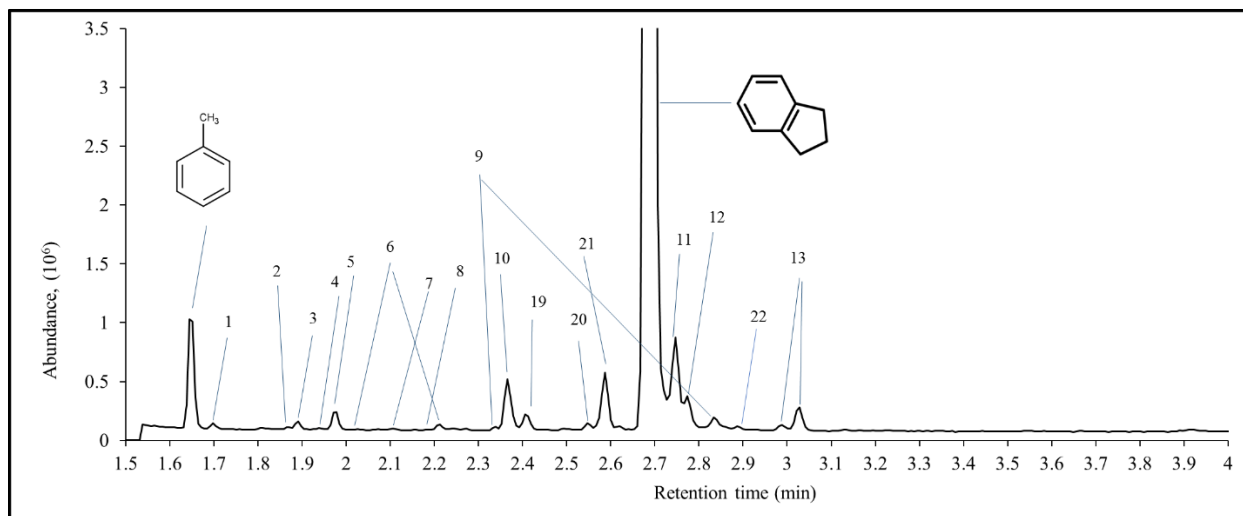


**Figure 5.13** Results from gas chromatography obtained for the *n*-pentane soluble fractions of indane and indene between the retention times of 1.5 to 20 minutes for a 60 min reaction at 2 MPa and 400 °C

**Table 5.5** Compound list from the GC-MS results for a 60 min reaction between indene and indane at 2 MPa and 400 °C

	Retention time (min)	Compound name	Chemical structure
1 - 18	-	Refer to table 2	-
19 <sup>b</sup> , 20 <sup>b</sup> , 21 <sup>b</sup>	2.41, 2.55, 2.59	Mass spectrum shown below (figure 16)	Unidentified
22 <sup>b</sup>	2.89	_a	-

a Mass spectrum for the respective retention time is shown in Appendix A.

b These compounds should be seen only as being indicative of the nature of the products. The true

identities of these compounds have not been confirmed.

For peak 19, 20 and 21, the mass spectrums obtained were very similar (figure 5.14). It is expected that they are isomers of the same compound. The expected molecular weight of the compound is approximately 120 g/mol. The compound contains a benzene ring (77 m/z). The compound also constitutes of 1 methyl group (120 m/z – 105 m/z) and an ethyl group (105 m/z – 77 m/z). The compound could be a product of ring-opening. A plausible structure for the compound could be 1-ethyl-2-methyl-benzene, having a molecular formula of  $C_9H_{12}$ .

Unknown; InLib=-284

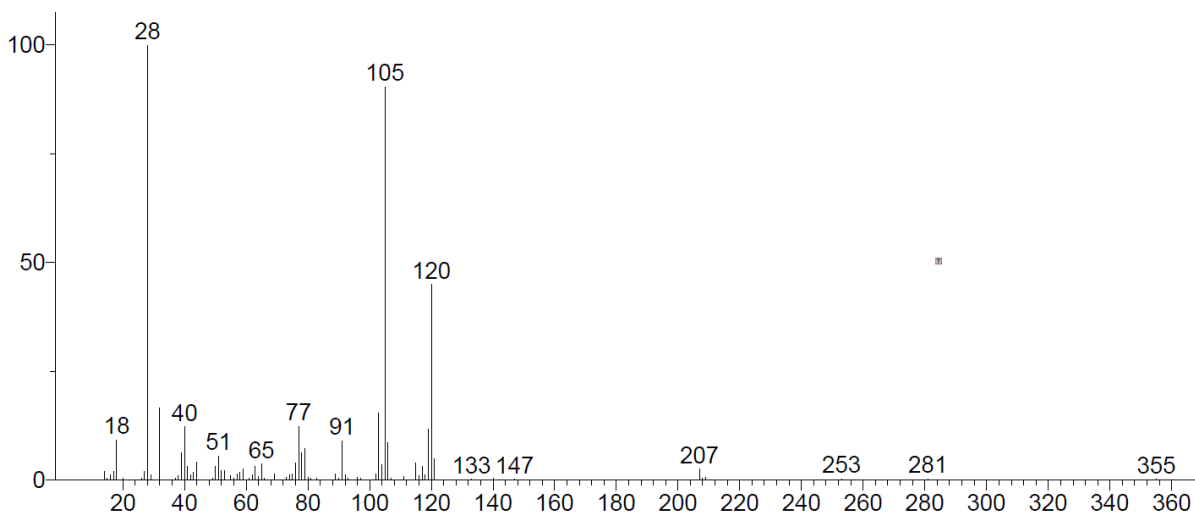


**Figure 5.14** Mass spectrum for peaks 19 from reaction of indene and indane for 60 min

On performing the asphaltene content, there was a reduced amount of asphaltene production in comparison to products from indene reaction. As can be seen in figure 5.15, only 22.8% solids were formed for 60 min reaction time. On normalizing the solid content with respect to the amount of indene present during the reaction, there was a 45.6% presence of solids, compared to 71.9% found after reaction of pure indene (figure 5.2).

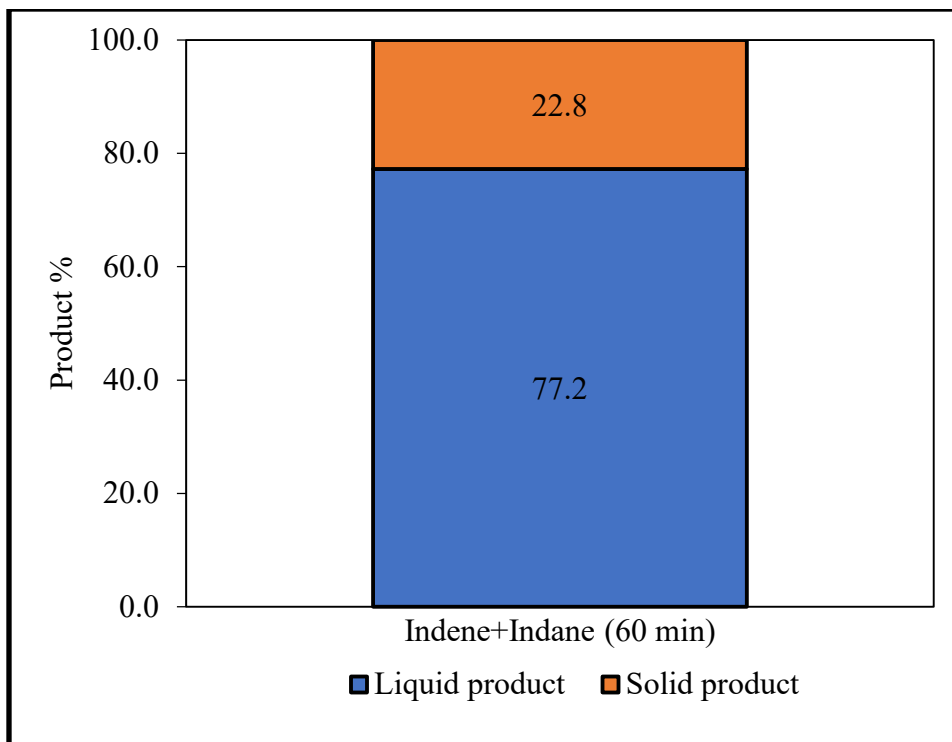


**Figure 5.15** Asphaltene content for a reaction with indane and indene in equal ratios performed at thermal cracking conditions for a reaction time of 60 min

When the *n*-pentane soluble fraction was analyzed using the SIMDIS (figure 5.16), a very similar graph was obtained in comparison to the samples from indene obtained previously in the chapter (figure 5.5). For the reaction between indene and indane, the maximum temperature reached by the heaviest product was 548 °C, with the presence of carbon chains constituting up to C<sub>44</sub>. However, in the case of indene for both reaction times of 30 and 60 min, there was a slightly higher maximum temperature of 588 °C, with a carbon composition of C<sub>52</sub>. The initial bump at the start of the graph is due to the presence of *n*-pentane used as solvent in the sample. The second bump at a temperature of 100 °C could be due to the ring-opening formed during the reaction of indene and indane.

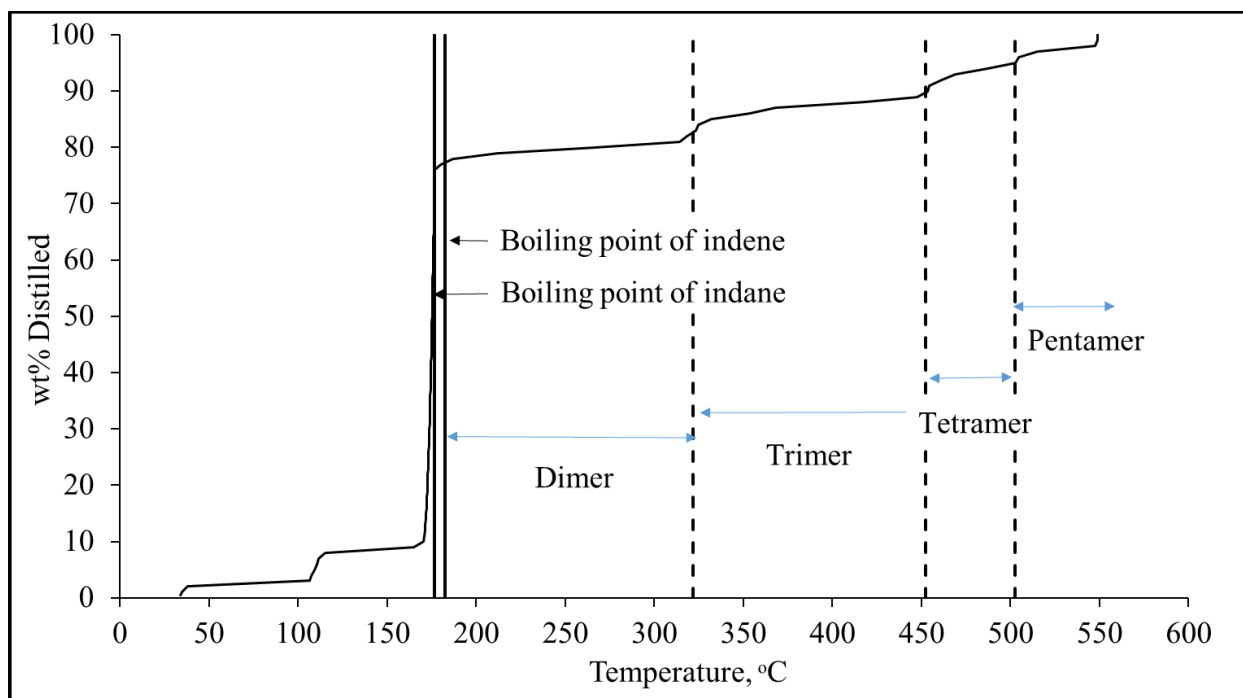


**Figure 5.16** Boiling curve acquired using SIMDIS for the product of indene and indane reacted together for 60 min in a batch reactor

From the ESR results obtained for the indene and indane sample (figure 5.17), there is a visible peak. The peak was not as clean as viewed for the previous samples but on quantifying the results, the ESR peaks contained  $7.8 \times 10^{17}$  spins/g of sample. The overall electron spin was much smaller (approximately half) than the products obtained from the reactions of pure indene.

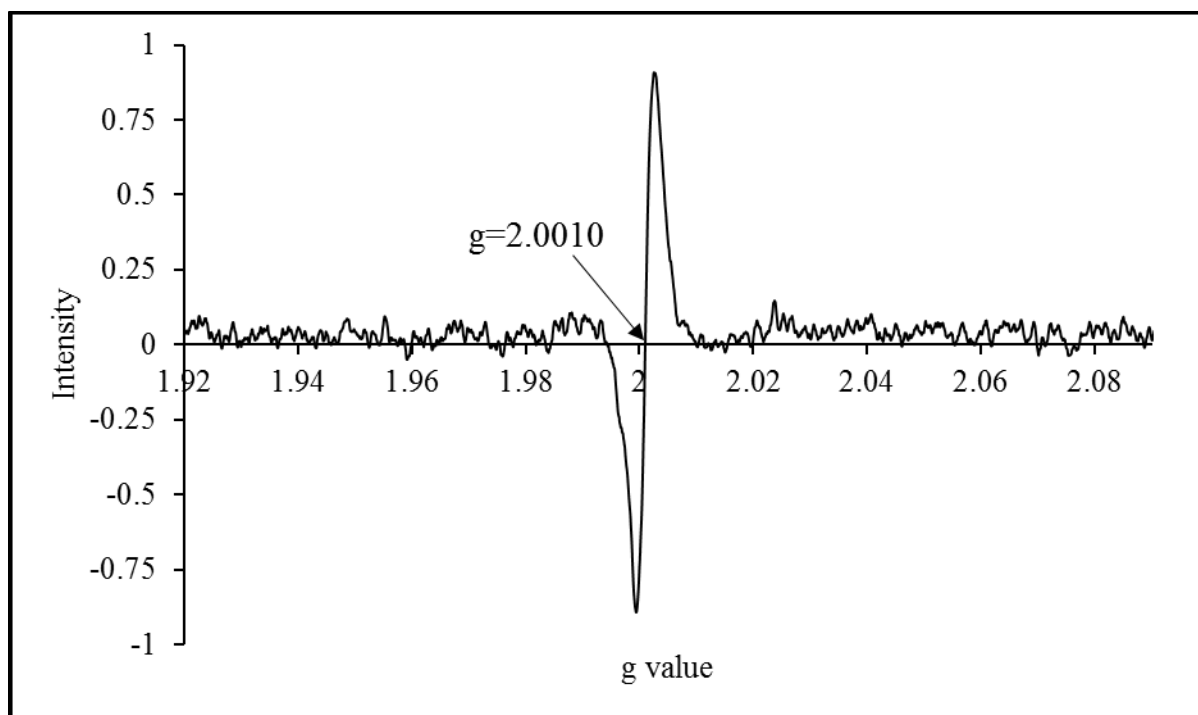


**Figure 5.17** First derivative electron spin resonance curve obtained using ESR for reaction between indene and indane for reactions at 60 min

## 5.4 Discussion

### 5.4.1 Heavier product formation and ring-opening reactions

Free radical reactions are an important class of addition reactions. Indene, benzofuran and indole were found to be capable of forming free radicals without external initiators and undergo self-reactions to form heavier compounds under thermal cracking conditions. Self-reactions are induced by hydrogen abstraction. Hydrogen transfer occurs as a principle reaction. The ESR results indicated that there was still large presence of free radicals in the products after reaction. Not all free radicals that were formed underwent a termination step and were still present in the product.

During the pyrolysis of indene, an indenyl radical is formed by a loss of hydrogen atom from the C(1) position by breaking the  $sp^3$  bond with the hydrogen atom.<sup>6</sup> The reaction mechanism of formation of heavier products from indene is shown in figure 5.18.

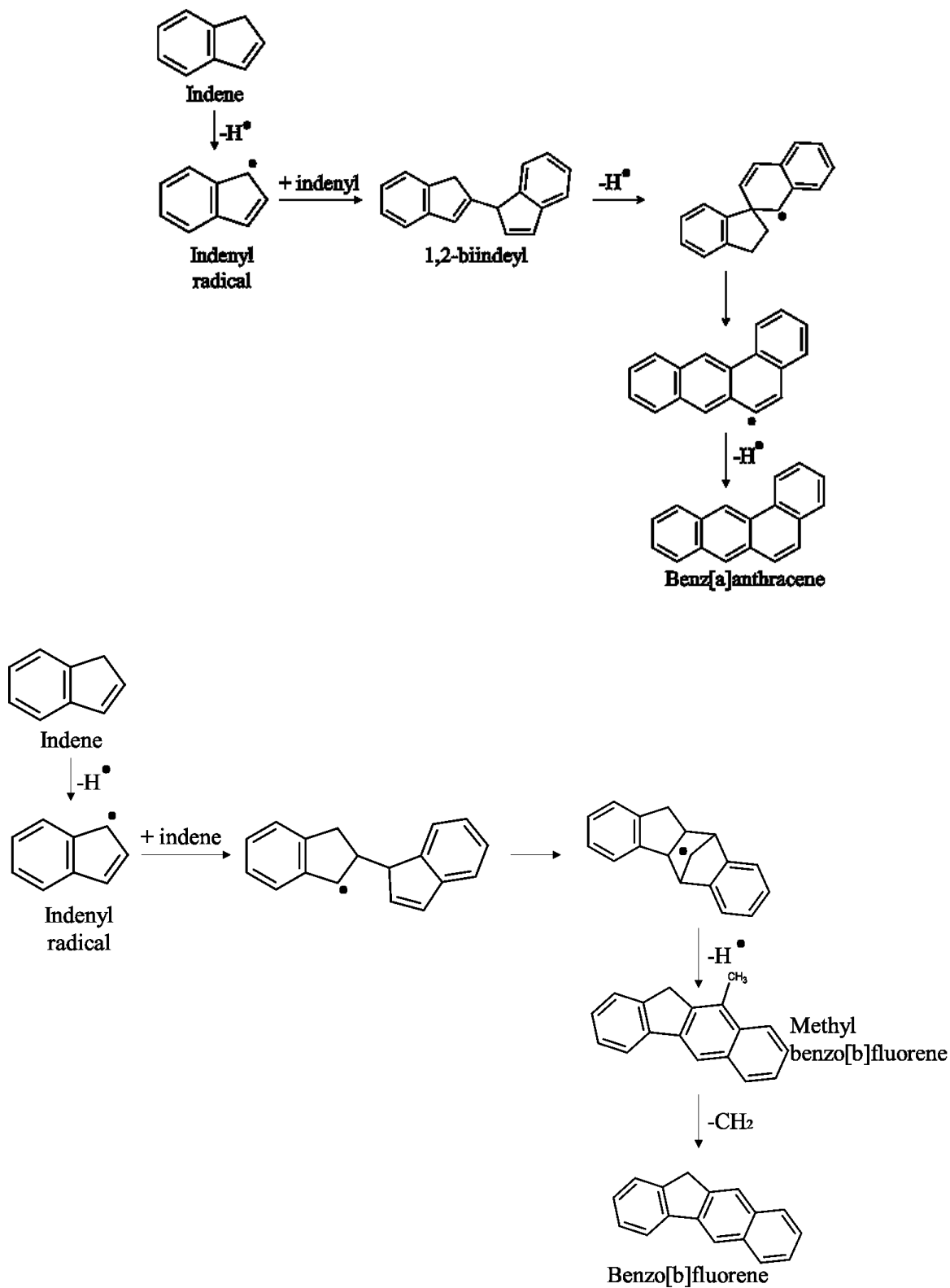


**Figure 5.18** Reaction mechanism of free radical addition reaction of indene under thermal cracking conditions <sup>7</sup>

In figure 5.18, the final product is not limited to the formation of benz[a]anthracene (peak 22). Possible isomers of benz[a]anthracene, such as chrysene and benzo[c]phenanthrene, could also form as a result of the above reaction mechanism proposed by Lu and Mulholland.<sup>7</sup>

Production of indane and, products from reaction of indene and indane are further explained in section 5.4.2.

From the SIMDIS, it is known that heavier products formed for the reaction of indole on exposure to thermal cracking conditions. Based on previous studies, under very high thermal conditions i.e. at temperatures of 777-1377 °C, indole undergoes polymerization and ring opening reactions. Isomers of benzyl cyanide, *o*- and *m*-tolunitriles were formed as a result of ring-opening reactions.<sup>8</sup> Polymerization takes place at the C(9) –N(1) positions in the indole ring. Some of the polymerization reaction require the formation of indolenine as an intermediate step, before further expansion.<sup>8</sup>

Benzofuran under thermal cracking conditions experienced ring-opening and addition reactions. The product was spiked with phenol and 2-ethylphenol to confirm the presence of the compounds. Both the spikes were effective and overlapped at the same retention time, confirming the presence of the two compounds in the product.

The ring-opening mechanism for the formation is shown in figure 5.19. Benzofuran on addition of a hydrogen radical, forms a resonance with the free radical inside the furan ring. In a three step hydrogen transfer reaction, the first step involves breaking of the furan ring at the C(1)-O position and forming 2-ethenylphenol. On addition of 2 more hydrogens, the final structure is of 2-ethylphenol.

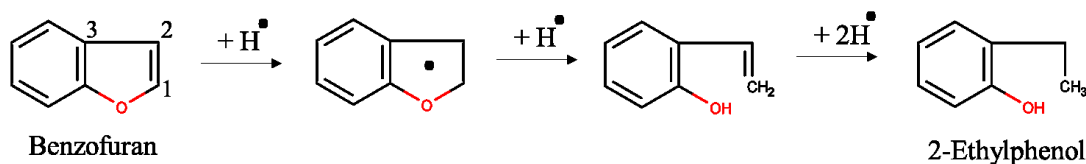


**Figure 5.19** Reaction mechanism for the ring opening of benzofuran under thermal cracking conditions

It is important to note that indene, indole and benzofuran on exposure to thermal cracking conditions, where cracking dominates, were still capable of forming polymers. Thus, at lower temperatures where polymerization is more dominant than cracking, these compounds have a high probability to polymerize.

#### 5.4.2 Reaction chemistry of indene and indane

A major concentration of indene was seen to convert to form indane. On hydrogen transfer, indene formed an indanyl radical (figure 5.20).

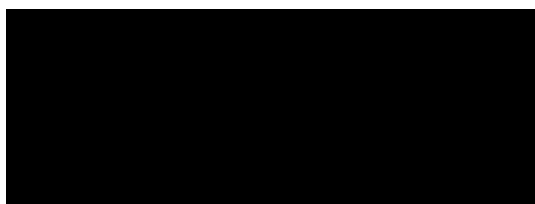


**Figure 5.20** Reaction mechanism for indanyl formation from indene under thermal cracking conditions <sup>6</sup>

Looking at the results obtained from indene, it was suspected that indene on formation of indane was leading to the formation of asphaltenes. Hence, indane was acting as a plausible intermediate between indene and asphaltenes production. For better understanding, indane was reacted by itself to examine if the hypothesis would agree with actual results but on performing the experiment it was observed that indane did not react. One explanation, and the most straightforward take, would be that indane is present in the most stable form and therefore, abstains from reacting further. Another plausible explanation could be that indane is highly susceptible to donate hydrogen but in the absence of hydrogen-accepting compounds, it does not react.

To test the second hypothesis, a reaction was performed with 50 wt% indene and 50 wt% indane. When compared to products formed with reactions of indene and reaction of indene and indane, very similar products were formed with additions of peaks 17-20 towards the lighter fraction (figure 5.13). The peaks were formed in the retention time of 2.4-2.9 min. The possible product

formation expected from the mass spectrum indicated towards ring-opening of indene, which might have led to the formation of 1-ethyl-2-methyl-benzene. This is possible by  $\beta$ -scission from the indanyl radical. The product then engages in three hydrogen transfer reactions. The first reaction involves the formation of 2-methyl styrene and with addition of two more hydrogen radicals, finally forms 2-methyl-1-ethylbenzene.

#### *5.4.3 No reaction in thianaphthene despite pyrolysis of benzofuran*

Thianaphthene is the least reactive of the naphtho-aromatic compounds selected for the study, hence, most stable. In the reaction of thianaphthene, there was a lack of hydrogen donors and hence no reaction was initiated. By itself, it has a very low propensity to form free radicals, it is highly stable and abstains from reacting at all.

### **5.5 Conclusion**

The free radical behavior of compounds containing 5-membered rings attached to an aromatic were the focus of this chapter. On exposing the selected model compounds to thermal cracking conditions, the following main conclusions can be derived from this study:

- a) On exposure of indene, indole and benzofuran to thermal cracking conditions of 400 °C and 2 MPa, free radical addition reactions took place. Heavier products were found in the products.
- b) Indane and thianaphthene did not react at all under thermal cracking conditions.
- c) Indene has a very high propensity to undergo free radical reactions. On undergoing hydrogen transfer, it formed asphaltenes and heavier products with the heaviest

composition constituting of C<sub>52</sub>. It was found that with increase in temperature, the asphaltenes content increased.

- d) Ring opening was observed in products from reactions of benzofuran and indene.
- e) On reaction of indane and indene, there was no increase in the addition products formed but there were observable peaks towards the lighter fraction. The peaks indicated towards ring-opening of the indene structure.
- f) The free radical content in the products formed from thermal cracking conditions of indene at a reaction time of 60 min was almost double in comparison to the free radicals observed in the reaction of indene and indane together for the same reaction time. Indane, therefore, did not contribute in the addition of free radicals to the system.

## 5.6 References

- (1) Gray, M. R. *Upgrading Oilsands Bitumen and Heavy Oil*, 1st ed.; The University of Alberta Press: Edmonton, **2015**.
- (2) Siddiquee, M. N.; De Klerk, A. Heterocyclic Addition Reactions during Low Temperature Autoxidation. *Energy and Fuels* **2015**, 29 (7), 4236–4244.
- (3) ASTM D7169-11. *Standard Test Method for Boiling Point Distribution of Samples with Residues Such as Crude Oils and Atmospheric and Vacuum Residues by High Temperature Gas Chromatography*; ASTM International: West Conshohocken, PA, 2016; Vol. 05.4.
- (4) Siddiquee, M. N.; De Klerk, A. Hydrocarbon Addition Reactions during Low-Temperature Autoxidation of Oilsands Bitumen. *Energy and Fuels* **2014**, 28 (11), 6848–6859.
- (5) Silverstein, R. M.; Webster, F. X.; Kiemle, D. J.; Bryce, D. L. *Spectrometric Identification of Organic Compounds*; John Wiley & Sons, Inc., 2014.
- (6) Lifshitz, A.; Suslensky, A.; Tamburu, C. Thermal Decomposition of 4-Methylpyrimidine.

- Experimental Results and Kinetic Modeling. *J. Phys. Chem. A* **2001**, *105* (14), 3542–3554.
- (7) Lu, M.; Mulholland, J. A. Aromatic Hydrocarbon Growth from Indene. *Chemosphere* **2001**, *42* (5–7), 625–633.
- (8) Laskin, A.; Lifshitz, A. Isomerization and Decomposition of Indole. Experimental Results and Kinetic Modeling †. *J. Phys. Chem. A* **1997**, *101* (42), 7787–7801.

## **CHAPTER 6 : HYDROGENATION OF AROMATIC COMPOUNDS CONTAINING 5-MEMBERED RINGS OVER A SUPPORTED METAL HYDROGENATION CATALYST IN A FLOW REACTOR IN THE PRESENCE OF H<sub>2</sub> GAS**

### **Abstract**

A lot of emphasis is given to the need to decrease the density and improve elemental composition in oilsands upgrading. These qualities can be obtained in the oil fractions by subjecting the fractions to hydrotreating. The process entails addition of molecular hydrogen at high partial pressures while heating the fractions at lower temperatures. The objective of this chapter was to expose the selected binuclear compounds to molecular hydrogen using a flow reactor at milder conditions compared to industrial practices to achieve incomplete conversion and study the possible implications. Reactions were performed under a hydrogen pressure of 1 MPag and a temperature range of 150-220 °C using a reduced Ni-alumina catalyst. On studying the results, it was found that even under mild conditions, at a space velocity of 4.5 h<sup>-1</sup>, indene was able to hydrogenate to indane, with a conversion of 27-15 %. Other model compounds i.e. indole, benzofuran and thianaphthene, also underwent hydrogenation. In addition, benzofuran and thianaphthene went through ring-opening reactions. No other side-reactions or byproducts were formed.

**Keywords:** Hydrogenation, flow reactor

## 6.1 Introduction

Catalytic hydrogenation in the upgrading process is employed to improve the density of the products, as well as, their elemental composition. This means that the density and heteroatom content of the hydrogenated product is decreased. Hydrogenation is known to suppress polymerization and coking in olefins. Highly active catalysts also help in reducing sulfur, nitrogen and aromatics from the oil fractions.<sup>1</sup> This is achieved by selectively subjecting the petroleum fractions to hydrogen in a reactor in the presence of an appropriate catalyst. It is used for a variety of fractions ranging from naphtha to atmospheric residue. In case of residual hydrotreating, controlled breaking of the bond at the point of nitrogen, sulfur or oxygen joined to the carbon atom using hydrogen molecule is achieved.<sup>1,2</sup>

From literature it is known that model compounds of interest namely indene, indole, benzofuran and thianaphthene in the presence of hydrogen go through hydrogenation under high pressure conditions between 5-14 MPa.<sup>3-6</sup> Even though hydrogen is used for hydroconversion and hydrocracking, this chapter will focus on hydrotreating of the distillate feed. Hydrotreating takes place at lower temperatures with a high partial pressure of molecular hydrogen.<sup>1</sup> The reactions were performed at a pressure of 1 MPa and temperature range of 150- 220 °C in the presence of a nickel catalyst. Compared to industrial practice these are mild conditions and were specifically selected to achieve incomplete conversion.

The objective of this chapter was to study the possible implications of hydrogenation reactions on selective binuclear compounds in the presence of metal promoted catalyst in a flow reactor. The reactions were performed by varying temperature and space velocity while keeping pressure and excess flow of hydrogen constant.

## 6.2 Experimental

### 6.2.1 Material

Refer to section 5.2.1 in Chapter 5 for the list of chemicals used. The catalyst preparation was done by using alumina support and nickel nitrate hexahydrate. The catalyst bed packing utilized silica carbide and the catalyst that was prepared. The  $\gamma$ -Al<sub>2</sub>O<sub>3</sub> support was supplied by Sasol. The tablets were cylindrical in shape with a diameter of 4.87 mm and length of 5.60 mm. Carborex® 16 was used as inerts, supplied by Ritchey supply. The silica carbide abrasive was of mesh 16 and 1.52 g/mL density. The chemicals that were used to build the calibration curve and catalyst preparation are listed in table 6.1.

**Table 6.1** Materials employed in this study

Compound	Formula	CASRN <sup>a</sup>	Mass fraction purity <sup>b</sup>	Supplier
<i>Chemicals</i>				
Indoline	C <sub>8</sub> H <sub>9</sub> N	496-15-1	0.99	Sigma-Aldrich
2,3-Dihydrobenzofuran	C <sub>8</sub> H <sub>8</sub> O	496-16-2	0.99	Sigma-Aldrich
Nickel (II) nitrate hexahydrate	Ni(NO <sub>3</sub> ) <sub>2</sub> ·6H <sub>2</sub> O	13478-00-7	0.999985	Fisher Scientific
Alumina tablets 5x5 mm	$\gamma$ -Al <sub>2</sub> O <sub>3</sub>	-	- <sup>c</sup>	Sasol
<i>n</i> -Heptane	C <sub>7</sub> H <sub>16</sub>	142-82-5	0.999	Fisher Scientific
<i>Cylinder gases</i>				
Hydrogen	H <sub>2</sub>	1333-74-0	0.99999 <sup>d</sup>	Praxair

<sup>a</sup> CASRN = Chemical Abstracts Services Registry Number

<sup>b</sup> This is the purity of the material guaranteed by the supplier; material was not further purified

<sup>c</sup> Mass fraction purity not specified

<sup>d</sup> Mole fraction purity

### 6.2.3 Preparation of catalyst<sup>7,8</sup>

Ni catalyst was prepared by incipient wetness impregnation on  $\gamma$ -Al<sub>2</sub>O<sub>3</sub> support. To achieve 5 wt% nickel impregnation, the amount of liquid that the support could absorb was tested. A known quantity of the alumina was taken in a beaker. A measured volume of deionized water

was added to the alumina dropwise until all of it was wet without any excess water collecting at the bottom of the beaker. This ratio of water and alumina was used to prepare a solution of nickel nitrate hexahydrate dissolved in deionized water. Based on the 20.3 % molar concentration of nickel in  $\text{Ni}(\text{NO}_3)_2 \cdot 6\text{H}_2\text{O}$ , the measurements were done to have a final concentration of 5 wt% of nickel with respect to the alumina support. The solution was added to a fresh unused quantity of support dropwise and constantly stirred using a glass rod. The wetted solid pellets were heated on a hot plate at 80 °C for 5 h. This was done to evaporate any excess water present. The dried sample was then placed in a CWF 1100 Carbolite chamber furnace for calcination. The temperature range for the furnace was between 30-1100 °C and temperature was controlled with a 3216 controller. The ramp on the furnace was set to start at 30 °C with increments of 10 °C/min until it reached 600 °C. The catalyst was calcined at a temperature of 600 °C for 3 h with a constant air flow of 100 mL/min, leaving behind nickel oxide impregnated on alumina support as the final product.

#### *6.2.4 Catalyst activation*

The catalyst activation to obtain activated nickel metal impregnated on  $\gamma\text{-Al}_2\text{O}_3$  support was performed in a flow reactor designed for the experimental work in this chapter. The reactor was packed with  $\gamma\text{-Al}_2\text{O}_3$  and carborex (inerts) with a mass ratio of 2:7. The reactor was loaded with 17.3 g of nickel impregnated alumina support and 59.9 g of inerts. The packing was done in a randomized order to ensure better heat distribution. The furnace was then heated to 350 °C for 3 h with a constant hydrogen gas flow of 88 mL/min. The heat was then turned off and the reactor was left to cool with the hydrogen flow running at the same flowrate until the temperature reached 100 °C. At a 100 °C, the reactor outlet was shut off and the hydrogen flow was stopped. At this point the catalyst was activated. The flow reactor was left with hydrogen blocked off in the reactor, to prevent oxidation prior to the hydrogenation experiments.

#### *6.2.5 Catalyst characterization*

The Autosorb iQ was used to perform the Brunauer–Emmett–Teller (BET) surface area analysis on the nickel catalyst and the plain alumina support. The samples were placed in a 9 mm cell. The samples were degassed to remove water and other adsorbed contaminations from the samples by heating the cells to 300 °C under vacuum. The sample was brought back to room temperature using liquid nitrogen in the dewer flask. The sample was moved to an evacuated sample chamber. The cell was then exposed to small amounts of gas which is expected to adsorb on the surface of the catalyst. The instrument measures the partial pressure of a gas after a known volume was introduced. The partial pressure versus volume of gas introduced curve is then used to determine the amount of gas used for monolayer adsorption and thereby the surface area. From the results, the surface area of the nickel catalyst was reported to be 151 m<sup>2</sup>/g and the area for the blank support was 166 m<sup>2</sup>/g. The evident decrease in the surface area of the support is indicative that part of the surface area of the support was absorbed by nickel particles and therefore blocked off. The average pore size of the impregnated catalyst was 4.59 x 10<sup>-9</sup> m compared to 4.71 x 10<sup>-9</sup> m for the blank, which agrees with the decreased surface area, since the pore size was calculated based on the measured surface area.

The ZEISS SIGMA field emission scanning electron microscope (FESEM) is mounted with an in-lens secondary electron (SE) detector and a backscatter (BSD) detector. The microscope is also equipped with Energy Dispersive X-ray (EDX) detection and Electron Back Scatter Diffraction (EBSD) which provide simultaneous acquisitions of chemical composition and crystal structures, respectively. SEM uses an electron beam to scan the catalyst surface that generates signals which the detectors pick up on for generation of images and spectrums. Samples were coated with 10 nm thickness of carbon before analyzing using the SEM to obtain better images and increasing electric conductivity of the samples. Figure 6.1 displays the use of SEM for generating high-quality images of the nickel impregnated on inside of the  $\gamma$ -Al<sub>2</sub>O<sub>3</sub> support. The EDX detector gave a nickel quantification of 3.3 % spread over the alumina surface.

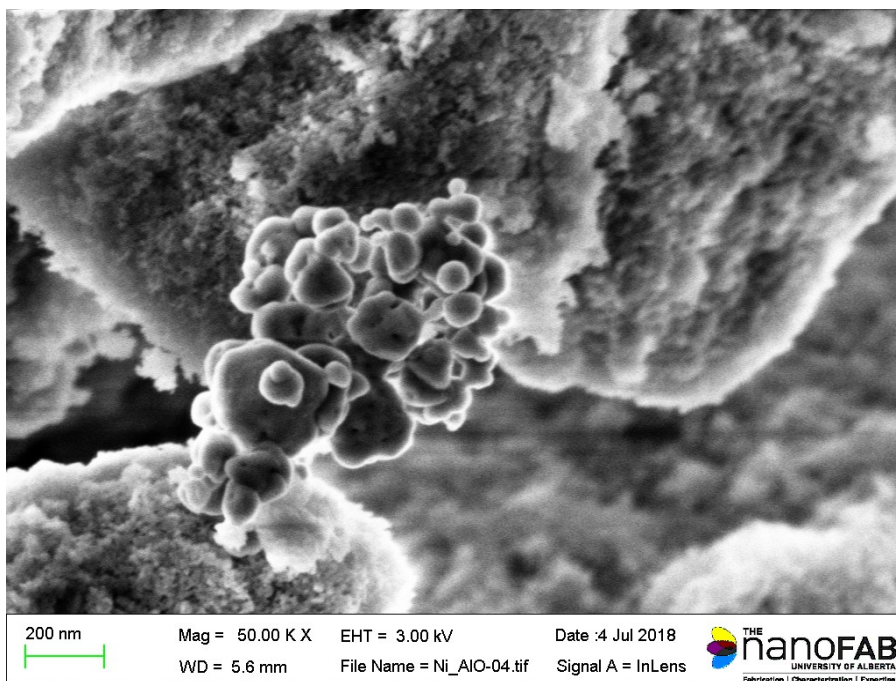
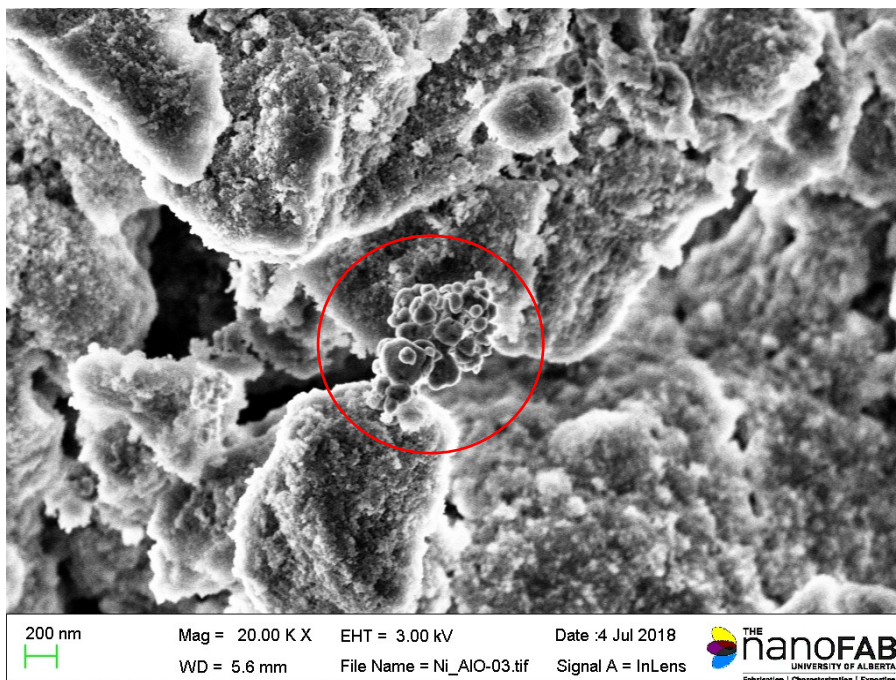


**Figure 6.1** SEM results for nickel catalyst impregnated on a  $\gamma$ -Al<sub>2</sub>O<sub>3</sub> support at magnifications of 20 and 50 K

Both the Autosorb iQ and the Scanning Electron Microscope (SEM) were performed under the guidance of technicians from the nanoFAB department at the University of Alberta.

### 6.2.6 Reactor design

Experiments for hydrogenation reaction using model compounds in the presence of excess hydrogen gas flow were performed in a flow reactor, designed and constructed, as shown in figure 6.2 and 6.3, respectively. No setup existed before the study was performed. The design and construction of the reactor were performed as part of this study.

The feed tank (F-1) consisted of a 500 mL vessel with a lid to facilitate easy addition of liquid, while reducing evaporative loss during use. A 1/8-inch hole was drilled in the lid of the vessel F-1 as an entrance for the pump inlet hose. A HPLC pump (P-1), i.e. a positive displacement pump, with a volumetric flow range of 0.01-10 mL/min was used to pump feed into the system. The changes in the weight of the feed were monitored using a Mettler Toledo Model ML3002E Balance with a range of 0-3200 g and readability of 0.01 g. A 30.5 cm long K-type thermocouple (T-01) with a 0.16 cm diameter, from Omega (Model KMQXL-062U-12) with a maximum reach of 1335 °C was installed after the feed inlet to keep track of the inlet temperature. The feed was subjected to a flow of hydrogen using a Brooks SLA5800 Series mass flowmeter (MF-1) with a flow capacity of 2-100 mL/min. The flowmeter was connected to a Brooks 0250-Series four channel power supply, readout and set point controller. To purge the system before and after each reaction, an inlet valve (BV-2) for nitrogen was present after the feed inlet. To prevent any backflow of liquids and gases, check valves were added after the pump, nitrogen inlet and mass flowmeter (CV-1, CV-3, CV-6). A relief valve (RV-7) designed for a set pressure of 2.90 MPa was added before the reactor to ensure the system was not over-pressurized.

The feed was then fed to the top of a packed bed reactor. Flow in the vertical packed bed reactor was from top to bottom, i.e. down-flow operation. The body of the reactor was a Swagelok 316 stainless steel tube with a length of 17 cm and diameter of 2.54 cm. The reactor was installed inside a Lindberg/Blue M single zone tube furnace (model HTF55122A) with a maximum temperature limit of 1000 °C. The furnace was connected to a UP150 programmable controller provided by the furnace from Thermo Fisher. It was well insulated with the help of glass wool on

the top and bottom. Reactor packing was explained in section 6.2.4. The total weight of the packing (alumina and inerts) inside the reactor was 77.3 g. A 0.64 cm wide thermowell (45.72 cm in length) was installed inside the reactor. The thermowell contained 3 omega K-type thermocouples (Model KMQXL-062U-36) that were all 0.16 cm in diameter and 60.96 cm long. The thermocouples were positioned at the top (0 cm), the middle (8.5 cm) and the bottom (17 cm) of the reactor, to monitor the temperatures at those three levels during the runs. The three temperature points are labelled as T-02, T-03 and T-04 in figure 2.

A co-current flow heat exchanger (E-1) was located right after the furnace. It was designed with an outer tube diameter of 1.27 cm and an inner tube diameter of 0.64 cm. The heat exchanger was 39 cm long. Water was used as the cooling fluid. The water was continuously cooled down to 5 °C and recirculated at a rate of 17 L/min at a delivery pressure of 30 kPa, by a Fisher Scientific Isotemp refrigerated/heated bath circulator 5150 R28 that had a temperature range of -28 °C to +150 °C. The feed was cooled down to room temperature as it passed through the heat exchanger tube. Another relief valve (RV- 8) was present at the outlet of the heat exchanger also designed for a set pressure of 2.90 MPa due to the pressure limitations on the backpressure regulator (BP-1). A thermocouple (T-05), similar in model and length to T-01, was installed after the relief valve to monitor the product temperature.

The product was then collected in a product tank designed by Swagelok (304L-HDF8-1000) using 316 stainless steel, with a capacity of 1 L. The liquid samples were collected at the bottom of the product tank while the gases were passed to the volumetric drum flowmeter through the backpressure. The backpressure regulator (BV-1) was designed with a pressure control range of 0.04-3.45 MPa, the relief valve (RV-8) ensured that it was not exposed to a pressure higher than 2.90 MPa. The backpressure regulator had a 316 stainless steel body with a Viton® O-ring seal and was manufactured by Sur-Flo Meters & Controls Ltd. After the backpressure, near atmospheric gas was passed through a Ritter TG-05 model #5 PVC volumetric gas meter to measure the gas volume precisely (GF-1). Since hydrogen gas was being fed to the system, the gas meter was connected to an explosion proof pulse generator V 2.0Ex (50 pulses per rev). The gas meter was designed for a 0.5 L of gas flow per revolution, with a flowrate range of 1-60 L/h

and maximum pressure rating of 50 kPa. The gas volume was measured and then released into the fumehood.

The system pressure was checked before and after the reactor using two pressure gauges (PG-01, PG-02). The HPLC pump, the Brooks controller, all the thermocouples and the Ritter's drum flowmeter were connected to a LabView program.

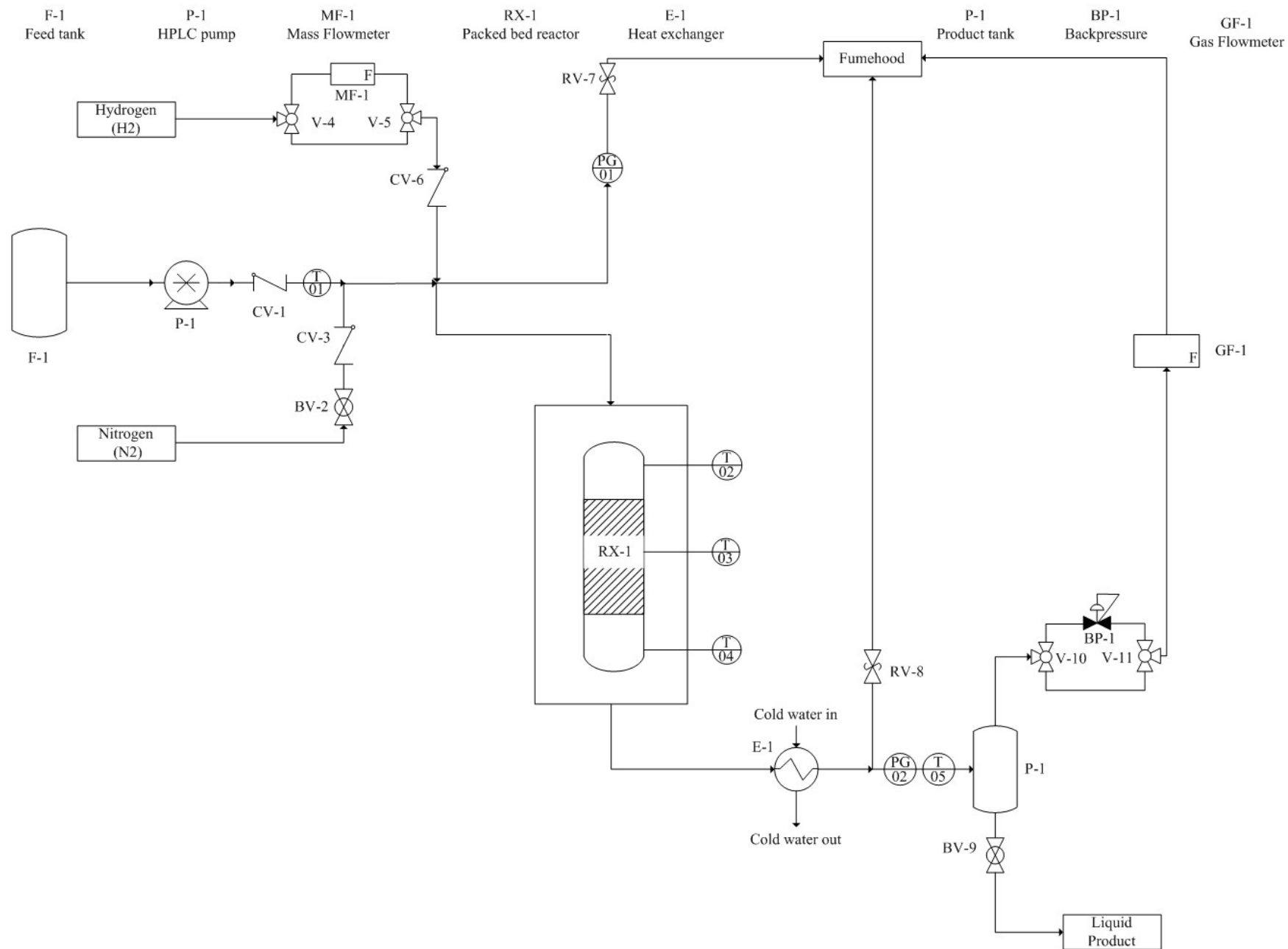


**Figure 6.2** Process flow diagram of plug flow reactor used for hydrogenation



**Figure 6.3** Images of lab scale reactor which was designed, constructed and commissioned as part of this project

### 6.2.7 Reactor operation

Experimental runs were performed under the operating conditions shown in table 6.2. An example of one of the runs is described below.

A solution of 200 mL of 5 wt% indene diluted in toluene was prepared and placed on the Mettler Toledo balance. The furnace temperature was increased to 150 °C with the help of the controller connected to the furnace. Hydrogen gas with a controlled flowrate of 88 mL/min and inlet pressure of 1.5 MPa was delivered to the system by the Brooks mass flow meter. Once the system was pressurized with hydrogen, the backpressure was used to maintain the overall system pressure at 1 MPa. HPLC pump started pushing the feed into the system at a flowrate of 1.47 mL/min ( $WHSV = 4.5 \text{ h}^{-1}$ , calculation shown in section 6.2.9). The feed passed over the packed bed in the reactor and the temperature profile was monitored with the help of the three thermocouples located at different points in the thermowell. Hydrotreating reactions are highly exothermic in nature, therefore, there was an increase in temperature inside the reactor. On observing increase in temperature as the reaction progressed, the furnace controller was manipulated manually to keep the temperature in the reactor close to desired temperature. After exposing the feed to the catalyst bed and increased temperatures, the solution was cooled in the heat exchanger after the furnace. During the process, hydrogen kept flowing through the system. The hydrogen flow was completely stopped, and the system was emptied of any hydrogen by slowly reducing the pressure in the system using the backpressure. When the system was at atmospheric pressure, the outlet valve from the product tank was opened and the product was collected in a vial.

**Table 6.2** Operating conditions for the flow reactor for each of the model compounds

<b>Model Compound</b>	<b>Temperature (°C)</b>	<b>Weight hourly space velocity (h<sup>-1</sup>)</b>
Indene	150	4.5
	150	8.9
	180	4.5
	180	8.9
Indole	150	4.5
	150	8.9
	180	4.5
	180	8.9
Benzofuran	150	4.5
	150	8.9
	180	4.5
	180	8.9
Thianaphthene	180	4.5
	180	8.9
	220	4.5
	220	8.9

The obtained product was weighed, and it was further analyzed. The gases from the reaction were not further analyzed. The same catalyst was used for all the runs performed in this chapter. After every run in the flow reactor, 67.53 g of toluene was pumped through the system without any gas flow. That certain amount was known to be the total capacity of the flow reactor when filled with toluene. This was done to collect all the product at the outlet, therefore, clearing the system of any remains and thus balancing the mass.

### 6.2.8 Analysis

Gas chromatography coupled with mass spectroscopy was used for characterization, to determine the composition of the liquid products. The detailed method description and working principle

can be found in section 5.2.3 of Chapter 5. The same method was used but with the detector switching off between retention times of 1.6-1.75 min, to avoid solvent saturation.

Gas chromatography with flame ionization detector (GC-FID) was used for quantitative analysis of the model compound and the hydrogenated compounds after the reaction using an internal standard. This was performed using an Agilent 7890A GC-FID/NPD equipped with a HP-5MS column (50 m x 0.2 mm x 0.5 μm). Helium was used as carrier gas with a flow of 1 mL/min. The method was created for the oven to start and stay at 35 °C for 10 min, then increase to 200 °C at increments of 5 °C/min followed by increments of 20 °C/min to 250 °C and stay at that temperature for 4.5 min. *n*-Heptane was used as an internal standard. Samples were prepared by diluting 0.1 mL of product and 0.1 mL of *n*-heptane in 10 mL of toluene. Three point-based calibration curves were built, to calculate the response factor of each of the model compounds separately. To create a calibration curve, each compound was weighed approximately to 50 mg, 100 mg and 150 mg, the exact weights were noted down. The standards were spiked with 68.4 mg of *n*-heptane and diluted in 10 mL of toluene. The standards were injected by triplicate in the GC and the response factor was calculated using the principle formula <sup>9</sup>-

$$Response\ factor = \frac{Area\ of\ compound\ X\ Weight\ of\ the\ internal\ standard}{Area\ of\ the\ internal\ standard\ X\ Weight\ of\ the\ compound} \quad (1)$$

The model compounds are quantified by the instrument based on their relative response factor with the internal standard. This is achieved by injecting samples to be analyzed with the same amount of internal standard for all runs. The response factors for each of the model compounds are shown in table 6.3.

**Table 6.3** Response factors for the selected model compounds acquired from the GC-FID

<b>Compound</b>	<b>Response factor</b>	<b>Standard deviation</b>
Indene	0.97	±0.04
Indane	0.76	±0.06
Indole	1.11	±0.03
Benzofuran	1.15	±0.04

Thianaphthene	1.18	±0.01
---------------	------	-------

---

An elemental analysis was performed on the fresh catalyst that was nickel oxide impregnated on  $\gamma$ -Al<sub>2</sub>O<sub>3</sub> support (before activation), and the spent catalyst after performing all the reactions in the plug flow reactor. The analysis was performed by the analytical and instrumentation laboratory located in the chemistry department at the University of Alberta.

### 6.2.9 Calculations

Weight hourly space velocity (WHSV) was used as a one of the comparison factors that was altered during the experimental runs. WHSV was calculated using equation 2,

$$\text{WHSV} = \frac{\text{Total mass flow rate}}{\text{Mass of the catalyst bed}} \quad (2)$$

Mass of the catalyst bed was calculated by taking the total weight of the alumina support impregnated with nickel. The mass flowrate was taken as the flow rate of the feed mixture.

## 6.3 Results

Products collected from the flow reactor were qualitatively analyzed using the GC-MS and then quantified using the GC-FID.

### 6.3.1 Identification of the peaks for hydrogenated products

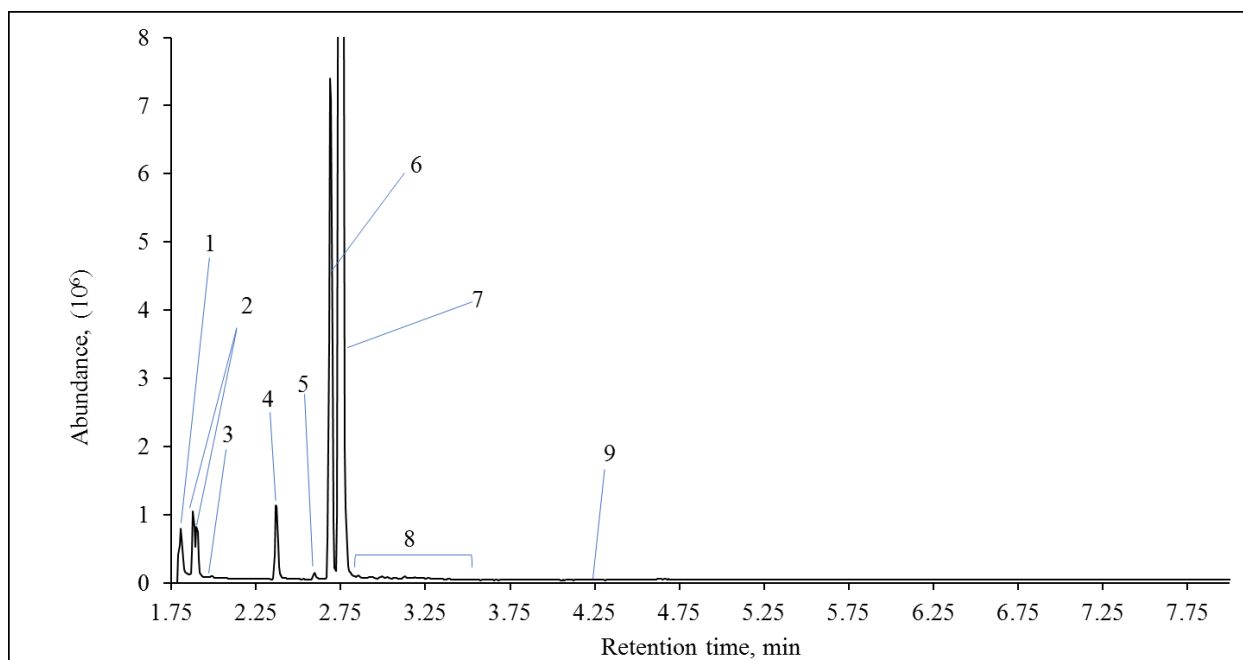
Peaks 1,2 and 3 in figures 6.4, 6.5, 6.6 and 6.8 were found to be representative of the same compounds and were also found to be of similar magnitudes. On further investigation, it was found that the corresponding eluents were due to the solvent used for dilution i.e. toluene. On

performing a run in the GC-MS under the same conditions with only toluene, the presence of peaks 1, 2 and 3 was observed.

### 6.3.1.1 Indene

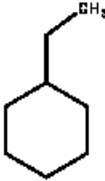
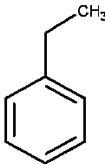
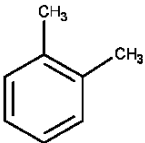
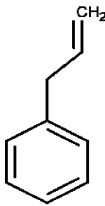
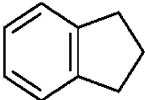
Product samples obtained for reactions with indene were analyzed using the GC-MS. No peaks were visible beyond a retention time of 3.75 min. Table 6.4, shows the compounds corresponding to each of the peaks in figure 6.4.

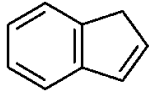
Indene hydrogenated to indane in the presence of excess hydrogen gas and nickel catalyst during all the experimental runs following the operating conditions listed in table 6.2. As can be seen from figure 6.4, the two major peaks on the chromatogram are those for indene (peak 7) and indane (peak 6). Presence of indane was further confirmed using the GC-FID (section 6.3.2). Peaks 1-5 and 8 represent impurities present in the toluene used for dilution and indene, as provided by the supplier.



**Figure 6.4** GC-MS result for the reaction of indene in the flow reactor

**Table 6.4** Products from hydrogenation reaction of indene in the presence of nickel catalyst

Peak	Retention time (min)	Compound name	Structure
1 <sup>e</sup>	1.81	Ethyl cyclohexane	
2 <sup>e</sup>	1.88, 1.99	Isomers of ethyl benzene	
3 <sup>e</sup>	1.90	o-Xylene	
4 <sup>a</sup>	2.37	- <sup>b</sup>	-
5 <sup>d</sup>	2.59	2-Propenyl benzene	
6	2.72	Indane	

7	2.80	Indene	
8	- <sup>c</sup>	- <sup>b</sup>	-

a Peak present in the pure compound acquired from the supplier as an existing impurity or unidentified compound.

b Mass spectrum for the respective retention time is shown in Appendix A.

c Representative of various peaks grouped together.

d These compounds should be seen only as being indicative of the nature of the products. The true identities of these compounds have not been confirmed.

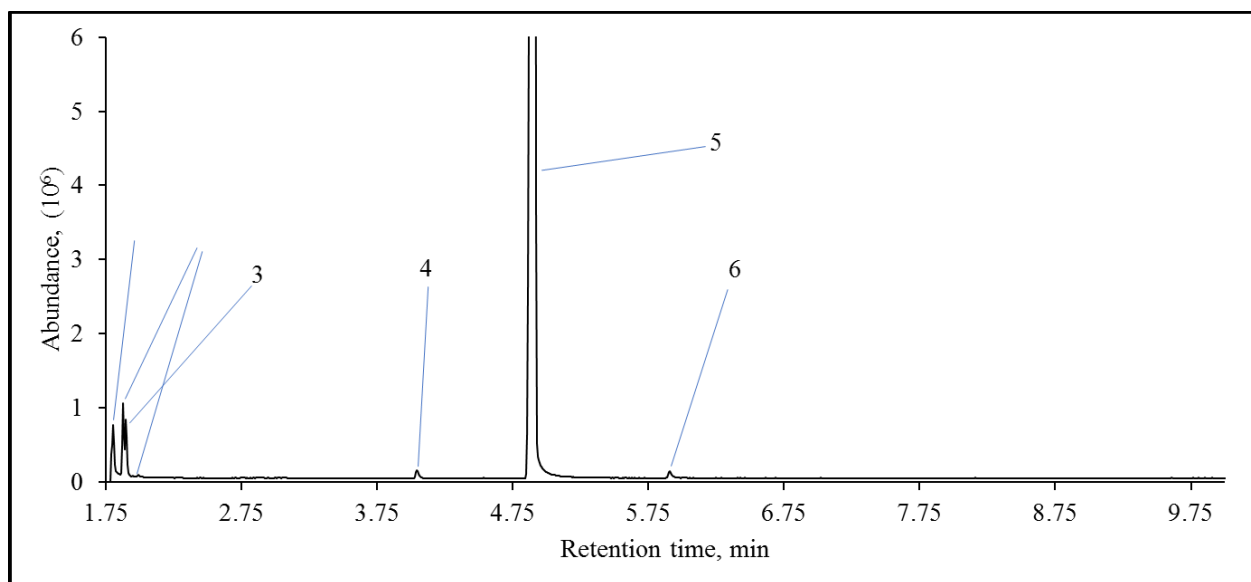
e Peak present in the solvent acquired from the supplier as an existing impurity or unidentified compound.

Hydrogenation to indane significantly varied based on different reaction conditions. This is further quantified and discussed in section 6.3.2.

#### 6.3.1.2 Indole

Hydrogenation of indole was not as evident for indole. The hydrogenated compound formed was indoline (peak 4). The sample was spiked with indoline and analyzed using the GC-MS, to confirm the suggestion by the mass spectrum. The peaks overlapped at the retention time of 4.05 min. Peak 6 is an impurity present in pure indole provided by the supplier, this was previously mentioned in Chapter 3 Acids.

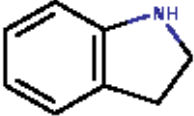
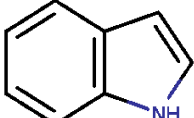
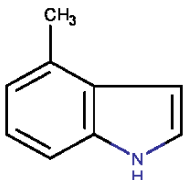
No visible peaks were present beyond the retention time of 6 min.



**Figure 6.5** GC-MS result for the reaction of indole in the flow reactor

**Table 6.5** Products from hydrogenation reaction of indole in the presence of nickel catalyst

Peak	Retention time (min)	Compound name	Structure
1 <sup>d</sup>	1.81	Ethyl cyclohexane	
2 <sup>d</sup>	1.88, 1.99	Isomers of ethyl benzene	
3 <sup>d</sup>	1.90	o-Xylene	

4	4.05	Indoline	
5	4.99	Indole	
6 <sup>a</sup>	2.72	4-Methyl-1H-indole <sup>b</sup>	

a Peak present in the pure compound acquired from the supplier as an existing impurity or unidentified compound.

b Mass spectrum for the respective retention time is shown in Appendix A.

c These compounds should be seen only as being indicative of the nature of the products. The true identities of these compounds have not been confirmed.

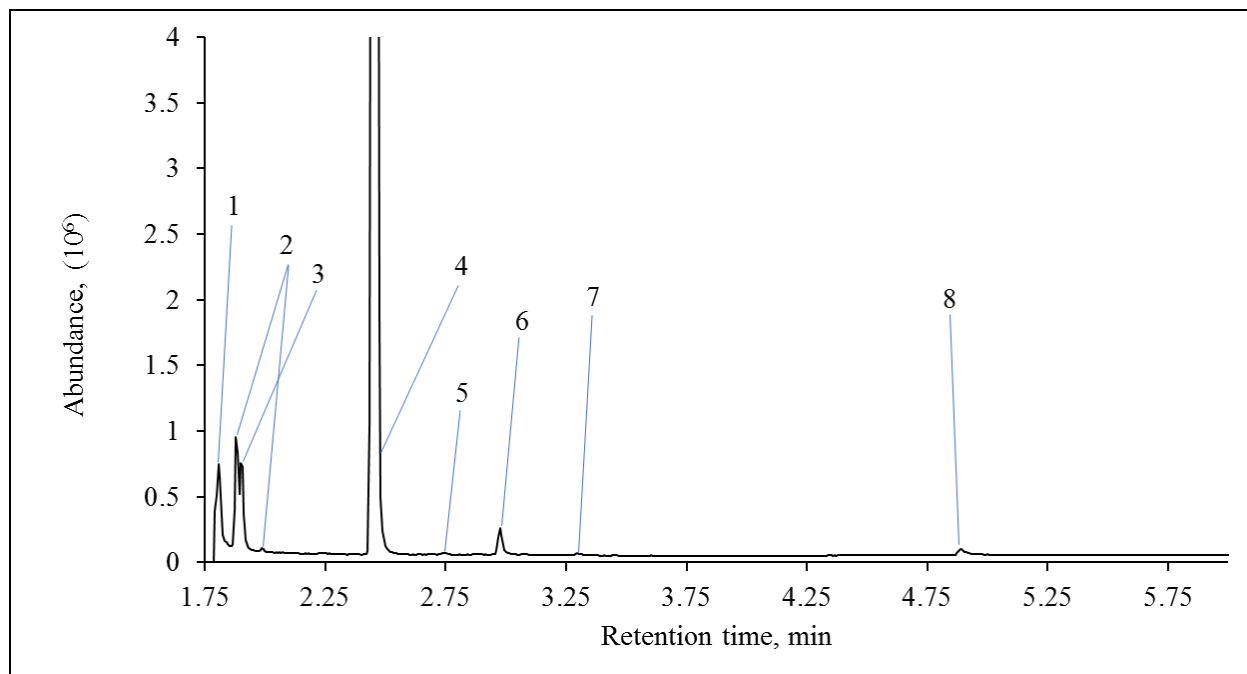
d Peak present in the solvent acquired from the supplier as an existing impurity or unidentified compound.

Despite low conversion rates, indole was able to undergo hydrogenation reactions at lower temperature ranges. An attempt was made to build the calibration curve for indoline but due to very low concentrations in the product sample, a linear plot was not achievable between concentrations of 1-10 % with respect to indole present in the feed (section 6.3.3).

### 6.3.1.3 Benzofuran

Benzofuran (peak 4) hydrogenated to form 2,3-dihydrobenzofuran (peak 6). The conversion was much lower for benzofuran in comparison to indene. However, like indole, benzofuran underwent hydrogenation under all operating conditions listed in table 6.2.

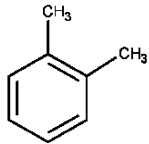
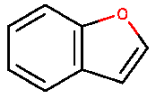
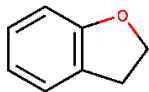
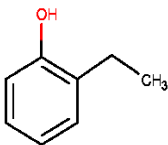
Ring opening was another possible reaction that took place during the runs, eluted at a retention time of 3.30 min (peak 7). A phenol is formed by breaking off the heterocyclic ring at the C<sub>1</sub> position.



**Figure 6.6** GC-MS result for the reaction of benzofuran in the flow reactor

**Table 6.6** Products from hydrogenation reaction of benzofuran in the presence of nickel catalyst

Peak	Retention time (min)	Compound name	Structure
1 <sup>d</sup>	1.81	Ethyl cyclohexane	
2 <sup>d</sup>	1.88, 1.99	Isomers of ethyl benzene	

3 <sup>d</sup>	1.90	o-Xylene	
4	2.50	Benzofuran	
5 <sup>c</sup>	2.75	Mass spectrum shown below (figure 6.7a)	Unidentified
6	2.98	2,3-Dihydrobenzofuran	
7 <sup>c</sup>	3.30	3-Ethyl phenol	
8 <sup>c</sup>	4.89	Mass spectrum shown below (figure 6.7b)	Unidentified

a Peak present in the pure compound acquired from the supplier as an existing impurity or unidentified compound.

b Mass spectrum for the respective retention time is shown in Appendix A.

c These compounds should be seen only as being indicative of the nature of the products. The true identities of these compounds have not been confirmed.

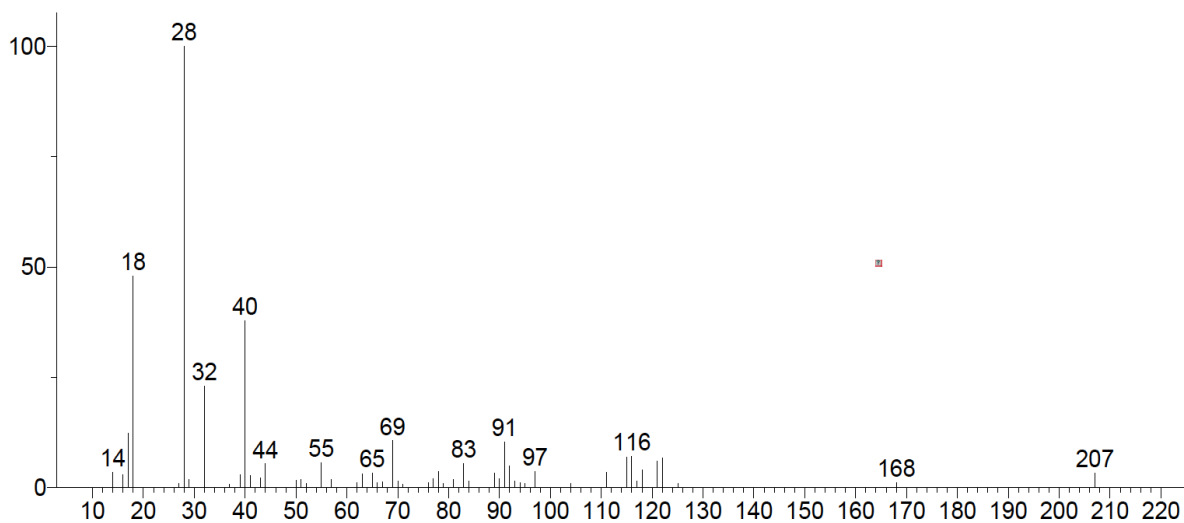
d Peak present in the solvent acquired from the supplier as an existing impurity or unidentified compound.

To understand peak 5, the mass spectrum at a retention time of 2.75 min was obtained (figure 6.7). An estimated molecular weight of the molecule is expected to be close to 116 m/z. Observing the two compounds prior to and after peak 5, the compound elutes between benzofuran and 2,3-dihydrobenzofuran. Both peaks 4 and 6, contain 8 carbons, implying that the unidentified compound comprises of 8 carbons. No strong 77 m/z to indicate a benzene ring, but 91 m/z indicative of toluene fragment.

Similarly, in the case of peak 8, the biggest molecular ion after the base ion is 117. From the suggestions given by the NIST library, it was suggested to be indole. On spiking the sample, it was confirmed that indole was still present in the system. It was a contaminant present in the benzofuran product samples, following the series of reactions of indoles prior to benzofuran.

a)

Unknown; InLib=-1558



b)

Unknown; InLib=-315

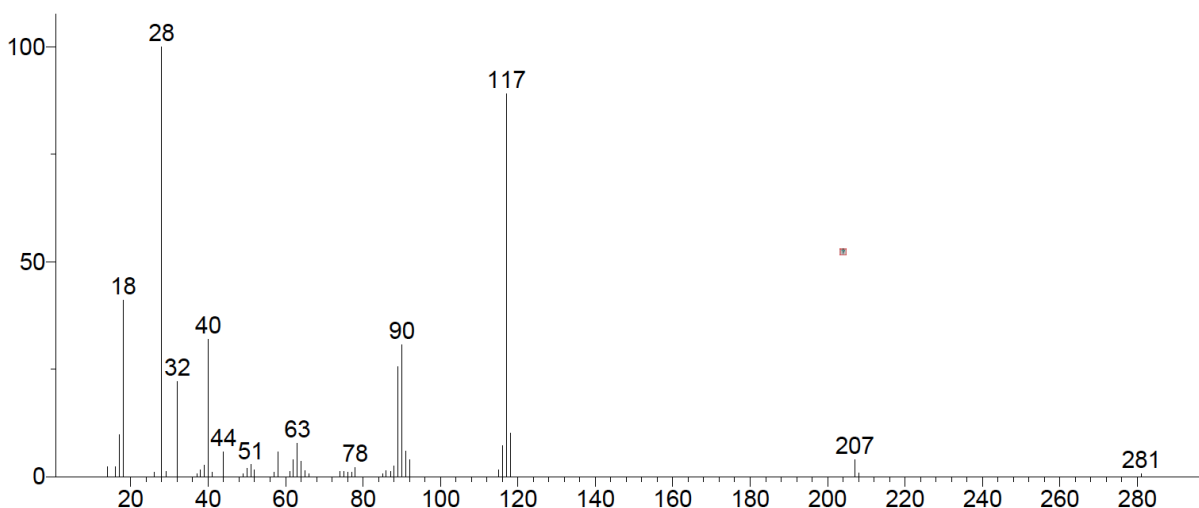


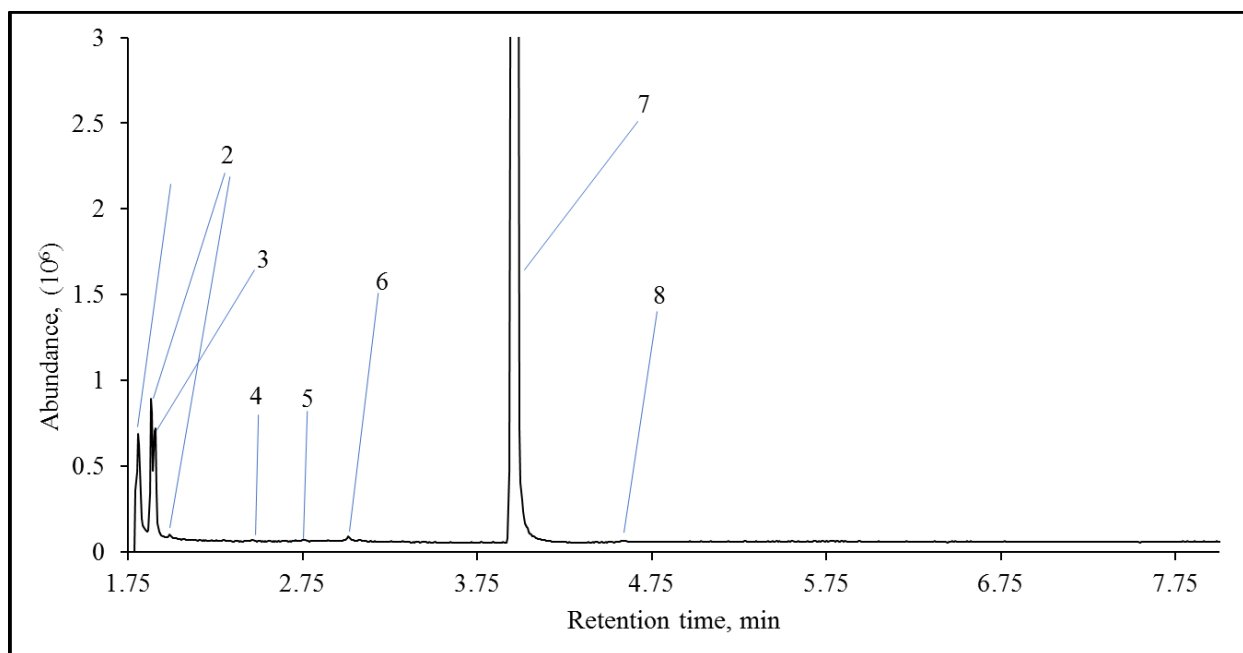
**Figure 6.7** Mass spectrums obtained for retention times of a) 2.75 min and b) 4.89 min, respectively, during the hydrogenation reaction of benzofuran in a plug flow reactor

Benzofuran, also, had an extremely low conversion rate in comparison to the inlet feed concentration of benzofuran. This is further explained in section 5.3.3.

#### 6.3.1.4 Thianaphthene

The first run performed with thianaphthene was run at a temperature of 180 °C under both space velocity of 4.5 and 8.9 h<sup>-1</sup>. On analyzing the products, no hydrogenation took place. The temperature was thus increased to 220 °C, to investigate whether temperature would affect the hydrogenation reaction.

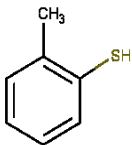
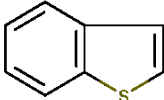
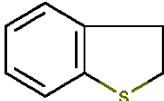
On analyzing the results from the experimental runs performed at a higher temperature, there was a peak for the hydrogenated compound at retention time of 4.60 min for both WHSV for the temperature of 220 °C. The presence of 2,3-dihydro-1-benzothiophene (peak 8) could not be confirmed with spiking because the compound was not for sale. Another ring opening reaction also took place and led to the formation of 3-methyl benzenethiol (peak 6). The intensity of peak 6 was seen to be relatively bigger than the peak for 2,3-dihydro-1-benzothiophene.



**Figure 6.8** GC-MS result for the reaction of thianaphthene in the flow reactor

**Table 6.7** Products from hydrogenation reaction of thianaphthene in the presence of nickel catalyst.

Peak	Retention time (min)	Compound name	Structure
1 <sup>d</sup>	1.81	Ethyl cyclohexane	
2 <sup>d</sup>	1.88, 1.99	Isomers of ethyl benzene	
3 <sup>d</sup>	1.90	o-Xylene	

4 <sup>c</sup>	2.47	Mass spectrum shown below (figure 6.9a)	Unidentified
5 <sup>c</sup>	2.76	Mass spectrum shown below (figure 6.9b)	Unidentified
6 <sup>c</sup>	3.01	3-Methyl benzenethiol	
7	3.30	Thianaphthene	
8 <sup>c</sup>	4.60	2,3-Dihydro-1-benzothiophene	

a Peak present in the pure compound acquired from the supplier as an existing impurity or unidentified compound.

b Mass spectrum for the respective retention time is shown in Appendix A.

c These compounds should be seen only as being indicative of the nature of the products. The true identities of these compounds have not been confirmed.

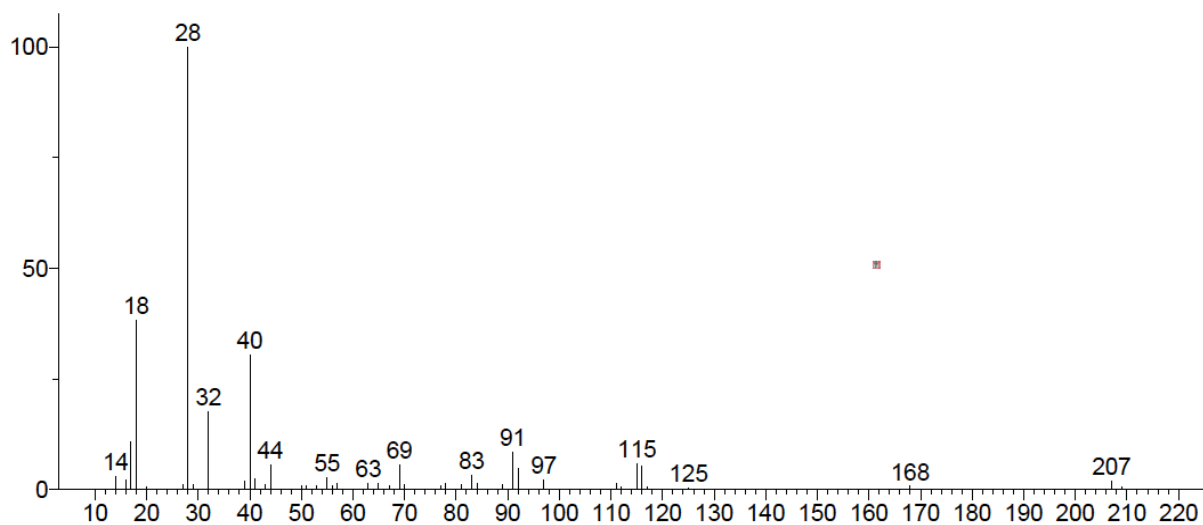
d Peak present in the solvent acquired from the supplier as an existing impurity or unidentified compound.

Peak 4 at retention time of 2.47 min was seen to have a molecular ion of 115 m/z. The closest molecular weight of the compound is expected to be at 115 g/mol. On analyzing the neighbouring peaks, the unidentified compound is composed of 8 carbon atoms.

Peak 5 was found in the same vicinity, at a retention time of 2.76 min. It most likely is also composed of a total of 8 carbons, with 2 carbons attached to a benzene ring (peak for 78 m/z). The molecular ion of 91 m/z in the spectrum indicates the presence of an alkyl benzene group. Given that the molecular weight of the compound is around 118 g/mol and since the molecular weight of sulfur is 32 g/mol, there was no sulfur present in the compound at peak 5.

a)

Unknown; InLib=-1774



b)

Unknown; InLib=-1187

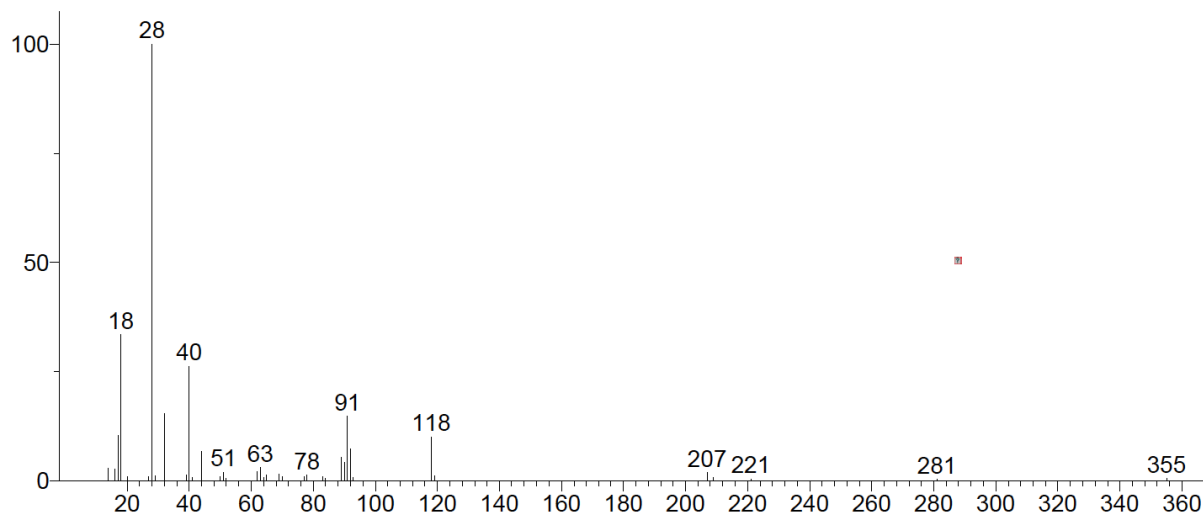


**Figure 6.9** Mass spectrums obtained for retention times of a) 2.47 min and b) 2.76 min, respectively, during the hydrogenation reaction of thianaphthene in a plug flow reactor

### 6.3.2 Effect of temperature and space velocity on conversion of indene

GC-FID was used for quantifying the indane formed after the hydrogenation reaction of indene as described in section 6.2.8. The quantification was performed using *n*-heptane as an internal standard for all the runs. The feed shown in table 6.8 was obtained by performing a mass balance for all the reactions. Therefore, the given concentration is the calculated feed concentration of indene. The feed was not quantified using the GC-FID.

The theoretical concentration from performing mass balances was not found to be a reasonable source of comparison for the feed.

One of the reason for discrepancy between the feed concentration and total product concentration is due to the fact that in some cases, there could be a possible contamination in the system from prior runs. Even though a toluene wash was performed between every run, it was evident through the contamination of indole in benzofuran in the gas chromatogram results from figure 6, that the runs could be contaminated.

Shown in table 8 are the theoretical concentrations for indene in the feed based on mass balance, and the concentrations of the indane and unreacted indene in the product obtained from the GC-FID. The conversion for the hydrogenation reaction was calculated based on the ratio of moles of indane in the product over the total moles present in the product.

**Table 6.8** GC-FID results obtained from product samples of experimental runs with indene compared to theoretical feed concentration

	Mass Recovery (%)	Feed (mg/mL of toluene) Indene	Product (mg/mL of toluene)		Conversion
			Indene	Indane	
T = 180 °C WHSV = 4.5 h <sup>-1</sup>	98.7	31.3	26.1	9.8	27.0
T = 180 °C WHSV = 8.9 h <sup>-1</sup>	99.2	29.1	31.0	1.2	3.6
T = 150 °C WHSV = 4.5 h <sup>-1</sup>	98.3	34.7	30.7	5.9	15.9
T = 150 °C WHSV = 8.9 h <sup>-1</sup>	97.4	38.4	37.2	1.5	3.9

The conversion of indene to indane for a space velocity of  $4.5 \text{ h}^{-1}$  at a temperature of  $180 \text{ }^\circ\text{C}$  was 27 % compared to 15.9 % at a lower temperature of  $150 \text{ }^\circ\text{C}$ . It is evident that with increase in temperature, the conversion to indane was greater which looking at results for a lower space velocity of  $4.5 \text{ h}^{-1}$ . However, at a faster flow rate of  $8.9 \text{ h}^{-1}$ , the conversion at both temperatures of 150 and  $180 \text{ }^\circ\text{C}$  is very close. A higher value of 3.9 % at a lower temperature of  $150 \text{ }^\circ\text{C}$ , in comparison with 3.6 % at a higher temperature of  $180 \text{ }^\circ\text{C}$  is due to analytical uncertainty.

For the same temperature, the ratio varies greatly with the different space velocities. At  $180 \text{ }^\circ\text{C}$ , the difference in the relative indane formation is almost 9.5 times less with increase in WHSV from  $4.5\text{-}8.9 \text{ h}^{-1}$ . At a temperature of  $150 \text{ }^\circ\text{C}$ , the product ratio reduced to 4.8 times with increase in WHSV. Hence, with increase in WHSV, the conversion rate decreases by a considerable amount. The feed requires more contact time with the catalyst to reach a higher conversion.

### *6.3.3 Low conversion rates after hydrogenation of indole, benzofuran and thianaphthene*

Unlike indene, the conversion to the hydrogenated counterpart for the remaining model compounds was lower than 5 %. It was difficult to build a calibration curve for such low concentrations of the hydrogenated products. On attempting to build a calibration curve for indole, with an expected low conversion rate lying between the range of 1-10 %, a parabolic calibration curve was obtained instead of a linear curve. In cases on benzofuran and thianaphthene, the peak area was not in the minimum area range for the GC-FID to quantify the hydrogenated product. Hence, the products could not be quantified using the GC-FID. The measure of hydrogenation was left to the comparison between the theoretical feed concentration and concentration of model compound in the analyzed product. The same assumptions, mentioned in section 6.3.2, are applied to the results obtained for the model compounds with lower conversion. The feed concentration was obtained by performing a mass balance for all the reactions. Therefore, the given concentration is the calculated feed concentration of the compounds. The feed was not quantified using the GC-FID.

For indole, the results were scattered. The product concentration in most of the experimental runs was greater than the feed concentration. % Discrepancy was calculated by obtaining a percent ratio of the difference between the product concentration and feed concentration with respect to the feed concentration. Since the discrepancy is seen to increase substantially, one of the reasons for larger concentration of indole in the product was suspected to be contamination of indole in the system from previous runs. A negative value in % discrepancy is because the concentration of product was higher than the theoretical feed concentration. The contamination could have accumulated which in turn led to such high discrepancies. An important aspect to be considered here is that there was contamination found in the chromatograms of products of benzofuran with indole. From the results, no claims can be made on the hydrogenation reaction, except the fact that hydrogenation does take place from the results obtained by the GC-MS in section 6.3.2.

**Table 6.9** GC-FID results obtained from product samples of experimental runs with indole compared to theoretical feed concentration

	<b>Mass recovery (%)</b>	<b>Feed (mg/mL of toluene) Indole</b>	<b>Product (mg/mL of toluene) Indole</b>	<b>Discrepancy %</b>
T = 180 °C WHSV = 4.5 h <sup>-1</sup>	100.3	30.9	32.7	-5.8
T = 180 °C WHSV = 8.9 h <sup>-1</sup>	99.6	33.7	38.0	-12.5
T = 150 °C WHSV = 4.5 h <sup>-1</sup>	102.2	30.4	35.9	-18.0
T = 150 °C WHSV = 8.9 h <sup>-1</sup>	100.0	32.5	29.5	9.2

From table 6.10, for benzofuran, there is a gradual decrease in concentration of benzofuran in the product from a temperature of 150 °C to 180 °C.

Even though the discrepancy between the concentrations is a positive value, based on previous assumptions and observations, observed patterns can not be used to draw conclusions on the rate of conversion for benzofuran with changes in temperature and WHSV. It can be concluded from

the results that there were possible reactions taking place in the products obtained from experimental runs of benzofuran.

**Table 6.10** GC-FID results obtained from product samples of experimental runs with benzofuran compared to theoretical feed concentration

	<b>Mass recovery (%)</b>	<b>Feed (mg/mL of toluene) Benzofuran</b>	<b>Product (mg/mL of toluene) Benzofuran</b>	<b>Discrepancy %</b>
T = 180 °C WHSV = 4.5 h <sup>-1</sup>	102.9	24.4	22.2	9.1
T = 180 °C WHSV = 8.9 h <sup>-1</sup>	101.5	24.8	23.2	6.7
T = 150 °C WHSV = 4.5 h <sup>-1</sup>	97.9	24.0	22.7	5.5
T = 150 °C WHSV = 8.9 h <sup>-1</sup>	100.6	26.2	25.1	4.2

The last four series of reactions were performed with thianaphthene. This was deliberately done due to the presence of sulfur in the heterocyclic ring of thianaphthene. Since the catalyst was not sulfided prior to the runs with thianaphthene, the sulfur had adsorbed onto the surface of the catalyst, this is further discussed in section 6.3.4. From the GC-MS, there was no visible peak for the hydrogenation of thianaphthene to 2,3-dihydro-1-benzothiophene at a temperature of 180 °C. However, there is a large discrepancy in the concentrations at 180 °C. This could be due to the loss of sulfur to the surface of the catalyst.

Compared to the rest of the model compounds, the largest discrepancy was observed for thianaphthene. The discrepancy can not be directly related to the rate of hydrogenation, but the loss of concentration could be as a result of hydrogenation, loss of sulfur and possible ring opening reactions.

**Table 6.11** GC-FID results obtained from product samples of experimental runs with thianaphthene compared to theoretical feed concentration

	Mass recovery (%)	Feed (mg/mL of Thianaphthene)	Product (mg/mL of toluene) Thianaphthene	Discrepancy %
T = 180 °C WHSV = 4.5 h <sup>-1</sup>	103.1	24.6	18.6	24.5
T = 180 °C WHSV = 8.9 h <sup>-1</sup>	100.2	26.9	24.1	10.7
T = 220 °C WHSV = 4.5 h <sup>-1</sup>	94.1	27.2	20.7	24.0
T = 220 °C WHSV = 8.9 h <sup>-1</sup>	101.5	24.5	20.9	15.0

#### 6.3.4 Elemental analysis of spent catalyst vs. fresh catalyst

After performing all the runs using the same activated catalyst pellets, the reactor was unloaded, and the catalyst was further analyzed. The CHNS results are presented in table 6.12. The spent catalyst was compared with the elemental composition of the freshly prepared catalyst. The largest increase was in the amount of carbonaceous deposits adsorbed on the spent catalyst. As mentioned in section 6.3.3, sulfur accumulated on the catalyst post-reaction with thianaphthene. There was an approximate increase of 8 times in the amount of sulfur. There was also an increase in the nitrogen and hydrogen content, in comparison to the fresh catalyst. It can be concluded from the elemental analysis that the spent catalyst accumulated impurities as the experiments proceeded which could have led to decrease in activity over time.

**Table 6.12** CHNS elemental analysis of the fresh catalyst and the spent catalyst

	%N	%C	%H	%S
<b>Fresh nickel catalyst</b>	0.01	0.12	0.59	0.03

<b>Spent nickel catalyst</b>	0.10	15.69	1.72	0.24
------------------------------	------	-------	------	------

## 6.4 Discussion

### 6.4.1 Hydrogenation of aromatic compounds containing 5-membered rings

The conditions needed to hydrogenate compounds in the presence of nickel catalyst required using high pressures, as mentioned in section 2.5 of chapter 2. A higher pressure of hydrogenation is known to work better for hydrogenation reactions. Using a higher pressure is linked with increase of hydrogen solubility and adsorption probability. This ensures increased hydrogen concentration on the surface of the catalyst. However, in this study a milder condition of 1 MPa used. However, from the results, it can be concluded that all compounds went through hydrogenation even under comparatively milder conditions.

In the heterogenous catalysis in the presence of nickel as a catalyst, the hydrogen gas in the system adsorbs to the nickel sites. The hydrogen binds to the surface on the catalyst. On adsorption of the model compounds on the catalyst, the model compounds also bind to the surface of the catalyst where the hydrogen transfer takes place. This leads to the formation of the hydrogenated compound (figure 6.10).

The results indicated that the relative rate of hydrogenation over Ni-alumina catalyst between a temperature of 150-220 °C and pressure of 1 MPag was: indene > benzofuran ~ indole > thianaphthene.

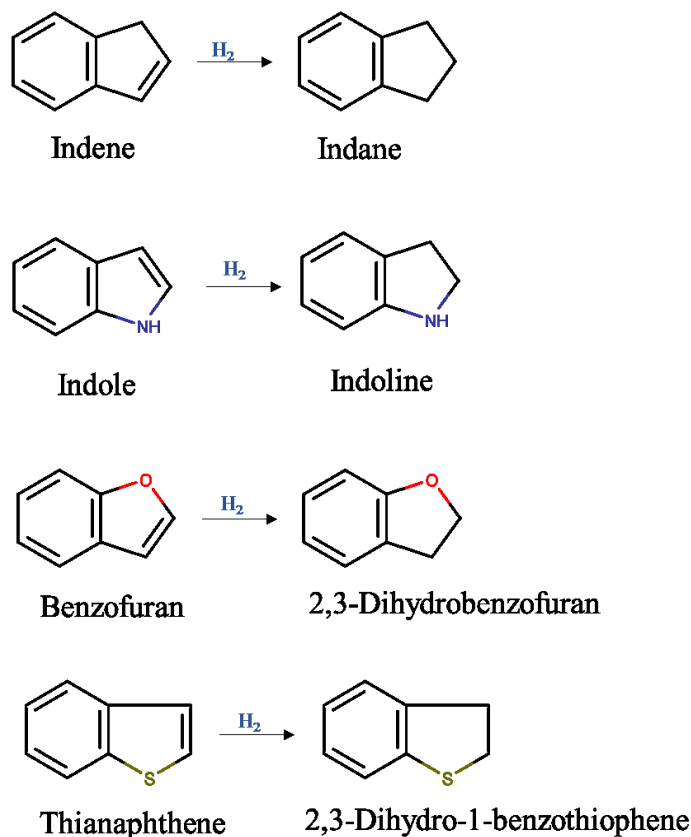


**Figure 6.10** Hydrogenation reactions for binuclear aromatic compounds with one 5-membered ring

#### 6.4.2 Ring-opening reactions followed by hydrogenation

Benzofuran and thianaphthene in the presence of excess hydrogen, proceeded towards ring-opening reactions. In the case of these two compounds, their hydrogenation compounds acted as intermediates in the reaction. Due to lower hydrogen pressure, there was a reduced selectivity towards reaction termination at the reduced products of benzofuran and thianaphthene. The possible mechanism for the ring-opening reaction is shown in figure 6.11. It is seen that the C-O and C-S scission takes place, forming ring-opening structures.

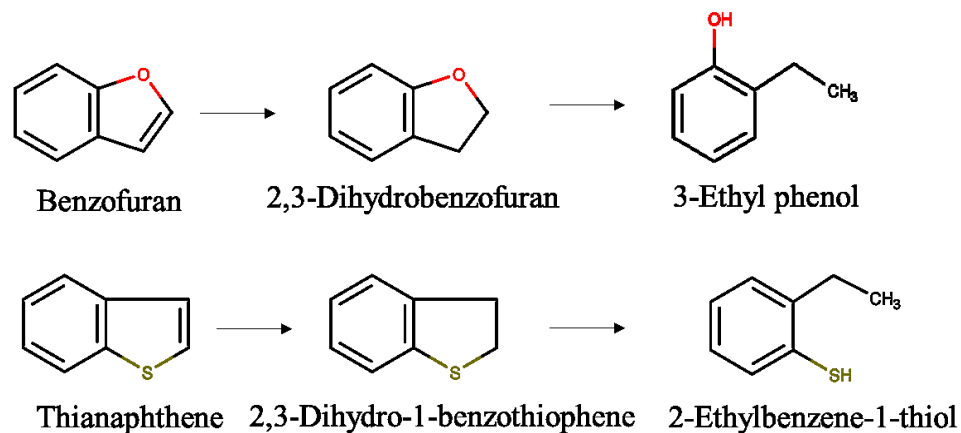


**Figure 6.11** Possible reaction sequence for the ring opening reaction of benzofuran and thianaphthene

## 6.5 Conclusion

A continuous flow reactor was used to implement hydrotreating of aromatic compounds containing 5-membered rings at a hydrogen pressure of 1 MPa and temperature between 150-220 °C. The reactions were performed to implications of hydrogenation reactions on selective binuclear compounds in the presence of metal promoted catalyst in a flow reactor. The main conclusions and observations were as follows:

- a) All the model compounds produced hydrogenated compounds on reaction, in the presence of molecular hydrogen at a pressure of 1 MPa and in the temperature range of

150-220 °C. Indene produced a much higher conversion than the other compounds which followed the order of benzofuran > indole > thianaphthene. Indene, indole and benzofuran were capable of hydrogenation starting at a temperature of 150 °C but no hydrogenation product was formed for thianaphthene at that temperature. Thianaphthene did hydrogenate at an increased temperature of 220 °C.

- b) Benzofuran and thianaphthene formed ring-opening products in addition to hydrogenated products.

## 6.6 References

- (1) Gray, M. R. *Upgrading Oilsands Bitumen and Heavy Oil*, 1st ed.; The University of Alberta Press: Edmonton, **2015**.
- (2) Hsu, C. S.; Robinson, P. R. *Practical Advances in Petroleum Processing*, 1st ed.; Springer Science & Business Media: New York, 2006.
- (3) Ipatieff, B. Y. V. N.; Meisinger, E. E.; Pines, H. Destructive Hydrogenation of Indan and Hexahydroindan. *J. Am. Chem. Soc.* **1949**, *71* (8), 2685–2687.
- (4) Haven, X. E. W.; Tretter, J. R. 1-Ketolilolidine and Some. **1953**, *23* (2).
- (5) Entel, J.; Ruof, C. H.; Howard, H. C. Reactions of Benzofurans with Hydrogen. *J. Am. Chem. Soc.* **1951**, *73* (9), 4152–4158.
- (6) Zirka, A. A.; Ryzhova, G. L.; Slizhov, Y. G.; Mashkina, A. V. Catalytic hydrogenation of benzothiophene to 2,3-dihydrobenzothiophene. *React. Kinet. Catal. Lett.* **1983**, *23* (1–2), 7–12.
- (7) Li, G.; Hu, L.; Hill, J. M. Comparison of reducibility and stability of alumina-supported Ni catalysts prepared by impregnation and co-precipitation. *Appl. Catal. A Gen.* **2006**, *301* (1), 16–24.
- (8) Cheng, Z.; Wu, Q.; Li, J.; Zhu, Q. Effects of promoters and preparation procedures on reforming of methane with carbon dioxide over Ni/Al<sub>2</sub>O<sub>3</sub> catalyst. *Catal. Today* **1996**, *30*

(1–3), 147–155.

- (9) Scanlon, J. T. Calculation of Flame Ionization Detector Relative Response Factors Using the Effective Carbon Number Concept. **1985**, *23*, 333–340.

## **CHAPTER 7: CONCLUSIONS AND FUTURE WORK**

### **7.1 Conclusions**

The objective of this study was to build a foundation for the fundamental understanding of the chemistry associated with binuclear aromatic compounds that contained 5-membered rings that could be present in the structure of larger molecules that are present in bitumen. By studying the different conversion types, thermal, acid, base and hydrogenation, for each compound a picture was formed of relative reactivity and the propensity of each compound to react under those conversion conditions. This was thought to be beneficial to gain a better insight into the side-

reactions that may be taking place when bitumen, or subfractions of bitumen, is converted under similar conditions. Listed below are the main conclusions that were drawn from this research:

- a) Indene, indole, benzofuran, and thianaphthene were all converted under acidic conditions. The most reactive of these compounds were indole and benzofuran. However, salts of indole were readily formed, as well as addition products, leading to solids precipitating from the reaction mixture. Benzofuran formed addition products. Indene required interaction with stronger acids before addition products were observed; no reaction was found with 1 M H<sub>2</sub>SO<sub>4</sub> or 1 N HCl at 120 °C, but addition products were formed at 70 °C over 85 % H<sub>3</sub>PO<sub>4</sub> and Amberlyst® 15 (acid resin catalyst). Thianaphthene was the most difficult to convert by acids and reaction products other than the starting material was observed only during conversion in the presence of Amberlyst® 15.
- b) Indole was light and air sensitive for polymerization.
- c) Indene, indole, and benzofuran were unaffected by 1 N NH<sub>4</sub>OH, Ambersep® 900 hydroxide (base resin catalyst) and NaH at 120 °C. Thianaphthene was reactive only towards NaH at 120 °C.
- d) Indane and thianaphthene, when thermally converted in the absence of other compounds, were thermally stable at 400 °C and 2 MPa over a period of 1 h.
- e) Indene, indole and benzofuran were reactive to thermal conversion at 400 °C. Addition products were found after thermal conversion and in the case of indene and indole solid products were also found after thermal conversion. Persistent free radicals were detected in the reaction products using electron spin resonance spectroscopy.

- f) Indene, indole, and benzofuran were reactive to hydrogenation over a reduced Ni-alumina catalyst at 150 °C and 1 MPa (gauge) H<sub>2</sub> pressure. The reactivity sequence under these conditions were indene >> benzofuran ~ indole.
  
- g) Thianaphthene was reactive to hydrogenation over a reduced Ni-alumina catalyst that was sulfided by reaction with thianaphthene, but it required a higher reaction temperature (220 °C) before conversion became noticeable.

## 7.2 Other deliverables

The design, construction and commissioning of a laboratory-scale flow reactor were performed as part of this study. This reactor was employed in the hydrogenation studies.

## 7.3 Future work

To better understand the intermediates formed during the reactions of the model compounds in the presence of acids and bases, it would be beneficial to analyze the aqueous layer collected while separating the acids and bases through water washing. Especially in the case of NaH where it was a key step to understand the reduction of thianaphthene, the aqueous layer could have provided the missing data to better describe the reaction chemistry.

## BIBLIOGRAPHY

- (1) Zou, C. Heavy Oil and Bitumen. *Unconv. Pet. Geol.* **2013**, 307–335
- (2) Gray, M. R. *Upgrading Oilsands Bitumen and Heavy Oil*, 1st ed.; The University of Alberta Press: Edmonton, **2015**.
- (3) Niizuma, S.; Steele, C. T.; Gunning, H. E.; Strausz, O. P. Electron spin resonance study of free radicals in Athabasca asphaltene. **1977**, *56*, 249–256.
- (4) Siddiquee, M. N.; De Klerk, A. Hydrocarbon addition reactions during low-temperature

- autoxidation of oilsands bitumen. *Energy and Fuels* **2014**, 28 (11), 6848–6859.
- (5) Strausz, O. P.; Lown, E. M. *The chemistry of Alberta oil sands, bitumens and heavy oils*; Alberta Energy Research Institute: Calgary, AB, 2003.
  - (6) Siddiquee, M. N.; De Klerk, A. Heterocyclic addition reactions during low temperature autoxidation. *Energy and Fuels* **2015**, 29 (7), 4236–4244.
  - (7) Solomons, T. W. G.; Fryhle, C. *Organic Chemistry*, 10th ed.; John Wiley & Sons, Inc.: Hoboken, N.J, 2011.
  - (8) Jovanović, J.; Spitteller, M.; Elling, W. Indene Dimerization Products. *J. Serbian Chem. Soc.* **2002**, 67 (6), 393–406.
  - (9) Jovanović, J.; Spitteller, M.; Spitteller, P. NMR Analysis of 2-(2', 3'-Dihydro-1'H-Inden-1'-Yl)-1H-Indene. *J. Serbian Chem. Soc.* **2001**, 66 (11–12), 753–763.
  - (10) Mizote, A.; Tanaka, T.; Higashimura, T.; Okamura, S. Cationic Polymerization of Cyclic Olefins. *J. Polym. Sci. Part A-1 Polym. Chem.* **1966**, 4 (4), 869–879.
  - (11) J. Houlihan, W. *Indoles*; Wiley-Interscience: New York, 1972.
  - (12) Kulkarni, A.; Zhou, W.; Török, B. Heterogeneous Catalytic Hydrogenation of Unprotected Indoles in Water: A Green Solution to a Long-Standing Challenge. *Org. Lett.* **2011**, 13 (19), 5124–5127.
  - (13) Clark, P. D.; Lesage, K. L.; Tsang, G. T.; Hyne, J. B.; Tn, C. Reactions of Benzo [B] Thiophene with Aqueous Metal Species: Their Influence on the Production and Processing of Heavy Oils. *Energy Fuels* **1988**, 2 (4), 578–581.
  - (14) Kotrel, S.; Knözinger, H.; Gates, B. C. The Haag-Dessau Mechanism of Protolytic Cracking of Alkanes. *Microporous Mesoporous Mater.* **2000**, 35–36, 11–20.
  - (15) Pines, H.; Stalick, W. M. *Base-Catalyzed Reactions of Hydrocarbons and Related Compounds*; Academic Press: New York, 1977.
  - (16) Styles, Y.; De Klerk, A. Sodium Conversion of Oilsands Bitumen-Derived Asphaltenes. *Energy Fuels* **2016**, 30 (7), 5214–5222.
  - (17) A. Pryor, W. *Free Radicals*; McGraw-Hill: New York, 1966.
  - (18) Lifshitz, A.; Suslensky, A.; Tamburu, C. Thermal Decomposition of 4-Methylpyrimidine. Experimental Results and Kinetic Modeling. *J. Phys. Chem. A* **2001**, 105 (14), 3542–3554.

- (19) Rüchardt, C.; Gerst, M.; Ebenhoch, J. Uncatalyzed Transfer Hydrogenation and Transfer Hydrogenolysis: Two Novel Types of Hydrogen-Transfer Reactions. *Angew. Chemie Int. Ed. English* **1997**, *36* (1314), 1406–1430.
- (20) Badger, B. G. M.; Kimber, R. W. L. The Formation of Aromatic Hydrocarbons at High Temperatures. Part V1. The Pyrolysis of Tetralin. *J. Chem. Soc.* **1960**, 266–270.
- (21) Laskin, A.; Lifshitz, A. Isomerization and Decomposition of Indole. Experimental Results and Kinetic Modeling. *J. Phys. Chem. A* **1997**, *101* (42), 7787–7801.
- (22) Organ, P. P.; Mackie, J. C. Kinetics of Pyrolysis of Furan. *J. Chem. Soc. Faraday Trans.* **1991**, *87* (6), 815–823.
- (23) Urness, K. N.; Guan, Q.; Golan, A.; Daily, J. W.; Nimlos, M. R.; Stanton, J. F.; Ahmed, M.; Ellison, G. B. Pyrolysis of Furan in a Microreactor. *J. Chem. Phys.* **2013**, *139* (12), 124305(1-10).
- (24) Winkler, J. K.; Karow, W.; Rademacher, P. Gas-Phase Pyrolysis of Heterocyclic Compounds, Part 1 and 2: Flow Pyrolysis and Annulation Reactions of Some Sulfur Heterocycles: Thiophene, Benzo[b]thiophene, and Dibenzothiophene. A Product-Oriented Study. *J. Anal. Appl. Pyrolysis* **2002**, *62* (1), 123–141.
- (25) Slotboom, H. W.; Penninger, J. Mechanism and Kinetics of the Thermal Hydrocracking of Single Polyaromatic Compounds. *ACS Symp. Ser.* **1975**, *32*, 444–456.
- (26) Chianelli, R. R. Fundamental Studies of Transition Metal Sulfide Hydrodesulfurization Catalysts. *Catal. Rev.* **1984**, *26* (3–4), 361–393.
- (27) Ipatieff, B. Y. V. N.; Meisinger, E. E.; Pines, H. Destructive Hydrogenation of Indan and Hexahydroindan. *J. Am. Chem. Soc.* **1949**, *71* (8), 2685–2687.
- (28) Kutz, W. M.; Nickels, J. E.; McGovern, J. J.; Corson, B. B. Catalytic Alkylation of Indan and Tetralin by Olefins, Alcohols and Diethyl Ether. *J. Am. Chem. Soc.* **1948**, *70* (12), 4026–4031.
- (29) Deng, D. S.; Han, G. Q.; Zhu, X.; Xu, X.; Gong, Y. T.; Wang, Y. Selective Hydrogenation of Unprotected Indole to Indoline over N-Doped Carbon Supported Palladium Catalyst. *Chinese Chem. Lett.* **2015**, *26* (3), 277–281.
- (30) Shaw, J. E.; Stapp, P. R. Regiospecific Hydrogenation of Quinolines and Indoles in the Heterocyclic Ring. *J. Heterocycl. Chem.* **1987**, *24* (5), 1477–1483.
- (31) Entel, J.; Ruof, C. H.; Howard, H. C. Reactions of Benzofurans with Hydrogen. *J. Am.*

- Chem. Soc.* **1951**, 73 (9), 4152–4158.
- (32) Karakhanov, É. A.; Drovyannikova, G. V.; Viktorova, E. A. Catalytic Alkylation of Benzofurans. *Chem. Heterocycl. Compd.* **1971**, 7 (8), 953–955.
- (33) Lee, C. L.; Ollis, D. F. Catalytic Hydrodeoxygenation of Benzofuran and O-Ethylphenol. *J. Catal.* **1984**, 87 (2), 325–331.
- (34) Zirka, A. A.; Ryzhova, G. L.; Slizhov, Y. G.; Mashkina, A. V. Catalytic Hydrogenation of Benzothiophene to 2,3-Dihydrobenzothiophene. *React. Kinet. Catal. Lett.* **1983**, 23 (1–2), 7–12.
- (35) Pines, H. Catalytic Versatility of Nickel as a Function of Its Preparation and Modification. *Adv. Catal.* **1987**, 35, 323–373.
- (36) Masliyah, J.; Zhou, Z. J.; Xu, Z.; Czarnecki, J.; Hamza, H. Understanding Water-Based Bitumen Extraction from Athabasca Oil Sands. *Can. J. Chem. Eng.* **2008**, 82 (4), 628–654.
- (37) Liu, J.; Xu, Z.; Masliyah, J. Interaction Forces in Bitumen Extraction from Oil Sands. *J. Colloid Interface Sci.* **2005**, 287 (2), 507–520.
- (38) Tamiz Bakhtiari, M.; Harbottle, D.; Curran, M.; Ng, S.; Spence, J.; Siy, R.; Liu, Q.; Masliyah, J.; Xu, Z. Role of Caustic Addition in Bitumen-Clay Interactions. *Energy Fuels* **2015**, 29 (1), 58–69.
- (39) Flury, C.; Afacan, A.; Tamiz Bakhtiari, M.; Sjoblom, J.; Xu, Z. Effect of Caustic Type on Bitumen Extraction from Canadian Oil Sands. *Energy Fuels* **2014**, 28 (1), 431–438.
- (40) Fink, T. E.; Bearden, R. Alkali Metal Desulfurization Process for Petroleum Oil Stocks Using Low Pressure Hydrogen. 3,787,315, 1974.
- (41) Sternberg, H. W.; Donne, C. L. D.; Markby, R. E.; Friedman, S. Reaction of Sodium with Dibenzothiophene. A Method for Desulfurization of Residua. *Ind. Eng. Chem. Process Des. Dev.* **1974**, 13 (4), 433–436.
- (42) Friedman, S.; Kaufman, M. L.; Wender, I. Alkali Metals As Hydrogenation Catalysts for Aromatic Materials. *J. Org. Chem.* **1971**, 36 (5), 694–697.
- (43) Price; Caole, C.; Oae, S. *Sulfur Bonding*; Ronald Press Co: New York, 1962.

- (44) ASTM D7169-11. *Standard Test Method for Boiling Point Distribution of Samples with Residues Such as Crude Oils and Atmospheric and Vacuum Residues by High Temperature Gas Chromatography*; ASTM International: West Conshohocken, PA, 2016; Vol. 05.4.
- (45) Silverstein, R. M.; Webster, F. X.; Kiemle, D. J.; Bryce, D. L. *Spectrometric Identification of Organic Compounds*; John Wiley & Sons, Inc., 2014.
- (46) Hsu, C. S.; Robinson, P. R. *Practical Advances in Petroleum Processing*, 1st ed.; Springer Science & Business Media: New York, 2006.
- (47) Haven, X. E. W.; Tretter, J. R. 1-Ketolilolidine and Some. **1953**, *23* (2).
- (48) Li, G.; Hu, L.; Hill, J. M. Comparison of reducibility and stability of alumina-supported Ni catalysts prepared by impregnation and co-precipitation. *Appl. Catal. A Gen.* **2006**, *301* (1), 16–24.
- (49) Cheng, Z.; Wu, Q.; Li, J.; Zhu, Q. Effects of promoters and preparation procedures on reforming of methane with carbon dioxide over Ni/Al<sub>2</sub>O<sub>3</sub> catalyst. *Catal. Today* **1996**, *30* (1–3), 147–155.
- (50) Scanlon, J. T. Calculation of Flame Ionization Detector Relative Response Factors Using the Effective Carbon Number Concept. **1985**, *23*, 333–340.

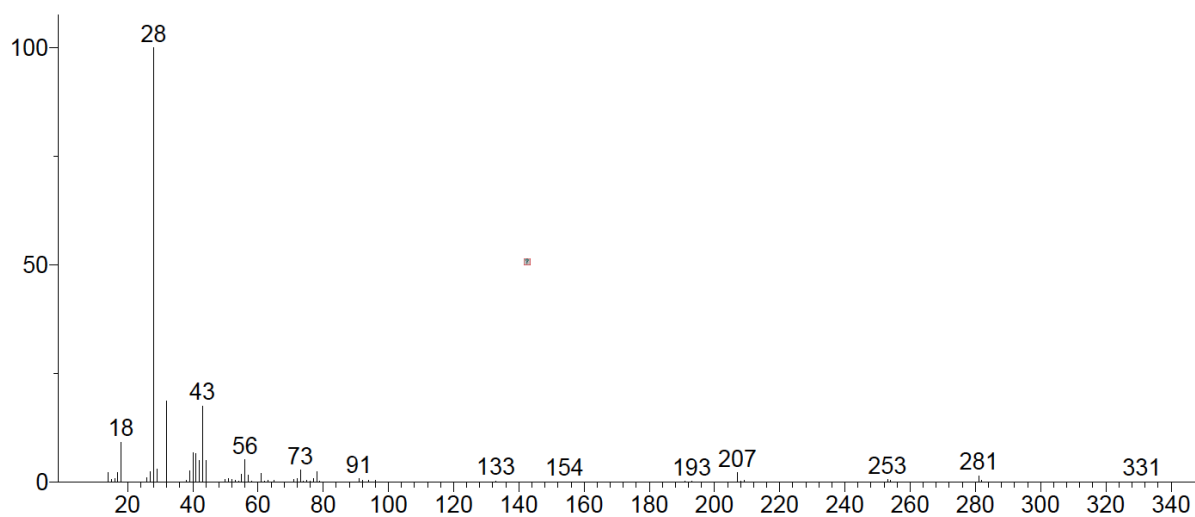
**APPENDIX A**  
**Mass Spectrums**

**Chapter 3**

**Indene**

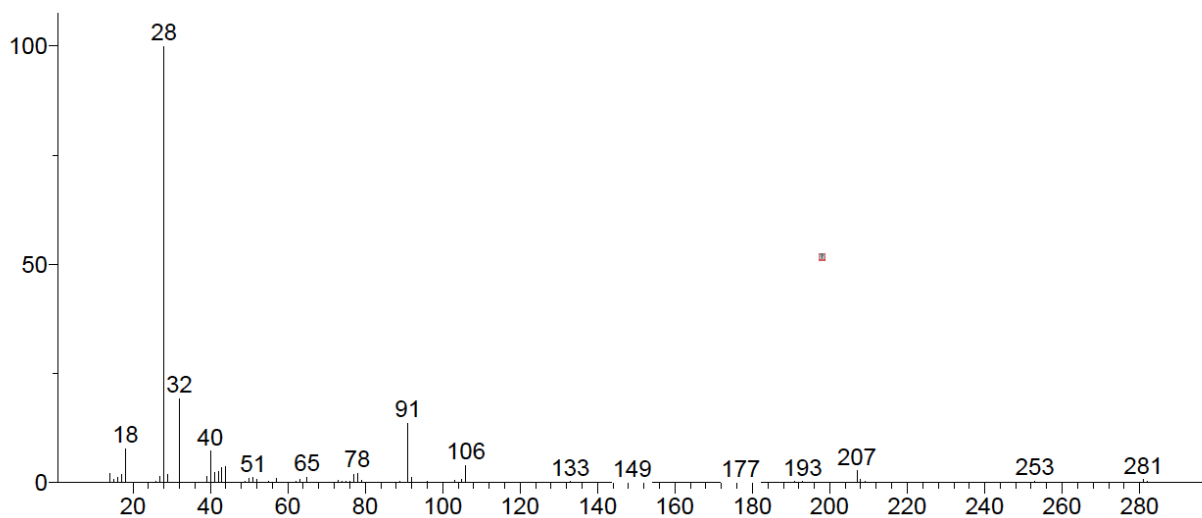
Retention time 1.73 min

Unknown; InLib=-1709



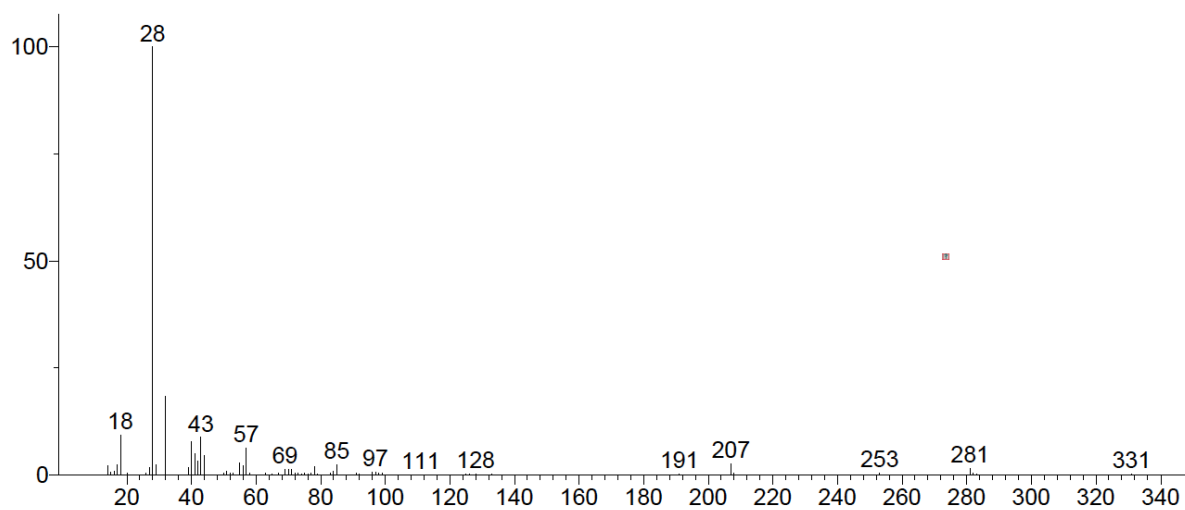
Retention time 1.90 min

Unknown; InLib=-1421



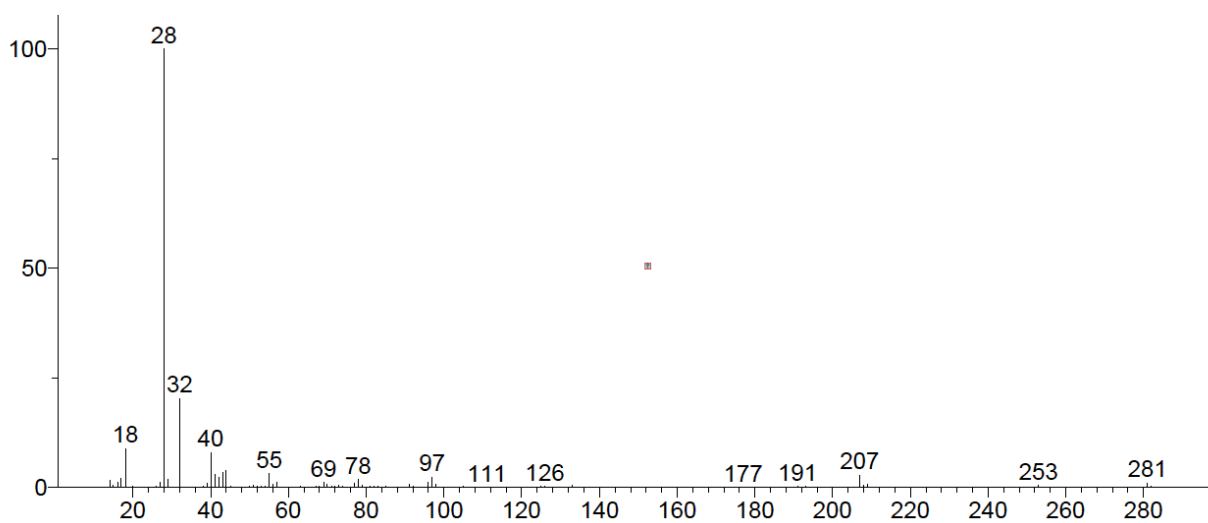
Retention time 1.97 min

Unknown; InLib=-1589



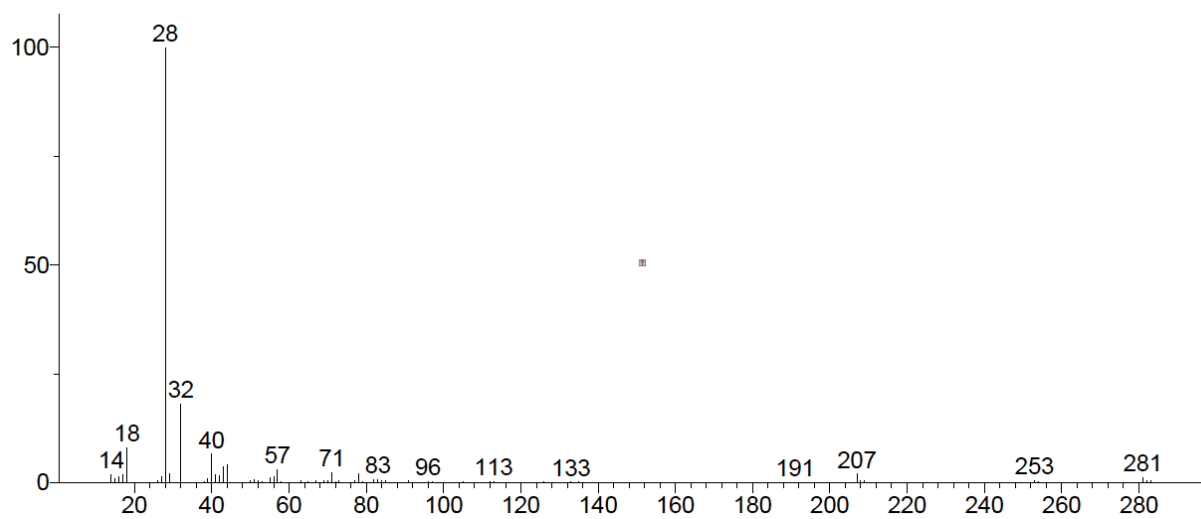
Retention time 2.06 min

Unknown; InLib=-1647



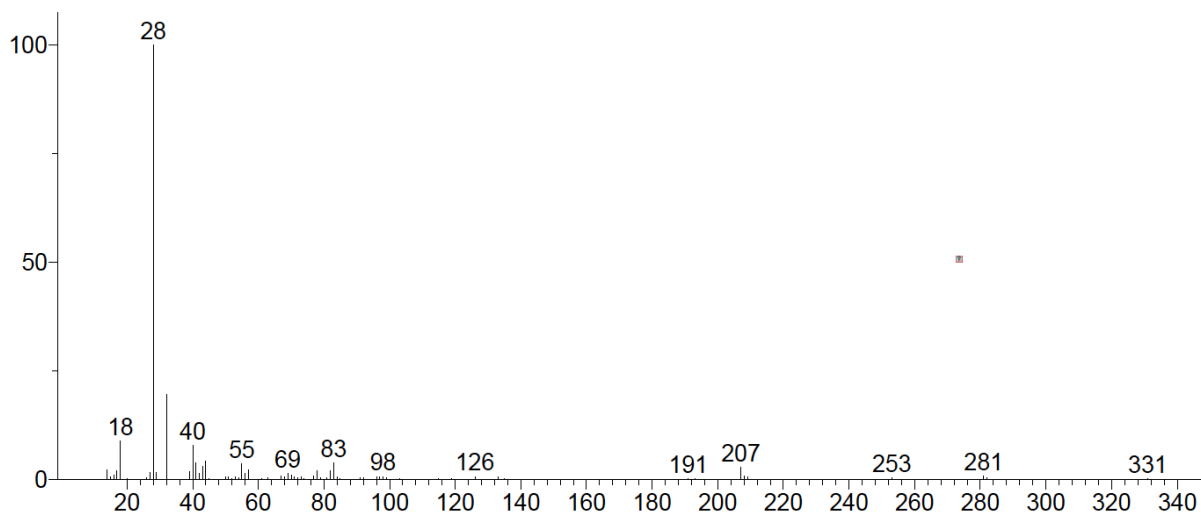
Retention time 2.11 min

Unknown; InLib=-1275



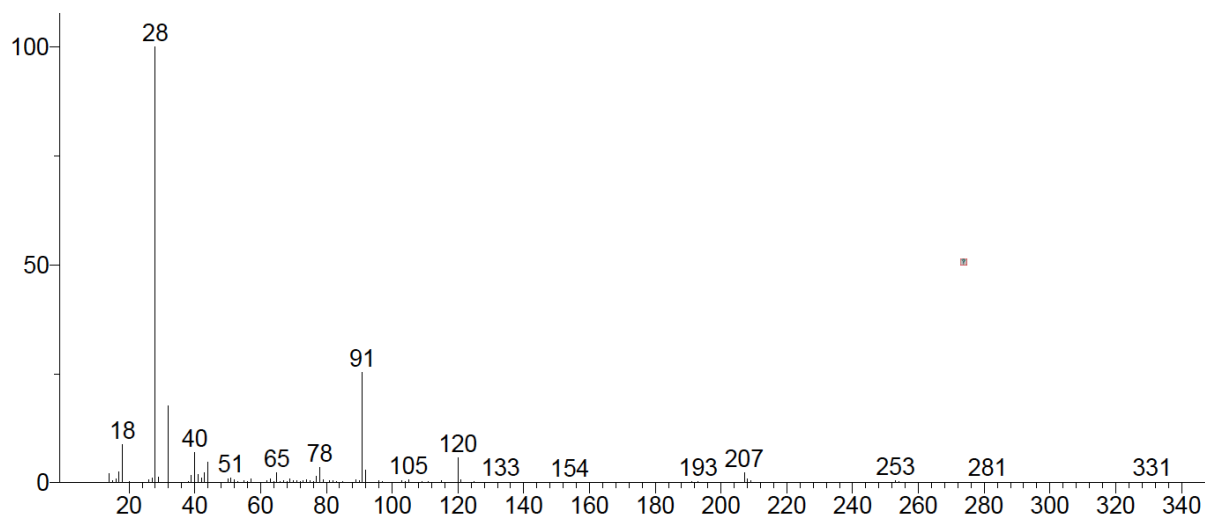
Retention time 2.14 min

Unknown; InLib=-1210



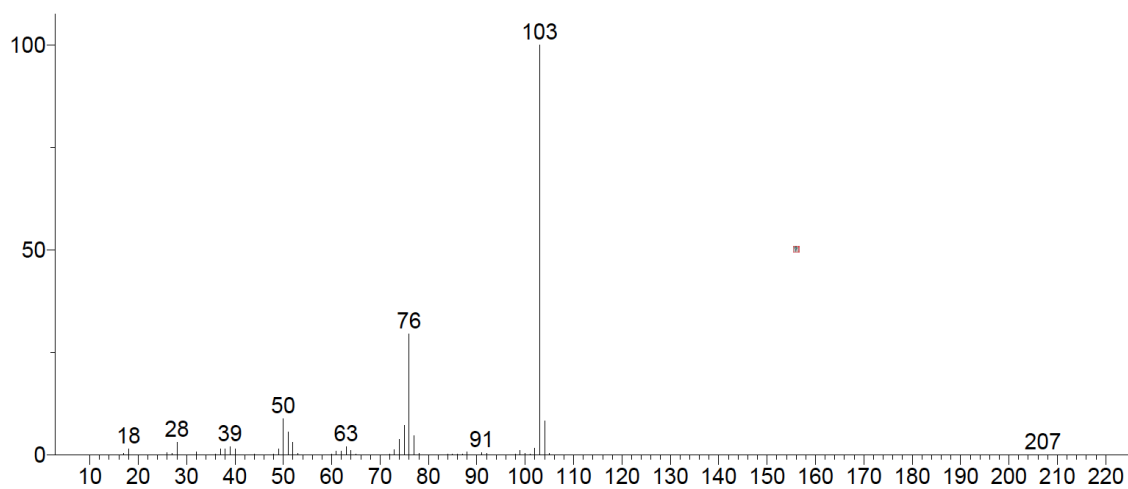
Retention time 2.25 min

Unknown; InLib=-1224



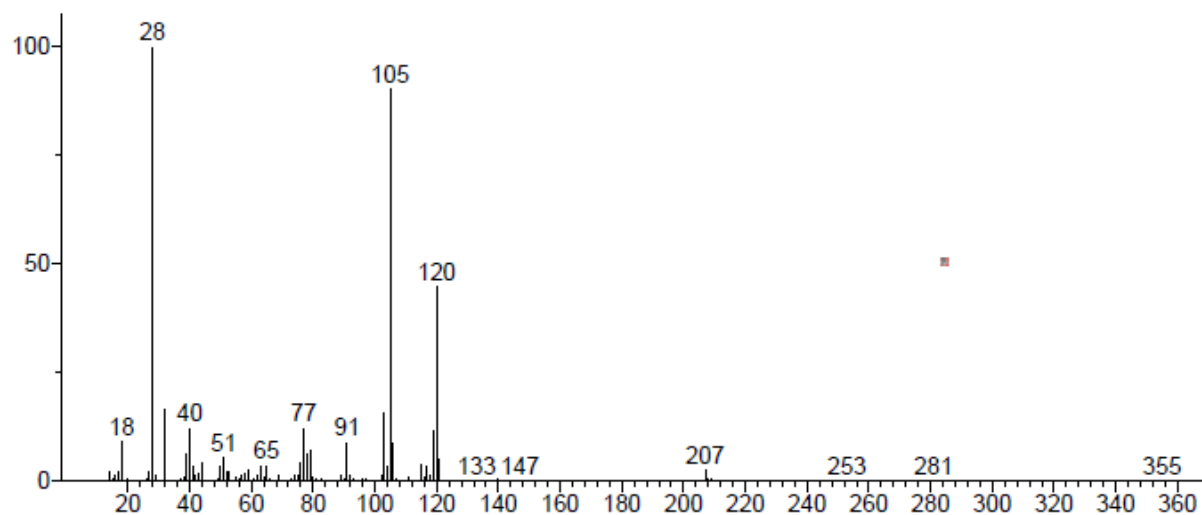
Retention time 2.37 min/ 2.49 min

Unknown; InLib=184



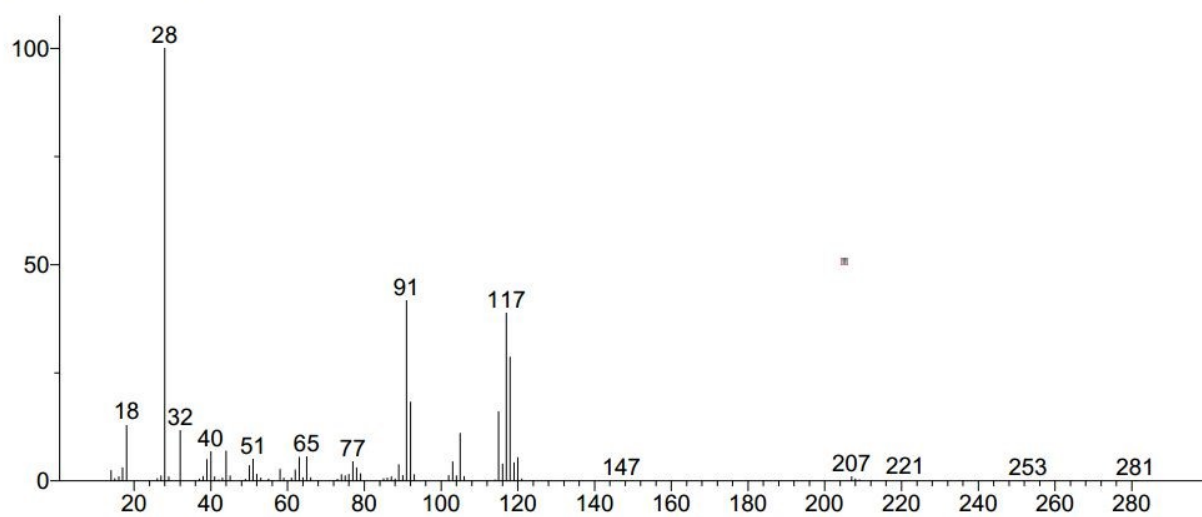
Retention time 2.41 min

Unknown; InLib=-284



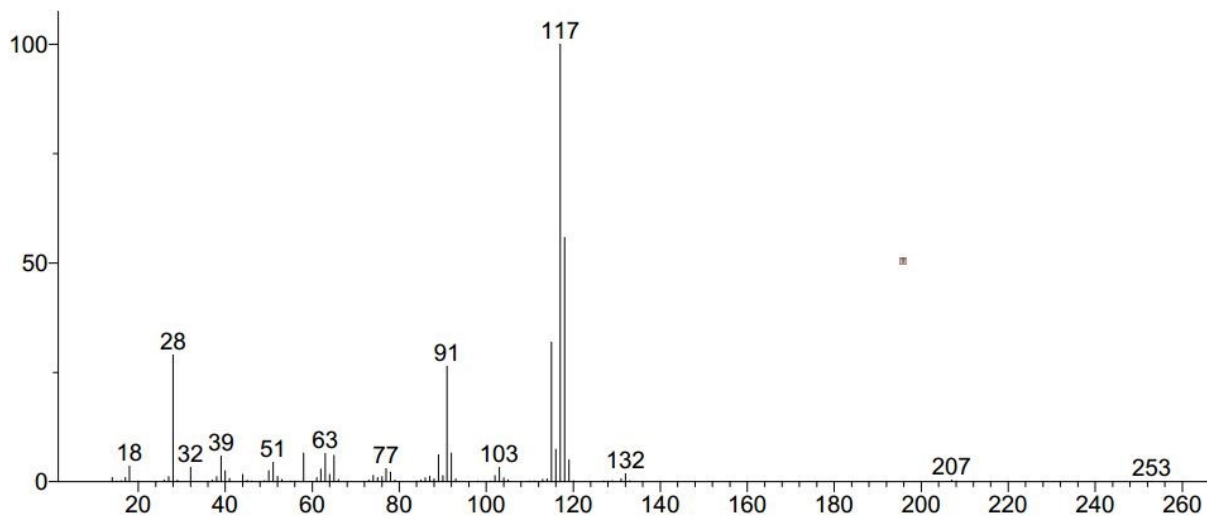
Retention time 2.75 min

Unknown; InLib=-509



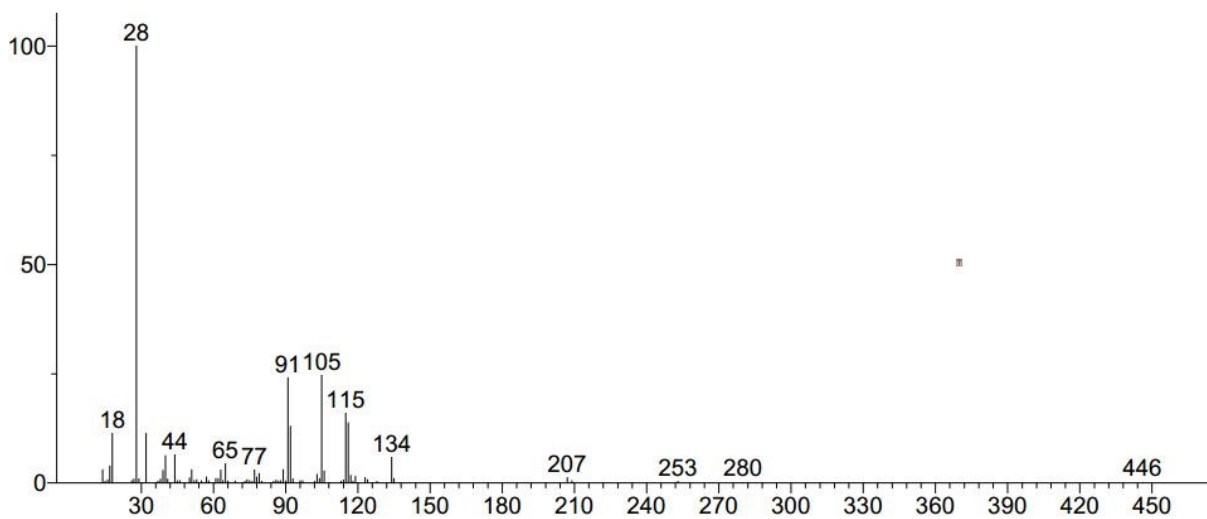
Retention time 2.85 min

Unknown; InLib=-122



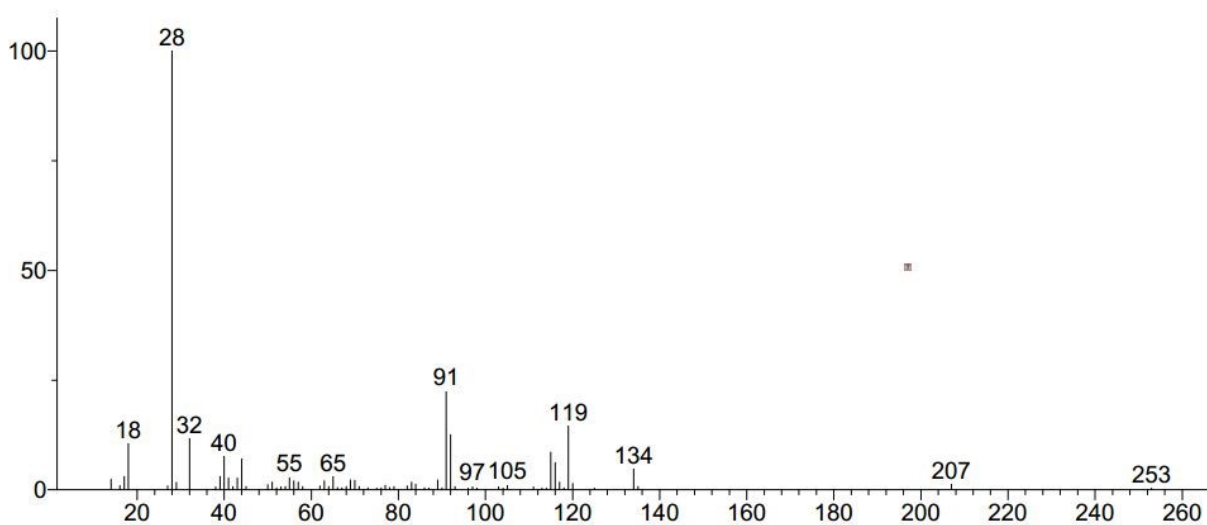
Retention time 3.03 min

Unknown; InLib=-1066



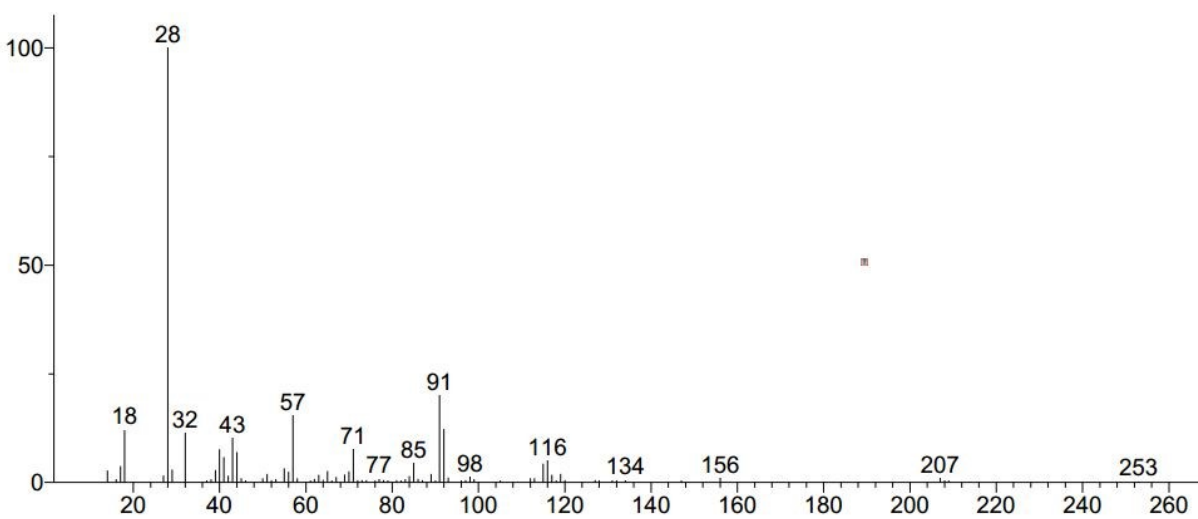
Retention time 3.12 min

Unknown; InLib=-905



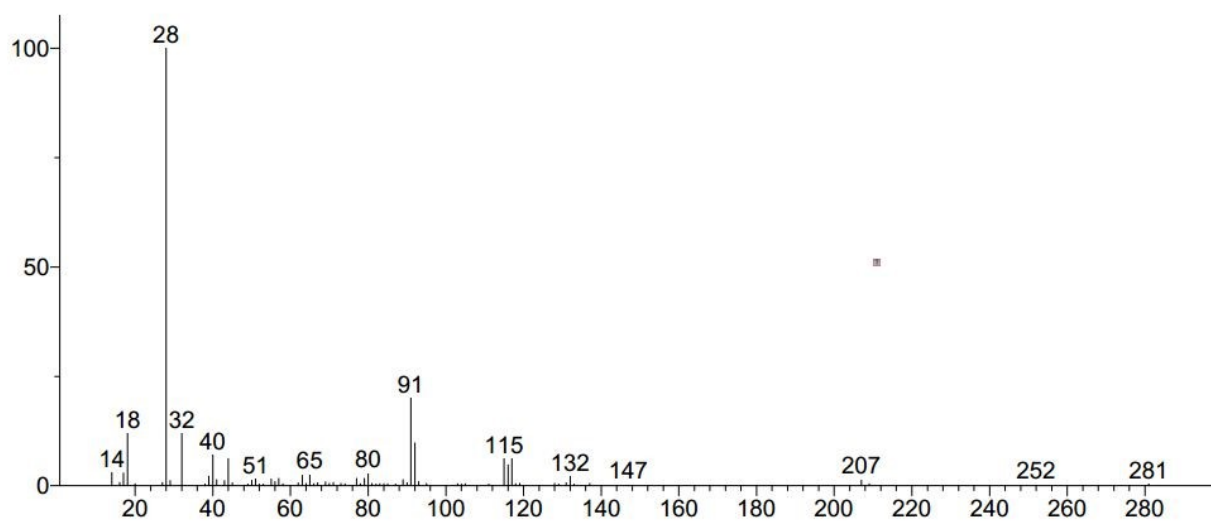
Retention time 3.18 min

Unknown; InLib=-1276



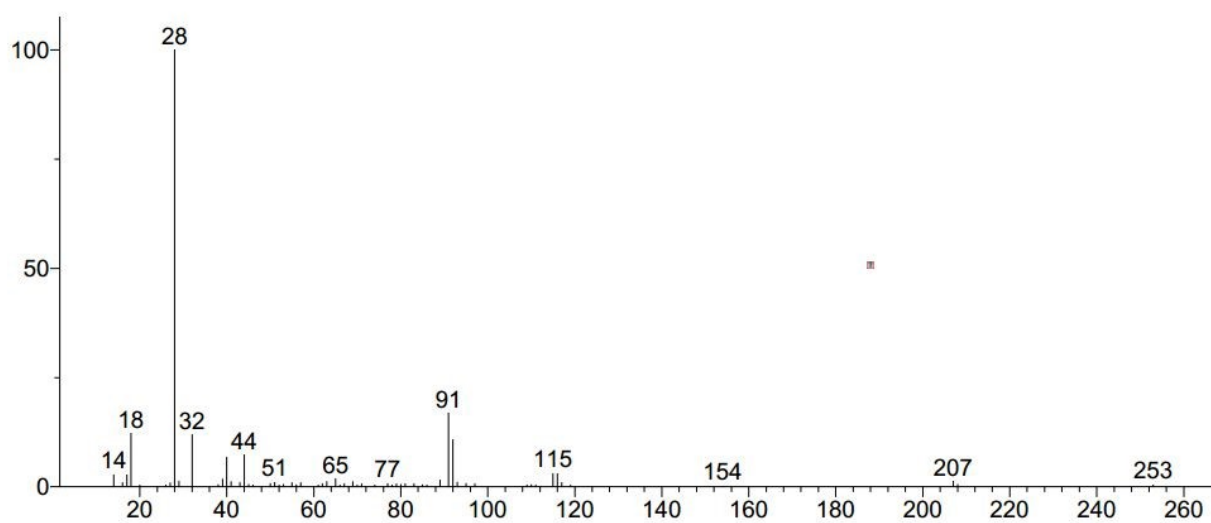
Retention time 3.22 min

Unknown; InLib=-549



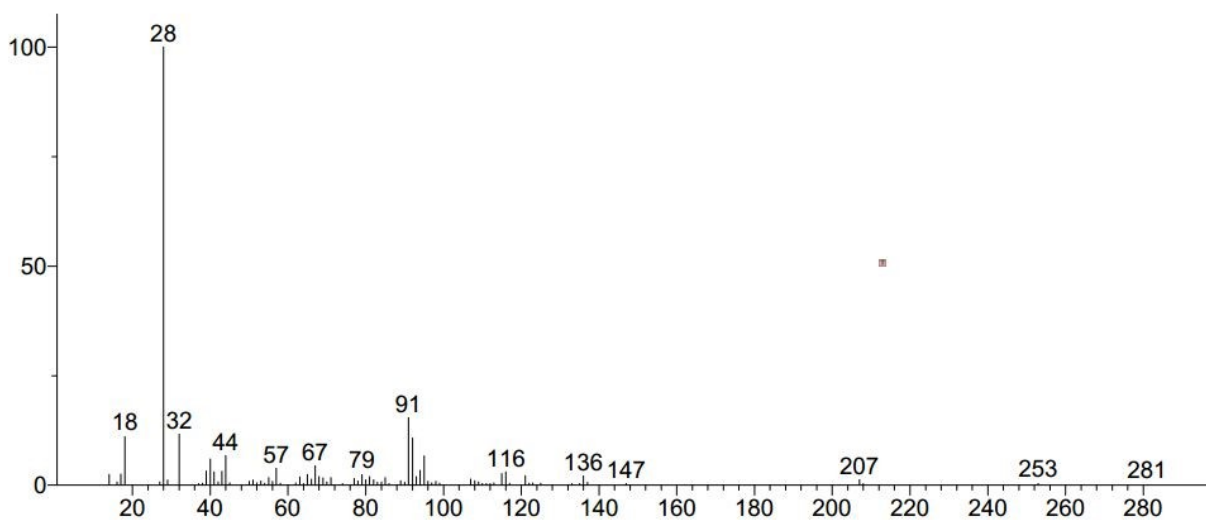
Retention time 3.26 min

Unknown; InLib=-1302



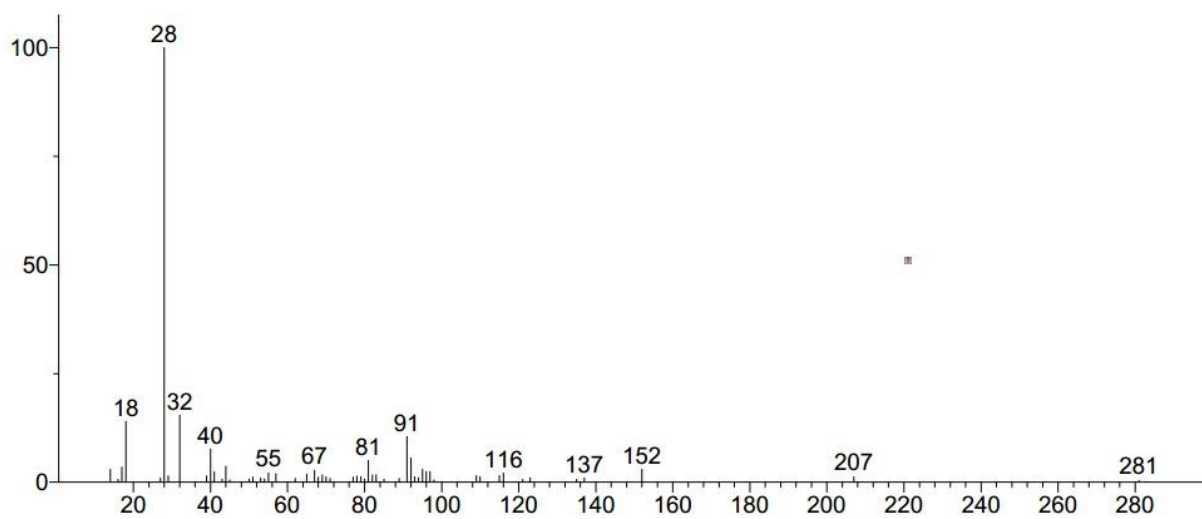
Retention time 3.32 min

Unknown; InLib=-1276



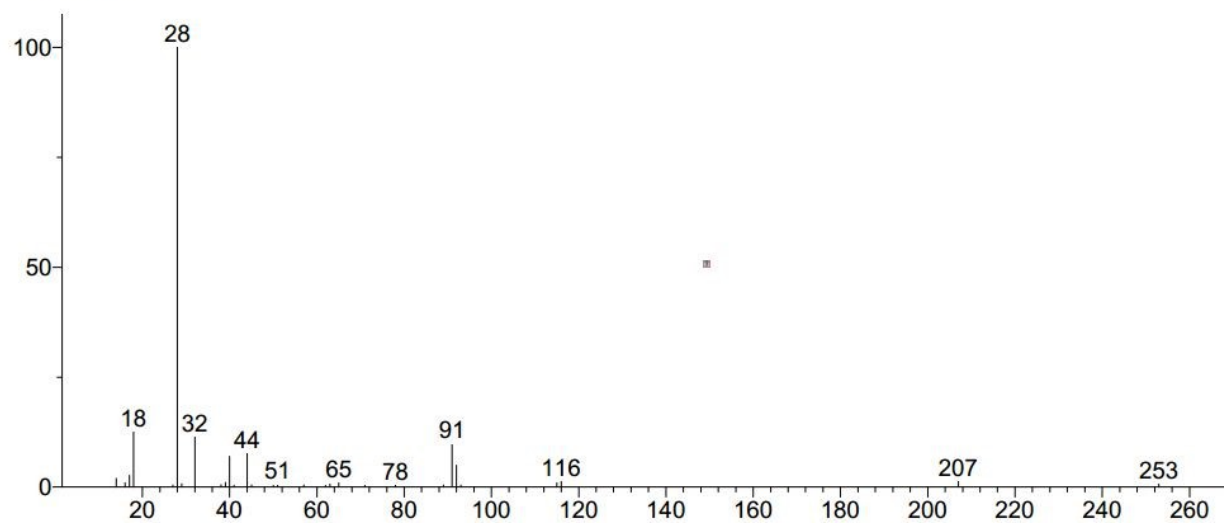
Retention time 3.44 min

Unknown; InLib=-1008



Retention time 4.10 min

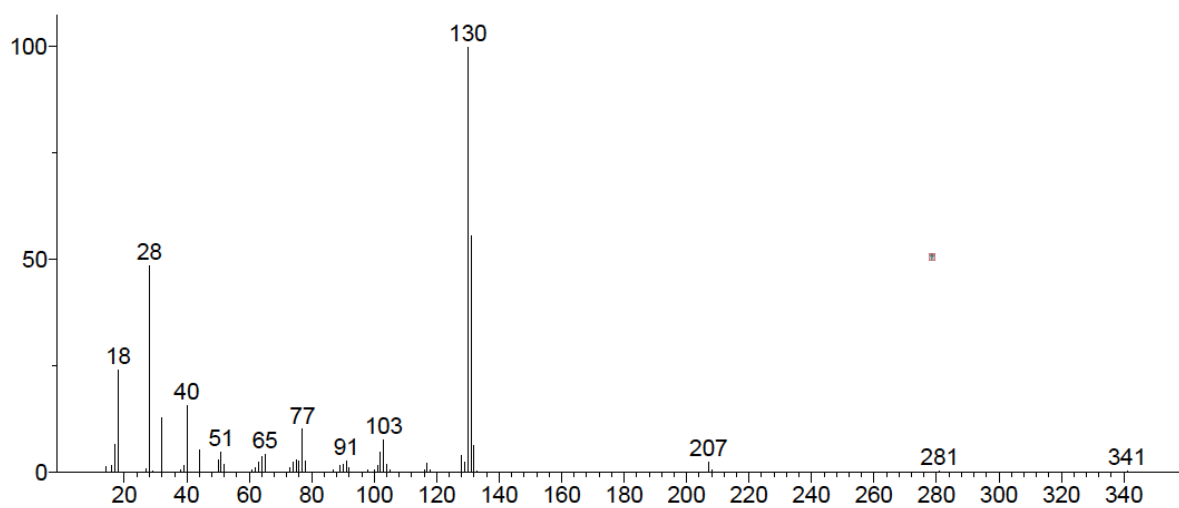
Unknown; InLib=-830



### Indole

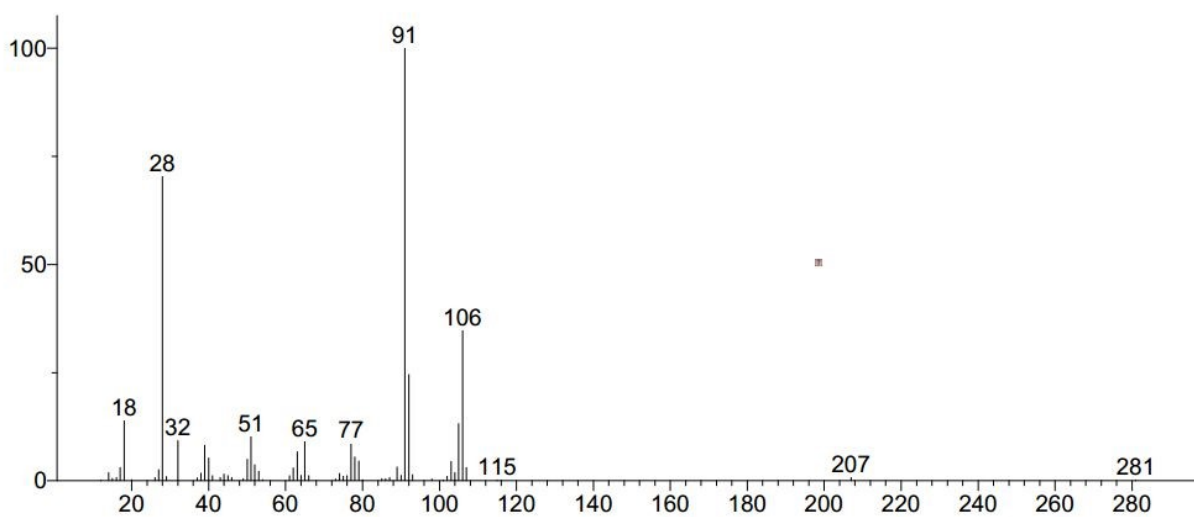
Retention time 5.91 min

Unknown; InLib=-197

**Benzofuran**

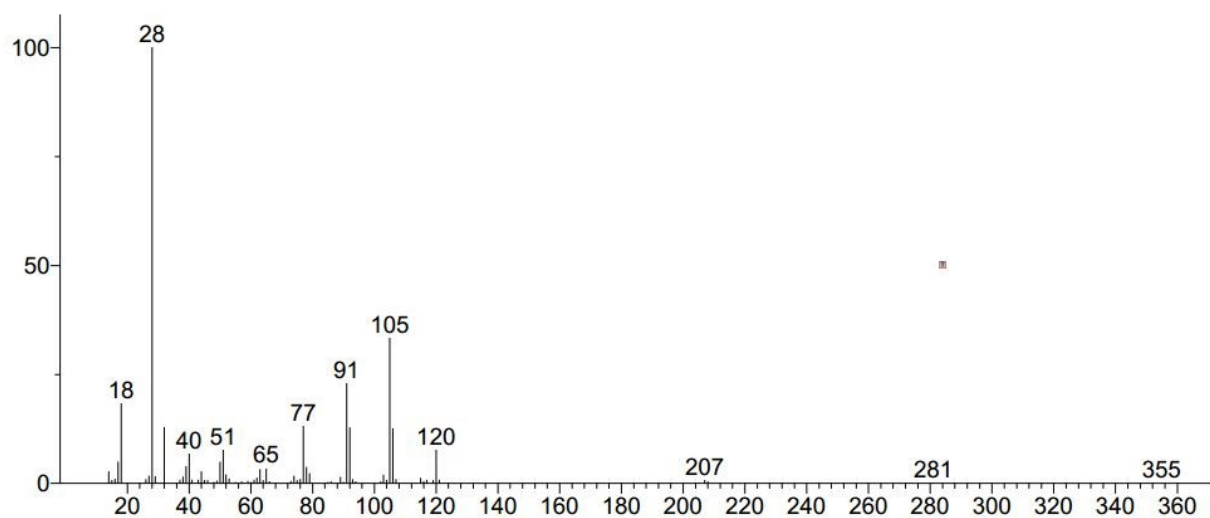
Retention time 2.07 min

Unknown; InLib=-135



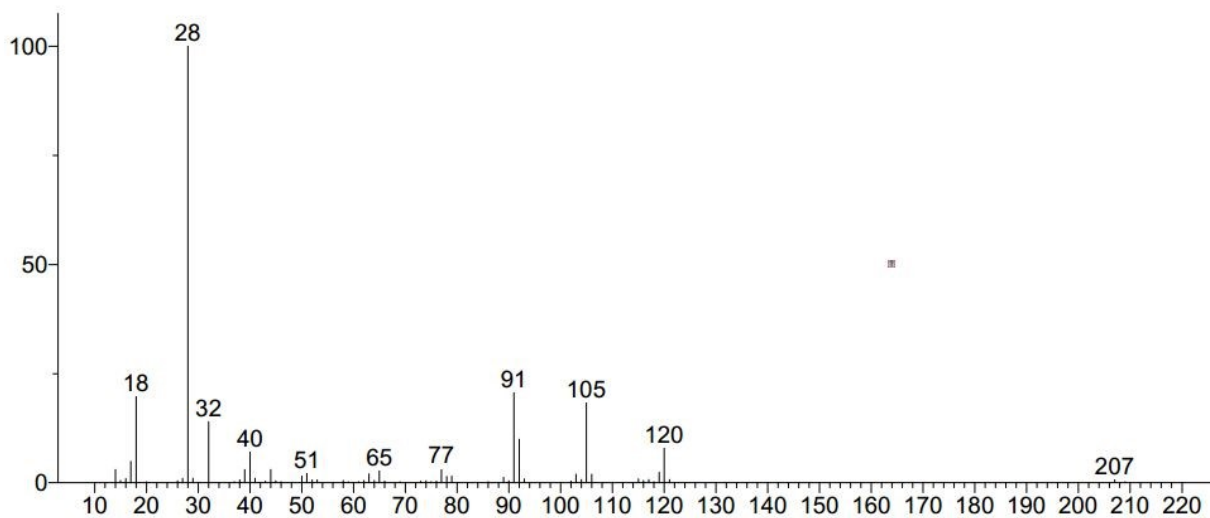
Retention time 2.37 min

Unknown; InLib=-744



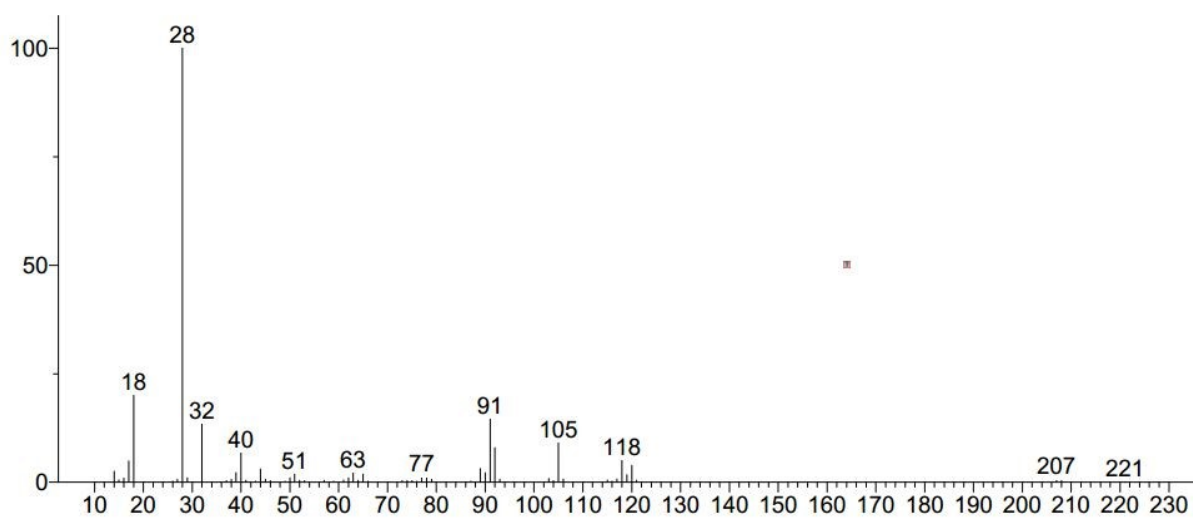
Retention time 2.55 min

Unknown; InLib=-474



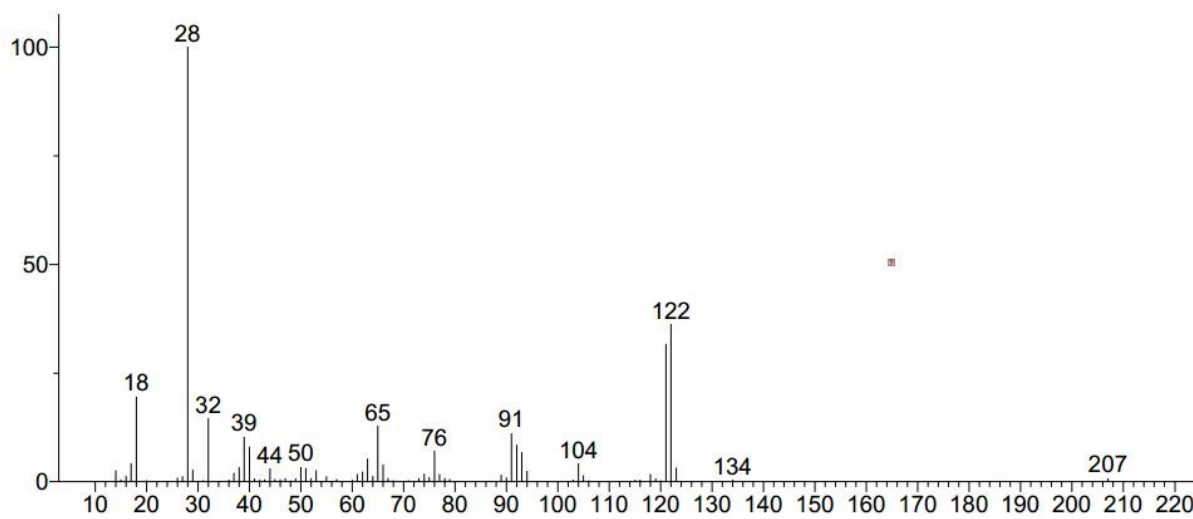
Retention time 2.73 min

Unknown; InLib=-1169



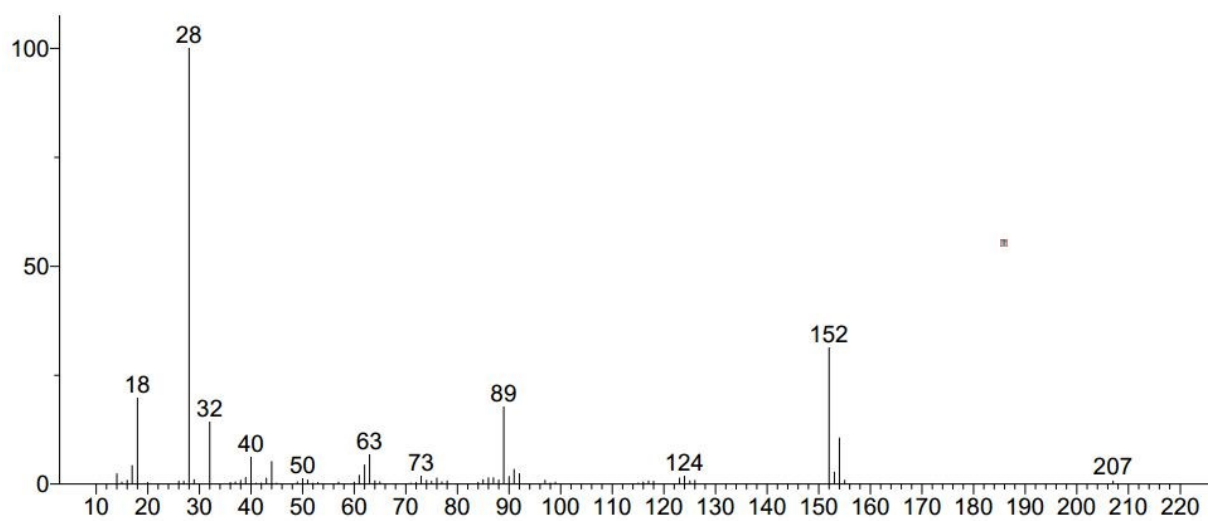
Retention time 2.89 min

Unknown; InLib=-496



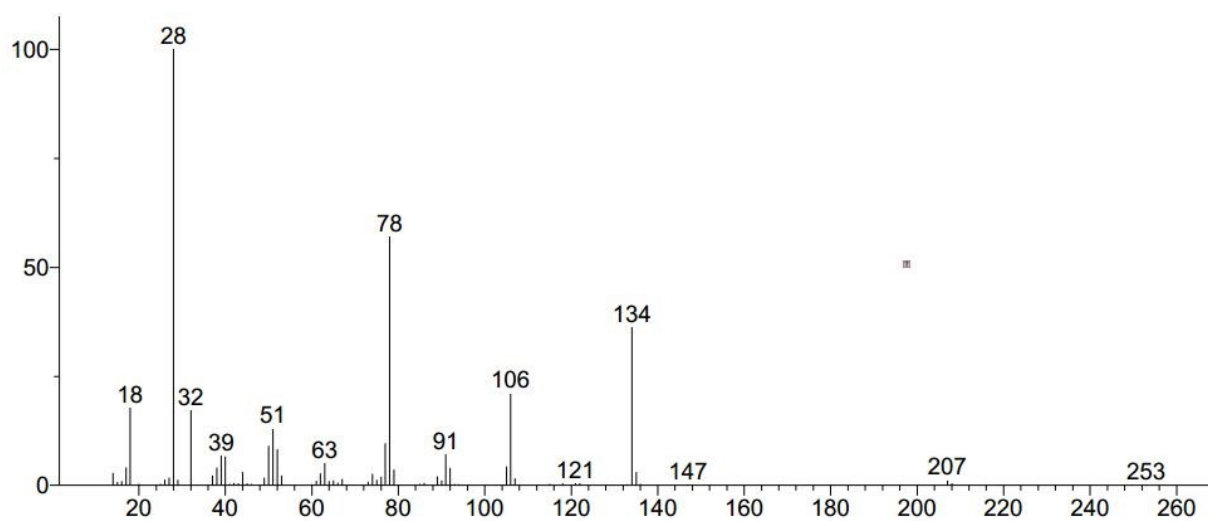
Retention time 4.11 min

Unknown; InLib=-778



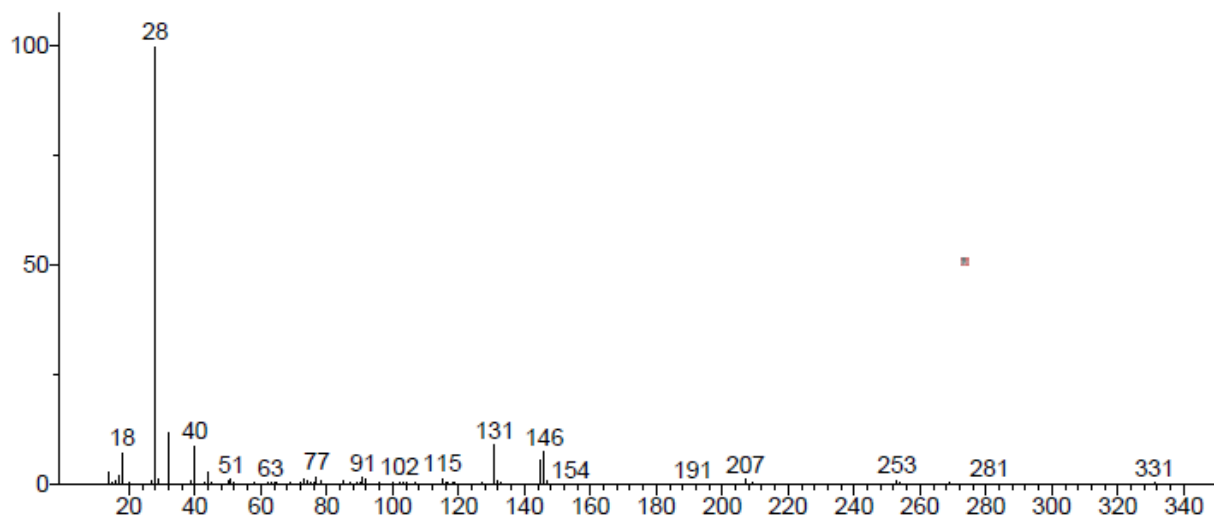
Retention time 4.55 min

Unknown; InLib=166



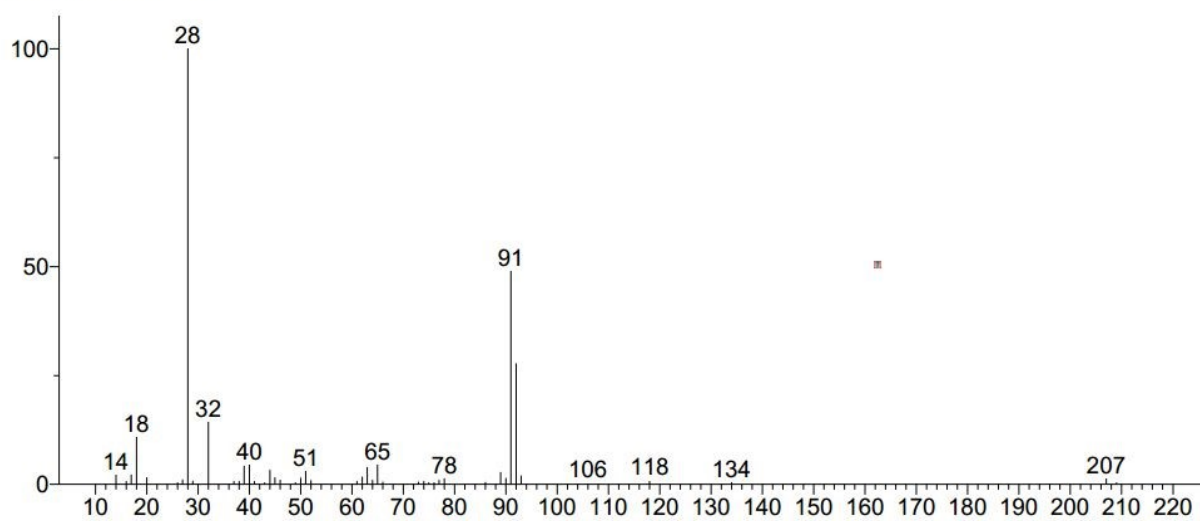
Retention time 4.26 min

Unknown; InLib=-1149



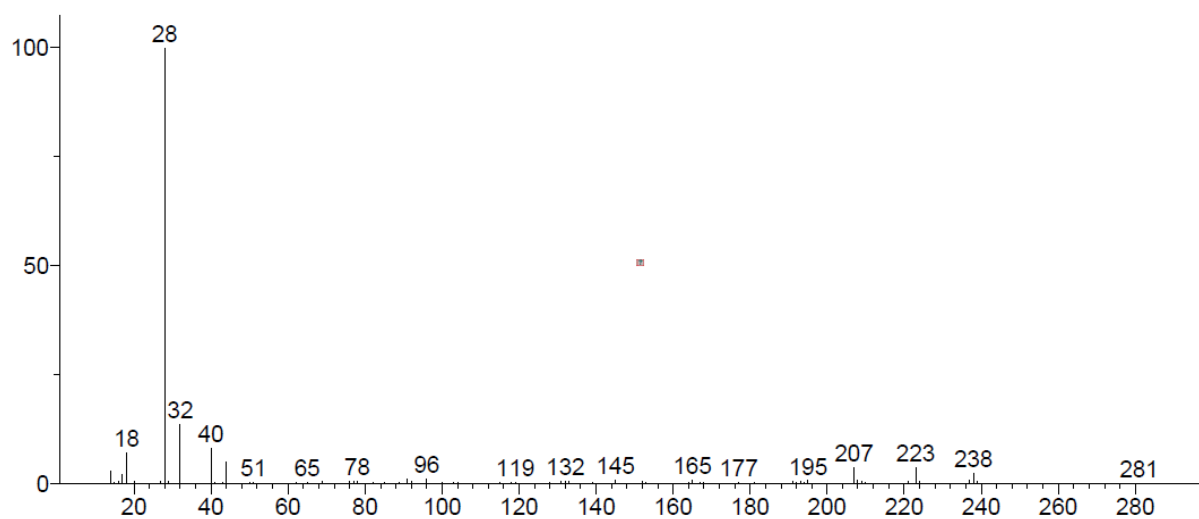
Retention time 5.14 min

Unknown; InLib=-591



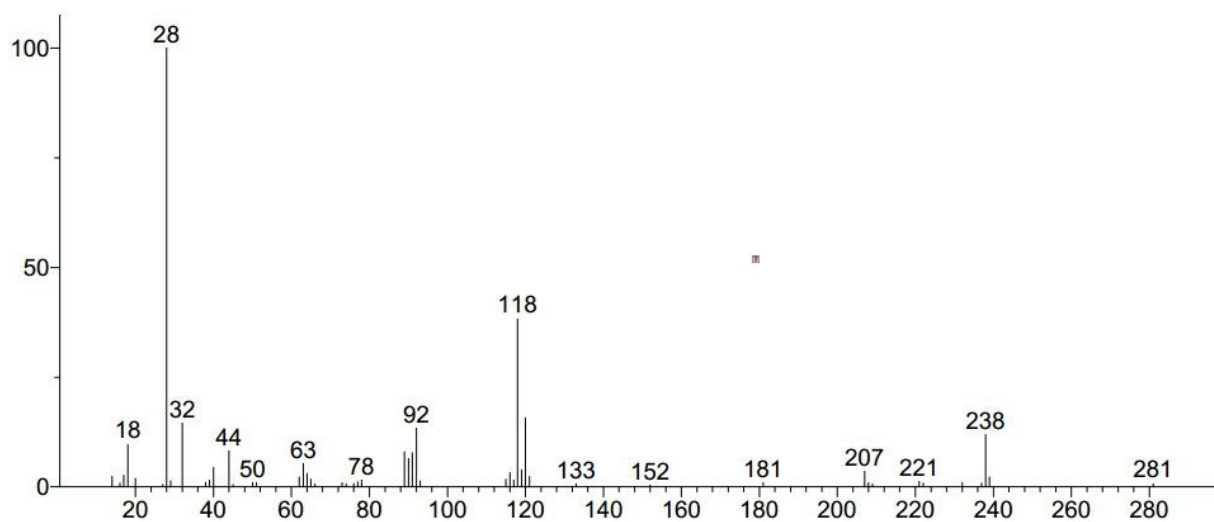
Retention time 10.77 min

Unknown; InLib=-610



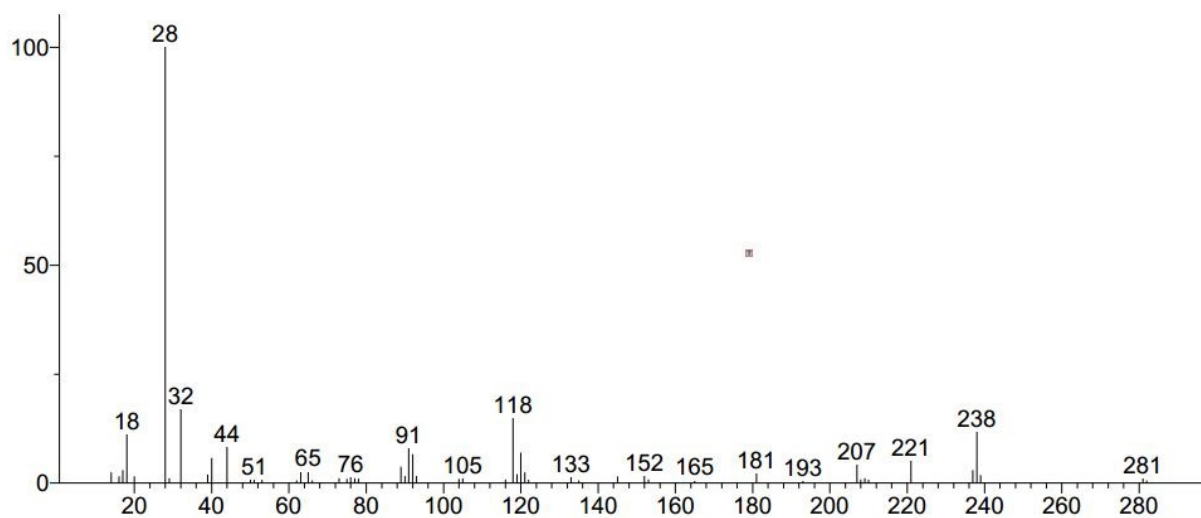
Retention time 14.12 min

Unknown; InLib=-830



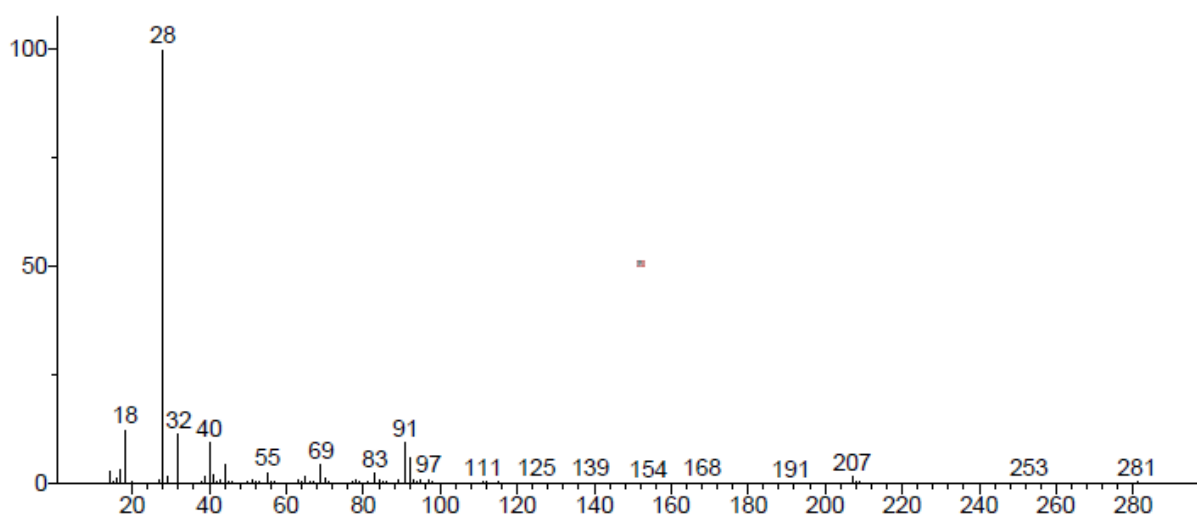
Retention time 14.37 min

Unknown; InLib=-550

**Thianaphthene**

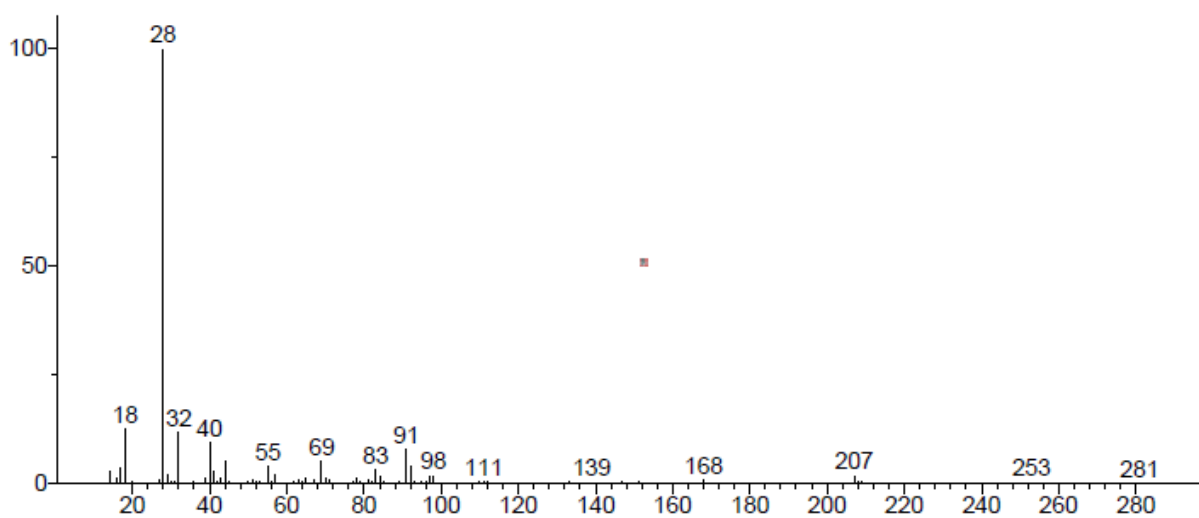
Retention time 2.77 min

Unknown; InLib=-1008



Retention time 2.91 min

Unknown; InLib=-1589

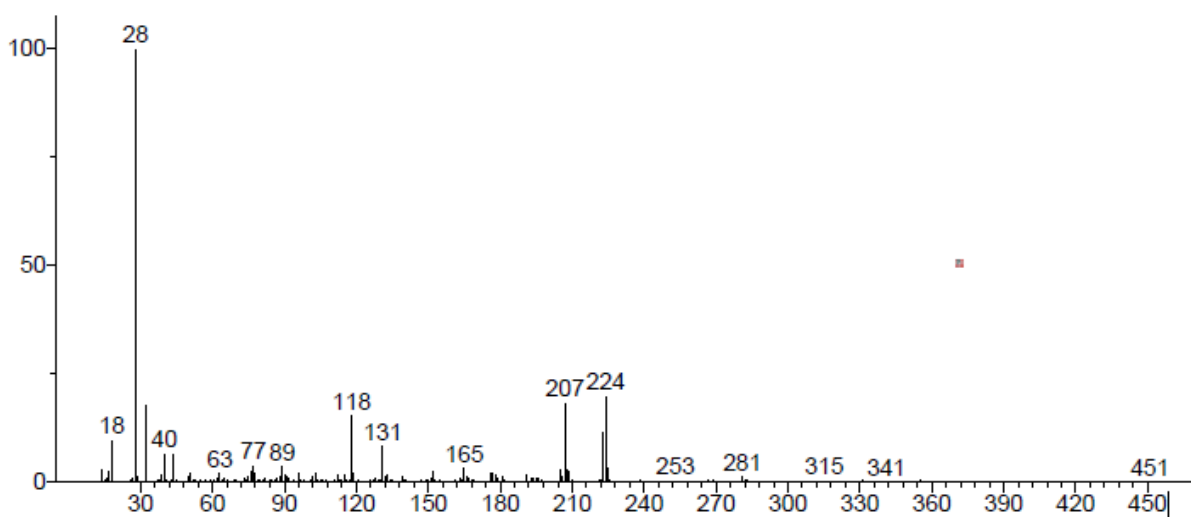


## Chapter 5

### Reaction of benzofuran for 60 min

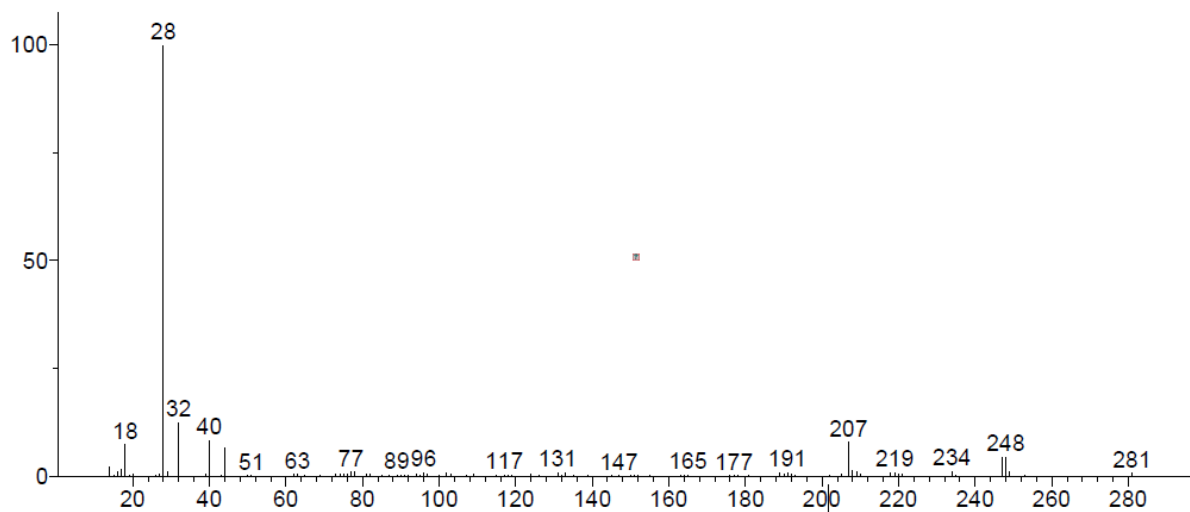
Retention time 13.23 min (peak 13)

Unknown; InLib=-1750



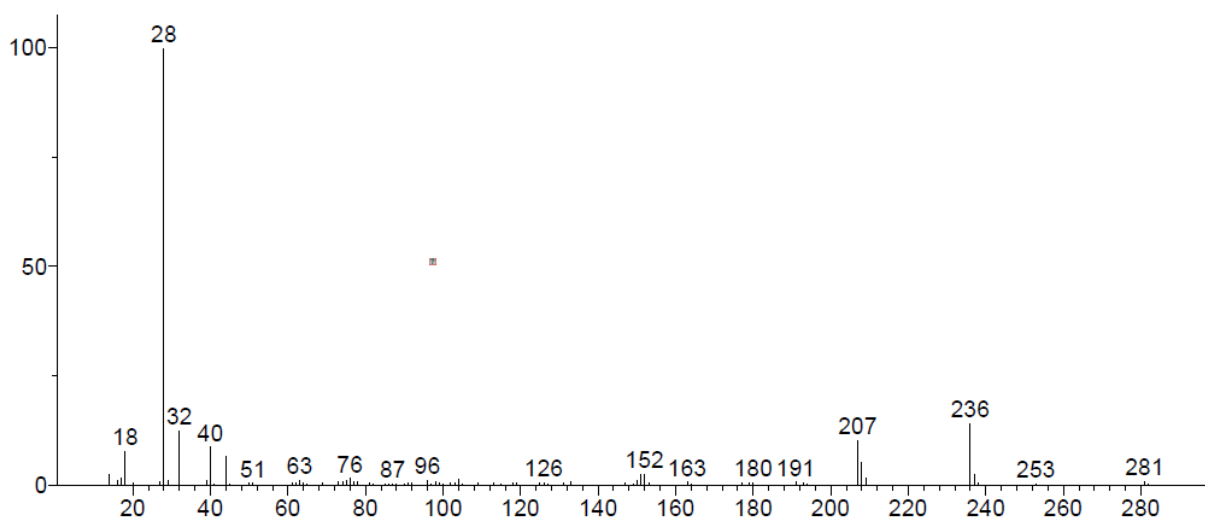
Retention time of 14.35, 14.67 min (peak 16)

Unknown; InLib=-1101



Retention time of 15.16 min (peak 17)

Unknown; InLib=-1066



### Reaction of Indene+Indane

Retention time 2.89 min

Unknown; InLib=-1660

